REACTIVITY STUDIES OF 1-Benzoyl-3-(2,4,6-tri-*tert*-butylphenyl)thiourea AND RELATED LIGANDS

A dissertation presented in partial fulfilment of the requirements for the degree of

Master of Philosophy
in
Chemistry

at Massey University, Palmerston North,
New Zealand.

I. K. G. Indira Chandrasena

2001

Dedication

To my dearest father… though you are far away across the Pacific you gave me strength and courage through your mind.

&

To my dearest mother… though you are not in this world to see this piece of work, your love and support lead me through to this stage.

Errata

P111 line 10 should read " .....two types of complex, one with a CT band in the 300 nm region and the other in the 350 nm region."

P113 line 3 from the bottom Method (b) not Method (a)

P115 line 11 from the bottom should read ".....derives from the instability of the compound in CHCl3/pentane."

P 150 In Table 5.2 the spectra were recorded at room temperature.

P47 reference 22 Weinhiem should be Weinheim.

Abstract

This thesis aims to investigate the coordination modes, reactivity, spectroscopy and structures of bulky 1-benzoyl-3-(aryl)thioureas, with metals and non-metals. The bulky ligand, 1-benzoyl-3-(2,4,6-tri-*tert*-butylphenyl)thiourea (Bz^tBPtuH) and the related ligands, 1-benzoyl-3-(2,4,6-triphenylphenyl)thiourea (BzPPtuH), 1-benzoyl-3-(2,6-diisopropylphenyl)thiourea (Bz^iPPtuH), 1-benzoyl-3-(4-fluorophenyl)thiourea (BzFPtuH), and 1-benzoyl-3-phenylthiourea (BzPtuH) are the focus of the research in this thesis.

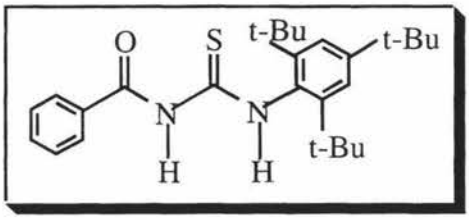

Bz^tBPtuH

Chapter One gives a brief review of the chemistry of thiourea and modified thiourea ligands.

In Chapter Two, the preparation, characterization and structure of Bz^tBPtuH are described and compounds of the type $[M(L)_2]$ (M = Cu, L = Bz^tBPtu or Bz^iPPtu), $[M(LH)_2X_2]$ (M = Cu(II) or Co(II), LH = Bz^tBPtuH or Bz^iPPtuH, X = Cl; M = Ni(II), LH = Bz^tBPtuH, X = I), $[M(LH)_2Cl]$ (M = Cu(I), LH = Bz^tBPtuH, BzPPtuH, Bz^iPPtuH or BzFPtuH), $[Cu(BzPtuH)_3Cl]$ and $[M(LH)_4]PF_6$ (M = Cu(I) or Ag(I), LH = Bz^tBPtuH or Bz^iPPtuH) have been synthesized. The deprotonated ligands, Bz^tBPtu and Bz^iPPtu, in the complexes $[Cu(Bz^tBPtu)_2]$ and $[Cu(Bz^iPPtu)_2]$ coordinate through the O and S atoms resulting in six-membered chelate rings from the anionic ligands. The electronic spectra give support for thiocarbonyl S being bound to the metal. This, combined with ESR spectra suggests square planar structures for $[M(L)_2]$ (L = Bz^tBPtu or Bz^iPPtu). For $[Cu(Bz^tBPtuH)_2Cl_2]$, the ligand remains neutral and binds through the S atom to form a distorted tetrahedral complex. The X-ray crystal structure of $[Cu(Bz^tBPtuH\text{-}\kappa^1\text{-}S)_2Cl]$ shows the ligand is bound through S and the complex has a

trigonal planar structure. The X-ray structure of $[Co(Bz^tBPtuH)_2Cl_2]$ shows it to be distorted tetrahedral with cobalt having an S_2Cl_2 donor set. The complexes $[M(LH)_4]PF_6$ (M = Cu(I) or Ag(I), LH = Bz^tBPtuH or Bz^iPPtuH) probably have tetrahedral structures.

In Chapter Three, $HgCl_2$ compounds of the type $[Hg(LH)_2Cl_2]$ (LH = Bz^tBPtuH, Bz^iPPtuH or BzFPtuH) are reported as well as $[Hg(BzPtuH)Cl_2]$. With $Hg(Ac)_2$, the ligands (in alcoholic solvents) are converted to $[C_6H_5CON{=}C(OX)NHR]$ (R = 2,4,6-tri-*tert*-butylphenyl, 2,4,6-tri-phenylphenyl, 2,6-diisopropylphenyl, *p*-fluorophenyl or phenyl, X = C_2H_5; and R = 2,4,6-tri-*tert*-butylphenyl, X = CH_3, or $CH_2C_6H_5$) while in CH_2Cl_2 $[C_6H_5CON(COCH_3)C(O)NHR]$ (R = 2,6-diisopropylphenyl) or NHCN-(2,4,6-tri-*tert*-butyl)phenyl are obtained. With sodium ethoxide in alcohol and water NH_2-C(S)NH-(2,4,6-tri-*tert*-butyl)phenyl was isolated. For $[Hg(LH)_2Cl_2]$ (LH = Bz^tBPtuH, Bz^iPPtuH or BzFPtuH) the ligand remains neutral and binds through the S atom to form a monomeric distorted tetrahedral complex. The structure of $[Hg(Bz^tBPtuH\text{-}\kappa^1S)_2Cl_2]$ was determined crystallographically. The complex $Hg(BzPtuH)Cl_2$ is possibly a polymer containing Cl and S bridges. The intermediate mercury complex formed with $Hg(Ac)_2$ in alcohol reaction was unstable, and it decomposed to form HgS and a new compound $[C_6H_5CON{=}C(OX)NHR]$. The X-ray crystal structure and spectroscopic data confirm the final product. $Cd(Ac)_2$ reacted with Bz^tBPtuH in ethanol to give some CdS, unreacted starting material and a little BzE^tBPA. No reaction was observed with Zn^{2+} or UO_2^{2+} acetate.

Chapter Four investigates the coordination chemistry and reactivity of Bz^tBPtuH and related ligands with halogens (I_2 and Br_2). The I_2 adducts of the type $[(LH)I_2]$ (LH = Bz^tBPtuH, BzPPtuH, Bz^iPPtuH, BzFPtuH or BzPtuH) were obtained in 1:1 molar ratio as well as the metastable Br_2 adduct $[(Bz^iPPtuH)Br_2]$. The X-ray crystal structure of $[(Bz^tBPtuH\text{-}\kappa^1S)I_2]$ shows a I–I bond distance of 2.8537(4) Å. The X-ray crystal structure of $[(Bz^iPPtuH\text{-}\kappa^1S)Br_2]$, shows a Br–Br bond distance of 2.6118(4) Å. The Br_2 adduct that initially formed in ice-cooled conditions with Bz^tBPtuH was converted to a novel heterocyclic ring compound, 2-benzamido-5,7-di-*tert*-butylbenzothiazole hydrobromide (B^tBBTH) at room temperature. This compound is ionic with Br^- anions and benzothiazole cations.

In Chapter Five, the complexes [Rh(COD)(LH)Cl] (LH = Bz^tBPtuH, BzPPtuH, Bz^iPPtuH, BzFPtuH or BzPtuH; COD = 1,5-cyclooctadiene) are prepared

from the reaction of $[Rh(COD)Cl]_2$ with the appropriate LH, and the complexes $[Pt(LH)_2Cl_2]$ (LH = Bz^tBPtuH or Bz^iPPtuH) by reacting $K_2[PtCl_4]$ with the appropriate LH. The X-ray structure of $[Rh(COD)(BzPPtuH\text{-}\kappa^1S)Cl]$ shows a square planar arrangement of the ligands about Rh, with LH binding through the sulfur atom. One of the π-bonds of COD is bound to Rh and is *trans* to the Cl group while the other π-bond is bound to Rh but is *trans* to the S atom. The two equivalent protons associated with the olefinic bonds *trans* to the Cl group have a different chemical shift from the two protons on the olefin arm *trans* to the S atom at low temperature (–20 to –40 °C), but coalesce into one broad band at higher temperature (20 to 40 °C). A preliminary X-ray structure on $[Pt(Bz^tBPtuH\text{-}\kappa^1S)_2Cl_2]$ shows the complex has a *cis* structure.

Acknowledgements

I take this opportunity to gratefully acknowledge the contribution from the following people, without which much of this work would not be possible.

It is with deep sense of gratitude and appreciation I thank my supervisors, Associate Professor Eric Ainscough and Professor Andrew Brodie for their excellent guidance, assistance, encouragement, valuable comments and giving their time, knowledge and experience freely from the beginning of my research project until the final review of the manuscript.

I would like to thank Professor Tony Burrell for assisting with the X-ray crystal structures, Dr Pat Edwards for assistance with the NMR experiments, Dr Allen Oliver of the University of Auckland for X-ray data collection, Associate Professor Graham A. Bowmaker of the University of Auckland for Raman Spectroscopy, Mr. John Allen of AgResearch for Mass Spectral data, Mrs. Marianne Dick of Otago University for elemental analysis, Mr. Terry Canton and Mrs. Penny Abercrombie for supplying everything I needed.

I would also like to take this opportunity to thank all the academic staff and other members of the department for their help during the course of my Masterate and who with their team effort make the place run.

Finally I would like to thank my husband, Dhamsiri and my two daughters Nadeeka and Kanchana for their continuous support, patience and encouragement until the completion of my thesis.

Table of Contents

List of Figures

List of Tables

List of Schemes

Abbreviations

ABz^{i}PPu	1-acetyl-1-benzoyl-3-(2,6-diisopropylphenyl)urea
Ac	acetate
Anal.	Analyses
B.M.	bohr magneton
bp	boiling point
B^{t}BBTH	2-benzamido-5,7-di-*tert*-butylbenzothiazole hydrobromide
Bu	butyl
BzEFPA	1-benzoyl-2-[ethoxyl-3-(4-fluorophenyl)amino]aldimine
BzE^{i}PPA	1-benzoyl-[2-ethoxyl-3-(2,6-diisopropylphenyl)amino]aldimine
BzEPA	1-benzoyl-2-[ethoxyl-3-(phenyl)amino]aldimine
BzEPPA	1-benzoyl-2-[ethoxyl-3-(2,4,6-tri-phenylphenyl)amino]aldimine
BzE^{t}BPA	1-benzoyl-2-[ethoxyl-3-(2,4,6-tri-*tert*-butylphenyl)amino]aldimine
BzFPtuH	1-benzoyl-3-(4-fluorophenyl)thiourea
Bz^{i}PPtuH	1-benzoyl-3-(2,6-diisopropylphenyl)thiourea
BzM^{t}BPA	1-benzoyl-2-[methoxyl-3-(2,4,6-tri-*tert*-butylphenyl)amino]aldimine
BzPM^{t}BPA	1-benzoyl-2-[phenylmethoxyl-3-(2,4,6-tri-*tert*-butylphenyl)amino]aldimine
BzPPtuH	1-benzoyl-3-(2,4,6-triphenylphenyl)thiourea
BzPtuH	1-benzoyl-3-phenylthiourea
Bz^{t}BPtuH	1-benzoyl-3-(2,4,6-tri-*tert*-butylphenyl)thiourea
$CDCl_3$	deuterated chloroform
COD	1,5-cyclooctadiene
CT	charge transfer
ESR	electron spin resonance
Et	ethyl
IR	Infrared
L	ligand
M	central metal atom in compound
m.p.	melting point
m/z	mass to charge ratio
M^+	molecular ion

Me	methyl
MS	mass spectra
MT	mull transmittance
NMR	nuclear magnetic resonance
ORTEP	the computer program used for crystal illustrations
Ph	phenyl
ppm	parts per million
Pr	propyl
R	organic group
rel. int.	relative intensity
^{t}BPc	2,4,6-tri-tert-butylphenylcyanamide
^{t}BPtu	2,4,6-tri-tert-butylphenylthiourea
TMS	tetramethylsilane
tu	thiourea
UV-vis	ultraviolet-visible
δ	chemical shift in ppm
ν(XY)	stretching frequency of X-Y bond (cm^{-1})
μ_{eff}	effective magnetic moment
2D	two dimensional

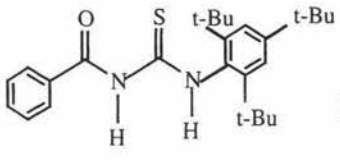

Bz^{t}BPtuH

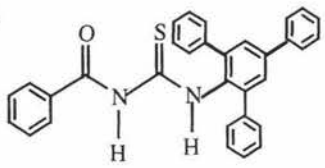

BzPPtuH

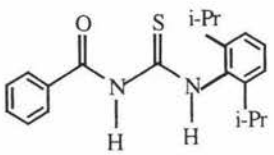

Bz^{i}PPtuH

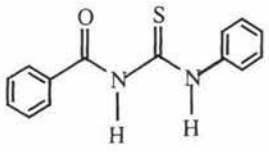

BzPtuH

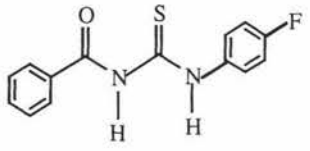

BzFPtuH

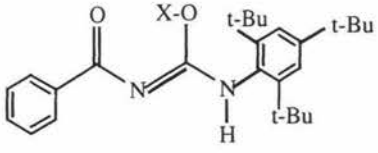

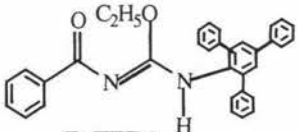

BzEPPA

BzE^{i}PPA

X = C_2H_5, 1-benzoyl-2-[ethoxyl-3-(2,4,6-tri-*tert*-butylphenyl)amino]aldimine (**BzE^{t}BPA**)

= CH_3, 1-benzoyl-2-[methoxyl-3-(2,4,6-tri-*tert*-butylphenyl)amino]aldimine (**BzM^{t}BPA**)

= $CH_2C_6H_5$1-benzoyl-2-[phenylmethoxyl-3-(2,4,6-tri-*tert*-butylphenyl)amino]aldimine (**BzPM^{t}BPA**)

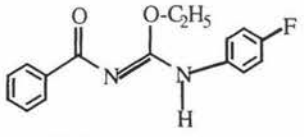

BzEFPA

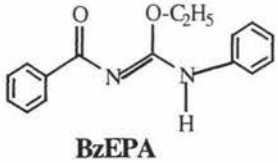

BzEPA

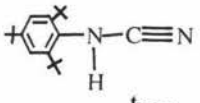

^{t}BPc

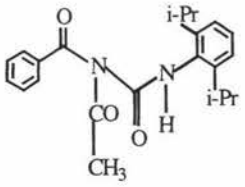

ABz^{i}PPu

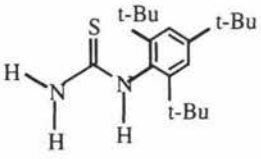

^{t}BPtu

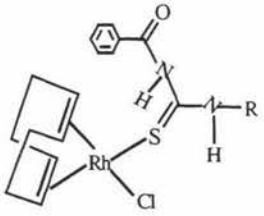

Rh(COD)(LH)Cl

LH = ^{t}BPtuH, BzPPtuH, Bz^{i}PPtuH, BzFPtuH or BzPtuH

R = 2,4,6-tri-*tert*-butylphenyl, 2,4,6-tri-phenylphenyl, 2,6-diisopropylphenyl, *p*-fluorophenyl or phenyl

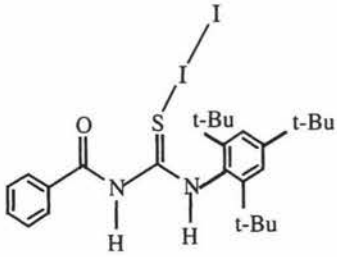

(Bz^{t}BPtuH)I_2

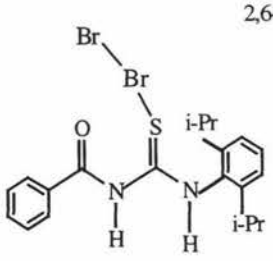

(Bz^{i}PPtuH)Br_2

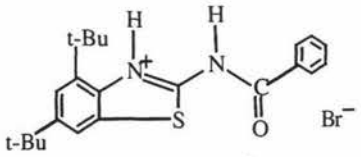

B^{t}BBTH

The structures and abbreviations of the molecules used in this thesis

CHAPTER ONE

Thiourea Complexes Containing Nitrogen, Sulfur and Oxygen-Donor Ligands

1.0 INTRODUCTION

The coordination chemistry of thiourea has been extensively studied and its complexes show a variety of structures with most transition metals. The parent thiourea ligand possesses potentially S and N donor atoms.

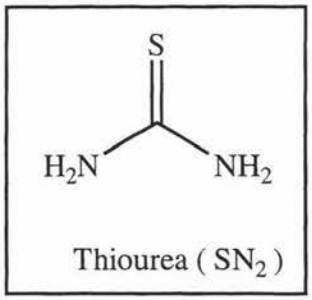

Thiourea (SN_2)

By adding appropriate moieties, the parent thiourea may be extended to systems containing SN_2O or SN_3O atoms as shown.

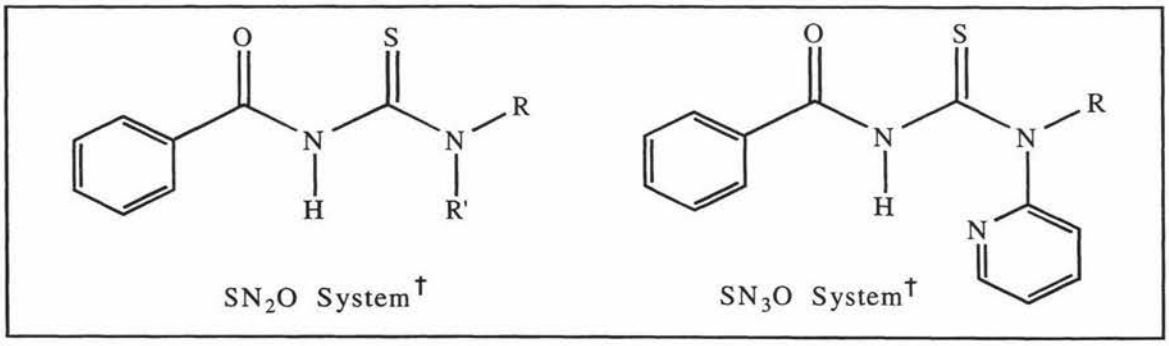

SN_2O System† SN_3O System†

† This is not meant to imply that all these atoms will bind at the same time.

This study aims to investigate the coordination chemistry of bulky thioureas of the type SN_2O where e.g. R' is bulky. As the chemistry of all these systems is expected to be dominated by the S donor ability, a summary of some of the known properties of S acting as a ligand will be undertaken first.

1.1 Properties Associated with Sulfur Donors

The particular features of sulfur as a donor atom have been discussed in some detail in an earlier review[1] and these do not appear to have been updated in a more recent review. Since they are relevant to this study, they are summarized here as follows.

(i) Whereas the permanent dipole moment and the coordinating ability decrease in the order: $H_2O > ROH > R_2O$, the reverse order holds for sulfur, viz. $H_2S < RSH < R_2S$.

(ii) From a consideration of both electrostatic and covalent models the strength of bonding to a metal ion is in the order: $RO^- > RS^-$ and $R_2O > R_2S$. However, sulfur has vacant d (and σ^*) orbitals, which can be used for d_π-d_π (or d_π-σ^*) bonding such as can occur with the later transition metals and with the early transition metals in unusually low oxidation states. Consequently, if π-bonding occurs, it can cause a reversal of the order to $RS^- > RO^-$ and $R_2S > R_2O$.

(iii) The polarizabilities of sulfur donors decrease in the order $S^{2-} > RS^- > R_2S$; furthermore, the number of lone pairs decreases in the same order. Consequently, thiolato ligands are more polarizable but not as effective π- electron acceptors as thioethers.

(iv) Sulfur donors bind more strongly to soft metals than do oxygen donors. Soft metals form a triangular area in the centre of the Periodic Table. The oxidation state of the metal affects the degree of soft character, which is strongest for transition metals in low oxidation states; i.e. metals having non-bonding d electrons and thus capable of forming d_π-d_π or d_π-σ^* bonds by donating a pair of electrons to the ligand.

---

[1] S.E. Livingstone, *Quart. Rev., Chem. Soc.*, 1965, **19**, 386.

(v) The spectrochemical series of ligands is arranged according to the spectroscopic splitting parameter Δ or 10Dq. Although some sulfur donors, including S-bonded SCN^-, $(RO)_2PS_2^-$, and S^{2-}, have a low position in the series near Cl^-, R_2S falls in the middle of series, probably between H_2O and N-bonded SCN^-, while S-bonded SO_3^{2-} has a later position near NO_2^-. The position of RS^- has not been established.

(vi) Sulfur ligands occupy a late position in the nephelauxetic series, which is, in effect, a measure of the degree of covalent bonding between metal and ligand. The series of donor atoms (arranged according to decreasing values of $1-\beta$) is roughly: $F < O < N < Cl < Br < S \approx I < Se$.

1.1.1 Some Additional General Observations

Sulfur atoms in heterocyclic rings have poor coordinating ability due to the pseudo-aromatic nature of the ring, which has the twofold effect of causing the lone pair on the sulfur atom to be less available for donation and the π-orbital to be less capable of accepting electrons from the metal. Towards soft and borderline metals, the coordinating ability of the various types of sulfur donors is:

$$RS^- > R_2S > RC{=}S \gg \text{ring sulfur}^{[1]}.$$

Some data are available on the nucleophilic reactivity of sulfur ligands[2]. The methylmercury cation CH_3Hg^+ has been used as a reference for bases L, since it acts as a Lewis acid as follows:

$$CH_3Hg^+ + L \rightarrow [CH_3HgL]^+$$

The values for $pK(CH_3Hg^+)$ are: S^{2-}, 21.3; RS^- in cysteine, 15.9; $S_2O_3^{2-}$, 10.95; SO_3^{2-}, 8.16; suggesting S^{2-} forms the strongest adduct.

1.1.2 Acid Dissociation Constants

Thiourea and its substituted analogs behave as monoacidic bases toward acids[3].

$$RH^+ \leftrightharpoons R + H^+$$

---

[2] F. Basolo and R.G. Pearson, *Mechanisms of Inorganic Reactions*, 2nd edn., John Wiley, New York, 1967, pp. 138, 396.

[3] J.L. Walter, J.A. Ryan and T.J. Lane, *J. Am. Chem. Soc.*, 1956, **78**, 5560,

It follows that

$$K_a = [H^+][R]/[RH^+]$$

Where K_a = acid dissociation constant of the protonated reagent RH^+

R = neutral reagent

The pK_a values obtained for thiourea and its analogs are given in **Table 1.1**. Thiourea (pK_a = 2.03) was found to be more basic than the corresponding urea (pK_a = 1.40). Because of the inductive and hyperconjugative effects exhibited by alkyl substituents on thiourea, the basicity increases in the order of H < ethyl < methyl < diethyl. The order of increasing basicity for the aromatic substituted thiourea compounds is *m*-tolyl ≤ *p*-tolyl < *o*-tolyl < phenyl < diphenyl. However, it would be expected that the *ortho*- and *para*-tolyl groups would contribute more to the basicity of thiourea than a phenyl group[6].

Table 1.1 Acid dissociation constants of thiourea analogs in 50% by volume dioxane at 25 °C

	pK_a		pK_a
1. Thiourea	2.03	5. Phenylthiourea	2.80
2. Urea	1.40	6. *o*-Tolylthiourea	2.78
3. Ethylthiourea	2.85	7. *m*-Tolylthiourea	2.70
4. Methylthiourea	2.90	8. *p*-Tolylthiourea	2.72

1.1.3 Mean Metal-Sulfur Coordinate Bond Energies and Formation Constants

A small amount of quantitative information on the strengths of the metal-ligand bond of thiourea complexes has been reported. An earlier thermochemical study[4] on the octahedral $[M(II)tu_4Cl_2]$ complexes of the first transition series metals showed that the mean metal-sulfur bond energy is comparable with the M-O and M-N bonds in

[4] S.J. Ashcroft, *J. Chem. Soc. A*, 1970, 1020.

H_2O and NH_3 complexes. Similar observations were also reported[5] for complexes of substituted thioureas.

The standard enthalpies of formation of crystalline complexes of thiourea (tu) with metal chlorides of the type $[M(II)tu_2Cl_2]$ [M(II) = Co, Zn, Cd, Hg] and $[M(I)tu_2Cl]$ [M(I) = Ag] were measured by reaction calorimetry at 298.15 K. The mean metal-sulfur coordinate bond dissociation energies range from 179kJ/mole for the Co complex to 104kJ/mol for the Hg complex[6].

Table 1.2 summarises the mean coordinate bond dissociation energies for cobalt, zinc, cadmium, silver and mercury thiourea complexes[6].

The mercury complex displays considerably weaker bonding. Direct comparison is probably unwise, however, owing to the uncertainty in the value of the enthalpy of sublimation (±20% for $\Delta_{cr}^{g}H$) and to the unusual structure of the complex. A consistent result for the enthalpy of sublimation could not be obtained for $[Hg(II)tu_2Cl_2]$, presumably due to decomposition[6].

Table 1.2 Mean Coordinate Bond Energies, D (M-tu) at 298.15 K

complex	D(M-tu) kJ/mol	complex	D(M-tu) kJ/mol
$[Cotu_2Cl_2]$	179	$[Agtu_2Cl]$	148
$[Zntu_2Cl_2]$	148	$[Hgtu_2Cl_2]$	104
$[Cdtu_2Cl_2]$	142		

The X-ray structures indicate similar tetrahedral structures for $[Zn(II)tu_2Cl_2]$[7] and for $[Cd(II)tu_2Cl_2]$[8]. The structure of the complex $[Hg(II)tu_2Cl_2]$ shows it to be $[Hg(II)tu_2Cl]^+Cl^-$ in which the chlorobis(thiourea) mercury ion is

[5] S.J. Ashcroft, *J. Chem. Thermodyn.*, 1971, **3**, 853.
[6] J. Ashcroft, *J.Chem. Eng. Data,* 1988, **33**, 73.
[7] N.R. Kunchur, and M.R. Truter, *J. Chem. Soc.,* 1958, 3478.
[8] M. Nardelli, L. Cavalca and A. Braibanti, *Gazz. Chim. Ital.,* 1957, **87**, 137.

trigonal planar. This structure was confirmed by Brotherton *et al.*[9]. $[Ag^{I}tu_2Cl]$ was shown to consist of infinite spiraling chains of -Ag-S-Ag-S-, each silver atom being surrounded by a distorted tetrahedron of ligands[10].

Toropova and Kirillova[11] have used a potentiometric method to measure the temperature dependence of the equilibrium between either Hg(II) or Ag(I) ions, in aqueous solution containing 0.8M $NaNO_3$, and thiourea. The derived thermodynamic data are shown in **Table 1.3**.

Table 1.3 Thermodynamic data for the reaction between Hg(II), Ag(I) and thiourea (tu), in 0.8M $NaNO_3$ at 25 °C[14]

	$[AgL_3]^+$			$[HgL_4]^{2+}$		
	ΔH° (KJ mol^{-1})	ΔG° (KJ mol^{-1})	ΔS° (J K^{-1} mol^{-1})	ΔH° (KJ mol^{-1})	ΔG° (KJ mol^{-1})	ΔS° (J K^{-1} mol^{-1})
L = tu	−84.00	−74.76	−29.4	−184.8	−150.36	−117.6

The enthalpy of formation of the silver thiourea complex [Ag(I) (thiourea)$_3$]$^+$, $\Delta H^\circ = -84.0 \pm 8.4$ kJ/mole, is much less negative than that of −126 kJ/mole found by direct calorimetric measurements by Yatsimirskii and Astasheva[12]. The data in **Table 1.3** show that $\Delta H^\circ/4$ for the Hg^{2+} complex is greater than $\Delta H^\circ/3$ for the Ag^+ complex implying that the former interaction is stronger. In both complexes the central atom is bonded to the ligand only through the sulfur atom[1].

Stability Constants of metal-ion complexes[13] are given in **Table 1.4**.

Table 1.4 Overall Stability Constants of Thiourea Complexes

Metal	Medium	β_2
Ag^+	0.5M KNO_3	9.83±0.11
Hg^{2+}	0.1M CH_3CN	21.3

[9] P.D. Brotherton, P.C. Healy, C.L. Raston and A.H. White, *J. Chem. Soc., Dalton Trans.*, 1973, 334.

[10] E.A. Vizzini and E.L. Amma, *J. Am. Chem. Soc.*, 1966, **88**, 2872.

[11] V.F. Toropova and L.S. Kirillova, *Russ. J. Inorg. Chem.*, 1960, **5**, 176.

[12] K.B. Yatsimirskii and A.A. Astasheva, *Zh. Fiz. Khim.*,1953, **27**, 1539.

[13] Stability Constants of Metal-ion Complexes: Part B, *Organic Ligands,* Pergamon Press, Oxford, 1979, p.16.

The above β_2 data indicates that the Hg^{2+} complex is more stable than the Ag^{+} complex. But in an apparent paradox, in **Table 1.2,** the mean coordinate bond energy is lower for $[Hgtu_2Cl_2]$. The reliability of the Hg-tu mean bond energy must remain in doubt and further attempts to measure it are needed.

1.2 Thiourea Complexes

Sulfur is considered to be a 'soft' atom in contrast to oxygen, which is a 'hard' atom, while the nitrogen atom ranges from 'borderline' to 'hard' [14]. Therefore, N and O donors are best suitable for higher oxidation state metal ions, and S is generally considered to be suitable for lower oxidation states.

Thiourea has been extensively studied over the last 60-70 years and a brief review of its chemistry will now be given.

The planar structure of thiourea can be represented by the three resonance structures:

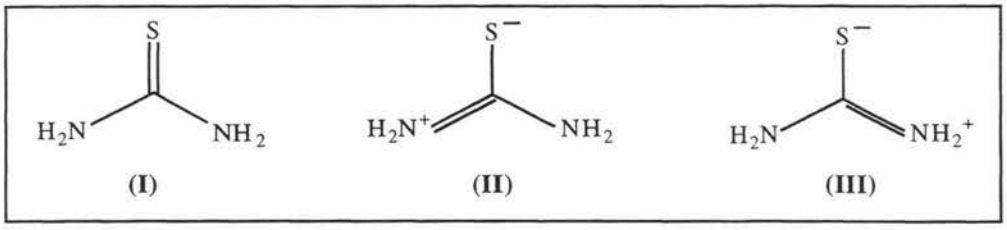

(I) **(II)** **(III)**

Complexation with sulfur as the donor site would enhance (II) and (III). The formation of S → M bounds is expected to increase the contribution of the highly polar structure to the thourea molecule, resulting in a greater double bond character for the nitrogen-to-carbon bond and a greater single bond character for the carbon-to-sulfur bond.

Thiourea $(H_2N)_2C{=}S$ (tu), acts as a unidentate ligand forming strong complexes with soft metal ions, in particular Cu(I), Au(I) and Hg(II). It reduces Cu(II) to Cu(I), Au(III) to Au(I), Pt(IV) to Pt(II) and Te(IV) to Te(II), forming complexes with the metal in the lower oxidation state[1]. The only metal reported to be N-bond is Ti(IV),

[14] R.G. Pearson, *Chemical Hardness*, 1997, Wiley-VCH, Weinhiem.

all others being S-bonded with ν(M-S) occurring at 300-200 cm^{-1} [15]. Thiourea, like other S-donor ligands, has a high *trans* effect [16,17].

Thiourea is remarkable for the number and variety of the addition compounds, which it forms, with salts of many metals. Its alkyl derivatives also share this property. Many of the interactions may serve as sensitive colour tests for the metal ions. Many addition compounds in solution have been detected by physical measurements. The relative stabilities of some metal complexes of thiourea and substituted thioureas have been investigated by means of a potentiometric procedure. Thiourea forms large complex metal cations, which can be precipitated by large anions [18].

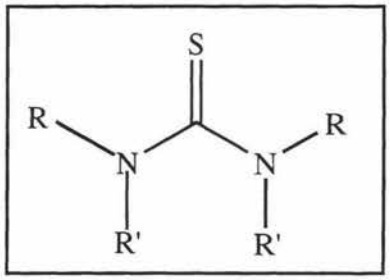

Complexes of N,N'-substituted thioureas, R = alkyl or aryl, R' = alkyl, aryl or H, have also been extensively studied[1].

1.3 Modified Thiourea Ligands

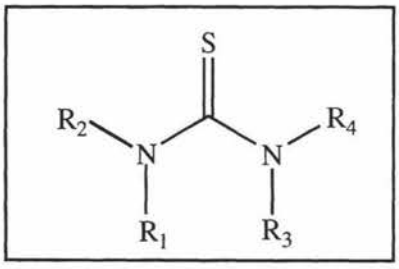

[15] K. Nakamoto, *Infrared Spectra of Inorganic and Coordination Compounds*, 2nd edn., Wiley-InterScience, New York, 1970, p. 210.
[16] J.V. Quagliano and L. Schubert, *Chem. Rev.*, 1952, **50**, 201.
[17] F. Basolo and R.G. Pearson, *Mechanisms of Inorganic Reactions,* Wiley, New York, 1958, p.172.
[18] E. Emmet Reid, *Organic Chemistry of Bivalent Sulfur*, Chemical Publishing Co., Inc., New York, 1963, **5**, 20.

The addition of appropriate moieties, R_1, R_2, R_3 and R_4, to thiourea (above) can modify the thiourea ligand. Interest in these systems commenced about 25 years ago and is continuing today.

1.3.1 1-Benzoyl-3,3-Dialkyl Thioureas and Related Ligands

One of the earliest studies[19] was done on a series of 1-benzoyl-3,3-dialkyl thioureas. The variety of R_3 and R_4 groups used are given in **Table 1.5** along with the complexes formed. In all cases the ligands act as monoanions[19].

Table 1.5 The ligands 1-benzoyl-3,3-disubstituted thioureas (HL) and their complexes with copper(II), nickel(II), palladium(II) and cobalt(III)

Structure	R_3R_4N	Complexes Formed
1-benzoyl-3,3-disubstituted thiourea 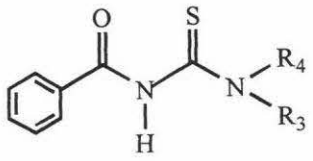	$(CH_3)_2N$	NiL_2 CuL_2 CoL_3
	$(C_2H_5)_2N$	NiL_2 CuL_2 PdL_2 CoL_3
	$(n\text{-}C_3H_7)_2N$	NiL_2 CuL_2 PdL_2 CoL_3
	$(i\text{-}C_4H_9)_2N$	NiL_2 CuL_2 PdL_2 CoL_3
	Morpholino 	NiL_2 CuL_2 PdL_2 CoL_3
	Piperidino 	NiL_2 CuL_2 PdL_2 CoL_3
	Pyrrolidino 	NiL_2 CuL_2 PdL_2 CoL_3

[19] L. Beyer, E. Hoyer, H. Hennig, R. Kirmse, H. Hartmann and J. Liebscher, *J. Prakt. Chem.*, 1975, **317**, 829.

ESR parameters and magnetic moment measurements have shown that 1-benzoyl-3,3-dialkyl thiourea complexes form chelates with transition metals which leads to square planar ML_2 (M = Ni, Cu, Pd) and octahedral CoL_3 compounds as shown below (**Fig. 1.1**). The ligand loses a proton and behaves as a bidentate anion.

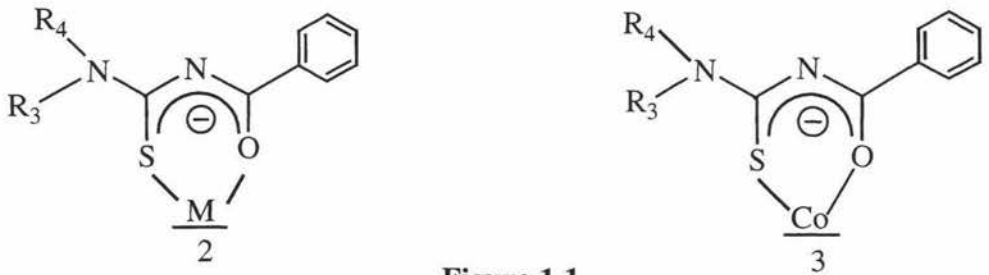

Figure 1.1

This work was followed up by Mohamadou *et al.*[20] nineteen years later and they claimed that the CoL_3 compounds were not very pure and the magnetic moments for the CoL_3 and NiL_2 compounds were abnormal because of purity problems. The ligands used in this study are given below (**Fig 1.2**).

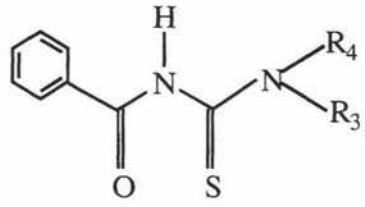

$R_3 = R_4 = CH_3, C_2H_5, n\text{-}C_3H_7, n\text{-}C_4H_9, C_6H_5$

$R_3 = CH_3, R_4 = C_6H_5\text{-}CH_2$ (Bz)

$R_3 = R_4 =$ morpholino 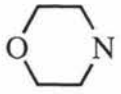

$R_3 = R_4 =$ piperidino 

Figure 1.2

Square planar complexes ML_2 (M = Cu, Ni) and *fac*-CoL_3 were formed, NiL_2 and CoL_3 were now diamagnetic indicating the ligand is a strong chelating agent. The CoL_3 complexes gave analytical compositions a little lower than expected. The authors extended their work to include NMR spectral and electrochemical studies. Reduction of

[20] A. Mohamadou, I. Déchamps-Oliver and J.P. Barbier, *Polyhedron,* 1994, **13**, 1363.

CuL_2 into CuL_2^- has been studied by cyclic voltammetry. **Table 1.6** shows the electrochemical data found for the irreversible Cu(II)/Cu(I) redox systems.

Table 1.6 Electrochemical data for copper compounds

R_3,R_4N-	E^o (V)
$(CH_3)_2N-$	-0.18
$(C_2H_5)_2N-$	-0.25
$(n\text{-}C_3H_7)_2N-$	-0.30
$(n\text{-}C_4H_9)_2N-$	-0.33
$(C_6H_5)_2N-$	-0.15
$CH_3,BzN-$	-0.18
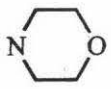	-0.16
	-0.22

From the above data it seems that the nature of the R_3 and R_4 substituent groups has a weak influence on the electrochemical properties of these complexes; even the aromatic or cyclic substituents have the same effect.

Mohamadou *et al.*[21] have extended their studies to 1-substituted benzoyl-3,3-diethyl or 3-morpholine thioureas as below (**Fig. 1.3**).

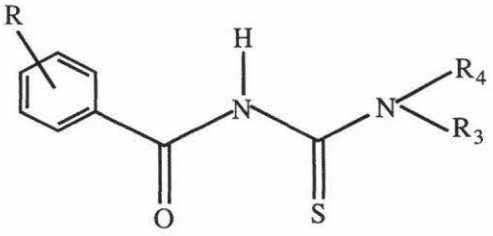

R = Cl, Br, OCH_3 or NO_2 in *ortho, meta and para* positions

Et_2RbtuH, $R_3 = R_4 = C_2H_5$.

morphRbtuH, R_3, R_4 = 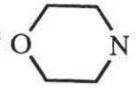

Figure 1.3

[21] A. Mohamadou, I. Déchamps-Olivier and J.P. Barbier, *Polyhedron*, 1994, **13**, 3277.

As before, complexes with copper were of the type CuL_2. Cyclic voltammetry for the irreversible copper(II)/copper(I) redox systems showed that the E^o values for a particular substituent are not influenced by the *ortho, meta* or *para* substituents, but were slightly influenced by the nature of the substituent. The E^o values for the quasi-reversible copper(III)/(II) redox systems are not influenced by the benzoyl substituents.

$$\text{copper(III) complexes} \underset{-e^-}{\overset{+e^-}{\leftrightharpoons}} \text{copper(II) complexes} \underset{-e^-}{\overset{+e^-}{\leftrightharpoons}} \text{copper(I) complexes.}$$

Déchamps-Olivier *et al.*[22] followed up this work and found the same ligands with Co and Ni, gave the square planar compounds NiL_2 and *fac*-CoL_3. Proton NMR and electronic spectral studies were used to characterize these compounds. The analytical compositions for the CoL_3 complexes were a little lower than expected as found before[20]. They explain that this may be due to the difficulty of drying these complexes. Also morpholine and *ortho* substituents on the benzoyl group gave no complexes with Co(III) and this may be due to the generation of strong steric hindrance by these groups.

Koch *et al.*[23] studied the coordinating properties of 1-benzoyl-3-(2-hydroxyethyl) (H_2Z) and 3,3-di(2-hydroxyethyl) thiourea (HY) ligands (**Fig. 1.4**) with platinum group metals such as, Pt(II), Pd(II) and Ni(II).

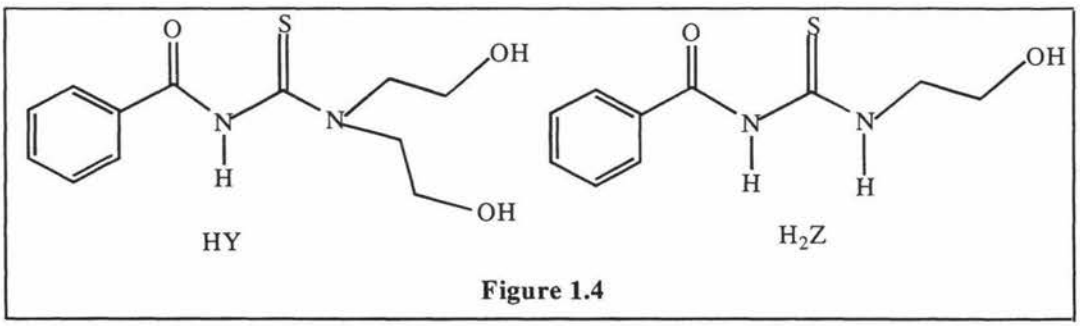

Figure 1.4

[22] I. Déchamps-Olivier, E. Guillon, A. Mohamadou and J. P. Barbier, *Polyhedron,* 1996, **15**, 3617.

[23] K.R. Koch, C. Sacht and S. Bourne, *Inorg. Chim. Acta*, 1995, **232**, 109.

[24] S. S. S. Raj, K. Puviarasan, D. Velmurugan, G. Jayanthi and H.K. Fun, *Acta Cryst.*, 1999, C**55**, 1318.

The ligands HY and H_2Z show remarkably different coordination chemistry to Pt(II), Pd(II) and Ni(II). This behavior is due to H-bonding which makes the H_2Z ligand behave more like a monodentate thiourea ligand since the carbonyl atom is prevented from coordination by an intramolecular hydrogen bond. A mixture of *cis* and *trans* complexes of $[Pt(H_2Z)_2Cl_2]$ with Pt(II) is obtained, whereas the HY ligand coordinates in a bidentate manner forming neutral complexes of the type *cis*-$[M(Y)_2]$ (M = Pt(II), Pd(II) and Ni(II))[23].

Possible intramolecular hydrogen bonding in the H_2Z ligand is depicted below (**Fig. 1.5**)[23] giving a 6-membered ring. This structure is based on a recently published crystal structure of 1-benzoyl-3-(3,4-dimethylphenyl)thiourea[24].

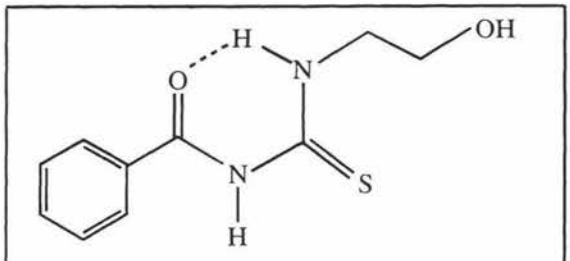

Figure 1.5

The coordination chemistry of this ligand (H_2Z) is strongly influenced by the intramolecular hydrogen bond between the carbonyl atom of the aroyl moiety and the thiourea N-H group on position 3. This favours coordination through the S atom only since O is *trans* to S [25].

In contrast, the free ligand, HY, does not possess a similar thiourea N-H group, but it does contain an intramolecular hydrogen bond between the thiourea N-H group on position 1 and the oxygen atom of one of the hydroxyethyl moieties, forming a 7-membered ring as shown in **Fig 1.6**. The O and S atoms are now *cis* to each other.

---

[25] K.R. Koch and S. Bourne, *J. Chem. Soc., Dalton Trans.*, 1993, 2071.

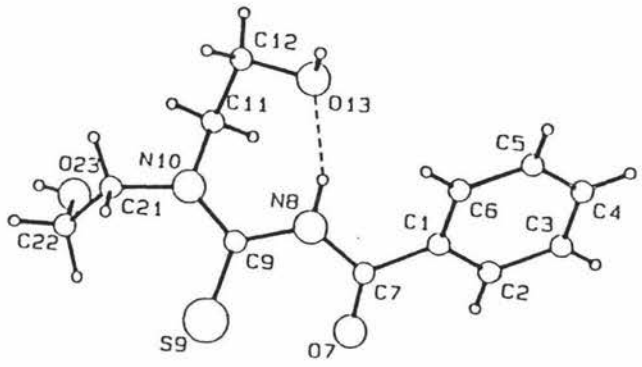

Figure 1.6 Molecular structure of 1-benzoyl-3,3-di(2-hydroxyethyl)thiourea (HY)

Therefore HY is geared up to bind through S and O atoms as a bidentate anion, *via* a loss of an N-H proton.

Koch *et al.*[26] also studied the coordination chemistry of similar ligands based on 1-benzoyl-3-alkyl and 3,3-dialkyl thioureas with the platinum group metals.

Koch *et al.*[27] and Fitzl et al.[28] studied the Pt(II) and Pd(II) complexes of 1-benzoyl-3-propyl thiourea (H_2L) and were able to obtain a crystal structure of *trans*-$[Pd(H_2L)_2Br_2]$ where H_2L binds through S. They have previously shown that the coordination of the 1-benzoyl-3,3-dialkyl thioureas usually leads to very stable bidentate-S,O coordination to Pd(II)[28], Pt(II)[29] and Rh(III)[30].

1.3.2 1-Ethoxycarbonyl- 3-Disubstituted Thiourea

Guillon *et al.*[31] have synthesized the ligands, such as 1-ethoxycarbonyl-3-disubstituted thioureas (**Fig. 1.7**), to study the influence of the substitution of a strong

---

[26] K.R. Koch, C. Sacht, T. Grimmbacher and S. Bourne, *S. Afr. J. Chem.,* 1995, **48**, 71.
[27] K.R. Koch,Y. Wang and A. Coetzee, *J. Chem. Soc., Dalton Trans.,* 1999, 1013.
[28] G. Fitzl, L. Beyer, R. Sieler, R. Richter, J. Kaiser and E. Hoyer, *Z. Anorg. Allg. Chem.,* 1977, **433**, 237.
[29] K.R. Koch, A. Irving and M. Matoetoe, *Inorg. Chim. Acta,* 1993, **206**, 193.
[30] W. Bensch and M. Schuster, *Z. Anorg. Allg. Chem.,* 1992, **615**, 93.
[31] E. Guillon, A. Mohamadou, I. Déchamps-Olivier and J.P. Barbier, *Polyhedron,*1996, **15**, 947.

donor group such as ethoxy for the phenyl ring on the properties of copper, nickel and cobalt complexes.

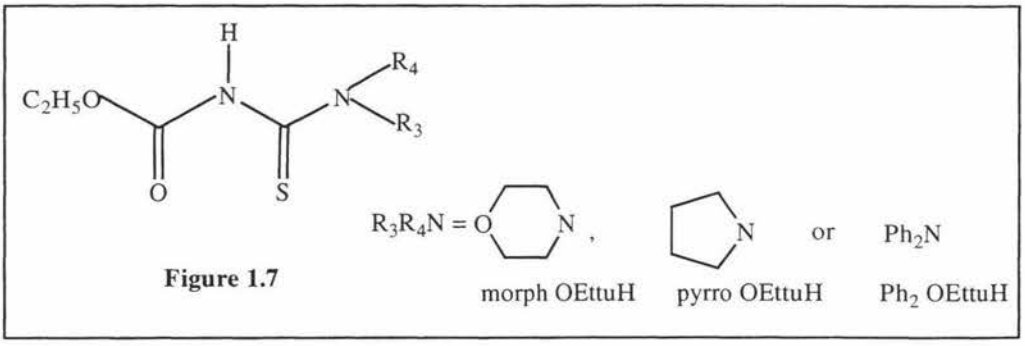

Figure 1.7

NMR spectra and magnetic data support the assignment of a square planar structure for NiL_2 and *fac or mer* structures for CoL_3 compounds. For unsymmetrical bidentate ligands, a single set of ethoxy group resonances for the ^1H NMR spectra is indicative of *fac*-Co(pyrro OEttu)$_3$, while two sets of resonances (intensity ratio 1:2) is obtained for *mer*-CoL_3 (L = morph OEttu or Ph_2 OEttu) as shown in **Fig. 1.8**[20,31]. These studies were confirmed by ^{13}C NMR data.

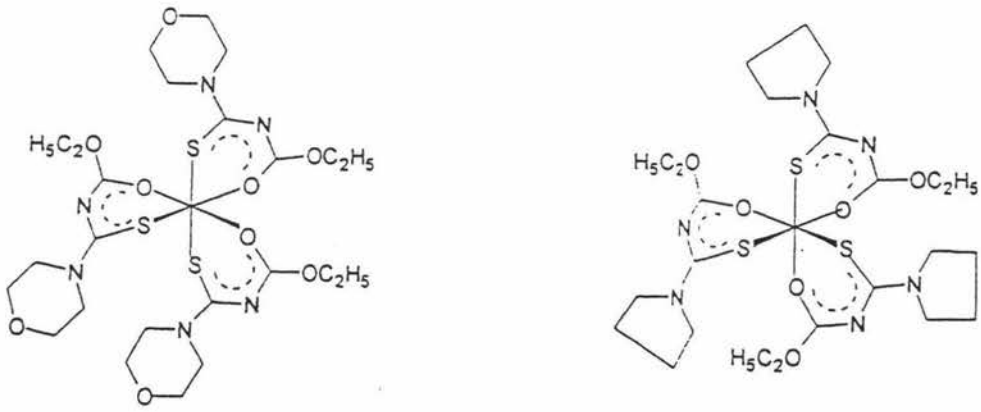

mer-Co(morph OEttu)$_3$ *fac*-Co(pyrro OEttu)$_3$

Figure 1.8

The electronic spectra of the metal complexes are similar to those obtained with 1-benzoyl-3,3-disubstituted thioureas [20]. The existence of copper(III), copper(II) and copper(II), copper(I) redox systems has been chemically and electrochemically determined in solution [31].

1.3.3 1-Benzoyl-3-Substituted Phenyl Thioureas

The previous studies relate to the coordination properties of 1-benzoyl or 1-ethoxy or 1-ethoxycarbonyl moieties with 3-mono or 3,3-disubstituted (aliphatic) thioureas. Recent studies are based on 1-benzoyl-3-unsubstituted[32] or *o*-, *m*- or *p*-substituted-phenyl thiocarbamides[33, 34,35]. **Figure 1.9** summarises the overall structures of some of the latter ligands. Important aspects of their limited coordination chemistry will be reviewed in Chapters 2 and 3.

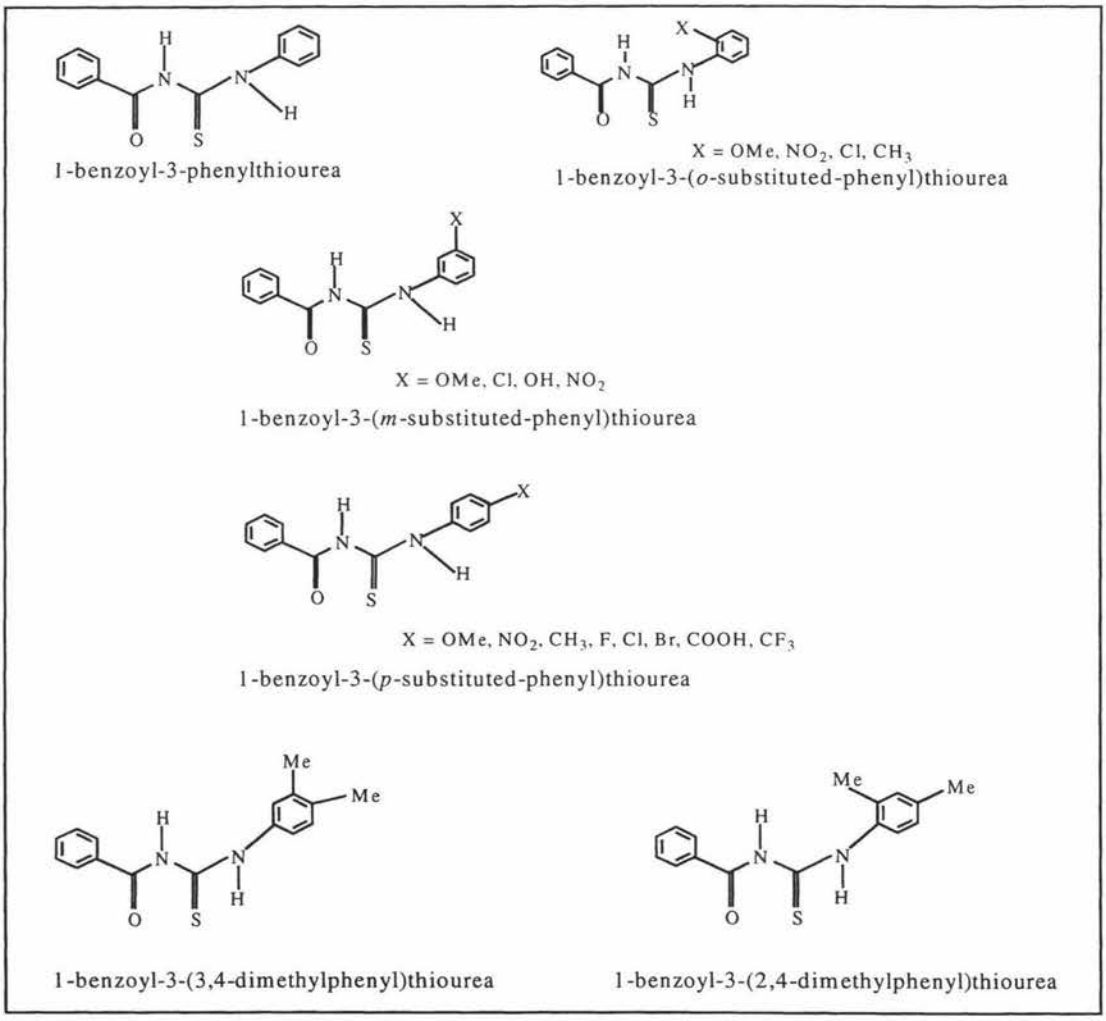

Figure 1.9 1-benzoyl-3-unsubstituted or *o, m* or *p*-substituted-phenyl thiocarbamides.

---

[32] F. Kurzer, *J. Chem. Soc.,* 1949, 3034-3048; R.L. Frank and P.V. Smith, *Org. Synth.,* 1955, Coll. Vol. **3**, 735-736.

[33] K.C. Satpathy and H.P. Mishra, *Indian J. Chem.,* 1981, **20**A, 1035.

[34] J.R. A. Cornejo, M. Valko, G. Ondrejovic and D. Valigura, *Conf. Coord. Chem.,* 1993, 14th (Contributions to Development of Coordination Chemistry), 107.

[35] D. Negoiu, V. Circu, T. Rosu and N. Badicu, *Rev. Chim. (Bucharest),* 1999, **50**, 88.

1.4 Uses of Thiourea Derivatives

While urea is an abundant natural product, thiourea is not although some fungi, under special conditions, produce it[36].

The effects of thiourea on the thyroid gland have been extensively studied with several thiourea derivatives having been found to have strong anti-thyroid activity. This was interpreted as due to the formation of disulfide by the reaction of I_2 with the –SH group (formed by enolization), thus interrupting the synthesis of thyroxine[37].

Thiourea has maximum inhibiting effect on corrosion of iron by acids at 50 mg per liter. It decreases the rate of solution of aluminum in acid by pure water or by potassium chloride solution. Various thiourea derivatives have also been studied in respect to altering the rate of attack of acids on steel and aluminum[38].

Metal complexes with ligands containing sulfur and nitrogen as donor atoms find use as pesticides[39] and fungicides[40,41]. Some of the applications are given below:

- The insecticidal activity of various substituted 1-benzoyl-3-phenyl-2-thioureas is determined by allowing seedcorn maggot larvae (*Hylemya platura*) to feed on lima bean seeds treated with these chemicals[42]. It was found that the most toxic thioureas were those containing a 2,6-difluorobenzoyl moiety combined with a 3,4-dichloro, 4-chloro, 4-trifluoromethyl or 4-nitrophenyl moiety which suggested that electron-withdrawing groups were important in conferring insecticidal activity [42].

---

[36] K.E. Ovcharov, *Compt. Rend. Acad. Sci. U. R. S. S.*, 1937, **16**, 461.
[37] G.M.A. El-Reash, F.I. Taha and G. Gadr, *Transition Met. Chem.*, 1990, **15**, 116.
[38] E.E. Reid, *Organic Chemistry of Bivalent Sulfur*, Chemical Publishing Co., Inc., New York, 1963, **5**, 58.
[39] C.W. Johnson, J.W. Foyner and R.P. Perry, *Antibiotics and Chemotherapy*, 1952, **2**, 636.
[40] H.W. Gansman, C.I. Rhykerd,, H.R. Hinderliter, E.S. Scott and L.F. Audrieth, *Bot. Gazz.*, 1953, **114**, 292.
[41] B.G. Benos, B.A. Gingras and C.H. Bayley, *Appl. Microbiol.*, 1961, **8**, 353.
[42] C.C. Yu, R.J. Kuhr, *J. Agric.Food Chem.*, 1976, **24**, 134.

- The copper(II) complexes of 1-benzoyl-3-*o*-substituted-phenyl thiocarbamides are fungitoxic against *Aspergillus niger, Fusarium oxysporium and Helminthosporium oryzae* [43].
- Thiourea complexes have shown antifungal activity against a major pathogen responsible for important crop damage, *Botrytis cinerea* [44].

Thiourea derivatives can be use as reagents in the solvent extraction of heavy metals. Some examples are given below:

- N-substituted benzoylthioureas are excellent reagents for the solvent extraction of gold [45].
- Cu(II) and 1-phenyl-3-benzoylthiocarbamide form a 1:1 complex that can be extracted with $CHCl_3$ from the aqueous phase at pH 5.8-6.3[46].
- N-mono- and N,N-disubstituted benzoylthioureas are excellent reagents for solvent extraction and have a high selectivity for Pt-group metals [47].
- The liquid-liquid extraction of the metals Pt, Pd, Ru, Rh and Ir with 1-benzoyl-3,3-diethylthiourea can be achieved by optimizing the concentration of acid, mole ratio of metal to chelating agent, temperature and extraction time [48].
- A 1-benzoyl-3-phenylthiourea solution was used for separation and purification of the Pt-group metals and Au from aqueous solutions by precipitation [49].

---

[43] K.C. Satpathy and H.P. Mishra, *Indian J. Chem.* 1981, **20A**, 1035.
[44] E. Rodriguez-Fernandez, E. Garcia, M.R. Hermosa, A. Jimenez-Sanchez, M.M. Sanchez, E. Monte and J.J. Criado, *J. Inorg. Biochem.*, 1999, **75**, 181.
[45] P. Vest, M. Schuster and K.H. Koenig, *Fresenius. J. Anal. Chem.*, 1991, **341,** (9), 566.
[46] V.R. Patil, R.B. Kharat and B.K. Deshmukh, *Chem. Anal. (Warsaw)*, 1984, **29**, 113.
[47] P. Vest, M. Schuster and K.H. Koenig, *Fresenius, Z. Anal. Chem.*, 1989, **335**, 759.
[48] M. Merdivan, R.S. Aygun and N. Kulcu, *Ann. Chim. (Rome)*, 2000, **90**, 407.
[49] D. Hollman, K.H. Koenig, M. Schuster and R. Gerner, *Ger.*, 1988, pp. 3.

- 1-benzoyl-3-(ethanol)thiourea and 1-benzoyl-3-(diethanol)thiourea can be use to extract and determine small amounts of Os in the presence of most of the Pt and common metals[50].
- Substituted thioureas can be use for separation of complexed heavy metals in wastewaters containing inorganic and organic complexing agents, by treatment of wastewater at pH 1-10 and 15-100 °C. Thus, Co(II) was precipitated from wastewater containing complexing agents by addition of 1-benzoyl-3,3-diethylthiourea[51].

Particular interest in the substituted thiourea ligands lies in their use as analytical reagents. For example 1-benzoyl-3-alkyl and 1-benzoyl-3,3-dialkylthioureas can be utilized in the high-performance chromatographic separation and determination of trace levels the platinum group metals[52,53], as well as in the online preconcentration of Pd(II) followed by its determination at ultra-trace level by means of electrothermal atomic absorption spectroscopy[54].

Thiourea derivatives, such as 1-benzoyl-3-(3,4-dimethylphenyl)thiourea and 1-benzoyl-3-methyl-3-phenylthiourea, have applications as rubber accelerators and as intermediate materials in dye preparation, and are very useful agrochemical intermediates. Recently, these derivatives were found to possess non-linear optical properties[24].

Bayón *et al.*[55] has shown that the thiourea-functionalized siloxane materials can be used as catalysts.

1.5 The Present Study

In Section 1.3 the coordination chemistry of simple 1-benzoyl-3-alkyl or unsubstituted or substituted-phenylthiourea or 3,3-dialkylthiourea ligands was reviewed.

---

[50] S.K. Bhowal, *Indian J. Chem.*, 1975, **13**, 92.
[51] M. Schuster, K.H. Koenig, H. Lotter and K. Drauz, *Ger. Offen.*, 1990, pp. 4.
[52] K.-H. König, M. Schuster, B. Steinbrech, G. Schneeweis and R. Schlodder, *Fresenius Z. Anal. Chem.*, 1985, **321**, 457; M. Schuster, *Fresenius Z. Anal. Chem.*, 1986, **324**, 127.
[53] M. Schuster, *Fresenius Z. Anal. Chem.*, 1992, **342**, 791.
[54] M. Schuster and M. Schwarzer, *Anal. Chim. Acta*, 1996, **328**, 1.
[55] J.C. Bayón, C. Claver and A.M. Masdeu-Bultó, *Coord. Chem. Rev.*, 1999, **193**, 73.

The ligand which is the focus of the research in this thesis is 1-benzoyl-3-(2,4,6-tri-*tert*-butylphenyl)thiourea (Bz^{t}BPtuH) (**Fig. 1.10**). The use of bulky anilino groups in ligands attached to metals has produced some interesting catalytic systems[56] and hence it was decided to study the fundamental chemistry of Bz^{t}BPtuH and compare it with the unsubstituted analogue. Bulky ligands of the type Bz^{t}BPtuH have not been studied before. As well as Bz^{t}BPtuH, other bulky and non-bulky ligands were studied, and these are given in **Fig. 1.11**.

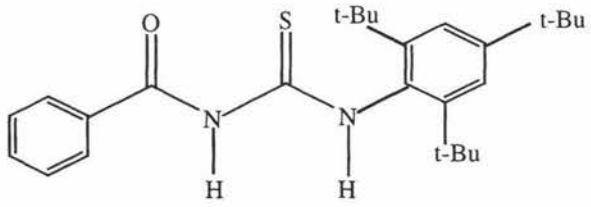

Figure 1.10 1-benzoyl-3-(2,4,6-tri-*tert*-butylphenyl)thiourea [**Bz^{t}BPtuH**]

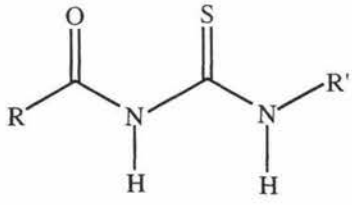

Figure 1.11

Where R is a phenyl group and

R' = 2,4,6-tri-phenyl (**BzPPtuH**), 2,6-diisopropylphenyl (**Bz^{i}PPtuH**), 4-fluorophenyl (**BzFPtuH**) or phenyl (**BzPtuH**).

These ligands may exist in various tautomeric forms and possible structures are shown for the unsubstituted phenyl ligand in **Fig. 1.12**.

On the basis of IR spectra the tautomeric forms (b), (d) and (c) are unlikely because of the absence of the ν(S-H) stretch in (b) and (d) and the ν(O-H) stretch in (c), suggesting that the ligand exists mainly in the form (a)[43] as found for H_2Z (**Fig. 1.5**).

[56] S.D. Ittel, L.K. Johnson and M. Brookhart, *Chem. Rev.*, 2000, **100**, 1169.

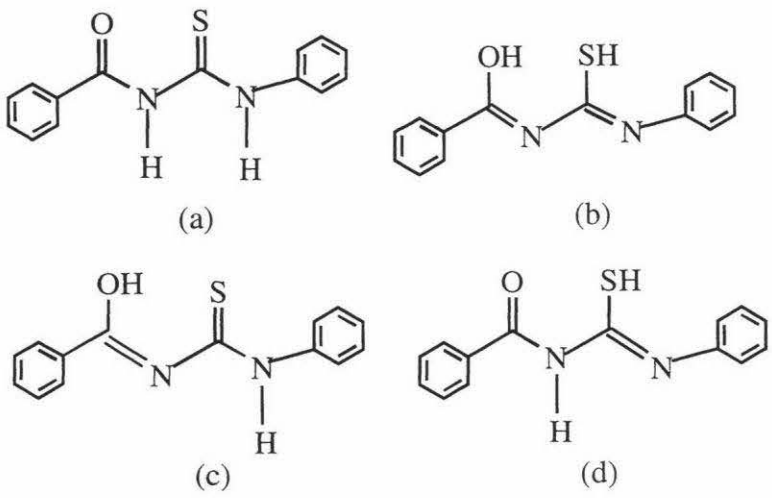

Figure 1.12 Possible Tautomeric Forms

This study aims to investigate:

(i) the synthesis and characterisation of bulky 1-benzoyl-3-substituted, phenylthiourea ligands,

(ii) the mode(s) of coordination of Bz^{t}BPtuH and related ligands to various metals,

(iii) the stoichiometry, coordination number, geometry of the metal centre and structure of the complexes,

(iv) the influence of the phenyl substituents (electronic effect, steric constraints, etc.) on the metallic complexes,

(v) the stability of the Cu^{2+} complexes towards reduction,

(vi) the ability of Bz^{t}BPtuH and related ligands to react with halogens (eg. I_2 and Br_2),

(vii) the reactivity of Bz^{t}BPtuH and related ligands towards metal acetates in different solvents.

The ligands contain both amide and thioamide linkages and possess 'soft' S atoms and 'hard' O and N atoms[14]. The modes of coordination of bulky thiourea ligands are unknown, but it should be possible to bind in neutral and anionic forms. In the neutral form it can bind from S, O, N or O and S, while in the anionic form it can bind from O and S or N. In this latter form it is a bidentate monoanionic ligand (**Fig. 1.13**).

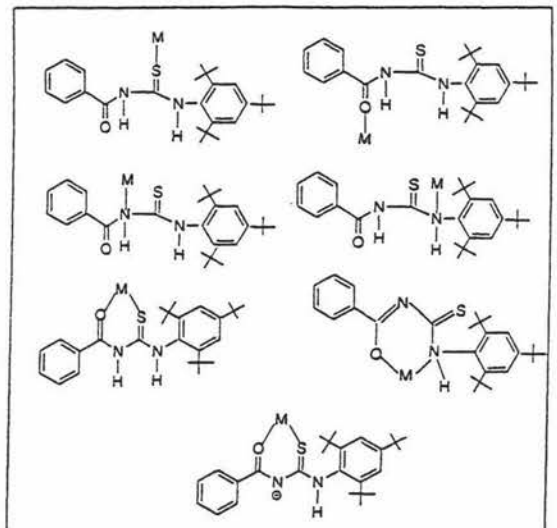

Figure 1.13 Some Possible Modes of Coordination (with respect to Bz^{t}BPtuH ligand)

An additional feature of these bulky ligands and their complexes is the enhanced solubility expected in organic solvents thus increasing the possibility of growing crystals. No X-ray structures have been reported for complexes of the parent ligand 1-benzoyl-3-phenylthiourea.

The thesis will be divided as follows:

- **Chapter 2** will describe the synthesis and characterisation of bulky 1-benzoyl-3-substituted, phenylthiourea ligands and discuss the reactivity, stoichiometry, coordination number, geometry and the structure of Cu(II) and Cu(I) complexes with these ligands, as well as those with Ag(I), Ni(II) and Co(II).

- **Chapter 3** will discuss the reactions of Bz^{t}BPtuH and related ligands towards metal acetates of Hg(II), Zn(II) and Cd(II) and UO_2^{2+} in various solvents.

- **Chapter 4** investigates the coordination chemistry and reactivity of Bz^{t}BPtuH and related ligands with halogens (e.g. I_2 and Br_2).

- **Chapter 5** describes a selected aspect of rhodium(I) chemistry, with emphasis on the synthesis of [Rh(COD)(Bz^{t}BptuH)Cl] and an NMR study of the olefin (alkene) site interchange of COD, as well as the coordination chemistry of the Bz^{t}BPtuH ligand with platinum(II).

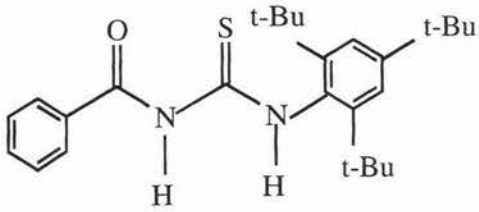

Bz^{t}BPtuH

1-benzoyl-3-(2,4,6-tri-*tert*-butylphenyl)thiourea

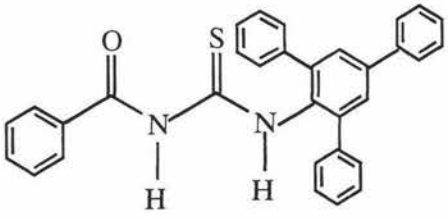

BzPPtuH

1-benzoyl-3-(2,4,6-tri-phenylphenyl)thiourea

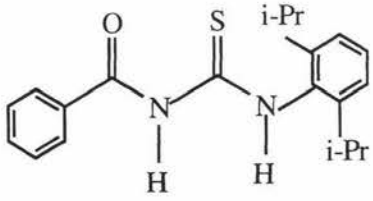

Bz^{i}PPtuH

1-benzoyl-3-(2,6-diisopropylphenyl)thiourea

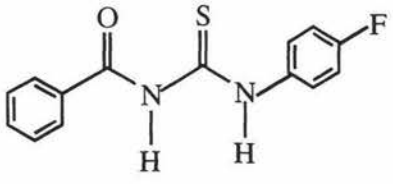

BzFPtuH

1-benzoyl-3-(4-fluorophenyl)thiourea

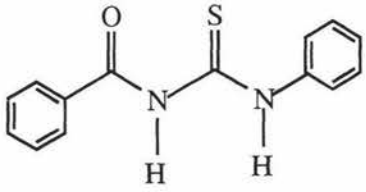

BzPtuH

1-benzoyl-3-phenylthiourea

Structures, Names and Abbreviations for the Ligands in Chapter Two

CHAPTER TWO

Synthesis of 1-Benzoyl-3-(2,4,6-tri-*tert*-butylphenyl)thiourea and Related Ligands and a Study of their Coordination Properties with Cu(II), Cu(I), Ag(I), Ni(II) and Co(II) Salts

2.0 INTRODUCTION

In this chapter the synthesis and characterisation of 1-benzoyl-3-(2,4,6-tri-*tert*-butylphenyl)thiourea (**Bz^{t}BPtuH**) and 1-benzoyl-3-(2,4,6-triphenylphenyl)thiourea (**BzPPtuH**) will be discussed. The reason for studying these new bulky systems has been given in **Section 1.5**. As well limited studies will be performed with the known compounds 1-benzoyl-3-(2,6-diisopropylphenyl)thiourea (**Bz^{i}PPtuH**)[1], 1-benzoyl-3-(4-fluorophenyl)thiourea (**BzFPtuH**)[2] and 1-benzoyl-3-phenylthiourea (**BzPtuH**)[3]. All the ligands have been prepared in a similar way according to the method described in the literature for BzPtuH[3].

The interactions of BzPtuH and Bz^{i}PPtuH with copper salts have been studied. Ibrahim[4] synthesised and characterized $[M(LH)Cl_2]$ (M = Cu, Ni, Co, Cd; LH = BzNHC(S)NHR, R = Ph, benzyl, naphthyl) and $[M(LH)_2]Cl_2$ (M = Ni, Cu; LH = BzNHC(S)NHPh] by elemental analyses, IR and electronic spectra as well as conductivity measurements. A tetrahedral or square planar geometry is proposed for the synthesised chelates[4].

---

[1] K. McBeth, 1999, Third Year Research Report, Massey University.
[2] E. Schroepl and R. Pohloudek-Fabini, *Pharmazie*, 1968, **23**, 484.
[3] F. Kurzer, *J. Chem. Soc.*,1949, 3034-3048; R.L. Frank and P.V. Smith, *Org. Synth.*, 1955, Coll. Vol. **3**, 735-736.
[4] S.A. Ibrahim, *Bull. Fac. Sci. Assiut Univ.*, 1991, **20**, 147.

Satpathy *et al.*[5] have isolated Cu(II) complexes of 1-benzoyl-3-(*o*-substituted and unsubstituted-phenyl)thioureas having the composition, $[Cu(HL)_2X_2]$, (where HL = 1-benzoyl-3-phenylthiourea and its 3-*o*-substituted OMe, NO_2 and Cl derivatives, X = Cl^-, Br^-, NO_3^-, ClO_4^- and SCN^-). They postulated these ligands to be bound through their O and S atoms and suggested an octahedral geometry for the complexes.

Similar studies were done by Cornejo *et al.*[6] with $C_6H_5C(O)NHC(S)NHR$ (R = *p*-C_6H_4COOH, *p*-C_6H_4OMe, Ph, *m*- C_6H_4OH, -CH_2-C_6H_5 and -CH_2-CH_3) ligands and 1:1 ratio of Cu(II) to ligand was observed for all complexes. From the stoichiometry and spectral properties of the complexes deprotonation from the N-H of the ligands was suggested.

Negoiu *et al* [7] prepared $[M(HL)_2Cl_2]$ (M = Pt and Hg; HL = 1-benzoyl-3-2,4-dimethylphenylthiourea) and $[ML_2]$ (M = Cu, Ni, Pd, Cd) complexes and characterized them EPR, IR and electronic spectroscopy. The geometry of the complexes was square-planar for Cu(II), Ni(II), Pt(II), Pd(II) and tetrahedral for Cd(II) and Hg(II). In the $[M(HL)_2Cl_2]$ complexes, the ligand acts as monodentate, being S-bonded to the metal ion while in the $[ML_2]$ complex, both S and O are bonded to the metal ion.

Bis(thiourea)silver(I) Chloride, $[(Ag(tu)_2Cl)]$, was first reported by Nardelli[8] and these studies were further extended by Vizzini *et al.*[9] who determined the crystal structure. The structure of $[Ag(tu)_2Cl]$ is composed of almost trigonal-planar $Ag(S)_3$ units bonded together by S bridges to form a spiraling linear polymer. As well, Udupa *et al.*[10] determined the crystal structure of tris(thiourea)silver(I) perchlorate which consists of binuclear $[(Ag_2(tu)_6)]^{2+}$ cations with C_2 symmetry and perchlorate anions.

In the above studies, apart from silver, structures have been proposed from infrared spectroscopy. Little information is available about the structures of the Co, Ni and Ag complexes. My aim will be to explore the chemistry of these metals with the

---

[5] K.C. Satpathy and H.P. Mishra, *Indian J. Chem.*, 1981, **20**A, 1035.
[6] J.R. Angulo Cornejo, M. Valko, G. Ondrejovic and D. Valigura, *Conf. Coord. Chem.*, 1993, 14th (Contributions to Development of Coordination Chemistry), 107.
[7] D. Negoiu, V. Circu, T. Rosu and N. Badicu, *Rev. Chim. (Bucharest)*, 1999, **50**, 88.
[8] M. Nardelli and A. Braibanti, *Gazz. Chim. Ital.*, 1957, **87**, 907.
[9] E.A.Vizzini, I.F. Taylor and E.L. Amma, *Inorg. Chem.*1968, **7**, 1351.
[10] M.R. Udupa and B. Krebs *Inorg. Chim. Acta*,1973, **7**, 271.

ligands **Bz^{t}BPtuH, BzPPtuH, Bz^{i}PPtuH, BzFPtuH** and **BzPtuH**, to confirm the above formulations for the copper complexes and to establish the structures of some of the complexes. Apart from BzPtuH and Bz^{i}PPtuH, no work has been done with the related ligands in this study.

2.1 Experimental

2.1.1 Instrumentation

All ^{1}H and ^{13}C NMR spectra were obtained in 5 mm tubes using a Bruker Avance 400 MHz spectrometer at 25 °C using $CDCl_3$ as solvent and TMS as internal standard.

Infrared (IR) spectra were carried out with a FT-IR Perkin-Elmer Paragon 1000 spectrometer as nujol mulls between NaCl discs.

Magnetic susceptibilities were determined by the Faraday method at room temperature using a Cahn Electrobalance model no. 7550.

The ESR spectra were recorded on a Varian E-104A ESR spectrometer at −160 °C using acetone as a solvent.

Electronic spectra were recorded using a Shimadzu UV-160 spectrophotometer on both solid and solution samples.

Melting points was determined using a Reichert hot-stage melting point apparatus.

Mass spectra were obtained using a Varian VG70-250S double-focusing magnetic sector spectrometer by the method of liquid secondary ion mass spectroscopy (LSIMS) using *m*-nitrobenzyl alcohol as the matrix by courtesy of John M. Allen, Mass Spectroscopy Unit, Hort. Research. Isotope abundance calculations were performed to identify the parent ion.

The Campbell Microanalytical Laboratory, University of Otago, Dunedin, carried out elemental analyses for carbon, hydrogen, nitrogen and sulfur.

2.1.2 Materials

All solvents and metal salts were laboratory grade quality, obtained from commercial suppliers and used without further purification. Ammonium thiocyanate

was obtained from AJAX Chemical Ltd.; benzoyl chloride, ethanol, cobalt(II) chloride hexahydrate and copper(II) acetate monohydrate from BDH Ltd.; 2,4,6-tri-*tert*-butylaniline, 2,4,6-tri-phenylphenylaniline, 4-fluoroaniline, aniline and copper(II) bromide from Aldrich Chemical Co Ltd. The ligand 1-benzoyl-3-(2,6-diisopropylphenyl)thiourea was synthesised by McBeth[1]. Acetone was obtained from Riedel deHaen Ltd; copper(II) chloride dihydrate and silver chloride from Hopkin and Williams; nickel(II) iodide hexahydrate from Johnson Matthey, acetonitrile from May and Baker; chloroform from Labscan Ltd.; dichloromethane from ASP Finechem Ltd.; hexane and diethyl ether were reagent-grade quality. $[Cu^{I}(CH_3CN)_4]PF_6$ and $[Ag(CH_3CN)_4]PF_6$ was prepared by an established method[11] and stored under nitrogen over silica gel. Acetone was dried over anhydrous magnesium sulphate.

2.1.3 Preparation of Ligands

2.1.3.1 1-Benzoyl-3-(2,4,6-tri-*tert*-butylphenyl)thiourea, Bz^{t}BPtuH

The ligand Bz^{t}BPtuH was prepared according to the method described in the literature for BzPtuH[3].

Benzoyl chloride (2ml, 2.4178g, 17.2 mmol) was added dropwisely *via* a dropping funnel with constant stirring to ammonium thiocyanate (2.1300g, 28 mmol) dissolved in dry acetone (~12ml) in a three necked flask (500ml). After the addition was complete the mixture was heated to reflux with stirring in an oil bath for 5 min at 75-80 °C and a solution of 2,4,6-tri-*tert*-butylaniline (4.5g, 17.2 mmol) in dry acetone (20ml) was added dropwise, while maintaining refluxing. The mixture was subsequently poured into water (1.0 l) with stirring and left sealed over night in a fume hood. The yellow precipitate was filtered and air-dried to give 7.414g of crude product, which was recrystallised from warm chloroform. Fine white flakes were isolated by vacuum filtration, washed well with hexane, and dried in *vacuo* to give 4.64g, 63.6% yield, m.p. 149-150 °C. Anal. Found: C, 69.93; H, 8.07; N, 6.31; S, 7.69%. Calculated for $C_{26}H_{36}N_2OS.¼\ CHCl_3$: C, 69.40; H, 7.99; N, 6.17; S, 7.05%.

The product recrystallised from ethanol gave a m.p. 151-154 °C. Anal. Found: C, 73.50; H, 8.66; N, 6.61; S, 7.36%. Calculated for $C_{26}H_{36}N_2OS$: C, 73.58; H, 8.49; N, 6.60; S, 7.55%.

---

[11] G.J. Kubas, *Inorg. Synth.*, 1979, **19**, 90.

Crystals suitable for X-ray analysis were grown by slow evaporation from ethanol. The equations for the synthesis of Bz^{t}BPtuH are given below.

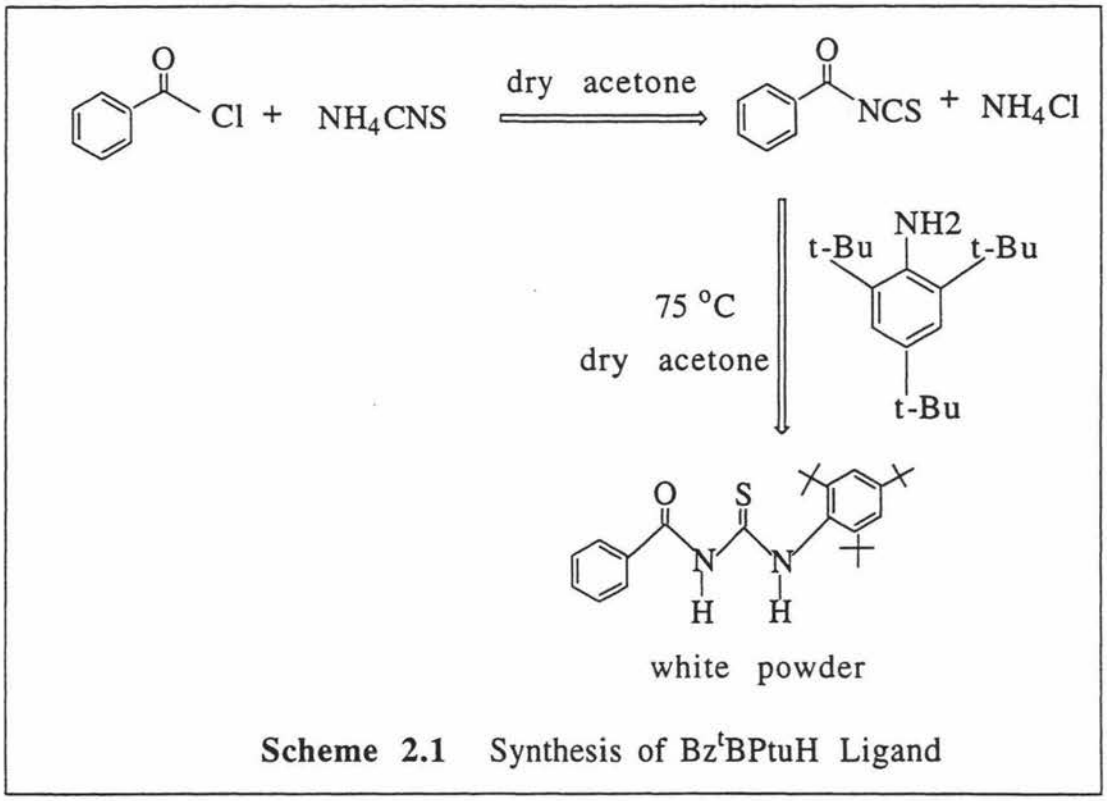

Scheme 2.1 Synthesis of Bz^{t}BPtuH Ligand

2.1.3.2 1-Benzoyl-3-(2,4,6-triphenylphenyl)thiourea, BzPPtuH

This ligand synthesis was based on the above method, which involved first converting benzoyl chloride to benzoyl isothiocyanate and then the condensation with 2,4,6-triphenylphenylaniline. The yellow crude product was recrystallized from hot ethanol-dichloromethane (1:1, v/v) and isolated by filtration, washed well with ethanol solution and dried in *vacuo* to give 4.40g, 73% yield, m.p. 189-191°C. Found: C, 78.66; H, 4.81; N, 6.05; S, 6.47%. Calculated for $C_{32}H_{24}N_2OS.1/10\ CH_2Cl_2$: C, 78.21; H, 4.91; N, 5.68; S, 6.49%.

The ligand 1-benzoyl-3-(2,6-diisopropylphenyl)thiourea (Bz^{i}PPtuH) was synthesised by McBeth[1], yield ~ 50%, m.p. is 188-189.5 °C.

The ligands, 1-benzoyl-3-(4-fluorophenyl)thiourea (BzFPtuH) and

1-benzoyl-3-phenylthiourea (BzPtuH), were also synthesised according to the same method described above with yields and m.p. 37%, 117-120 °C (128-9.5 °C)[12] and 44%, 126-127 °C (148-9 °C)[12] respectively. Variations from literature melting points may be due to presence of two isomers.

2.1.4 Preparation of Metal Complexes

[Cu(Bz^{t}BPtu-κ^2S,O)$_2$]

To Bz^{t}BPtuH 0.1000g (0.2358 mmol) dissolved in ~5 ml of ethanol, was added 0.0235g (0.1177 mmol) of copper(II) acetate monohydrate in ~5 ml of ethanol. This reaction mixture was warmed for a few seconds and the flask scratched after cooling to room temperature. The resulting fine dark green powder was filtered and washed with ethanol and dried in air. Yield, 0.0089g (8%). Anal. Found: C, 68.43; H, 7.68; N, 6.18; S, 6.41%. Calculated for $C_{52}H_{70}CuN_4O_2S_2$: C, 68.61; H, 7.70; N, 6.16; S, 7.04%.

[Cu(Bz^{i}PPtu-κ^2S,O)$_2$] was synthesised by McBeth[1] according to the same method as above.Yield, 0.0810g (29%). Anal. Found: C, 59.43; H, 5.72; N, 7.09; S, 8.08%. Calculated for $C_{40}H_{46}CuN_4O_2S_2.3.5H_2O$: C, 59.66; H, 6.58; N, 6.96; S, 7.96%.

[Cu(Bz^{t}BPtuH-κ^1S)$_2$Cl$_2$]

A solution of $CuCl_2.2H_2O$ (0.0402g, 0.2358 mmol) in ethanol (~5 ml) was added to a solution of Bz^{t}BPtuH (0.100g, 0.2358 mmol) in ethanol (~5 ml). The resultant mixture was kept in room temperature. The reddish brown fine powdery product that formed was filtered, washed with ethanol and air-dried to give 0.0600g (26%). Anal. Found: C, 63.41; H, 7.73; N, 5.63; S, 7.42%. Calculated for $C_{52}H_{72}Cl_2$ $CuN_4O_2S_2$: C, 63.51; H, 7.33; N, 5.70; S, 6.51%.

Attempted synthesis of *[Cu(Bz^{t}BPtuH)$_2$Cl$_2$]* complex

This was synthesised according to the same method as above. The product that formed was unstable with respect to its transformation to the Cu(I) complex, and hence it could not be analysed. Its electronic spectrum was similar to the [Cu(Bz^{t}BPtuH-κ^1S)$_2$Cl$_2$] complex, suggesting it has the same stoichiometry and structure.

---

[12] E. Schroepl and R. Pohloudek-Fabini, *Pharmazie*, 1968, **23**, 484.

[Cu(Bz^{t}BPtuH-κ^1S)$_2$Cl]

A solution of $CuCl_2.2H_2O$ (0.0213g, 0.1249 mmol) in acetone (~5 ml) was added to a solution of Bz^{t}BPtuH (0.1060g, 0.2500 mmol) in acetone (~5 ml). The reddish brown solution was left to stand and after a week, pale yellow crystals suitable for X-ray analysis were isolated. These were washed with ethanol and air-dried to yield 0.0450g, 38%. Anal. Found: C, 66.09; H, 8.15; N, 5.80; S, 6.56%. Calculated for $C_{52}H_{72}ClCuN_4O_2S_2$: C, 65.89; H, 7.60; N, 5.91; S, 6.76%.

The reaction goes equally well if the acetone is replaced by ethanol. Yield 0.0320g, 34%.

[Cu(BzPPtuH-κ^1S)$_2$Cl]

A solution of $CuCl_2.2H_2O$ (0.0852g, 0.4997 mmol) in ethanol (~3 ml) was added to a solution of Bz^{t}BPtuH (0.484g, 1.000 mmol) in dichloromethane (~15 ml). The resultant dark reddish brown solution was left to cool and the green yellow complex was filtered off and washed with ethanol. Yield 0.4196g (79%), m.p 148-150.6 °C. Anal. Found: C, 72.95; H, 4.71; N, 5.31; S, 5.98%. Calculated for $C_{64}H_{48}ClCuN_4O_2S_2$: C, 72.05; H, 4.50; N, 5.25; S, 6.00%. Crystals suitable for X-ray analysis were grown by recrystallisation from CH_2Cl_2/pentane.

[Cu(Bz^{i}PPtuH-κ^1S)$_2$Cl]

A solution of $CuCl_2.2H_2O$ (0.0850g, 0.4986 mmol) in ethanol (~5 ml) was added to a solution of Bz^{i}PPtuH (0.3400g, 1.000 mmol) in ethanol (~5 ml). The reddish brown product, which formed immediately, was left in the solvent at room temperature. After 4 days, a dark yellow product was isolated, washed with ethanol and air-dried to give 0.1500g, 39%. Anal. Found: C, 61.45; H, 6.38; N, 7.32; S, 8.01%. Calculated for $C_{40}H_{48}ClCuN_4O_2S_2$: C, 61.6; H, 6.16; N, 7.18; S, 8.21%.

[Cu(BzFPtuH-κ^1S)$_2$Cl]

A solution of $CuCl_2.2H_2O$ (0.1704g, 1.000 mmol) in ethanol (~5 ml) was added to a solution of BzFPtuH (0.2740g, 1.000 mmol) in ethanol (~5 ml). The reddish brown product, which formed at once, turned to a dark yellow pulp-like precipitate on further addition of excess $CuCl_2$. The resulting precipitate was filtered, washed with ethanol and air-dried to give 0.0768g, 12%. Anal. Found: C, 51.83; H, 3.46; N, 8.71; S, 9.91%. Calculated for $C_{28}H_{22}ClCuF_2N_4O_2S_2$: C, 51.93; H, 3.40; N, 8.65; S, 9.89%.

[Cu(BzFPtuH-κ^{1}S)$_2$Br]

A solution of anhydrous $CuBr_2$ (0.2235g, 1.000 mmol) in ethanol (~5 ml) was added to a solution of BzFPtuH (0.2740g, 1.000 mmol) in ethanol (~5 ml). The pale yellow thick precipitate, which formed at once was filtered, washed with ethanol to give 0.2500g, 36%. The complex was not analysed since its IR spectrum and colour was similar to $[Cu(BzFPtuH)_2Cl]$.

[Cu(BzPtuH-κ^{1}S)$_3$Cl]

A solution of $CuCl_2.2H_2O$ (0.0852g, 0.4997 mmol) in ethanol (~5 ml) was added to a solution of BzPtuH (0.2560g, 1.000 mmol) in ethanol (~5 ml). The yellow precipitate, which formed at once, was filtered and recrystallized from chloroform-acetone (1:1, v/v) to yield a yellow powder, which were collected by filtration. Yield 0.0800g, 26%. Anal. Found: C, 58.09; H, 4.25; N, 9.82; S, 11.16%. Calculated for $C_{42}H_{36}ClCuN_6O_3S_3$: C, 58.13; H, 4.15; N, 9.69; S, 11.07%.

[Cu(Bz^{t}BPtuH-κ^{1}S)$_4$]PF$_6$

To a solution of Bz^{t}BPtuH (0.1696g, 0.4000 mmol) in acetonitrile (10 ml) was added $[Cu(CH_3CN)_4]PF_6$ (0.0372g, 0.1000 mmol) in acetonitrile (10 ml). The resulting yellow cloudy solution was gently heated. The silvery white complex was filtered, washed with hot acetonitrile to give a pale yellow powder. Yield: 0.0484g, 25%. Anal. Found: C, 65.20; H, 7.66; N, 6.27; S, 6.56%. Calculated for $C_{104}H_{144}CuF_6N_8O_4PS_4$: C, 65.52; H, 7.56; N, 5.88; S, 6.72%.

[Cu(Bz^{i}PPtuH-κ^{1}S)$_4$]PF$_6$

To a solution of Bz^{i}PPtuH (0.2720g, 0.8000 mmol) in acetonitrile (10 ml) was added $[Cu(CH_3CN)_4]PF_6$ (0.0745g, 0.2000 mmol) in acetonitrile (10 ml). The resulting yellow cloudy solution was gently heated, then diethyl ether was added until a white precipitate formed which was filtered off and washed with diethyl ether. Yield 0.0540g, 17%. Anal. Found: C, 61.28; H, 6.12; N, 7.32; S, 8.16%. Calculated for $C_{80}H_{96}CuF_6N_8O_4PS_4$: C, 61.20; H, 6.12; N, 7.14; S, 8.16%.

[Ni(Bz^{t}BPtuH-κ^{1}S)$_2$I$_2$]

To Bz^{t}BPtuH 0.2000g (0.4717 mmol) dissolved in ~5 ml of ethanol, was added 0.1980g (0.4708 mmol) of $NiI_2.6H_2O$ in ~5 ml of ethanol. The resulting solution

was warmed gently for 0.25 h maintaining the volume at 10 ml. The brown yellow powder was filtered and washed with ethanol and dried in air. Yield, 0.0900g (16%). Anal. Found: C, 53.65; H, 6.44; N, 4.89; S, 5.21%. Calculated for $C_{52}H_{72}I_2N_4NiO_2S_2$: C, 53.77; H, 6.20; N, 4.82; S, 5.51%.

Crystals suitable for X-ray analysis were grown by slow evaporation of the filtrate. The result of this analysis will be discussed in Chapter 4.

[Co(Bz^{t}BPtuH-κ^1S)$_2$Cl$_2$]

To Bz^{t}BPtuH 0.1060g (0.2500 mmol) dissolved in ~5 ml of ethanol, was added 0.0595g (0.2500 mmol) of $CoCl_2.6H_2O$ in ~5 ml of ethanol. The resulting solution was warmed gently and left to stand at room temperature. After one day, blue crystals of the product were collected and washed with ethanol. Yield, 0.0300g (12%). Anal. Found: C, 63.83; H, 7.50; N, 5.77; S, 6.35%. Calculated for $C_{52}H_{72}Cl_2CoN_4O_2S_2$: C, 63.80; H, 7.36; N, 5.72; S, 6.50%.

Attempted synthesis of *[Ag(Bz^{t}BPtuH)$_2$Cl]*

To a solution of Bz^{t}BPtuH 0.0848g (0.2000 mmol) in ~7 ml of ethanol was added a suspension 0.0143g (0.1000 mmol) of AgCl in ~10 ml of ethanol. This reaction mixture was refluxed for 1 hour, then the resulting solution was reduced to dryness by rotary evaporation and the white oil formed was triturated in 1:10 (v/v) ethanol/petroleum spirit. The white product, which formed, was filtered, washed with ethanol/petroleum spirit (1:10, v/v). Yield, 0.0267g, m.p. 139-140 °C. It was found by mass spectroscopy that no single pure compound could be isolated.

[Ag(Bz^{t}BPtuH-κ^1S)$_4$]PF$_6$

To a solution of Bz^{t}BPtuH (0.1696g, 0.4000 mmol) in acetonitrile (10 ml) was added $[Ag(CH_3CN)_4]PF_6$ (0.0417g, 0.1000 mmol) in acetonitrile (10 ml). The resulting white cloudy solution was gently heated until the complex precipitated. The yellow precipitate, which formed, redissolved upon heating. The volume of the resulting solution was reduced using a rotary evaporator and diethyl ether was added until a precipitate occurred. The white fine complex was filtered, and washed with diethyl ether. Yield, 0.0990g, 51%, m.p. 194-196 °C. Anal. Found: C, 63.55; H, 7.24; N, 5.85; S, 6.41%. Calculated for $C_{104}H_{144}AgF_6N_8O_4PS_4$: C, 64.03; H, 7.39; N, 5.75; S, 6.57%.

[Ag(Bz^{i}PPtuH-κ^1S)$_4$]PF$_6$

To a solution of Bz^{i}PPtuH (0.1360g, 0.4000 mmol) in acetonitrile (10 ml) was added [Ag(CH$_3$CN)$_4$]PF$_6$ (0.0417g, 0.1000 mmol) in acetonitrile (10 ml). The pale yellow solution which formed at once was reduced in volume using a rotary evaporator and diethyl ether was added until a white precipitate formed which was filtered off and washed with diethyl ether. Yield 0.1000g, 62%, m.p. 178-179 °C. Anal. Found: C, 58.41; H, 5.95; N, 7.05; S, 7.74%. Calculated for $C_{80}H_{96}AgF_6N_8O_4PS_4$: C, 59.52; H, 5.95; N, 6.94; S, 7.93%.

2.2 Results and Discussion

2.2.1 Synthesis and Characterization of the Ligands

2.2.1.1 Synthesis of the Ligands

The new ligands were prepared as described in the experimental Section **2.1.3** with yields ranging from 37 to 73%. The microanalytical data is in agreement with the expected formulations.

2.2.1.2 Infra Red Spectra and Mass Spectral Results

The ligands have characteristic IR spectra with a strong peak in the range 1667-1673 cm^{-1} (see **Table 2.1**). This peak can be assigned to the ν(C=O) stretching frequency of the benzoyl moiety. However, the repeat synthesis of the Bz^{t}BPtuH ligand (with slow recrystallisation from ethanol) gave a product with two peaks at 1667 and 1647 cm^{-1} suggesting two isomeric forms of the ligand (*cis* and *trans*). The spectra are also characterized by the presence of one broad band in the region 3131-3284 cm^{-1}, assigned to the ν(N-H) stretching frequencies suggesting both frequencies are similar. However for the BzPPtuH ligand two absorptions occur at 3407 and 3208 cm^{-1} indicating the ν(N-H) frequencies are more dissimilar. The ν(C=S) frequency is hard to assign due to its low intensity[13]. For thioketones the ν(C=S) stretch may occur at 1180 or 1224-1207 cm^{-1} region, but unfortunately this vibration cannot be located in the

---

[13] L.J. Bellamy, *Advances in IR Group Frequencies*, 1968, Richard Clay Ltd., Suffolk, p. 214.

present work. These ligands adopt the thione form in the free state and in their complexes, which is evident by the absence of the ν(S–H) stretch, in the 2600- 2550 cm^{-1} region, and by the presence of ν(N-H) in the range 2890-3310 cm^{-1}.

Mass spectral data give further evidence for the integrity of the ligands. In all these ligands the parent ion [MH^+ or M^+] has a very low intensity. The calculated masses of the ligands along with the isotope abundance calculations compare well with the experimental values. Suggested assignments for some of the other peaks are given in **Table 2.1**.

Table 2.1 Selected IR band positions and MS data for the ligands

	IR[a] (cm^{-1})		
Ligand	ν(C=O)	ν(N-H)	(+)FAB Mass spectra[b] m/z (rel. int., %)
Bz^tBPtuH[c]	1670vs	3221sbr	MH^+ 425 (12) 391(7) $[M-(S+H)]^+$ 367 (100) $[M-(C(CH_3)_3)]^+$ 105 (78) $[C_6H_5CO]^+$
Bz^tBPtuH[d]	1667vs 1647w	3214sbr	—
BzPPtuH	1670vs	3407w 3208mbr	MH^+ 485 (12) 451 (10) $[M-(S+H)]^+$ 105 (69) $[C_6H_5CO]^+$
Bz^iPPtuH	1667vs	3237w	M^+ 340 (v.low) 307 (13) $[M-(S+H)]^+$ 297 (27) $[M-(CH(CH_3)_2]^+$ 219 (32) $[M-C_7H_7ON]^+$ 105 (100) $[C_6H_5CO]^+$
BzFPtuH	1669vs	3131w	—
BzPtuH	1673vs	3284mbr	—

[a] As nujol mull on NaCl. vs = very strong, s = strong, m = medium, w = weak, br = broad. [b] In 3-nitrobenzylalcohol matrix. [c] Recrystallised from $CHCl_3$.
[d] Recrystallised from EtOH.

2.2.1.3 ^{1}H and ^{13}C NMR Data

The ^{1}H NMR spectra of some ligands show signals due to two N-H groups (δ = 8.82-12.25 ppm) whereas for Bz^{i}PPtuH and BzFPtuH ligands but the second ν(N-H) peak is not always detected (see **Table 2.2**). The aromatic protons show signals at 7.09-7.97 ppm. The ligands with *tert*-butyl and isopropyl moieties show signals due to methyl protons in the range 1.21-1.45 ppm for both ligands and 3.11 ppm for the isopropyl C-H proton. The methyl groups of the isopropyl moiety have become nonequivalent as shown by the two doublets that occur due to the rotational restriction as a result of steric hindrance. This non-equivalence does not appear in the CH resonance of the isopropyl moiety, which is a single septuplet. Interestingly restricted rotation does not occur for the *t*-butyl group. The intensities of the signals are given in **Table 2.2** and the area under the peaks is in accordance with the ratio of the expected proton types. In the ^{13}C NMR spectra (**Table 2.3**) the peak at about 181 ppm has been assigned to the thiocarbonyl (C=S) carbon while the peak near 167 ppm is consistent with the carbonyl (C=O) carbon. These peaks were assigned from the 2D NMR spectrum of the Bz^{t}BPtuH ligand, which is shown in **Fig. 2.1.** Coupling of the *ortho* protons of the benzoyl group with the CO carbon occurs and identifies the ^{13}C assignment of CO.

The number of Ar-CH and Ar-$C_{(quat.)}$ resonances listed in **Table 2.3** are in accordance with the proposed ligand structures. In the Bz^{t}BPtuH ligand there are two peaks in the 31.8-32.8 ppm region for tri-*tert*-butyl groups representing all 9C atoms while Bz^{i}PPtuH displays two peaks in the 23.5-24.8 ppm region for the diisopropyl groups representing all 4C atoms, instead of one strong peak. These results are in agreement with the proton spectra.

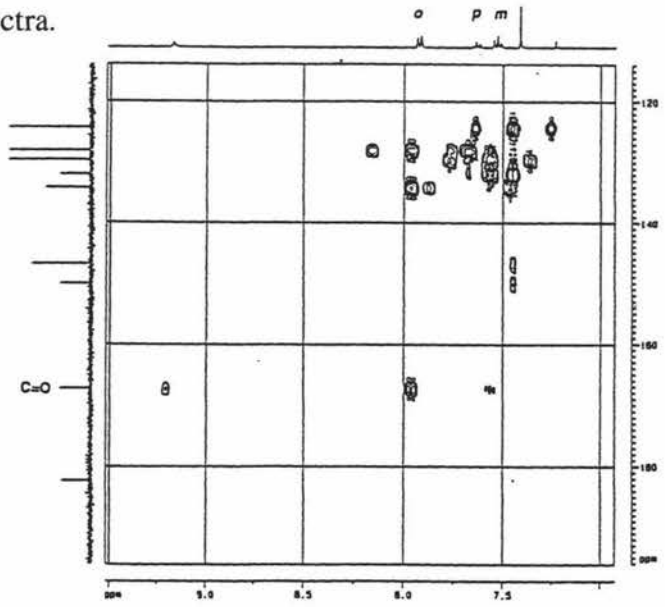

Figure 2.1 The 2D NMR spectrum of the Bz^{t}BPtuH ligand

Table 2.2 ^{1}H chemical shift data for the ligands[a]

	^{1}H NMR ($CDCl_3$, TMS, ppm)		
Ligand	δ_{N-H}	δ_{Ar-CH}	$\delta^{t}_{B-CH3\ or}\ ^{i}_{P-CH3\ and\ CH}$
Bz^{t}BPtuH	12.25s (1H) 9.23s (1H)	7.26-7.96m (7H)	1.34s (18H), 1.45s (9H)
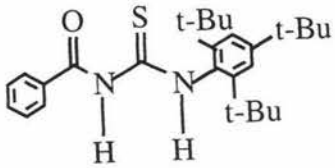			
BzPPtuH	11.98s (1H) 8.82s (1H)	7.27-7.73m (22H)	
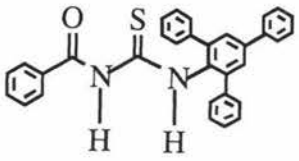			
Bz^{i}PPtuH	9.29s (1H)	7.26-7.97m (8H)	1.22d (6H), 1.34d (6H) 3.13sept. (2H)
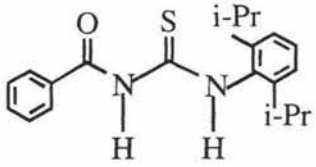			
BzFPtuH	9.15s (1H)	7.09-7.90m (9H)	
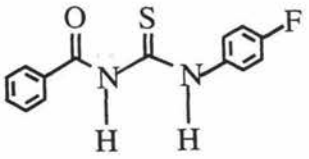			
BzPtuH	10.06s (1H) 9.07s (1H)	7.14-7.91m (10H)	
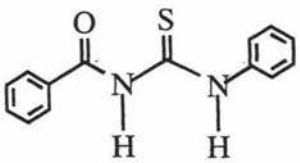			

[a] Recorded at 400MHz, chemical shifts are relative to $Si(CH_3)_4$ [TMS]. solvent $CDCl_3$. S = singlet, d = doublet, m = multiplet, sept = septuplet.

Table 2.3 ^{13}C chemical shift data for the ligands[a]

Ligands	^{13}C NMR ($CDCl_3$, ppm) $\delta_{C=S}$	$\delta_{C=O}$	$\delta_{Ar\text{-}CH}\delta_{Ar\text{-}C\ (quat.)}$	$\delta^{t}_{B\text{-}CH3\ and\ C(quat.)}$ or $\delta^{i}_{P\text{-}CH3\ and\ CH}$
Bz^{t}BPtuH	181.6	166.6	124.2–150.0 [7Ar-CH, 5Ar- $C_{(quat.)}$]	31.8 (3C), 32.8 (6C) 35.4 ($1C_{(quat.)}$) 37.2 ($2C_{(quat.)}$)
BzPPtuH	180.5	166.8	127.7–141.8 [22Ar-CH, 8Ar-$C_{(quat.)}$]	
Bz^{i}PPtuH	181.7	167.4	124.2–145.9 [8Ar-CH, 4Ar-$C_{(quat.)}$]	23.5 (2C), 24.8 (2C) 29.28 ($2C_{(tert.)}$)
BzFPtuH	179.3	167.4	116.1–162.6 [9Ar-CH, 3Ar-$C_{(quat.)}$]	
BzPtuH	178.7	167.4	124.6–137.9 [10Ar-CH, $2C_{(quat.)}$]	

[a] Recorded at 400MHz, solvent $CDCl_3$. quat = quaternary, tert = tertiary.

2.2.1.4 Description of the crystal structure of 1-benzoyl-3-(2,4,6-tri-*tert*-butylphenyl)thiourea (Bz^{t}BPtuH)

The white crystals of Bz^{t}BPtuH were grown by slow evaporation of an ethanol solution. The two independent molecules are contained in the asymmetric unit show no significant differences from one another. One of the independent molecules (molecule 1) has been arbitrarily selected for the purpose of this discussion. The structure of the Bz^{t}BPtuH molecule is shown in **Fig. 2.2**, with crystal data and structure refinement details given in **Table 2.4**, selected bond lengths and angles given in **Table 2.5** and selected torsion angles given in **Table 2.6**. In the structure, the O and S atoms adopt a *trans* orientation with respect to one another, so as to minimise non-bonded steric interactions. Particular interest in this ligand is the intramolecular hydrogen bond between the N(2)–H hydrogen and the carbonyl moiety (O(1)), analogous to that observed in the crystal structures of 1-benzoyl-3-butylthiourea[14], 1-benzoyl-3-propyl

[14] S. Bourne, T. Grimmbacher and K.R. Koch, (1993) unpublished results.

thiourea[15], 1-benzoyl-3-methyl-3-phenylthiourea[16], 1-benzoyl-3-(3,4-dimethylphenyl)-thiourea[16] and 1-benzoyl-3-(4-methoxyphenyl)thiourea[17]. The intramolecular hydrogen bond distance between N(2)–H and O(1) is 1.977(6) Å. This results in an almost planar six-membered ring with the C(25), N(1) and C(26) atoms in the central part of the molecule (torsion angles C(25)–N(1)–C(26)–N(2) = 3.5(4)° and O(1)–C(25)–N(1)–C(26) = 0.8(5)°). Similar observations have been made in 1-benzoyl-3-(3,4-dimethylphenyl)thiourea[16] and 1-benzoyl-3-(4-methoxyphenyl)-thiourea[17]. Also there are intermolecular hydrogen bonds with ethanol molecules in the lattice with N(1)–H(1)...O(ethanol) = 2.134(4) Å, C(26)–S...O(ethanol) = 2.385(5) Å and C(20)–H...O(ethanol) = 2.452(4) Å. As well in the crystal, the molecules are linked through weak intermolecular C–H...S interactions (C(22)–H...S = 2.834(5) Å). As will be seen later, the intramolecular hydrogen bond has significant implications on the coordination chemistry of the ligand.

The other bond lengths and angles are typical for thiourea compounds[16]. The C(25)–O(1) distance (1.226(3) Å) is similar to the calculated C=O (1.22 Å) double bond distance. The short C(26)–S distance (1.679(3) Å) clearly shows its double-bond character (calculated C–S single bond distance is 1.81 Å) and is very close to the unweighted mean value of 1.681 Å for the C=S distance found in other thioureas[16].

The conformation of the molecule with respect to the phenyl rings is shown by the torsion angles. For example, the torsion angle, C(24)–C(19)–C(25)–O(1) involving the benzoyl ring is -160.8(3)° and the angle C(2)–C(1)–N(2)–C(26) involving the *tert*-butyl substituted phenyl ring is 81.1(3)° (see **Fig. 2.2(b)**). The *ortho-tert*-butyl groups are pushed back, the angles not being 120°, one angle is bigger and one is smaller than 120°. All these orientations occur to minimise steric interactions within the molecule.

The bond lengths of C(19)–C(25) and C(1)–N(2) (1.488(4) and 1.438(3) Å respectively) are comparable with values in the literature[17]. The C–N bond lengths in the central part of the molecule are all shorter than the average single C–N bond length

---

[15] A. Drago, Y. Shepelev, F. Fajardo, F. Alvarez and R. Pomes, *Acta Cryst. C*, 1989, **45**, 1192.

[16] S.S.S. Raj, K. Puviarasan, D. Velmurugan, G. Jayanthi and H-K. Fun, *Acta Crystallorgr. C*, 1999, **55**, 1318.

[17] Y. Cao, B. Zhao, Y-Q Zhang and D-C Zhang, *Acta Cryst. C*, 1996, **52**, 1772.

of 1.479 Å[18], but longer than the average double C=N bond length of ~1.29 Å, being C(25)–N(1) = 1.379(4) Å, C(26)–N(1) = 1.395(4) Å and C(26)–N(2) = 1.326(4). This shows varying degrees of double bond character in these C–N bonds suggesting electron delocalisation throughout the imine system. Bond lengths and angles are very similar to those found in the molecular structure of 1-benzoyl-3,3-di(2-hydroxyethyl)thiourea[19].

The ligand may exist in various tautomeric forms and possible structures are shown for the unsubstituted phenyl ligand (**Fig. 2.3**). On the basis of IR spectra the tautomeric forms (b), (d) and (c) are unlikely because of the absence of the ν(S-H) stretch in (b) and (d) and the ν(O-H) stretch in (c). This suggests that the ligand exists mainly in the form (a), as well as zwitterions (e) and (f).

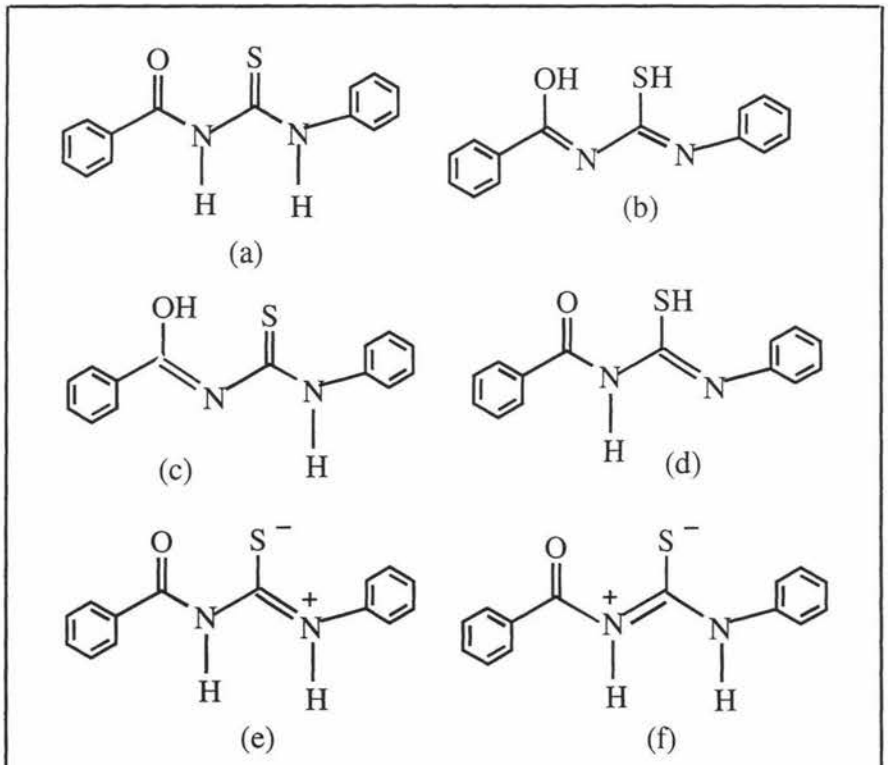

Figure 2.3 Possible Tautomeric Forms and Zwitterions

[18] R.C.Weast (ed.), *Handbook of Chemistry and Physics*, CRC, Boca Raton, FL, 64th edn., 1983-1984, p. 171.

[19] K.R. Koch, C. Sacht and S. Bourne, *Inorg. Chim. Acta,* 1995, **232**, 109.

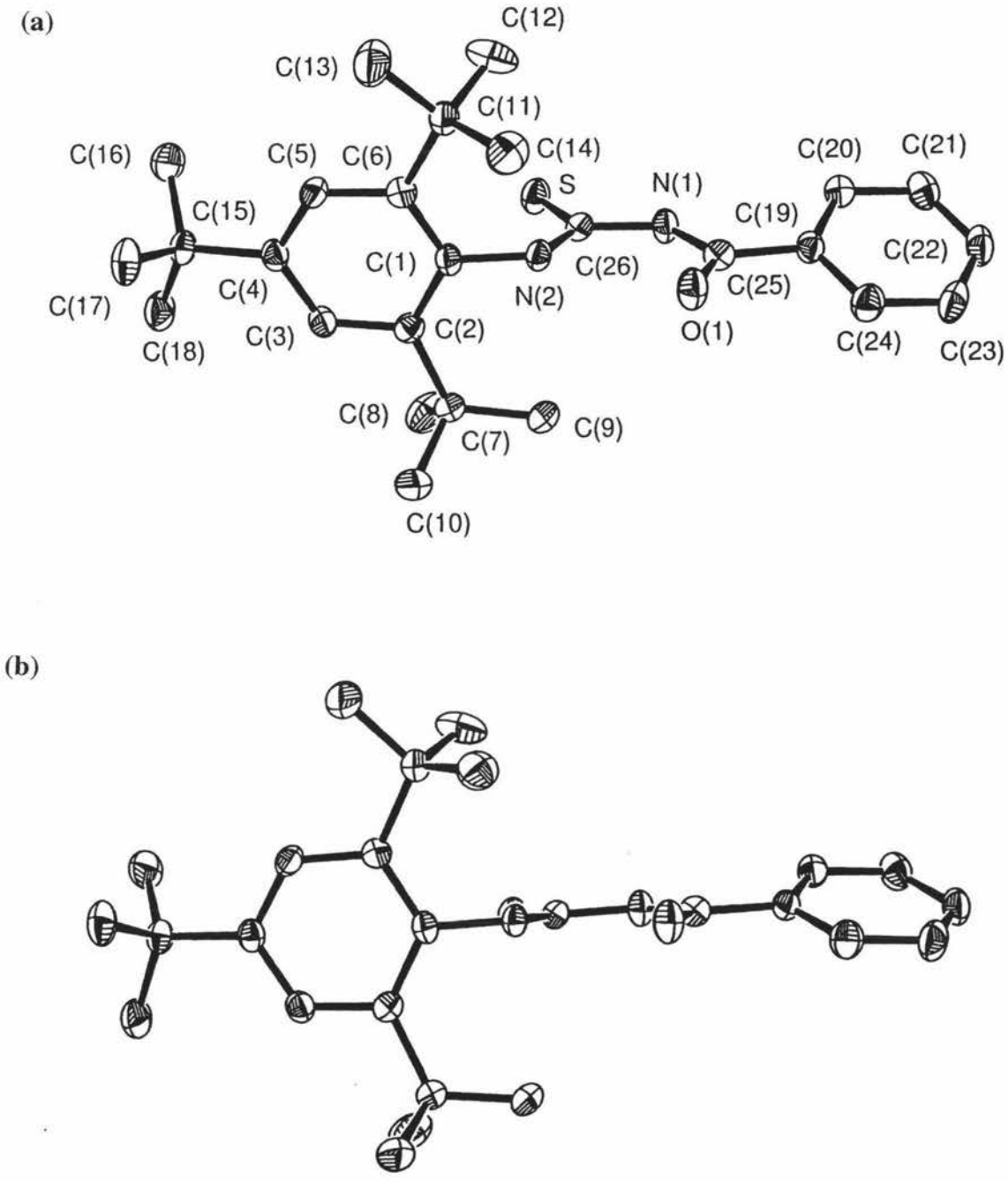

Figure 2.2 **(a)** ORTEP diagram of the ligand Bz^{t}BPtuH showing the numbering system used. Thermal ellipsoids are at the 50% probability level. Hydrogen atoms and solvent molecules have been omitted for clarity. **(b)** Orientation of the benzoyl ring and the *tert*-butyl substituted phenyl ring

Table 2.4 Crystal data and structure refinement for Bz^{t}BPtuH

Identification code	ic3a	
Empirical formula	$C_{28}H_{42}N_2O_2S$ ($C_{26}H_{36}N_2OS \cdot C_2H_5OH$)	
Formula weight	470.70	
Temperature	150(2) K	
Wavelength	0.71073 Å	
Crystal system	Monoclinic	
Space group	P2(1)/c	
Unit cell dimensions	a = 18.0946(5) Å	$\alpha = 90°$
	b = 20.9118(2) Å	$\beta = 110.795(1)°$
	c = 15.4054(4) Å	$\gamma = 90°$
Volume	5449.5(2) Å^3	
Z	8	
Density (calculated)	1.147 Mg/m^3	
Absorption coefficient	0.145 mm^{-1}	
F(000)	2048	
Crystal size	1.60 x 0.24 x 0.11 mm^3	
Theta range for data collection	1.20 to 25.04°.	
Index ranges	$-21 \leq h \leq 21$, $-24 \leq k \leq 23$, $-18 \leq l \leq 15$	
Reflections collected	27767	
Independent reflections	9592 [R(int) = 0.0531]	
Absorption correction	Semi-empirical from equivalents	
Max. and min. transmission	0.9843 and 0.8017	
Refinement method	Full-matrix least-squares on F^2	
Data / restraints / parameters	9592 / 0 / 595	
Goodness-of-fit on F^2	1.032	
Final R indices [I>2sigma(I)]	R1 = 0.0637, wR2 = 0.1311	
R indices (all data)	R1 = 0.1077, wR2 = 0.1547	
Largest diff. peak and hole	0.287 and -0.322 e.Å^{-3}	

Table 2.5 Selected bond lengths [Å] and angles [°] for Bz^{t}BPtuH with estimated standard deviations in parentheses

Bond lengths:

	Molecule 1	*Molecule 2*
C(1)-N(2)	1.438(3)	1.446(4)
C(19)-C(25)	1.488(4)	1.485(4)
C(25)-O(1)	1.226(3)	1.226(3)
C(25)-N(1)	1.379(4)	1.377(4)
N(1)-C(26)	1.395(4)	1.399(4)
C(26)-N(2)	1.326(4)	1.325(4)
C(26)-S	1.679(3)	1.677(3)

Bond angles:

C(2)-C(1)-N(2)	119.0(3)	118.3(3)
C(6)-C(1)-N(2)	118.2(2)	119.5(2)
C(3)-C(2)-C(7)	115.4(3)	119.1(3)
C(1)-C(2)-C(7)	128.6(3)	123.8(3)
C(3)-C(4)-C(15)	122.3(3)	120.3(3)
C(5)-C(4)-C(15)	120.4(3)	122.6(3)
C(5)-C(6)-C(11)	119.7(3)	115.8(3)
C(1)-C(6)-C(11)	123.8(2)	127.6(3)
C(24)-C(19)-C(25)	117.8(3)	117.4(3)
C(20)-C(19)-C(25)	123.0(3)	124.3(3)
O(1)-C(25)-N(1)	122.6(3)	121.8(3)
O(1)-C(25)-C(19)	122.0(3)	121.5(3)
N(1)-C(25)-C(19)	115.4(3)	116.6(3)
C(25)-N(1)-C(26)	128.3(3)	128.8(3)
N(2)-C(26)-N(1)	116.6(2)	116.8(3)
N(2)-C(26)-S	124.4(2)	125.4(2)
N(1)-C(26)-S	118.9(2)	117.8(2)
C(26)-N(2)-C(1)	122.3(2)	123.6(2)

Table 2.6 Selected torsion angles [°] for Bz^{t}BPtuH

	Molecule 1	*Molecule 2*
N(2)-C(1)-C(2)-C(3)	-170.8(3)	-176.6(3)
N(2)-C(1)-C(6)-C(5)	171.0(3)	175.5(3)
C(25)-C(19)-C(20)-C(21)	-176.3(3)	-176.2(3)
C(25)-C(19)-C(24)-C(23)	175.1(3)	175.7(3)
C(24)-C(19)-C(25)-O(1)	21.5(4)	10.8(5)
C(20)-C(19)-C(25)-O(1)	-160.8(3)	-171.2(3)
C(24)-C(19)-C(25)-N(1)	-155.8(3)	-167.2(3)
C(20)-C(19) C(25)-N(1)	21.9(4)	10.8(5)
O(1)-C(25)-N(1)-C(26)	0.8(5)	2.8(5)
C(19)-C(25)-N(1)-C(26)	178.1(3)	-179.2(3)
C(25)-N(1)-C(26)-N(2)	3.5(4)	-3.3(4)
C(25)-N(1)-C(26)-S	-175.5(2)	177.6(2)
N(1)-C(26)-N(2)-C(1)	179.9(2)	179.6(2)
S-C(26)-N(2)-C(1)	-1.1(4)	-1.4(4)
C(2)-C(1)-N(2)-C(26)	81.1(3)	95.8(3)
C(6)-C(1)-N(2)-C(26)	-97.6(3)	-85.5(4)

2.2.2 Physicochemical Studies and Characterization of the Complexes

2.2.2.1 Synthesis of the Complexes

The copper, nickel, cobalt and silver complexes were prepared by conventional methods and these are outlined in the Experimental Section **2.1.4** and listed with colors in **Table 2.7** and **2.8**. In the reaction of $CuCl_2$ with the ligands, only one copper(II) complex, *viz.* [Cu(Bz^{t}BPtuH)$_2$Cl$_2$], was isolated analytically pure. The ligands Bz^{t}BPtuH, BzPPtuH, Bz^{i}PPtuH and BzFPtuH produced dark red brown precipitates as intermediates, but these were transformed to the Cu(I) complexes [Cu(HL)$_2$X] (HL = Bz^{t}BPtuH, BzPPtuH, Bz^{i}PPtuH and BzFPtuH, X = Cl^-) upon aging in acetone and ethanol. BzPtuH produced the yellow complex [Cu(BzPtuH)$_3$Cl]. The yields of copper(II) and copper(I) complexes varied from 8% - 79%.

The stability of the copper(II) chloride complexes is apparently dependent on the presence of a bulky group on the anilino-ring. The presence of tertiary butyl groups conferred good stability on the copper(II) complex in that it remained unchanged for more than one year in the solid state. The pathway for copper(II) reduction in the solid

state is more hindered for this complex, possibly because steric constraints prevent the easy formation of the oxidized disulfide ligand.

When Bz^{t}BPtuH reacts with $CuCl_2$ in acetone the initial product is $[Cu(Bz^tBPtuH)_2Cl_2]$, which is soluble in the solvent, but after one week the reddish brown colour of the solvent is discharged and pale yellow crystals of $[Cu(Bz^tBPtuH)_2Cl]$ are isolated. In this process one of the ligands attached to the Cu(II) reduces it to Cu(I) while the oxidised ligand, presumably the disulfide (shown in **Fig. 2.4**) is formed, similar to that found for thiourea oxidation[20].

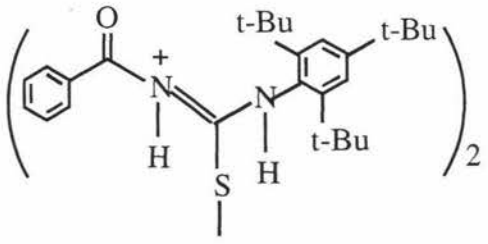

Figure 2.4

The remaining ligand interacts with half of the CuCl to give the product.
The overall reaction could be as follows:

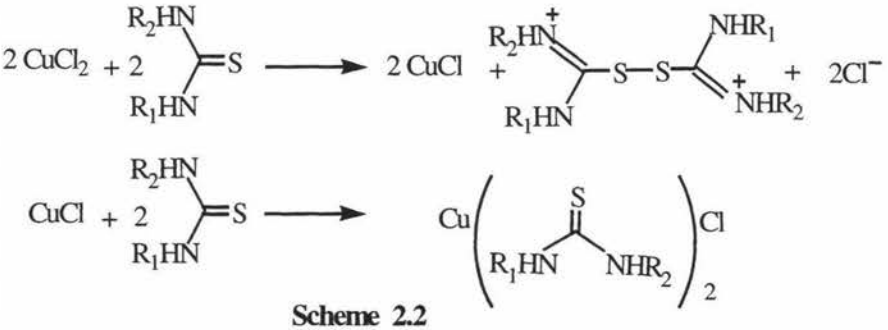

Scheme 2.2

Where R_1 = benzoyl group, R_2 = tri-*tert*-butyl-, triphenyl-, diisopropyl- or p-fluoro- phenyl or phenyl.

[20] D.A. Zatko and B. Kratochvil, *Anal. Chem.*, 1968, **40**, 2120.

The bulky anilino-groups appear to decrease the reduction rate. The qualitative order of stability for the $CuCl_2$ complexes was tri-*tert*-butyl > diisopropyl >tri-phenyl > *p*-fluoro > unsubstituted phenyl anilino derivatives. The red copper(II) species were more stable at low temperatures (< 0 °C).

There are many literature reports on the reduction of Cu(II) in the presence of thiourea derivatives. For example, Zatko *et al.*[20] investigated oxidation of a series of thioureas by copper(II) in acetonitrile, observing a 1:1 stoichiometry in most cases. They considered the oxidized product of the substituted thioureas to be the cationic disulfides and the order of stability of the red copper(II) species to be tetramethyl > N,N-dimethyl-N'-*o*-tolyl > *m*- and *p*-tolyl derivatives > N,N'-di-*o*-tolyl > N,N'-diphenyl > N,N-di-*tert*-butyl > mono- and di-substituted alkyl derivatives. Shen *et al.*[21] have isolated Cu(I) complexes of 1-(butoxycarbonyl)-3-(*p*-nitrophenyl)thiourea (H_2nbt) and 1-(ethoxycarbonyl)-3-(*o*-nitrophenyl)thiourea (H_2net) having the compositions, $[Cu(H_2nbt)_2Cl]_2$ and $[Cu(H_2net)_2Cl]$ respectively. X-ray crystallographic studies show a dimeric structure for the $[Cu(H_2nbt)_2Cl]_2$ complex in which the Cu(I) atom has a distorted tetrahedral coordination, whereas in $[Cu(H_2net)_2Cl]$ the copper(I) atom has a trigonal planar geometry.

When Bz^tBPtuH or Bz^iPPtuH is allowed to react with $Cu(Ac)_2.H_2O$ (Ac = acetate) in a 2 :1 molar ratio, a dark green complex forms according to the following equation:

$$Cu(Ac)_2.H_2O + 2LH \rightarrow [CuL_2] + 2HAc + H_2O$$

where L = Bz^tBPtu or Bz^iPPtu.

$[Ni(Bz^tBPtuH)_2I_2]$ and $[Co(Bz^tBPtuH)_2Cl_2]$ were formed by reacting the Bz^tBPtuH ligand in 1:1 molar ratio with $NiI_2.6H_2O$ and $CoCl_2.6H_2O$ respectively.

$[Cu(LH)_4]PF_6$ (LH = Bz^tBPtuH or Bz^iPPtuH) as well as $[Ag(LH)_4]PF_6$ were formed according to the stoichiometric molar ratios from $[Cu(CH_3CN)_4]PF_6$ and $[Ag(CH_3CN)_4]PF_6$. Each metal is thus able to bind four bulky ligands.

---

[21] Xu Shen, T.B. Wen, Q.T. Liu, X.Y. Huang, B.S. Kang, X.L. Wu, Z.S. Huang and L.Q. Gu, *Polyhedron*, 1997, **16**, (15), 2605.

All the compounds were characterized by elemental analysis, infrared and FAB(+) mass spectra. ^{1}H and ^{13}C NMR spectra were used to characterize Ag(I) and some of the Cu(I) compounds. Electronic spectra were used to characterize $[Cu(L)_2]$ (L = Bz^tBPtu or Bz^iPPtu), $[Cu(LH)_2Cl_2]$, $[Ni(Bz^tBPtuH)_2I_2]$ and $[Co(Bz^tBPtuH)_2Cl_2]$, also ESR spectra were used for $[CuL_2]$ and $[Cu(LH)_2Cl_2]$. X-ray diffraction was used for $[Cu(Bz^tBPtuH\text{-}\kappa^1S)_2Cl]$ and $[Co(Bz^tBPtuH\text{-}\kappa^1S)_2Cl_2]$.

2.2.2.2 IR and Mass Spectroscopic Studies of the Compounds

For the complexes, $[Cu(Bz^tBPtu)_2]$ and $[Cu(Bz^iPPtu)_2]$, the intensities of the ν(N-H) peaks have dropped from strong to weak, implying a loss of a proton. The ν(CO) stretching frequencies of $[Cu(Bz^tBPtu)_2]$ and $[Cu(Bz^iPPtu)_2]$ occur at 1605 and 1586 cm^{-1}, whereas for the free ligands the band appears at 1670 and 1667 cm^{-1} respectively. The lowering of the ν(CO) stretch (~ 65 and 81 cm^{-1}) is consistent with the coordination through the oxygen atom. A large decreased shift should also be observed for the C=S stretching vibration, but unfortunately this vibration could not be located because of its low intensity[13]. These results may be interpreted in terms of the ligand acting as a bidentate monoanion binding through O and S atoms (**Fig. 2.5**).

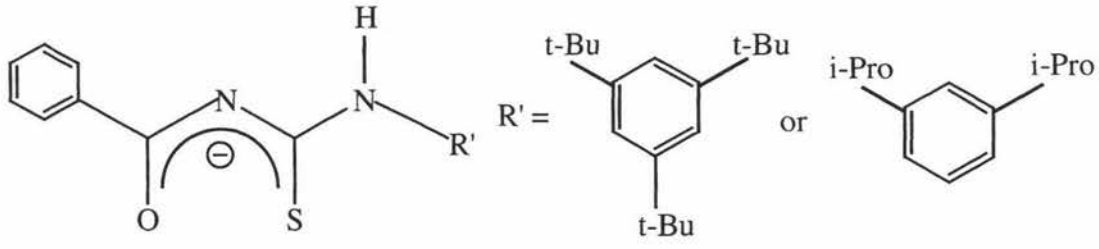

Figure 2.5

In contrast, all the other complexes (**Table 2.7** and **2.8**) show only a small shift to higher wave numbers for the ν(CO) stretch, consistent with the non-coordination of the carbonyl oxygen atom. The ν(C=O) stretching frequencies of $[M(HL)_4]PF_6$ [M = Cu(I), Ag(I), HL = Bz^tBPtuH, Bz^iPPtuH] complexes are higher (8-15 cm^{-1}) than the ligand ν(C=O) stretch which again is direct evidence that C=O is not coordinated to the metal. The magnitude of the lowering of the ν(N-H) stretch in $[Cu(Bz^tBPtuH)_2Cl_2]$, $[Cu(Bz^iPPtuH)_2Cl]$, $[Co(Bz^tBPtuH)_2Cl]$ and $[Ni(Bz^tBPtuH)_2I_2]$ as well as one of the

ν(N-H) frequencies of [Cu(Bz^{t}BPtuH)$_2$Cl] does not indicate the involvement of the N-H group in coordination. Instead hydrogen bonding to the C=O group of the benzoyl moiety or a weakening of the N-H bond when S binds to the metal may be factors. The infra red evidence suggest the C=S group is bound to the metal ions and this is confirmed by the X-ray structures of [Cu(Bz^{t}BPtuH)$_2$Cl] and [Co(Bz^{t}BPtuH)$_2$Cl$_2$] complexes which are shown in Section **2.2.2.6**. The crystal structures clearly indicate the involvement of the C=S group in the coordination. Bonding through the sulfur atom is also favoured because copper(II) is a 'borderline soft' atom, and should interact with a 'soft' donor such as sulfur[22].

All the compounds of **Table 2.7** exhibited molecular ion peaks with isotope abundance calculations in agreement with the experimental values. Suggested assignments for some of the other peaks are given in the same table. In [Cu(Bz^{t}BPtu)$_2$] both the ligands are protonated under the conditions of the mass spectral experiment, whereas in [Cu(Bz^{i}PPtu)$_2$] only one ligand is protonated. The $[MH]^+$ species of [Cu(Bz^{t}BPtu)$_2$] is formulated as $[Cu(Bz^tBPtu)(Bz^tBPtuH)]^+$ (m/z = 910). For [Cu(Bz^{t}BPtuH)$_2$Cl$_2$], [Ni(Bz^{t}BPtuH)$_2$I$_2$], [Cu(Bz^{t}BPtuH)$_2$Cl] and [Cu(BzFPtuH)$_2$Cl] the parent ion loses the halide first and then a ligand, whereas for [Co(Bz^{t}BPtuH)$_2$Cl$_2$] one Cl^- ion is lost in the first step and in the second step it loses the other Cl^- ion followed by a ligand. [Cu(BzPtuH)$_3$Cl] is exceptional, it loses one ligand first and then the Cl^- in the second step. The [M(LH)$_4$]PF$_6$ [M = Cu, Ag, LH = Bz^{t}BPtuH, Bz^{i}PPtuH] complexes lose ligands sequentially.

---

[22] R.G. Pearson, *Chemical Hardness*, 1997, Wiley-VCH, Weinhiem.

Table 2.7 Selected IR and MS data for copper complexes

Compounds	IR[a] (cm^{-1}) ν(C=O)	ν(N-H)	ν(P-F)	(+)FAB Mass spectra[b] m/z (rel. int., %)
$[Cu(Bz^tBPtu)_2]$ (green)	1605vs	3207wbr		[c] $[(MH_2)(^{63}Cu)]^+$ 911 (22) 910 (3) $[MH]^+$ 487 (90) $[MH_2\text{-}L]^+$ 367 (67) $[L\text{-}(C(CH_3)_3)]^+$ 105 (100) $[C_6H_5CO]^+$
$[Cu(Bz^iPPtu)_2]$[1] (dark green)	1586s	3286wbr		$[(MH))(^{63}Cu)]^+$ 742 (43) 403 (94) $[CuL]^+$ 105 (100) $[C_6H_5CO]^+$
$[Cu(Bz^tBPtuH)_2Cl_2]$ (red brown)	1676vs	3157mbr		$[(M\text{-}Cl_2)(^{63}Cu)]^+$ 911 (100)
$[Cu(Bz^tBPtuH)_2Cl]$ (pale yellow)	1668vs	3231w 3144mbr		$[(M\text{-}Cl)(^{63}Cu)]^+$ 911 (30) 487 (53) $[(M\text{-}Cl)\text{-}L]^+$ 367 (100) $[L\text{-}(C(CH_3)_3)]^+$ 105 (49) $[C_6H_5CO]^+$
$[Cu(BzPPtuH)_2Cl]$ (greenish yellow)	1669vs	3200sh 3140wbr		
$[Cu(Bz^iPPtuH)_2Cl]$ (dark yellow)	1662s	3140wbr		—
$[Cu(BzFPtuH)_2Cl]$ (dark yellow)	1671s 1611s	3130w		$[(M\text{-}Cl)(^{63}Cu)]^+$ 611 (13) 337 (8) $[(M\text{-}Cl)\text{-}L]^+$ 275 (100) $[HL]^+$ 105 (36) $[C_6H_5CO]^+$
$[Cu(BzFPtuH)_2Br]$ (pale yellow)	1672s 1611s	3277sh 3219s		—
$[Cu(BzPtuH)_3Cl]$ (yellow)	1671vs	3283w 3134w		$[(M\text{-}L)(^{63}Cu)]^+$ 610 (5) 575 (20) $[(M\text{-}L)\text{-}Cl]^+$ 257 (100) $[HL]^+$ 105 (28) $[C_6H_5CO]^+$
$[Cu^I(Bz^tBPtuH)_4]PF_6$ (pale yellow)	1682vs	3321s 3193wbr	845vs	911 (62) $[CuL_2]^+$ 487 (100) $[CuL]^+$ 367 (61) $[L\text{-}(C(CH_3)_3]^+$ 105 (61.5) $[C_6H_5CO]^+$
$[Cu^I(Bz^iPPtuH)_4]PF_6$ (white)	1675vs	3315s 3185s	842vs	743 (70) $[CuL_2]^+$ 403 (100) $[CuL]^+$ 105 (42) $[C_6H_5CO]^+$

[a] As nujol mull on NaCl, [b] 3-nitrobenzylalcohol matrix, [c] MH_2^+ is equivalent to $[(^{63}Cu)(Bz^tBptuH)_2]^+$, vs = very strong, s = strong, m = medium, w = weak, br = broad, sh = shoulder.

Table 2.8 Selected IR and MS data for Ni, Co and Ag complexes

Compounds	IR[a] (cm^{-1}) ν(C=O)	ν(N-H)	ν(P-F)	(+)FAB Mass spectra[b] m/z (rel. int., %)
$[Ni(Bz^tBPtuH)_2I_2]$ (brown yellow)	1673vs	3265mbr 3191mbr		$[(M-I_2)(^{58}Ni)]^+$ 905 (16) 482(36) $[M-I_2-(L-H)]^+$ 367(100) $[L-(C(CH_3)_3]^+$ 105 (25) $[C_6H_5CO]^+$
$[Co(Bz^tBPtuH)_2Cl_2]$ (blue)	1674vs	3160mbr		$[(M-Cl)(^{59}Co)]^+$ 942 (9) 906(4) $[M-Cl_2]^+$ 518(40) $[(M-Cl)-L]^+$ 367(100) $[L-(C(CH_3)_3]^+$ 105 (72) $[C_6H_5CO]^+$
$[Ag(Bz^tBPtuH)_4]PF_6$ (white)	1684vs	3346s 3203mbr	845vs	—
$[Ag(Bz^iPPtuH)_4]PF_6$ (white)	1682vs	3314mbr 3152mbr	846vs	789 (52) $[AgL_2+H]^+$ 447 (100) $[AgL-H]^+$ 105 (93) $[C_6H_5CO]^+$

[a] As nujol mull on NaCl. [b] 3-nitrobenzylalcohol matrix. vs = very strong, s = strong, m = medium, w = weak, br = broad

2.2.2.3 ^1H and ^{13}C NMR Spectroscopic Studies of Selected Compounds

NMR spectra may be useful in determining the coordination behavior of ligands in diamagnetic metallic complexes. The ^1H NMR data for selected compounds are shown in **Table 2.9**. In all the complexes only one N-H proton was observed and its resonance was slightly higher than the free ligand, suggesting non-coordination of the N-H group. The proton signals of the aromatic rings are found to be slightly shifted.

^{13}C NMR spectra are reported in **Table 2.10**. The ^{13}C chemical shifts for the C=S (and to a lesser extent C=O) carbons are relatively constant with little change from the free ligands. This suggests that at room temperature dissociation of the M-S bond is

occurring. Similar results have been obtained for a related rhodium system[23]. Other peaks due to phenyl rings and alkyl groups are observed in the expected range.

Table 2.9 ^{1}H chemical shift data for the complexes[a]

	^{1}H NMR ($CDCl_3$, TMS, ppm)		
Complexes	δ_{N-H}	δ_{Ar-CH}	$\delta^{t}_{B-CH3\ or}\ ^{i}_{P-CH3\ and\ CH}$
$[Cu(BzFPtuH)_2Cl]$	10.97s (1H)	6.96-8.23m (9H)	
$[Cu^{I}(Bz^{i}PPtuH)_4]PF_6$	9.90s (1H)	6.88-8.14m (8H)	1.04d (6H), 1.11d (6H) 2.69sept. (2H)
$[Ag^{I}(Bz^{t}BPtuH)_4]PF_6$	9.76s (1H)	7.25-7.70m (7H)	1.28s (18H), 1.59s (9H)
$[Ag^{I}(Bz^{i}PPtuH)_4]PF_6$	9.44s (1H)	7.17-7.69m (8H)	1.18d (6H), 1.27d (6H) 2.93sept. (2H)

[a] Recorded at 400MHz, chemical shifts are relative to $Si(CH_3)_4$ [TMS], solvent $CDCl_3$, s = singlet, d = doublet, m = multiplet, sept = septuplet.

Table 2.10 ^{13}C chemical shift data for the complexes[a]

	^{13}C NMR ($CDCl_3$, ppm)			
complexes[b]	$\delta_{C=S}$	$\delta_{C=O}$	$\delta_{Ar-CH}\delta_{Ar-C\ (quat.)}$	$\delta^{t}_{B-CH3\ and\ C(quat.)}$ or $\delta^{i}_{P-CH3\ and\ CH}$
$[Cu(Bz^{i}PPtuH)_4]PF_6$	181.4	168.0[c]	124.3-145.6 [8Ar-CH, 4Ar-$C_{(quat.)}$]	23.3 (2C), 24.6 (2C) 29.2 ($2C_{(tert.)}$)
$[Ag(Bz^{t}BPtuH)_4]PF_6$	182.3	168.5	123.8-150.0 [7Ar-CH, 5Ar- $C_{(quat.)}$]	31.4-34.9 (9C) 36.7 ($3C_{(quat.)}$)
$[Ag(Bz^{i}PPtuH)_4]PF_6$	181.8	167.9	124.3-145.8 [7Ar-CH, 5Ar- $C_{(quat.)}$]	23.5 (2C), 24.8 (2C) 29.3 ($2C_{(tert.)}$)

[a] Recorded at 400MHz, solvent $CDCl_3$. [b] The ^{13}C NMR spectrum for $[Cu(BzFPtuH)_2Cl]$ was not recorded. quat = quaternary, tert = tertiary.

[23] D. Cauzzi, M. Lanfranchi, G. Marzolini, G. Predieri, A. Tiripicchio, M. Costa, R. Zanoni, *J. Organomet. Chem.*, 1995, **488**, 115.

2.2.2.4 Electronic Absorption and Magnetic Susceptibility Data for the Complexes

The electronic absorption spectra for $[CuL_2]$ [L = Bz^tBPtu or Bz^iPPtu] in solution (**Table 2.11**) display d-d bands at 585 (and 567) nm (ε = 566 and 1230) respectively which is consistent with copper in a square planar geometry [24]. As well, absorptions appearing at 396 and 346 nm (ε = 7630 and 9420) respectively may be assigned as S $\rightarrow$ Cu(II) charge transfer (CT) bands and this indicates that S is coordinated to copper. The high ε values for the d-d bands suggest some intensity stealing from the CT bands. These data are similar to that observed for bis(1-benzoyl-3,3-diethylthioureato)copper(II) whose structure is known to be planar.[25,26] Here the d-d band occurs at 585 nm ($\varepsilon \approx 250$) and the charge transfer band at $\approx$375 nm ($\varepsilon \approx 7000$)[27].

For $[Cu(LH)_2Cl_2]$ [LH = Bz^tBPtuH or Bz^iPPtuH] in CH_2Cl_2 the d-d bands move to lower energy (935 and ~920 nm respectively) which is consistent with a distorted tetrahedral arrangement of ligands about copper(II). As well, absorptions appearing at 565 and 536 nm respectively may be assigned as S $\rightarrow$ Cu(II) CT bands which supports the coordination of S to copper. Pure compounds of the type $[Cu(LH)_2Cl_2]$ have not been prepared before for substituted thioureas, hence the electronic absorption spectra cannot be compared with similar compounds. Our data are similar to that for $[CuLCl_2]$ (L = $(C_6H_5)_2P(S)CH_2(S)P(C_6H_5)_2$) where a distorted tetrahedral structure was proposed[28]. The magnetic moments for both types of complexes are consistent with the presence of one unpaired electron as expected for Cu(II) with a d^9 configuration.

When $CuCl_2$ was added to excess Bz^tBPtuH or Bz^iPPtuH in ethanol, red solutions formed and they displayed CT bands at 537 nm or 512 nm and d-d bands at 760 nm or 710 nm respectively. Within about two minutes the red colour was discharged. The fact that the d-d bands are at higher energy than the value of ~930 nm seen for $[Cu(LH)_2Cl_2]$

---

[24] F.A. Cotton and G. Wilkinson, *Advanced Inorganic Chemistry,* Interscience Publishers, 4th Ed., 1972, 915.
[25] R. Richter, L. Beyer and J. Kaiser, *Z. Anorg. Allg. Chem.*, 1980, **461**, 67.
[26] R. Kirmse, L. Beyer and E. Hoyer, *Chem. Phys. Lett.*, 1976, **44**, 173.
[27] A. Mohamadou, I. Déchamps-Olivier and J.P. Barbier, *Polyhedron*, 1994, **13**, 3277.
[28] E.W. Ainscough, H.A. Bergen, A.M. Brodie and K.A. Brown, *J. Chem. Soc., Dalton Trans.*, 1976, 1649.

(LH = Bz^{t}BPtuH or Bz^{i}PPtuH) is consistent with a different geometry. We speculate that the species may be formulated as $[Cu(LH)_4(EtOH)_2]Cl_2$ or $[Cu(LH)_4Cl_2]$ and the geometry is octahedral.

When $CuCl_2$ was added to excess BzPPtuH in 10 ml of dichloromethane and ~3-4 drops of ethanol, a red solution formed which displayed a CT band at ~540 nm and a d-d band at 883 nm. The red colour discharged within about one and a half minutes. The spectrum was similar to that obtained when $CuCl_2$ and BzPPtuH are reacted in a 1:2 ratio. It appears that possibly $[Cu(BzPPtuH)_2Cl_2]$ is the main species in both these reactions.

$[Co(Bz^tBPtuH)_2Cl_2]$ shows a broad structured band at around 674 nm (ε = 299) which is assigned to a $^4A_{2g} \rightarrow {}^4T_1(P)$ transition[29]. This and the magnetic moment of 4.30 B.M. is consistent with a tetrahedral structure and this is verified from the X-ray crystal structure (see Section **2.2.2.6**).

For $[Ni(Bz^tBPtuH)_2I_2]$, the three d-d bands at 1059, 735 and 520 nm (ε = 110, 160 and 640 respectively) are characteristic of octahedral nickel(II) compounds and are assigned to the $^3A_{2g} \rightarrow {}^3T_{2g}$ and $^3A_{2g} \rightarrow {}^3T_{1g}$ (F) and $^3A_{2g} \rightarrow {}^3T_{1g}$ (P) transitions respectively[30]. The possibility of it having a pseudo-tetrahedral structure cannot be dismissed either. As well in the spectrum the 365nm absorption is presumably a S $\rightarrow$ Ni(II) or I $\rightarrow$ Ni(II) CT band. This is supported by the magnetic moment measurement of 2.94 B.M. indicative of the presence of two unpaired electrons. It is difficult to envisage an octahedral structure for this complex especially if the carbonyl or N-H groups are not bound. Attempts to grow crystals were unfortunately unsuccessful.

---

[29] F.A. Cotton and G. Wilkinson, *Advanced Inorganic Chemistry,* Interscience Publishers, 4th Ed., 1972, 881.

[30] F.A. Cotton and G. Wilkinson, *Advanced Inorganic Chemistry*, Interscience Publishers, 4th Ed., 1972, 894.

Table 2.11 Electronic absorption and Magnetic susceptibility data for the complexes

Compounds	UV-vis λ/nm (ε_{max}/dm^3 mol^{-1}cm^{-1}) CT	d-d	Solvent[a]	μ_{eff}[b] B.M.
[Cu(Bz^{t}BPtu)$_2$]	396 (7630)	750 (sh) (260) 585 (566)	CH_2Cl_2	1.95
	419	600	MT	
[Cu(Bz^{i}PPtu)$_2$][d]	346 (9420)	567 (1230)	$CHCl_3$	1.90
[Cu(Bz^{t}BPtuH)$_2$Cl$_2$]	565 (2585)	935 (375)	CH_2Cl_2	1.90
	562	850	MT	
[Cu(Bz^{i}PPtuH)$_2$Cl$_2$]	536	≈920	CH_2Cl_2	—
[Cu(BzPPtuH)$_2$Cl$_2$]	≈540(sh)	883	CH_2Cl_2/EtOH[c]	—
[Ni(Bz^{t}BPtuH)$_2$I$_2$]	365 (2418)	1059 (110) 735 (160) ≈520 (sh) (640)	$CHCl_3$	2.94
	358	1000 740 500	MT	
[Co(Bz^{t}BPtuH)$_2$Cl$_2$]	332 (1409)	674 (299) 637 (sh) (240) 617 (sh) (200) 577 (158)	$(CH_3)_2CO$	4.30
	—	771 648 602	MT	

[a]MT is nujol mull transmittance. [b]B.M. = 0.927×10^{-23} A m^2. [c]CH_2Cl_2/EtOH (10ml/~3-4 drops). [d]From ref.1.

2.2.2.5 ESR Spectra for the Copper(II) Complexes

The ESR spectra of a frozen solution of [Cu(Bz^{t}BPtu)$_2$] at 77K is characterized by an axial g tensor with the $g_{//}$ value > $g_{\perp}$ value. Three of the four parallel hyperfine features are well resolved while the fourth one at high field is overlapped by

the broad $g_{\perp}$ signal. Only one set of four-line patterns is observed suggesting the presence of one species. A similar study on bis(1-benzoyl-3,3-diethylthioureato)copper(II) and related systems show the simultaneous presence of a planar *trans* and a nearly planar *cis* isomers in a 1:2 ratio for all "S, O" compounds[31]. The X-ray structure of a similar molecule supports this[32]. In our case the spectral parameters (**Table 2.12**) are consistent with a planar CuS_2O_2 moiety, but it is not clear whether it is *cis* or *trans*. The latter may be preferred from molecular models where steric influences come into play.

The ESR spectra of $[Cu(LH)_2Cl_2]$ (LH = Bz^{t}BPtuH or Bz^{i}PPtuH) at 77 K also show axial spectra. The $A_{//}$ value has decreased from 186×10^{-4} cm^{-1} in the square planar case to 157×10^{-4} cm^{-1} in the distorted tetrahedral case (see Table 2.14). For $[Cu(Bz^iPPtuH)_2Cl_2]$, the $g_{\perp}$ region is unusually multiply split but the $g_{//}$ and $A_{//}$ values are similar for both complexes. These data are similar to other systems that have an CuS_2Cl_2 donor set, which may have an out of plane geometry[28].

Table 2.12 ESR spectral data for the copper(II) complexes at 77K

Compounds	$g_{//}$	$g_{\perp}$	$10^4 \times A_{//}$ (cm^{-1})	Solvent
$[Cu(Bz^tBPtu)_2]$	2.273	~2.099	186	acetone
$[Cu(Bz^iPPtu)_2]$	[a]	2.155	[a]	acetone
$[Cu(Bz^tBPtuH)_2Cl_2]$[b]	2.270	2.176	157	acetone
$[Cu(Bz^iPPtuH)_2Cl_2]$	2.277	[a]	152	acetone

[a] Not resolved, [b] minor species is due to $CuCl_2$ in acetone: $g_{//} = 2.48$, $g_{\perp} = 2.23$, $A_{//}$ = not calculated.

[31] E. Guillon, I. Déchamps-Olivier and J.P. Barbier, *Polyhedron*, 1998, **17**, 3255.
[32] R. Richter, J. Sieler, E. Ludwig, E. Uhlemann and L. Golic, *Z. Anorg. Allg. Chem.*, 1984, **513**, 114.

2.2.2.6 Description of the Crystal Structures

2.2.2.6.1 Crystal Structure of [Cu(Bz^{t}BPtuH-κ^1*S*)$_2$Cl]

The structure of the complex [Cu(Bz^{t}BPtuH-κ^1*S*)$_2$Cl] is shown in **Fig. 2.6** with crystal data and structure refinement details given in **Table 2.13**, selected bond lengths and angles in **Table 2.14** and selected torsion angles in **Table 2.15**. The complex has a monomeric structure with the Cu(I) atom is a trigonal planar geometry. The angles about the Cu are: S(1)–Cu(1)–Cl = 122.58(2), S(1A)–Cu(1)–Cl = 118.85(2) and S(1)–Cu(1)–S(1A) = 118.39(2)°. The two Cu–S bonds are 2.2257(7) and 2.2285(6) Å respectively and the Cu–Cl distance is 2.2420(6) Å. These parameters are similar to those found in the trigonal planar complex [Cu(H$_2$net)$_2$Cl] [H$_2$net = 1-(ethoxycarbonyl)-3-(*o*-nitrophenyl)thiourea][21], with angles about the Cu being: S(1)–Cu–Cl 120.53(5), S(2)–Cu–Cl 118.43(5) and S(1)–Cu–S(2) 119.16(5)° and the bond distances being: Cu–S 2.228(1) Å and 2.232(1) Å, Cu–Cl 2.251(1) Å.

The Cu–S bond distances are close to the Cu–S distances for [Cu{Ph$_2$PS)$_2$CH$_2$}Cl][33] (2.23, 2.25 Å) which also has a trigonal planar geometry. The Cu–S distances are shorter than those found for other tetrahedral complexes,[34,35,36] showing they are sensitive to the coordination environment of the copper(I) atom.

The conformation of the central part of the two ligands is shown by the torsion angle C(25)–N(1)–C(26)–S(1). Ligand 1 is ~ planar (174.0(2)°) but ligand 2 is ~12° out of plane (-168.1(2)°). The conformation of the rest of the two ligands is same as the free ligand. An interesting feature of the two ligands is that, one is the approximate mirror image of the other.

The intramolecular hydrogen bond distance between N(2)–H and O(1) is 1.912(6) Å in ligand 1 and 1.883(6) Å in ligand 2. As in the free ligand, this results in

---

[33] E.W. Ainscough, A.M.Brodie and K.L. Brown, *J. Chem. Soc.,Dalton Trans.*, 1980, 1042.
[34] A. Pignedoli and G. Peyronel, *Acta Crystallorgr. Sect. B,* 1979, **35**, 2009.
[35] M.M. Olmstead, W.K. Musker and R.M. Kessler, *Trans. Met. Chem.*, 1982, **7**, 140.
[36] K.D. Karlin, P.L. Dahlstrom, J.R. Hyde and J. Zubieta, *J. Chem. Soc., Chem. Commun.*, 1980, 906.

the formation of an approximately planar six-membered ring, for example, the C(25)–N(1)–C(26)–N(2) torsion angle is -4.6(3)° for ligand 1 and 10.4(3)° for ligand 2. (free ligand value = 3.5(4)°).

The chlorine atom forms an intramolecular hydrogen bonds between N(1)–H and Cl with N(1)–H...Cl = 2.441(6) Å and N(1a)–H and Cl with N(1a)–H...Cl = 2.562(6) Å.

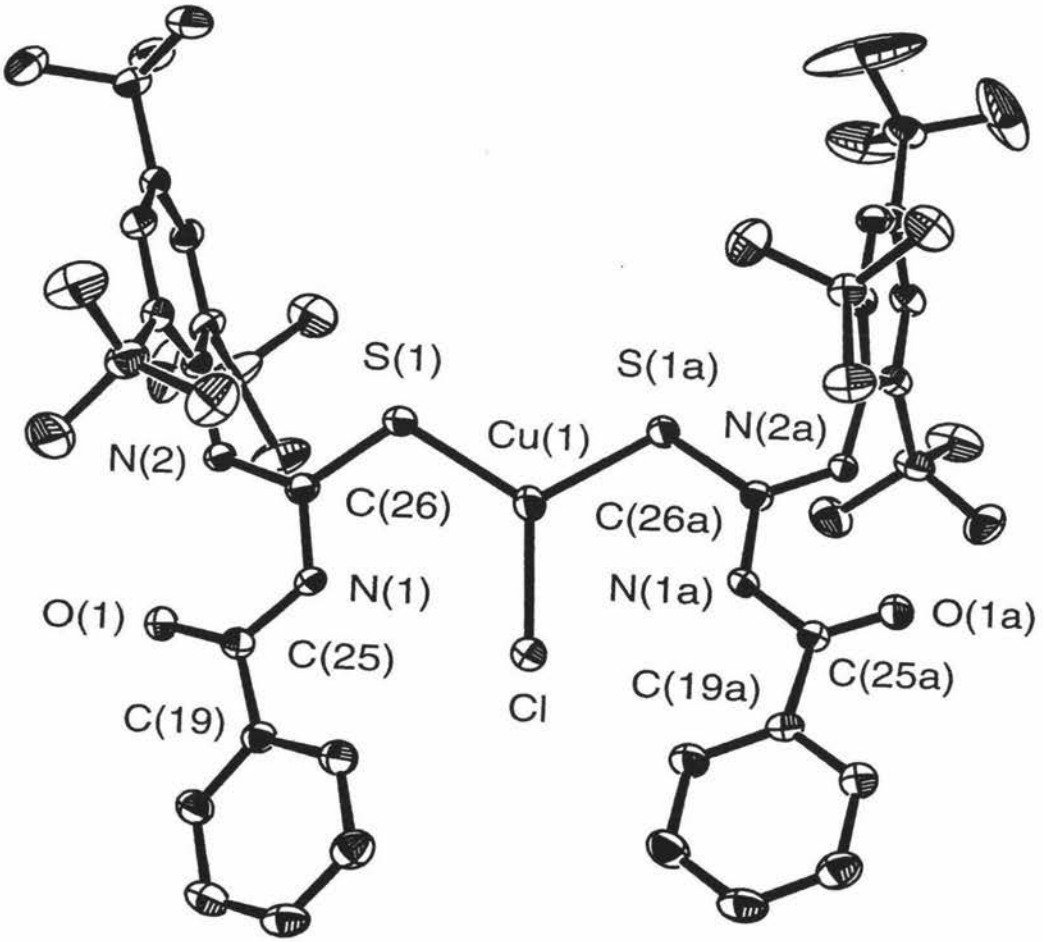

Figure 2.6 ORTEP diagram for the complex [Cu(Bz^{t}BPtuH-κ^1*S*)$_2$Cl] showing the numbering system used. Thermal ellipsoids are at the 50% probability level. Hydrogen atoms have been omitted for clarity

Table 2.13 Crystal data and structure refinement for [Cu(Bz^{t}BPtuH-κ^1S)$_2$Cl]

Identification code	ic8	
Empirical formula	$C_{52}H_{72}ClCuN_4O_2S_2$	
Formula weight	948.25	
Temperature	150(2) K	
Wavelength	0.71073 Å	
Crystal system	Monoclinic	
Space group	P2(1)/c	
Unit cell dimensions	a = 11.9675(3) Å	$\alpha = 90°$
	b = 26.5010(5) Å	$\beta = 92.605(1)°$
	c = 16.0507(3) Å	$\gamma = 90°$
Volume	5085.23(19) Å^3	
Z	4	
Density (calculated)	1.239 Mg/m^3	
Absorption coefficient	0.606 mm^{-1}	
F(000)	2024	
Crystal size	0.42 x 0.38 x 0.32 mm^3	
Theta range for data collection	1.48 to 26.38°.	
Index ranges	$-13 \leq h \leq 14$, $-33 \leq k \leq 33$, $-20 \leq l \leq 10$	
Reflections collected	29052	
Independent reflections	10334 [R(int) = 0.0179]	
Absorption correction	Semi-empirical from equivalents	
Max. and min. transmission	0.8296 and 0.7848	
Refinement method	Full-matrix least-squares on F^2	
Data / restraints / parameters	10334 / 2 / 587	
Goodness-of-fit on F^2	1.024	
Final R indices [I>2sigma(I)]	R1 = 0.0440, wR2 = 0.1123	
R indices (all data)	R1 = 0.0516, wR2 = 0.1183	
Largest diff. peak and hole	1.125 and -0.986 e.Å^{-3}	

Table 2.14 Selected bond lengths [Å] and angles [°] for [Cu(Bz^{t}BPtuH-κ^1*S*)$_2$Cl] with estimated standard deviations in parentheses

Bond lengths:

	Ligand 1		*Ligand 2 (labelled a)*
S(1)-Cu(1)	2.2257(7)	Cu(1)-S(1A)	2.2285(6)
Cu(1)-Cl	2.2420(6)		
C(1)-N(2)	1.446(3)	C(1A)-N(2A)	1.443(3)
C(19)-C(25)	1.490(3)	C(19A)-C(25A)	1.492(3)
C(25)-O(1)	1.228(3)	C(25A)-O(1A)	1.225(3)
C(25)-N(1)	1.390(3)	C(25A)-N(1A)	1.387(3)
N(1)-C(26)	1.388(3)	N(1A)-C(26A)	1.395(3)
C(26)-N(2)	1.323(3)	C(26A)-N(2A)	1.323(3)
C(26)-S(1)	1.699(2)	S(1A)-C(26A)	1.695(2)

Bond angles:

S(1)-Cu(1)-Cl	122.58(2)	S(1A)-Cu(1)-Cl	118.85(2)
S(1)-Cu(1)-S(1A)	118.39(2)		
C(26)-S(1)-Cu(1)	110.64(8)	C(26A)-S(1A)-Cu(1)	112.18(8)
C(2)-C(1)-N(2)	119.8(2)	C(2A)-C(1A)-N(2A)	119.9(2)
C(6)-C(1)-N(2)	117.9(2)	C(6A)-C(1A)-N(2A)	117.6(2)
C(3)-C(2)-C(7)	116.1(2)	C(3A)-C(2A)-C(7A)	115.9(2)
C(1)-C(2)-C(7)	127.1(2)	C(1A)-C(2A)-C(7A)	127.7(2)
C(3)-C(4)-C(15)	122.9(2)	C(3A)-C(4A)-C(15A)	121.8(2)
C(5)-C(4)-C(15)	119.5(2)	C(5A)-C(4A)-C(15A)	120.4(2)
C(5)-C(6)-C(11)	119.2(2)	C(5A)-C(6A)-C(11A)	119.8(2)
C(1)-C(6)-C(11)	124.0(2)	C(1A)-C(6A)-C(11A)	123.5 (2)
C(20)-C(19)-C(25)	122.8(2)	C(20A)-C(19A)-C(25A)	124.6(2)
C(24)-C(19)-C(25)	117.6(2)	C(24A)-C(19A)-C(25A)	115.9(2)
O(1)-C(25)-N(1)	122.0(2)	O(1A)-C(25A)-N(1A)	121.6(2)
O(1)-C(25)-C(19)	121.4(2)	O(1A)-C(25A)-C(19A)	120.2(2)
N(1)-C(25)-C(19)	116.6 (2)	N(1A)-C(25A)-C(19A)	118.2(2)
C(26)-N(1)-C(25)	126.52)	C(25A)-N(1A)-C(26A)	125.7(2)
N(2)-C(26)-N(1)	117.0(2)	N(2A)-C(26A)-N(1A)	116.9(2)
N(2)-C(26)-S(1)	122.9 (2)	N(2A)-C(26A)-S(1A)	122.3(2)
N(1)-C(26)-S(1)	120.1(2)	N(1A)-C(26A)-S(1A)	120.9(2)
C(26)-N(2)-C(1)	125.7 (2)	C(26A)-N(2A)-C(1A)	124.1(2)

Table 2.15 Selected torsion angles [°] for [Cu(Bz^{t}BPtuH-κ^1S)$_2$Cl]

	Ligand 1	*Ligand 2 (labelled a)*
N(2)-C(1)-C(2)-C(3)	-178.1(2)	-171.3(2)
N(2)-C(1)-C(6)-C(5)	177.6(2)	172.7(2)
C(25)-C(19)-C(20)-C(21)	175.3(2)	180.0(2)
C(25)-C(19)-C(24)-C(23)	-176.0(2)	179.5(2)
C(24)-C(19)-C(25)-O(1)	15.0(3)	0.9(3)
C(20)-C(19)-C(25)-O(1)	-159.9(2)	-179.7(2)
C(24)-C(19)-C(25)-N(1)	-166.1(2)	-178.1(2)
C(20)-C(19) C(25)-N(1)	18.9(3)	1.3(3)
O(1)-C(25)-N(1)-C(26)	12.8(4)	-5.6(4)
C(19)-C(25)-N(1)-C(26)	-166.1(2)	173.3(2)
C(25)-N(1)-C(26)-N(2)	-4.6(3)	10.4(3)
C(25)-N(1)-C(26)-S(1)	174.0(2)	-168.1(2)
N(1)-C(26)-N(2)-C(1)	174.5(2)	-178.7(2)
S(1)-C(26)-N(2)-C(1)	-4.1(3)	-0.2(3)
C(2)-C(1)-N(2)-C(26)	88.8(3)	79.2(3)
C(6)-C(1)-N(2)-C(26)	-94.6(3)	-100.8(3)

2.2.2.6.2 Crystal Structure of [Co(Bz^{t}BPtuH-κ^1S)$_2$Cl$_2$]

The ORTEP diagram of the complex [Co(Bz^{t}BPtuH-κ^1S)$_2$Cl$_2$] is shown in **Fig. 2.7** with crystal data and structure refinement details given in **Table 2.16,** selected bond lengths and angles in **Table 2.17** and selected torsion angles in **Table 2.18**. The complex has a distorted tetrahedral monomeric structure. The two Bz^{t}BPtuH ligands are bound to the Co atom through two sulfur atoms and the remaining two coordination sites are occupied by Cl ligands. The Co–S bond distances (2.316(8) Å and 2.329(9) Å) and the Co–Cl bond distances (2.230(9) and 2.229(9) Å) are similar to those found for [Co(tu)$_2$Cl$_2$][37] [Co–S 2.30(1) and 2.32(1) Å and Co–Cl 2.29(1) and 2.27(1) Å] (Co–Cl is little longer)]. One bond angle is greater than the tetrahedral angle (Cl(2)–Co–Cl(1) = 122.69(3)), but the other three angles are closer to the tetrahedral angle (109°28'). As observed in the free ligand, the O and S atoms are *trans* to each other. The two C–S distances are similar at 1.699(3) and 1.693(3) Å, but slightly longer than the free ligand C–S distance (1.679(3) Å), due to the coordination with Co. There is no significant

---

[37] D. Dew. Hall, W. DeW. Horrocks Junior, *Inorg. Chem.*, 1969, **8**, 1809.

change in the carbonyl C=O bond lengths (1.219(4) and 1.227(4) Å) when compared with the free ligand (1.226(3) Å). The bond lengths of the imine system are similar to those found in the free ligand.

The intramolecular hydrogen bond between N(2)–H and O(1) is 1.954(6) Å in ligand 1 and 1.943(6) Å in ligand 2. This results in an almost planar six-membered ring with the C(25), N(1) and C(26) atoms in the central part of the molecule. For example, the C(25)–N(1)–C(26)–N(2) torsion angle is -6.1(5)° in ligand 1 and 5.3(4)° in ligand 2. As well in the crystal there are weak intermolecular hydrogen bonds between different molecules (N(2)–H...O(1) = 2.428(6) Å and C–H(*tert*-butyl)...O(1) = 2.523(6) Å).

The phenyl rings are twisted out of the plane of the central part of the ligands. For example, the torsion angle involving the benzoyl ring, C(24)–C(19)–C(25)–O(1) is -167.3(3)° for ligand 1 and -152.7(3)° for ligand 2. The *tert*-butyl substituted ring is twisted out of the plane even further with the C(2)–C(1)–N(2)–C(26) torsion angles being 94.4(4) and -90.0(4)°.

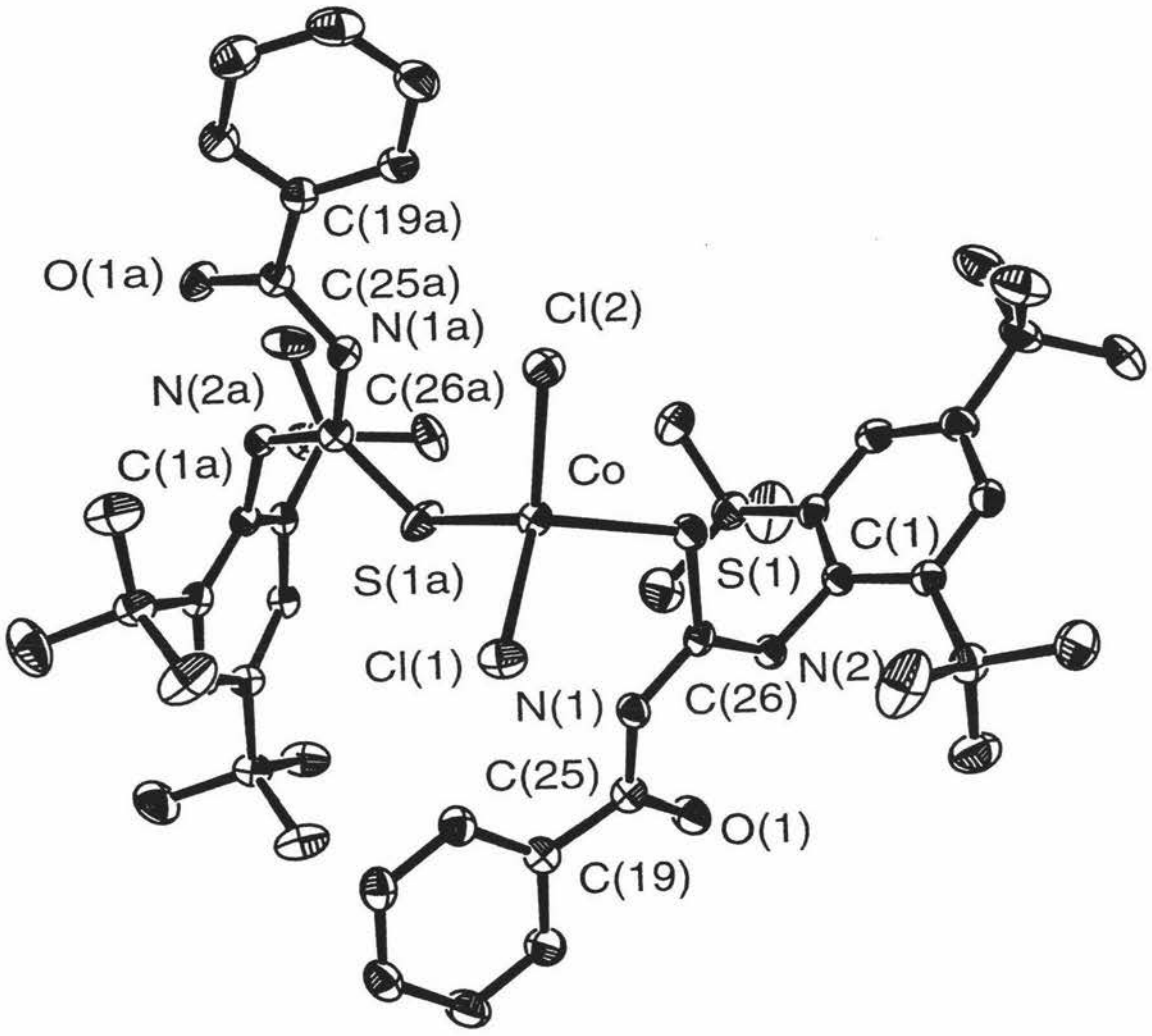

Figure 2.7 ORTEP diagram for the complex $[Co(Bz^tBPtuH\text{-}\kappa^1S)_2Cl_2]$ showing the numbering system used. Thermal ellipsoids are at the 50% probability level. Hydrogen atoms have been omitted for clarity

Table 2.16 Crystal data and structure refinement for $[Co(Bz^tBPtuH\text{-}\kappa^1S)_2Cl_2]$

Identification code	ic7a	
Empirical formula	$C_{52}H_{72}Cl_2CoN_4O_2S_2$	
Formula weight	979.09	
Temperature	150(2) K	
Wavelength	0.71073 Å	
Crystal system	Triclinic	
Space group	P-1	
Unit cell dimensions	a = 9.2734(1) Å	α= 97.62°
	b = 15.7403(1) Å	β= 96.249(1)°
	c = 18.6447(2) Å	γ = 92.064(1)°
Volume	2677.89(4) $Å^3$	
Z	2	
Density (calculated)	1.214 Mg/m^3	
Absorption coefficient	0.539 mm^{-1}	
F(000)	1042	
Crystal size	0.32 x 0.22 x 0.16 mm^3	
Theta range for data collection	1.11 to 26.51°	
Index ranges	$-11 \leq h \leq 11$, $-19 \leq k \leq 19$, $-23 \leq l \leq 23$	
Reflections collected	25477	
Independent reflections	10900 [R(int) = 0.0457]	
Absorption correction	Semi-empirical from equivalents	
Max. and min. transmission	0.9187 and 0.8464	
Refinement method	Full-matrix least-squares on F^2	
Data / restraints / parameters	10900 / 0 / 568	
Goodness-of-fit on F^2	1.048	
Final R indices [I>2sigma(I)]	R1 = 0.0557, wR2 = 0.1593	
R indices (all data)	R1 = 0.0785, wR2 = 0.1748	
Largest diff. peak and hole	1.676 and -1.042 $eÅ^{-3}$	

Table 2.17 Selected bond lengths [Å] and angles [°] for $[Co(Bz^tBPtuH\text{-}\kappa^1S)_2Cl_2]$ with estimated standard deviations in parentheses

Bond lengths:

	Ligand 1		*Ligand 2 (labelled a)*
Co-Cl(1)	2.2302(9)	Co-Cl(2)	2.2295(9)
Co-S(1)	2.3161(8)	Co-S(1A)	2.3299(9)
S(1)-C(26)	1.699(3)	S(1A)-C(26A)	1.693(3)
C(1)-N(2)	1.446(4)	N(2A)-C(1A)	1.438(4)
C(19)-C(25)	1.487(4)	C(19A)-C(25A)	1.480(4)
C(25)-O(1)	1.219(4)	C(25A)-O(1A)	1.227(4)
C(25)-N(1)	1.381(4)	C(25A)-N(1A)	1.384(4)
N(1)-C(26)	1.381(4)	N(1A)-C(26A)	1.377(4)
C(26)-N(2)	1.315(4)	C(26A)-N(2A)	1.314(4)

Bond angles:

Cl(2)-Co-Cl(1)	122.69(3)	S(1)-Co-S(1A)	107.71(3)
Cl(1)-Co-S(1)	108.28(3)	Cl(1)-Co-S(1A)	104.71(4)
Cl(2)-Co-S(1)	101.28(3)	Cl(2)-Co-S(1A)	111.42(3)
C(26)-S(1)-Co	110.5(1)	C(26A)-S(1A)-Co	114.9(1)
C(6)-C(1)-N(2)	119.1(3)	C(6A)-C(1A)-N(2A)	118.7(3)
C(2)-C(1)-N(2)	117.6(3)	C(2A)-C(1A)-N(2A)	119.1(3)
C(3)-C(2)-C(7)	119.5(3)	C(3A)-C(2A)-C(7A)	117.4(2)
C(1)-C(2)-C(7)	123.9(3)	C(1A)-C(2A)-C(7A)	125.7(3)
C(5)-C(4)-C(15)	123.0(3)	C(5A)-C(4A)-C(15A)	119.1(3)
C(3)-C(4)-C(15)	119.6(3)	C(3A)-C(4A)-C(15A)	123.6(3)
C(1)-C(6)-C(11)	128.4(3)	C(1A)-C(6A)-C(11A)	126.8(3)
C(5)-C(6)-C(11)	115.5(3)	C(5A)-C(6A)-C(11A)	116.6(3)
C(20)-C(19)-C(25)	117.0(3)	C(20A)-C(19A)-C(25A)	117.5(3)
C(24)-C(19)-C(25)	124.0(3)	C(24A)-C(19A)-C(25A)	123.1(3)
O(1)-C(25)-N(1)	121.5(3)	O(1A)-C(25A)-N(1A)	121.5(3)
O(1)-C(25)-C(19)	122.3(3)	O(1A)-C(25A)-C(19A)	121.2(3)
N(1)-C(25)-C(19)	116.2(3)	N(1A)-C(25A)-C(19A)	117.3(3)
C(25)-N(1)-C(26)	126.8(3)	C(26A)-N(1A)-C(25A)	126.6(3)
N(2)-C(26)-N(1)	118.3(3)	N(2A)-C(26A)-N(1A)	118.4(3)
N(2)-C(26)-S(1)	120.8(2)	N(2A)-C(26A)-S(1A)	120.6(2)
N(1)-C(26)-S(1)	120.9(2)	N(1A)-C(26A)-S(1A)	121.0(2)
C(26)-N(2)-C(1)	121.2(3)	C(26A)-N(2A)-C(1A)	122.3(2)

Table 2.18 Selected torsion angles [°] for $[Co(Bz^tBPtuH\text{-}\kappa^1S)_2Cl_2]$

	Ligand 1	*Ligand 2 (labelled a)*
N(2)-C(1)-C(2)-C(3)	-168.9(3)	166.7(3)
N(2)-C(1)-C(6)-C(5)	169.7(3)	-167.7(3)
C(25)-C(19)-C(20)-C(21)	179.1(3)	-179.1(3)
C(25)-C(19)-C(24)-C(23)	-179.0(3)	178.0(3)
C(24)-C(19)-C(25)-O(1)	-167.3(3)	-152.7(3)
C(20)-C(19)-C(25)-O(1)	12.4(5)	24.4(4)
C(24)-C(19)-C(25)-N(1)	12.6(5)	29.2(4)
C(20)-C(19) C(25)-N(1)	-167.8(3)	-153.7(3)
O(1)-C(25)-N(1)-C(26)	8.0(5)	0.1(5)
C(19)-C(25)-N(1)-C(26)	-171.9(3)	178.2(3)
C(25)-N(1)-C(26)-N(2)	-6.1(5)	5.3(4)
C(25)-N(1)-C(26)-S(1)	174.6(3)	-175.8(2)
N(1)-C(26)-N(2)-C(1)	177.3(3)	-177.9(2)
S(1)-C(26)-N(2)-C(1)	-3.3(4)	3.2(4)
C(2)-C(1)-N(2)-C(26)	94.4(4)	-90.0(4)
C(6)-C(1)-N(2)-C(26)	-82.0(4)	86.0(4)

2.3 Conclusions

Compounds of the type $[M(L)_2]$ (M = Cu, L = Bz^tBPtu or Bz^iPPtu), $[M(LH)_2X_2]$ (M = Cu(II) or Co(II), LH = Bz^tBPtuH or Bz^iPPtuH, X = Cl; M = Ni(II), LH = Bz^tBPtuH, X = I), $[M(LH)_2Cl]$ (M = Cu(I), LH = Bz^tBPtuH, BzPPtuH, Bz^iPPtuH or BzFPtuH), $[Cu(BzPtuH)_3Cl]$ and $[M(LH)_4]PF_6$ (M = Cu(I) or Ag(I), LH = Bz^tBPtuH or Bz^iPPtuH) have been synthesized. The deprotonated ligands, Bz^tBPtu and Bz^iPPtu, in the complexes $[Cu(Bz^tBPtu)_2]$ and $[Cu(Bz^iPPtu)_2]$ coordinate through the O and S atoms resulting in six-membered chelate rings from the anionic ligands. The electronic spectra give support for thiocarbonyl S being bound to the metal. This, combined with ESR spectra suggests square planar structures for $[M(L)_2]$ (L = Bz^tBPtu or Bz^iPPtu).

For $[Cu(Bz^tBPtuH)_2Cl_2]$, the ligand remains neutral and binds through the S atom to form a distorted tetrahedral complex. Generally most of the ligands gave red solutions with $CuCl_2$ indicative of the presence of species similar to the above, but they quickly lost their colour to give yellow or green-yellow $[Cu(LH)_2Cl]$ (LH = Bz^tBPtuH, Bz^iPPtuH, BzPPtuH or BzFPtuH) or $[Cu(BzPtuH)_3Cl]$ complexes. A report by Satpathy *et al.*[5] that an ice-green Cu(II) complex of stoichiometry $[Cu(BzPtuH)_2Cl_2]$ was isolated

under thermal conditions must be in doubt. Instead in this work a copper(I) complex has been formed. Their claim that the ligand binds through O and S atoms should also be challenged. The X-ray crystal structure of the light yellow [Cu(Bz^tBPtuH-κ^1-*S*)$_2$Cl] complex shows the ligands bound through S and the copper(I) complex has a trigonal planar structure. As well the yellow complex [Cu(BzPtuH)$_3$Cl] shows no signs of oxygen binding from the IR spectrum.

The structure of [Co(Bz^tBPtuH)$_2$Cl$_2$] is distorted tetrahedral with cobalt having an S_2Cl_2 donor set, while the structure for [Ni(Bz^tBPtuH)$_2$I$_2$] remains uncertain.

The complexes [M(LH)$_4$]PF_6 (M = Cu(I) or Ag(I), LH = Bz^tBPtuH or Bz^iPPtuH) probably have tetrahedral structures but the ligands dissociate at room temperature in solution.

CHAPTER THREE

The Coordination Characteristics and Reactivity of 1-Benzoyl-3-(2,4,6-tri-*tert*-butylphenyl)thiourea and Related Ligands with $HgCl_2$ and Mercury and Silver Acetates

3.0 INTRODUCTION

To the best of our knowledge no studies have been done on the interaction of $Hg(Ac)_2$ with the title ligands. The main focus of this chapter will be a study of these interactions and to compare the results with those for $HgCl_2$.

Hiremath *et al.*[1] have prepared a 1:1 complex of Hg(II) chloride with benzoylthiourea and characterised it by microanalysis.

Negoiu *et al.*[2] have prepared $[Hg(HL)_2Cl_2]$ (HL = 1-benzoyl-3-(2,4-dimethylphenyl)thiourea) and characterized it by IR spectroscopy and postulated a tetrahedral geometry for the Hg(II) complex, where the ligand acts as a monodentate, being S-bonded to the metal ion.

However thiourea (tu) reacts with $HgCl_2$ to give a variety of complexes viz. $[Hg(tu)Cl_2]$[3], $[Hg(tu)_2Cl_2]$[4], $[Hg(tu)_3Cl_2]$[5] and $[Hg(tu)_4]Cl_2$ [6]. The mercury complex $[Hg(II)(tu)_2Cl_2]$ is formulated as $[Hg(II)(tu)_2Cl]Cl$ in which the

---

[1] A.C. Hiremath and A.S.R. Murthy, *Indian J. Chem., A*, 1977, **15A**, 55.
[2] D. Negoiu, V. Circu, T. Rosu and N. Badicu, *Rev. Chim. (Bucharest)*, 1999, **50**, 88.
[3] *Inorg. Synth.*, 1960, **6**, 27.
[4] P.D. Brotherton, P.C. Healy, C.L. Raston and A.H. White, *J. Chem. Soc. Dalton Trans.*, 1973, 334.
[5] A. Korczynski, *Rocz. Chem.*, 1968, **42**, 1207.
[6] A. Korczynski, M. Nardelli, M.A. Pellinghelli, *Rocz. Chem.*, 1973, **47**, 905.

chlorobis(thiourea)mercury ion is trigonal planar. This structure was confirmed by Brotherton *et al.*[4], whereas [Ag(I)$(tu)_2$Cl] was shown to consist of infinite spiraling chains of -Ag-S-Ag-S-, each silver atom being surrounded by a distorted tetrahedron of ligands[7].

Lessmann *et al.*[8] have synthesised the first chloro-bridged thiourea mercury(II) complex which is formulated as $[C_6H_5C(OCH_3)NC(S)N(C_2H_5)_2HgCl_2]_2$. FAB mass spectrometry, IR spectroscopy and NMR spectroscopy characterized the compound. The dimeric structure was established crystallographically. In this structure each mercury atom takes a tetragonal distorted geometry and is coordinated by two bridging chloride atoms, one terminal chloride atom and one thiocarbonyl sulfur atom of the ligand [8].

In this chapter the interactions of the ligands with the acetates, $M(Ac)_2$ (M = Zn(II), Cd(II) and UO_2^{2+}) and NaOEt will be investigated.

3.1 Experimental

3.1.1 Instrumentation

Elemental analyses, ^1H and ^{13}C NMR spectra, IR spectra, mass spectra and melting points were performed as described previously.

3.1.2 Materials

All the reagents and solvents were of analytical grade and used without further purification. Uranyl acetate, mercuric acetate and chloride were supplied by May and Baker Ltd., zinc chloride from Scharlau Chemie S.A., cadmium acetate dihydrate and zinc acetate dihydrate from BDH Chemicals Ltd., silver acetate from Hopkin and Williams Ltd., sodium from Riedel-de-Haen Ltd., sodium acetate from Ajax Chemicals Ltd., and thiourea, thioacetamide, thiobenzamide, phenylthiourea, 4,4'-bis(dimethylamino)thiobenzophenone, thiocaprolactam, dithizone, thiocamphor, and bis(diphenyl-thiophosphoryl)amide from Aldrich Chemical Company, Inc.

---

[7] E. A. Vizzini and E.L. Amma, *J. Am. Chem. Soc.,* 1966, **88**, 2872.
[8] F. Leßmann, L. Beyer and J. Sieler, *Inorg. Chem. Commun.*, 2000, **3**, 62.

3.1.3 Preparation of Metal Complexes and Derived Organic Products

The abbreviations used in this chapter for the ligands are given in Chapter 2, and the abbreviations for the other compounds along with their names and structures are given in **Fig. 3.1**.

3.1.3.1 Reactions with MCl_2 (M = Hg or Zn)

[Hg(Bz^{t}BPtuH-κ^1S)$_2$Cl$_2$]

To Bz^{t}BPtuH 0.0530g (0.1250 mmol) dissolved in ~10 ml of ethanol, was added 0.0339g (0.1248 mmol) of $HgCl_2$ in ~10 ml of ethanol. The resulting solution was warmed gently and left to stand at room temperature. The white product was filtered and washed with ethanol. Yield, 0.0500g (35.77%). Anal. Found: C, 55.75; H, 6.52; N, 5.12; S, 5.77; Cl, 6.00%. Calculated for $C_{52}H_{72}Cl_2HgN_4O_2S_2$: C, 55.73; H, 6.43; N, 5.00; S, 5.71; Cl, 6.34%.

[Hg(Bz^{i}PPtuH-κ^1S)$_2$Cl$_2$]

This complex was prepared by either Method (a) or Method (b).

Method (a): A solution of $HgCl_2$ (0.0678g, 0.2497 mmol) in ethanol (~5 ml) was added to a solution of Bz^{i}PPtuH (0.1700g, 0.5000 mmol) in ethanol (~10 ml). The resultant solution was kept at room temperature and a white crystalline product was filtered, washed with ethanol and air-dried to give 0.1930g (81%). Anal. Found: C, 50.36; H, 5.19; N, 5.91; S, 6.68%. Calculated for $C_{40}H_{48}Cl_2HgN_4O_2S_2$: C, 50.47; H, 5.05; N, 5.88; S, 6.73%.

Method (b): A solution of $HgCl_2$ (0.0678g, 0.2497 mmol) and Bz^{i}PPtuH (0.3400g, 1.000 mmol) in ethanol (~12 ml) was kept at room temperature, and after 3 days, white crystals of the product were collected and washed with ethanol. Yield: 0.0640g (67%). Anal. Found: C, 50.10; H, 5.10; N, 5.94; S, 6.71%. Calculated for $C_{40}H_{48}Cl_2Hg\,N_4O_2S_2$: C, 50.47; H, 5.05; N, 5.88; S, 6.73%.

[Hg(BzFPtuH-κ^1S)$_2$Cl$_2$]

A solution of $HgCl_2$ (0.1357g, 0.4998 mmol) in ethanol (~5 ml) was added to a solution of BzFPtuH (0..2740g, 1.000 mmol) in ethanol (~10 ml). The white product, which formed at once, turned to a white pulp-like precipitate. This precipitate was filtered, washed with ethanol and air-dried to give 0.1230g, 30%. Anal. Found: C, 41.03; H, 2.66; N, 6.86; S, 7.77%. Calculated for $C_{28}H_{22}Cl_2F_2HgN_4O_2S_2$: C, 41.03; H, 2.69; N, 6.84; S, 7.81%.

[Hg(BzPtuH-κ^1S)Cl$_2$]

A solution of $HgCl_2$ (0.1357g, 0.4998 mmol) in ethanol (~5 ml) was added to a solution of BzPtuH (0.2560g, 1.000 mmol) in ethanol (~10 ml). The white precipitate, which formed at once, was filtered and washed with ethanol. Yield 0.1970g, 74.8%. Anal. Found: C, 31.85; H, 2.59; N, 5.33; S, 6.15%. Calculated for $C_{14}H_{12}Cl_2HgN_2OS$: C, 31.85; H, 2.27; N, 5.31; S, 6.07%.

Attempted syntheses of [Zn(LH)$_2$Cl$_2$] (LH = Bz^{t}BPtuH or Bz^{i}PPtuH or BzFPtuH or BzPtuH)

Reacting LH with $ZnCl_2$ in 2:1 molar ratio in ethanol gave white crystals, after leaving the reaction mixture for 1 to 2 days. The products, which separated, were filtered and washed with ethanol and characterized by elemental analyses, melting points, IR, FAB(+) MS and ^1H and ^{13}C NMR spectroscopy. All the data were identical to the free ligands showing no chemical reaction occurred.

3.1.3.2 Reactions with Hg(Ac)$_2$ and Ag(Ac)

1-benzoyl-2-[ethoxyl-3-(2,4,6-tri-tert-butylphenyl)amino]aldimine (BzE^{t}BPA)

This compound was prepared according to Method (a), Method (b) or Method (c) with the first method being the best.

Method (a): To a solution of Bz^{t}BPtuH 0.2120g (0.5000 mmol) in ~15 ml of ethanol, was added 0.1592g (0.4995mmol) of mercuric acetate in ~15 ml of ethanol. A yellow coloured precipitate formed at once which turned dark brown and then black. The

precipitate was filtered and found quantitatively to be HgS. From the filtrate, white needle shaped crystals was isolated after 3 days. Yield, 0.1040g (47.7%), m.p. 157.6-158.0 °C. Anal. Found: C, 77.28; H, 9.89; N, 6.46%; S, nil. Calculated for $C_{28}H_{40}N_2O_2$: C, 77.06; H, 9.17; N, 6.42%.

Method (b): To a solution of $Hg(Bz^tBPtuH)_2Cl_2$ 0.0559g (0.0499 mmol) in ~10 ml of ethanol, was added 0.0164g (0.1999 mmol) of sodium acetate in ~10 ml of ethanol. The light brown precipitate turned to black HgS and this was filtered and the solvent volume reduced using a rotary evaporator. The white product was filtered off and washed with ethanol. Yield, 0.0150g (69%), m.p. 155-156 °C. From the IR spectroscopy and mass spectrum the compound was identified mainly as BzE^tBPA with a trace of Bz^tBPtuH.

Method (c): To a solution of Bz^tBPtuH 0.0530g (0.1250 mmol) in ethanol (~10 ml), was added 0.0208g (0.1246 mmol) of silver acetate in ethanol (~10 ml). A similar sequence of color changes was observed as before upon heating and the black Ag_2S was filtered off. The volume of the filtrate was reduced using a rotary evaporator. The white product, which separated, was filtered off and washed with ethanol. The yield was very low. The melting point (157-158.0 °C) and IR spectrum was similar to the product obtained in (a) which supports BzE^tBPA being the major product, with a trace of Bz^tBPtuH.

1-benzoyl-[2-ethoxyl-3-(2,6-diisopropylphenyl)amino]aldimine (BzE^iPPA)

This compound was prepared by Method (a) or Method (b).

Method (a): BzE^iPPA was synthesised by McBeth[9] by reacting mercuric acetate and Bz^iPPtuH in 1:1 ratio in ethanol (~30 ml). A yellow coloured precipitate formed at once which turned dark brown and then to black HgS. From the filtrate white cubic shaped crystals were isolated with a m.p. of 104.5-107 °C. Anal. Found: C, 75.17; H, 8.24; N, 7.99%; S, nil. Calculated for $C_{22}H_{28}N_2O_2$: C, 75.00; H, 7.95; N, 7.95%.

Method (b): A mixture of Bz^iPPtuH (0.1700g, 0.5000 mmol) and silver acetate (0.1693g, 1.0142 mmol) in 15 ml of chloroform stabilised with 1% ethanol, was heated

[9] K. McBeth, 1999, Third Year Research Report, Massey University.

to reflux for 4 h. A similar sequence of colour changes was observed as before and the Ag_2S was filtered, and the filtrate was reduced to dryness using a rotary evaporator. The white oil was triturated in hexane in an ice-bath and the white product which formed, was filtered and washed with hexane. Yield, 0.1025g (47%), m.p. 53-54 °C. The product was identified mainly as BzE^{i}PPA from the mass spectral and IR results.

1-benzoyl-2-[methoxyl-3-(2,4,6-tri-tert-butylphenyl)amino]aldimine (BzM ^{t}BPA)

To a solution of Bz^{t}BPtuH 0.2120g (0.5000 mmol) in methanol (~10 ml), was added 0.1592g (0.4995 mmol) of mercuric acetate in methanol (~10 ml). A similar sequence of colour changes was observed as above and the HgS was filtered. The filtrate was left standing for a week, whereupon white chunky crystals of the product deposited. Yield, 0.0900g (43%), m.p. 183-188 °C. Anal. Found: C, 76.93; H, 9.09; N, 6.80%; S, nil. Calculated for $C_{27}H_{38}N_2O_2$: C, 76.77; H, 9.00; N, 6.64%.

1-benzoyl-2-[phenylmethoxyl-3-(2,4,6-tri-tert-butylphenyl)amino]aldimine (BzPM ^{t}BPA)

To a solution of Bz^{t}BPtuH 0.053g (0.1250 mmol) in benzyl alcohol (~10 ml), was added 0.0339g (0.1063 mmol) of mercuric acetate in benzyl alcohol (~10 ml). A similar sequence of colour changes was observed as above and the HgS was filtered. The filtrate was left standing for four weeks. The white product, which separated, was filtered off and washed with benzyl alcohol. Yield, 0.0150g (28%), m.p. 169-173 °C Anal. Found: C, 79.26; H, 8.62; N, 5.64%; S, nil. Calculated for $C_{33}H_{42}N_2O_2$: C, 79.52; H, 8.43; N, 5.62%.

1-benzoyl-2-[ethoxyl-3-(2,4,6-tri-phenylphenyl)amino]aldimine (BzEPPA)

To a solution of BzPPtuH 0.2420g (0.5000 mmol) in ethanol (~10 ml), was added 0.1593g (0.4998 mmol) of mercuric acetate in ethanol (~10 ml). A similar sequence of colour changes was observed as above and the HgS was filtered. The filtrate was reduced in volume using a rotary evaporator. The white product, which separated, was filtered off and washed with ethanol. Yield, 0.1680g (68%), m.p. 180-180.6 °C Anal. Found: C, 82.33; H, 5.58; N, 5.75%; S, nil. Calculated for $C_{34}H_{28}N_2O_2$: C, 82.25; H, 5.64; N, 5.64%.

1-benzoyl-2-[ethoxyl-3-(4-fluorophenyl)amino]aldimine (BzEFPA)

To a solution of BzFPtuH 0.5480g (2.000mmol) in ~10 ml of ethanol, was added 0.6374g (2.000 mmol) of mercuric acetate in ~15 ml of ethanol. A yellow coloured precipitate formed at once which turned dark brown and upon heating to black HgS. After filtration the filtrate was reduced in volume using a rotary evaporator, and left to stand for one day in a fridge. The white crystals were filtered and washed with ethanol, and dried in *vacuo*. Yield, 0.0860g (15%), m.p. 60.0-60.9 °C. Anal. Found: C, 67.13; H, 5.31; N, 10.04; F, 6.35%; S, nil. Calculated for $C_{16}H_{15}N_2O_2$: C, 67.13; H, 5.24; N, 9.79; F, 6.64%.

1-benzoyl-2-[ethoxyl-3-(phenyl)amino]aldimine (BzEPA)

To a solution of BzPtuH 0.5120g (2.000 mmol) in ~10 ml of ethanol, was added 0.6360g (1.9956 mmol) of mercuric acetate in ~15 ml of ethanol. A yellow precipitate formed at once which turned dark brown and then to black HgS, which was filtered. The filtrate was reduced in volume using a rotary evaporator, and left to stand for one day in a fridge. The white crystals were filtered and washed with ethanol, and dried in *vacuo*. Yield, 0.1560g (29%), m.p. 35-38 °C. Anal. Found: C, 71.22; H, 5.89; N, 11.24%; S, nil. Calculated for $C_{16}H_{16}N_2O_2$: C, 71.64; H, 5.97; N, 10.45%.

3.1.3.3 The Reactions of other Thiocarbonyls with $Hg(Ac)_2$

The following reactions all produced HgS. The products of the reactions were known compounds and were generally characterized by IR, mass spectroscopy or the melting point.

Reaction with thiourea to form cyanamide

To a solution of $Hg(Ac)_2$ (0.6374g, 2.000 mmol) in ethanol (50 ml) was added thiourea (0.1520g, 2.000 mmol) in ethanol (10 ml). A yellow coloured precipitate formed at once, which turned dark brown and then to black HgS (100%) which was filtered off. The filtrate was reduced in volume using a rotary evaporator to give a white oil which turned to a white oily solid upon cooling. The product was dried in *vacuo* and was identified as cyanamide (NH_2-C≡N) by mass spectroscopy and IR. FAB (+) MS

(meta-nitrobenzylalcohol): M^+ 42 (100%), 41 (12%) $[NH\text{-}C\equiv N]^+$, IR (cm^{-1}): ν(NH) 3384, ν(C≡N) 2261 (cf. lit. 2269 cm^{-1} from SDBS N° 22210).

Reaction with thioacetamide to form acetonitrile

To a solution of $Hg(Ac)_2$ (0.6374g, 2.000 mmol) in ethanol (10 ml) was added thioacetamide (0.1502g, 2.000 mmol) in ethanol (10 ml). The black HgS (~96%) was filtered. The product acetonitrile (bp 81 °C), has a similar boiling point to ethanol (bp 78 °C) and could not be easily separated. IR (cm^{-1}): ν(C≡N) 2349. (cf. with an authentic sample ν(C≡N) 2349 cm^{-1}).

Reaction with thiobenzamide to form benzonitrile

To a solution of $Hg(Ac)_2$ (0.3187g, 1.000 mmol) in ethanol (10 ml) was added thiobenzamide (0.1370g, 1.000 mmol) in ethanol (10 ml) . A similar sequence of colour changes was observed as above and the HgS (~96%) was filtered. The filtrate was reduced in volume using a rotary evaporator. The yellow oil and the white gel like product, which separated, was filtered off and washed with petroleum ether. The solid 'cracked' when filtering. The yellow oil was identified as benzonitrile ($C_6H_5\text{-}C\equiv N$). IR (cm^{-1}): ν(C≡N) 2229 cm^{-1} (cf. with an authentic sample ν(C≡N) 2229 cm^{-1}). FAB (+) MS (meta-nitrobenzylalcohol): M^+ 103 (22%).

Reaction with phenylthiourea to give phenylcyanamide

To a solution of $Hg(Ac)_2$ (0.3187g, 1.000 mmol) in ethanol (10 ml) was added phenylthiourea (0.1520g, 1.000 mmol) in ethanol (10 ml) . A similar sequence of colour changes was observed as above and the HgS (~98%) was filtered. The filtrate was reduced to dryness using a rotary evaporator. The white oil, which formed, was left to stand for one day in a fridge and then dried in *vacuo*. It was identified as phenylcyanamide ($C_6H_5NH\text{-}C\equiv N$) from IR ($cm^{-1}$): ν(N-H) 3172 (cf 3145)[10] and ν(C≡N) 2228 (cf. 2231 cm^{-1})[10] and FAB (+) MS (meta-nitrobenzylalcohol): M^+ 118 (100%), 91 (48%) $[M\text{-}CNH]^+$, 77 (25%) $[C_6H_5]^+$.

---

[10] M.L. Brader, 1988, Ph.D. Thesis and S.L. Ingham, 1987, Hons. Thesis, Massey University.

Reaction with 4,4'-bis(dimethylamino)thiobenzophenone to give 4,4'- bis(dimethylamino)benzophenone

To a solution of $Hg(Ac)_2$ (0.3187g, 1.000 mmol) in ethanol (10 ml) was added 4,4'-bis(dimethylamino)thiobenzophenone (0.2844g, 1.000 mmol) in ethanol (150 ml) . The reaction mixture was refluxed for 2 days. The black yellow product, which separated, was filtered off and washed with ethanol to give 0.1400g of HgS (60% yield). The filtrate was reduced to dryness using a rotary evaporator to give three bands of the colour: green, yellow and red. The yellow and red bands were dissolved in hot ethanol (~5 ml) and red crystals separated from the solution within 15 minutes. These were filtered and washed with ethanol. Anal. Found: C, 74.20; H, 7.44; N, 10.36%; S, 4.00%. Calculated for $C_{17}H_{20}N_2S$: C, 71.83; H, 7.04; N, 9.86; S, 11.27% and for $C_{17}H_{20}N_2O$: C, 76.12; H, 7.46; N, 10.44%. The product was a mixture of the starting thiobenzophenone and the benzophenone. The yellow filtrate was reduced in volume by rotary evaporation to give a yellow product, which was filtered and washed with ethanol. Yield: 0.06g (22%), m.p. 146-150 °C (lit. 174-176 °C from the Aldrich Handbook of Fine Chemicals). Anal. Found: C, 74.27; H, 7.54; N, 10.14%; S, nil. Calculated for $C_{17}H_{20}N_2O$: C, 76.12; H, 7.46; N, 10.44%. Analytical data shows some contamination with the starting material. FAB (+) MS (meta-nitrobenzylalcohol): MH^+ 269 (100%), 148 (30%) $[M\text{-}C_6H_5N_2O]^+$, IR (cm^{-1}): ν(C=O) 1604.

Reaction with thiocaprolactam

To a solution of $Hg(Ac)_2$ (0.3187g, 1.000 mmol) in ethanol (10 ml) was added thiocaprolactam (0.1290g, 1.000 mmol) in ethanol (10 ml) . A similar sequence of colour changes was observed as above and the HgS (80%) was filtered. The filtrate was reduced to dryness using a rotary evaporator. The yellow oil, which formed, was dried in *vacuo* for 2 days. The oil was difficult to characterize from IR and mass spectroscopy. This will be discussed in section **3.2**.

The following thiocarbonyls did not produce HgS.

Reaction with dithizone

To a solution of $Hg(Ac)_2$ (0.3187g, 1.000 mmol) in ethanol (5 ml) was added dithizone (0.2560g, 1.000 mmol) in ethanol (5 ml). The dark red precipitate was heated

for 0.5 h., but this did not result in the production of HgS and the reaction was not followed up.

Reaction with thiocamphor

To a solution of $Hg(Ac)_2$ (0.3187g, 1.000 mmol) in ethanol (10 ml) was added thiocamphor (0.1680g, 1.000 mmol) in ethanol (5 ml). The reaction mixture was heated for ~5 minutes and a pale yellow complex was precipitated, instead of the black HgS precipitate. This reaction was not worked up any further.

Reaction with bis(diphenylthiophosphoryl)amide

To a solution of $(Ph_2PS)_2NH$ (0.1123g, 0.2498 mmol) in ethanol (10 ml) was added $Hg(Ac)_2$ (0.0790g, 0.2478 mmol) in ethanol (10 ml). The reaction mixture was heated for ~10 minutes and a white complex precipitated, instead of HgS, so the reaction was not followed up.

1-acetyl-1-benzoyl-3-(2,6-diisopropylphenyl)urea (ABz ^{i}PPu)

This compound was prepared by Method (a) or Method (b).

Method (a): A mixture of Bz^{i}PPtuH (0.1700g, 0.5000 mmol) and silver acetate (0.1693g, 1.0142 mmol) in 15 ml of dichloromethane was heated to reflux for 1 h. A black precipitate of Ag_2S (~40%) was filtered, and the filtrate was reduced to dryness using a rotary evaporator. The white oil formed was triturated in cold hexane and the white product, was filtered, and washed with hexane. Yield, 0.0413g (22%). m.p. 118-119 °C. Anal. Found: C, 71.64 ; H, 7.18 ; N, 7.88; S, 2.81%. Calculated for $C_{22}H_{26}N_2O_3$: C, 72.13; H, 7.10; N, 7.65%. Crystals suitable for X-ray analysis were grown by recrystallisation from CH_2Cl_2/pentane. Even though the X-ray structure shows no sulfur in the compound, analytical figures show some contamination with the free ligand.

Method (b): A mixture of Bz^{i}PPtuH (0.0680g, 0.2000 mmol) and mercuric acetate (0.0637g, 0.1998 mmol) in 15 ml of dichloromethane was heated to reflux for 1 h. A white precipitate formed at once which turned yellow, dark brown and then black. The black precipitate of HgS (~30%) was filtered and the filtrate was reduced to dryness

using a rotary evaporator. The white oil, which formed, was triturated in hexane in an ice-bath and the white product, was filtered and washed with hexane. Yield, 0.0043g (6%). m.p. 118.4-119 °C. The yield was less and the compound was characterized by the IR (same as for the Method (a) product) and mass spectroscopy.

Reaction of Bz^{t}BPtuH with mercuric acetate (in CH_2Cl_2) to form 2,4,6-tri-tert-butylphenylcyanamide (^{t}BPc)

A mixture of Bz^{t}BPtuH (0.1060g, 0.2500 mmol) and mercuric acetate (0.0796g, 0.2497 mmol) in 15 ml of dichloromethane was heated to reflux for 1 h. A white precipitate formed at once which then turned yellow, dark brown and then black. The black precipitate of HgS (0.0280g, 48% yield) was filtered, and the filtrate was reduced to dryness using a rotary evaporator. The white oil, which formed, was very soluble in hexane, petroleum spirit or diethyl ether, so the product was dried in *vacuo* for 2 days. The IR and ^{1}H and ^{13}C NMR spectroscopy identified a cyanamide group and an acetyl moiety. The reaction mixture was then purified by thin layer chromatography, eluting with a 1:9 (v/v) $CHCl_3$/ *n*-hexane mixture, to give three bands. The top band was identified by its IR and mass spectrum [M^+ = 286 (12%)] to be 2,4,6-tri-*tert*-butylphenylcyanamide (^{t}BPc). Yield, ~0.0050g (7%), m.p. 97-99 °C. The other two bands were a mixture of ^{t}BPc and Bz^{t}BPtuH. Insufficient sample precluded elemental analysis.

Reaction of Bz^{t}BPtuH with C_2H_5ONa to give 2,4,6-tri-tert-butylphenylthiourea (^{t}BPtu)

To Bz^{t}BPtuH 0.0848g (0.2000 mmol) dissolved in 20 ml of ethanol, was added 0.0046g (0.2000 mmol) of sodium in 15 ml of ethanol. The pale yellow solution was stirred at room temperature for 2 days. The white product, which separated, was filtered off and the filtrate was reduced in volume using a rotary evaporator. A suck-back resulted in water filling the flask by accident and the white crude precipitated product was filtered and dried in *vacuo*. It was recrystallized from ethanol to yield a white powder, which was collected by filtration. Yield: 0.0090g, (14%), m.p. 86-90 °C. Anal. Found: C, 71.48; H, 9.86; N, 8.75; S, 9.74%. Calculated for $C_{19}H_{32}N_2S$: C, 71.47; H, 9.72; N, 8.78; S, 10.03%.

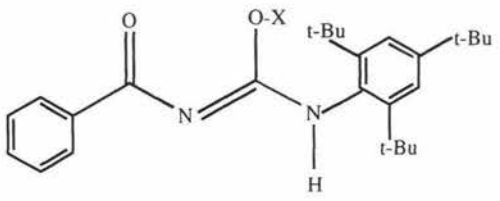

X = C_2H_5, 1-benzoyl-2-[ethoxyl-3-(2,4,6-tri-*tert*-butylphenyl)amino]aldimine (**BzE^{t}BPA**)

= CH_3, 1-benzoyl-2-[methoxyl-3-(2,4,6-tri-*tert*-butylphenyl)amino]aldimine (**BzM^{t}BPA**)

= $CH_2C_6H_5$, 1-benzoyl-2-[phenylmethoxyl-3-(2,4,6-tri-*tert*-butylphenyl)amino]aldimine

(**BzPM^{t}BPA**)

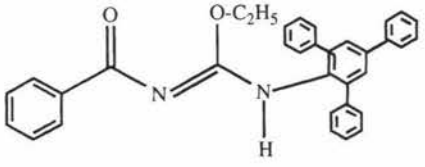

1-benzoyl-2-[ethoxyl-3-(2,4,6-tri-phenylphenyl)amino]aldimine

BzEPPA

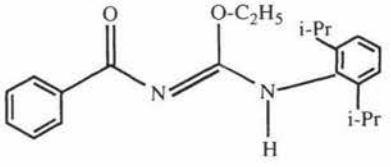

1-benzoyl-2-[ethoxyl-3-(2,6-diisopropylphenyl)amino]aldimine

BzE^{i}PPA

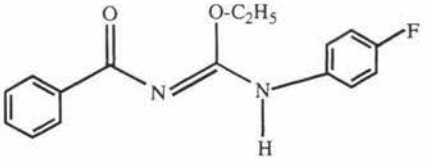

1-benzoyl-2-[ethoxyl-3-(4-fluorophenyl)amino]aldimine

BzEFPA

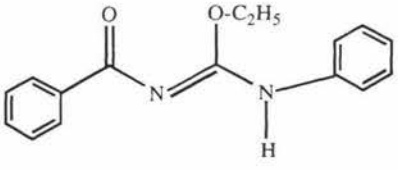

1-benzoyl-2-[ethoxyl-3-(phenyl)amino]aldimine

BzEPA

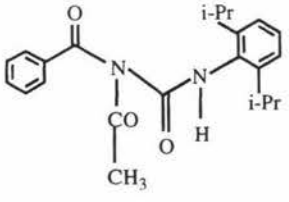

1-acetyl-1-benzoyl-*3*-(2,6-diisopropylphenyl)urea

ABz^{i}PPu

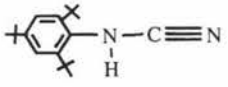

2,4,6-tri-*tert*-butylphenylcyanamide

^{t}BPc

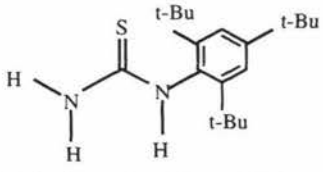

2,4,6-tri-*tert*-butylphenylthiourea

^{t}BPtu

Figure 3.1 Abbreviations, names and the structures of the compounds synthesised in this chapter.

3.2 Results and Discussion

3.2.1 Physicochemical Studies and Characterization of the Complexes

3.2.1.1 Synthesis and Reactivity of the Complexes

The complexes $[Hg(LH)_2Cl_2]$ (LH = Bz^tBPtuH, Bz^iPPtuH or BzFPtuH) were prepared by reacting $HgCl_2$ with the appropriate ligand LH in a 1:2 molar ratio. Yields ranged from 30-81%. $[Hg(Bz^tBPtuH)_2Cl_2]$ was also prepared when the molar ratio was 1:1 and , $[Hg(Bz^iPPtuH)_2Cl_2]$ was prepared when the ratio was 1:4, indicating that their formation was independent of the reactant ratios. However for BzPtuH, only $[Hg(BzPtuH)Cl_2]$ was isolated when the ratio was 1:2. This compound was insoluble in all solvents suggesting it have a polymeric structure. The other complexes are probably monomeric and this may possibly be determined by the bulkiness of the ligand.

Attempts to synthesize $ZnCl_2$ complexes with Bz^tBPtuH, Bz^iPPtuH, BzFPtuH or BzPtuH were unsuccessful.

The Reactions of $HgCl_2$ with LH

When $HgCl_2$ reacts with Bz^tBPtuH in a 1:1 molar ratio or Bz^iPPtuH or BzFPtuH in 1:2 molar ratio or Bz^iPPtuH in 1:4 molar ratio, the colourless complexes $[Hg(LH)_2Cl_2]$ were isolated according to the following equation:

$$HgCl_2 + 2LH \rightarrow [Hg(LH)_2Cl_2]$$

where LH = Bz^tBPtuH, Bz^iPPtuH, BzFPtuH or BzPtuH.

Reacting BzPtuH with $HgCl_2$ in 2:1 molar ratio, resulted in the formation of a colourless complex $[Hg(LH)Cl_2]$ according to the following equation:

$$HgCl_2 + 2LH \rightarrow [Hg(LH)Cl_2]$$

The Reactions of $Hg(Ac)_2$ with LH

Reacting $Hg(Ac)_2$ with Bz^{t}BPtuH, BzPPtuH, Bz^{i}PPtuH, BzFPtuH or BzPtuH (**Fig. 3.2**) did not result in the isolation of stable complexes, instead S is removed (desulfurisation) as black HgS and the ligands were transformed into new organic compounds (**Fig 3.3**), where the -OX moiety depends on the solvent. ^1H and ^{13}C NMR spectroscopy verified the products.

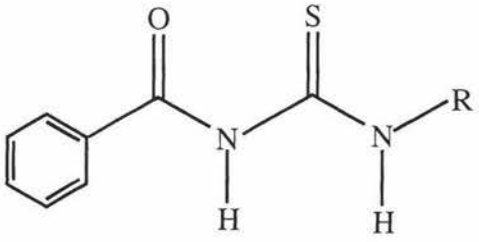

Figure 3.2

R = 2,4,6-tri-*tert*-butylphenyl (Bz^{t}BPtuH), 2,4,6-tri-phenylphenyl (BzPPtuH), 2,6-diisopropylphenyl (Bz^{i}PPtuH), *p*-fluorophenyl (BzFPtuH) or phenyl (BzPtuH)

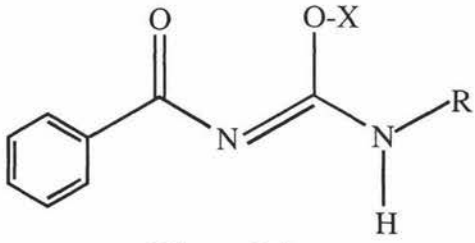

Figure 3.3

R = 2,4,6-tri-*tert*-butylphenyl, X = C_2H_5, (BzE^{t}BPA)
= CH_3, (BzM^{t}BPA)
= $CH_2C_6H_5$, (BzPM^{t}BPA)

X = C_2H_5, R = 2,4,6-tri-phenylphenyl, (BzEPPA)
= 2,6-diisopropylphenyl, (BzE^{i}PPA)
= *p*-fluorophenyl, (BzEFPA)
= phenyl, (BzEPA)

In these studies, 1-benzoyl-[2-ethoxyl-3-(2,4,6-tri-*tert*-butylphenyl)-amino]aldimine (BzE^tBPA) was also derived from the desulfurization of $Hg(Bz^tBPtuH)_2Cl_2$ with CH_3COONa in ethanol. This shows the importance of a good base for these reactions as discussed in this section later. Bz^tBPtuH was also converted to BzE^tBPA in ethanol when $Hg(Ac)_2$ is replaced by AgAc.

By reacting 1-ethoxycarbonyl-3-(*p*-nitrophenyl)thiourea with the strong nucleophilic reagent $NaOCH_3$ in ethanol, Shen *et al.*[11] prepared the similar methoxy product 1-ethoxycarbonyl-[2-methoxyl-3-(*p*-nitrophenyl)amino]aldimine.

The novel 1-acetyl-1-benzoyl-3-(2,6-diisopropylphenyl)urea (ABz^iPPu) (see **Fig. 3.1**) was derived from the desulfurization of Bz^iPPtuH in the presence of mercuric acetate or silver acetate in dichloromethane (see the X-ray crystal structure **Fig. 3.8**). A similar reaction of Bz^tBPtuH with mercuric acetate in dichloromethane produced 2,4,6-tri-*tert*-butylphenylcyanamide (^tBPc) by hydrolysis of the ligand. As well the reaction of Bz^tBPtuH with C_2H_5ONa in ethanol/water gave 2,4,6-tri-*tert*-butylphenylthiourea (^tBPtu).

Reactions of other Thiocarbonyl Substrates with $Hg(Ac)_2$

To probe the universality of the desulfurisation reaction, the interaction of $Hg(Ac)_2$ with other substrates containing thiocarbonyl groups was studied. Desulfurisation of thiourea to cyanamide, thioacetamide to acetonitrile, thiobenzamide to benzonitrile, phenylthiourea to phenylcyanamide and 4,4'-bis(dimethylamino)thiobenzophenone to 4,4'-bis(dimethylamino)benzophenone occurred, whereas dithizone, thiocamphor and bis(diphenylthiophosphoryl)amide did not produce HgS under the same conditions.

---

[11] X. Shen, X. Shi, B. Kang, Y. Tong, Y. Liu, L. Gu, Q. Liu and Y. Huang, *Polyhedron*, 1999, **18**, 33.

Further discussion on the reactions of $Hg(Ac)_2$ with LH

Reactions in alcoholic solvents

The addition of LH (Bz^{t}BPtuH, BzPPtuH, Bz^{i}PPtuH, BzFPtuH or BzPtuH) to a solution of $Hg(Ac)_2$ in 1:1 molar ratio at room temperature in ethanol, resulted in formation of a yellow precipitate which turned dark brown and then to black HgS. White crystals of BzE^{t}BPA, BzEPPA, BzE^{i}PPA, BzEFPA or BzEPA (see **Fig. 3.3**) were recovered from the filtrate according to the following equation:

$$Hg(CH_3COO)_2 + C_6H_5C(O)NHC(S)NHR + C_2H_5OH \rightarrow HgS\downarrow + C_6H_5CON{=}C(OX)NHR + 2CH_3COOH$$

where X = C_2H_5, R = 2,4,6-tri-*tert*-butylphenyl (Bz^{t}BPtuH), 2,4,6-tri-phenylphenyl (BzPPtuH), 2.6-diisopropylphenyl (Bz^{i}PPtuH), *p*-fluorophenyl (BzFPtuH) or phenyl (BzPtuH),

For Bz^{t}BPtuH, similar reactions occur upon changing the solvent to methanol or benzyl alcohol (X = CH_3 or $CH_2C_6H_5$) and the products are BzM^{t}BPA or BzPM^{t}BPA respectively (see **Fig. 3.3**).

Replacing ethanol by acetone or water, resulted in the formation of HgO from $Hg(Ac)_2$, but there was no further reaction.

Reactions in $CHCl_3$/EtOH

Refluxing Bz^{i}PPtuH with AgAc in $CHCl_3$ stabilised with 1% ethanol for four hours resulted in the formation of a black precipitate of Ag_2S and the colourless compound BzE^{i}PPA (**Fig. 3.3**). The IR and NMR data were similar to the ethoxy compound (BzE^{t}BPA). This reaction is very specific and may be used to detect the presence of EtOH.

Reactions in CH_2Cl_2

Refluxing Bz^{i}PPtuH with $Hg(Ac)_2$ or $Ag(Ac)_2$ in CH_2Cl_2 for one hour resulted in the same colour change as above forming a black precipitate of HgS or Ag_2S and a new colourless compound. The IR and NMR spectra of the product are now different from that obtained in $CHCl_3$/EtOH. The new compound was confirmed by the

X-ray crystal structure (see **Fig. 3.8**) to be ABz^{i}PPu. The following equation can be proposed for this reaction.

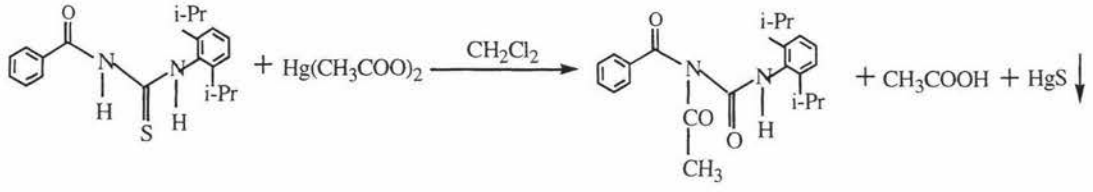

ABz^{i}PPu

Reacting Bz^{t}BPtuH with $Hg(Ac)_2$ in CH_2Cl_2 on the other hand resulted in the new compound ^{t}BPc. The following equation can be proposed for this reaction.

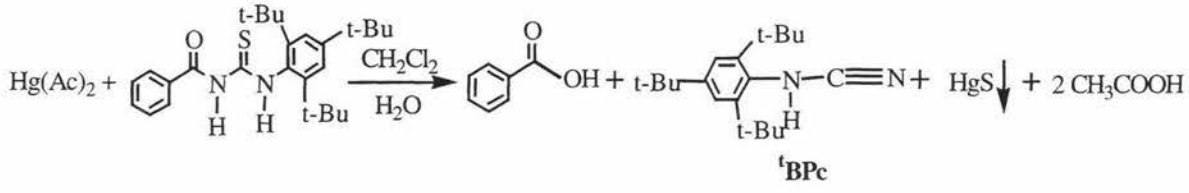

^{t}BPc

The reaction of $[Hg(Bz^{t}BPtuH)_2Cl_2]$ with CH_3COONa in ethanol produced a black HgS precipitate and white crystals of BzE^{t}BPA were isolated from the filtrate according to the following equation:

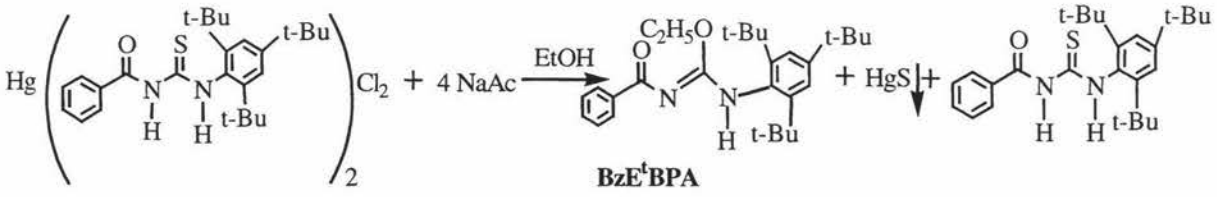

BzE^{t}BPA

This reaction shows that the chloro complex may be converted to BzE^{t}BPA in the presence of acetate, which acts as a base to remove protons from Bz^{t}BPtuH and ethanol and promotes the reaction.

The free ligand Bz^{t}BPtuH, however, reacts with C_2H_5ONa in ethanol to give ^{t}BPtu according to the following equation:

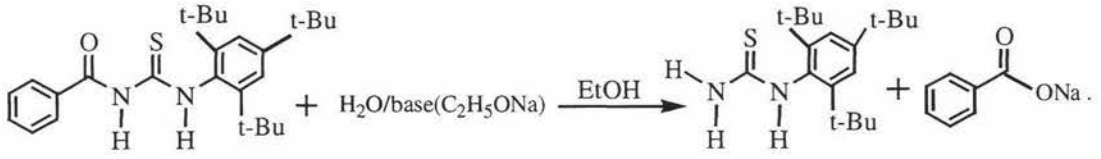

^{t}BPtu

3.2.1.2 IR and Mass Spectroscopic Studies of the Compounds

The compounds $[Hg(LH)_2Cl_2]$ (LH = Bz^{t}BPtuH, Bz^{i}PPtuH, BzFPtuH or BzPtuH) display a small shift to higher wave number in the ν(C=O) stretching frequency, indicating that the carbonyl oxygen is not coordinated to the metal. Similarly ν(N-H) stretching frequencies are a little less than those of the ligands, but one of the ν(N-H) frequencies of $[Hg(Bz^{t}BPtuH)_2Cl_2]$ and $[Hg(BzFPtuH)_2Cl_2]$ is slightly greater (~25 and ~70 cm^{-1}). Together this does not indicate the coordination of the N-H group in any of these compounds. A large decreased shift should be expected for the ν(C=S) stretching vibration, however this vibration cannot be located. The coordination of the ligand to the S atom was confirmed by the X-ray crystal structure of $[Hg(Bz^{i}PPtuH)_2Cl_2]$ (see **Fig. 3.6**).

The IR spectrum of $C_6H_5CON{=}C(OX)NHR$ (X = CH_3 or C_2H_5 or $CH_2C_6H_5$, R = 2,4,6-tri-*tert*-butylphenyl, X = C_2H_5, R = 2,4,6-tri-phenylphenyl or 2,6-diisopropylphenyl or *p*-fluorophenyl or phenyl) shows no ν(C=O) stretch, instead displays a new broad amide type band (~1571-1618 cm^{-1}) which is consistent with a ν(C=O) + ν(C=N) stretch. The ν(N-H) stretching region has become simplified, this may be due to the loss of an N-H proton in the product (**Fig.3.4**).

Phenylcyanamides have very characteristic IR spectra with an extremely strong peak in the range 2221-2245 cm^{-1} [12]. The peak at 2259 cm^{-1} in ^{t}BPc can be assigned to the ν(C≡N) stretching frequency of the cyanamide moiety. As expected no bands due to a ν(N-H) stretching frequency appears in the spectrum in the range 3350-3310 cm^{-1} [13].

---

[12] S.L. Ingham, 1987, BSc. Honours Project Report, Massey University.
[13] R.M. Silverstein, G.C. Bassler and T.C. Morrill, *Spectrometric Identification of Organic Compounds*, 1991, 5th Ed., John Wiley & Sons, Inc., New York, p 123.

Three ν(N-H) stretching frequencies appear in the spectrum of the ^{t}BPtu in the range 3151-3439 cm^{-1} region. These are associated with the primary $\nu(NH_2)$ and secondary amine ν(N-H) stretches.

ABz^{i}PPu displays 3 bands in the region 1674-1734 cm^{-1} which may be assigned to the benzoyl (1675 cm^{-1}), acetyl (1711 cm^{-1}) and urea (1734 cm^{-1}) C=O groups respectively. A single medium peak at 3239 cm^{-1} can be assigned to the ν(N-H) stretch.

The compounds BzE^{t}BPA, BzE^{i}PPA, BzM^{t}BPA, BzPM^{t}BPA, BzEFPA, BzEPA in **Table 3.1** exhibit molecular ion peaks, with isotope abundance calculations, that compare well with the experimental values. $[Hg(LH)_2Cl_2]$ (LH = Bz^{i}PPtuH or BzFPtuH) however display a loss of Cl^- and ligand, similar to the cobalt and copper complexes discussed in Chapter 2. From the mass spectral data, we can conclude that the molecular formula of the complexes and organic derivatives are correct.

The spectroscopic characterization of the products formed from the reaction of selected thiocarbonyls with $Hg(Ac)_2$ is listed in **Table 3.2**. For example, the presence of a ν(C≡N) stretch at 2261 cm^{-1}, as well as M^+ at 42 showed the conversion of thiourea to cyanamide. The other products were characterized in a similar way; thus thioacetamide was converted to acetonitrile, thiobenzamide to benzonitrile, phenylthiourea to phenylcyanamide.

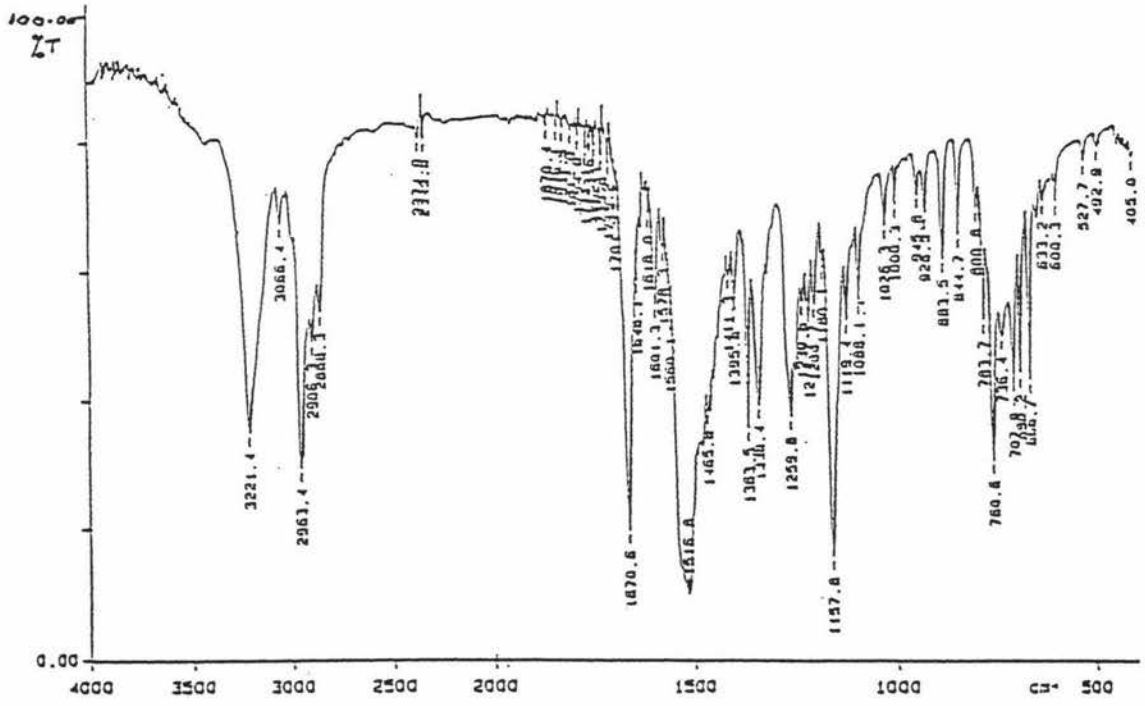

(a) Infrared Spectrum of the Free Ligand (Bz^{t}BPtuH).

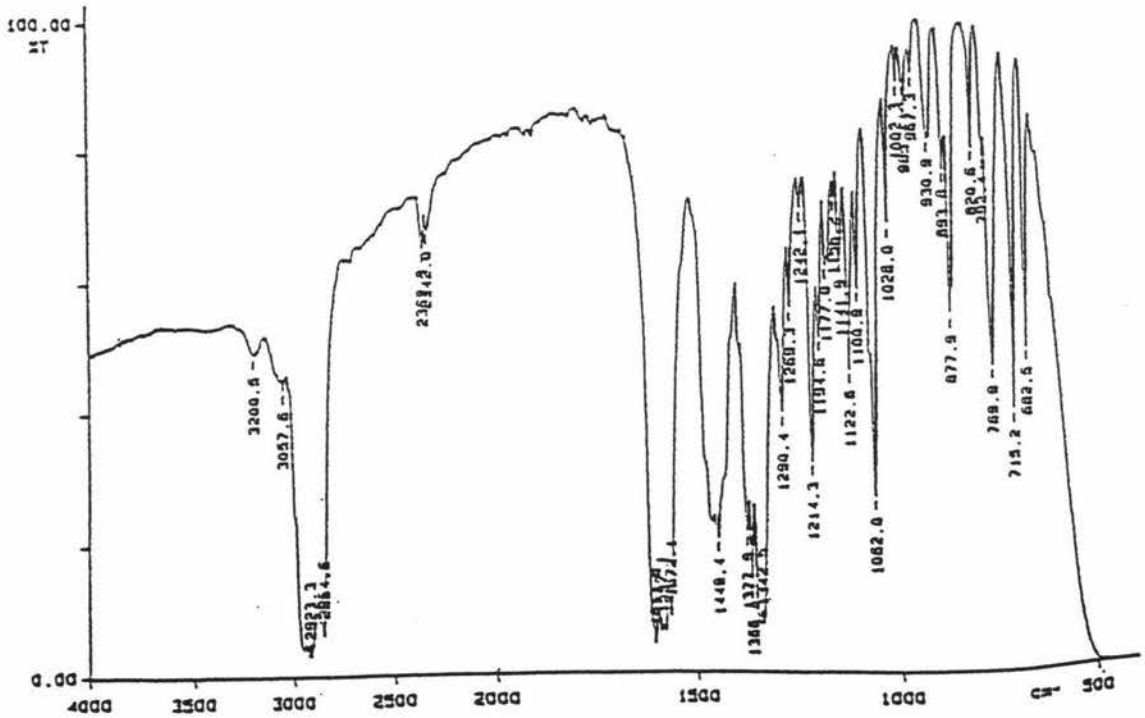

(b) Infrared Spectrum of BzE^{t}BPA.

Figure 3.4 Infrared Spectra of **(a)** Bz^{t}BPtuH **(b)** BzE^{t}BPA.

Table 3.1 Selected IR and MS data for mercury complexes and organic derivatives

	IR[a] (cm^{-1})				
Compounds	ν(C=O)	ν(N-H)	ν(C=O) + ν(C=N)[14]	ν(C-OC_nH_{2n+1})[11]	(+)FAB Mass spectra[b] m/z (rel. int., %)
$[Hg(Bz^tBPtuH)_2Cl_2]$	1672s	3245sh 3135vw			—
$[Hg(Bz\ ^iPPtuH)_2Cl_2]$	1681s	3194w			$[(M-Cl)+HL]^+(^{202}Hg)(^{35}Cl)$ 1258 (5) 917 (7) $[M-Cl)]^+$ 577 (57) $[Hg(L)Cl]^+$ 105 (100) $[C_6H_5CO]^+$
$[Hg(BzFPtuH)_2Cl_2]$	1678s	3200sh 3100br			$[(M-Cl)\ (^{202}Hg)\ (^{35}Cl)]^+$ 785 (3) 511 (12) $[Hg(L)Cl]^+$ 275 (100) $[HL]^+$ 105 (49) $[C_6H_5CO]^+$
$[Hg(BzPtuH)Cl_2]$	1678s	3148w			[c]
BzE^{t}BPA		3199vw 3058vw	1614,1586,1571 br	1214 s ν(C-OC_2H_5)	M^+ 436 (1) 421 (1) $[M-CH_3]^+$ 390 (9) $[M-(C_2H_5OH)]^+$ 105 (100) $[C_6H_5CO]^+$
[d,e]BzE^{i}PPA[9]		3207w 3073w	1615, 1597, 1583 br	[f]	M^+ 352 (7) 309 (26) $[M-(OC_2H_5)]^+$ 105 (100) $[C_6H_5CO]^+$
BzM^{t}BPA		3228m 3073w	1618, 1588, 1576 br	1213 s ν(C-OCH_5)	MH^+ 423 (100) 365 (91) $[M-(C(CH_3)_3]^+$ 105 (100) $[C_6H_5CO]^+$
BzPM^{t}BPA	[g]				MH^+ 499 (37)
BzEPPA		3219vw	1614, 1584, 1574 br	[f]	—
BzEFPA		3192m 3075w	1614, 1595, 1575 br	1225s	M^+ 286 (21) 137 (7) $[C_6H_4FNHC(CH_3)]^+$ 105 (100) $[C_6H_5CO]^+$
BzEPA		3066m	1614, 1595, 1579 br	1213s ν(C-OC_2H_5)	M^+ 268 (40) 147 (18) $[C_8H_5NO_2]^+$ 77 (48) $[C_6H_5]^+$
ABz^{i}PPu	1734s 1711s (CH_3CO or -NCON-) 1675m (C_6H_5CO)	3239m			MH^+ 367 (88) 105 (100) $[C_6H_5CO]^+$ 43 (6) $[CH_3CO]^+$
^{t}BPc ν(C≡N) 2259s		[h]			M^+ 286 (12) 105 (100) $[C_6H_5CO]^+$
^{t}BPtu[e]		3439m 3209wbr ν(NH_2) 3151sbr ν(NH)			MH^+ 321 (100) 319 (55) $[M-H]^+$

[a] As nujol mull on NaCl. [b] 3-nitrobenzylalcohol matrix. [c] Sample insoluble. [d] FTIR (KBr). [e] EI(+) MS. [f] Not detected because of overlap of bands. [g] Not enough sample. [h] No peak; s = strong, m = medium, w = weak, br = broad, sh = shoulder.

[14] R.M. Silverstein, G.C. Bassler and T.C. Morrill, *Spectrometric Identification of Organic Compounds*, 1991, 5th Ed., John Wiley & Sons, Inc., New York, pp 123, 112.

Table 3.2 Selected IR and Mass Spectral data for the products of other $Hg(Ac)_2$ reactions

Substrate	Product	IR[a] (cm^{-1}) ν(C≡N)	ν(N-H)	ν(NH_2)	(+)FAB Mass spectra[b] m/z (rel. int., %)
Thiourea	Cyanamide	2261vs	—	3384br	M^+ 42 (100) 41 (12) $[NH\text{-}C{\equiv}N]^+$
Thioacetamide	Acetonitrile	2349vw			[c]
Thiobenzamide	Benzonitrile	2228vs			M^+ 103 (22) $[C_6H_5C{\equiv}N]^+$
Phenylthiourea	Phenylcyanamide	2228vs	3172sbr		M^+ 118 (100) 91 (48) $[M\text{-}(CNH)]^+$ 77 (25) $[C_6H_5]^+$
$(C_6H_4NMe_2)_2CS$	$(C_6H_4NMe_2)_2CO$	1604vs ν(C=O)			MH^+ 269 (100) 148 (30) $[OCC_6H_4N(CH_3)_2]^+$
Thiocaprolactam	[d]	[e]			[f]

[a] As nujol mull on NaCl. [b] 3-nitrobenzylalcohol matrix. [c] CH_3-C≡N not detected. [d] Major product not identified. [e] IR not conclusive. [f] A minor product was detected only with M^+ = 167 (42%). This compound is C-6-thiazole (MF: $C_9H_{13}NS$).

3.2.1.3 ^1H and ^{13}C NMR Spectroscopic Studies of Selected Compounds

The ^1H NMR data for selected compounds are shown in **Table 3.3** and ^{13}C NMR data in **Table 3.4**. The complex $[Hg(Bz^tBPtuH)_2Cl_2]$ exhibits two singlets for the N-H protons, whose chemical shifts are slightly lower than the free ligand. In the ^{13}C NMR spectrum, even though the thiocarbonyl sulfur binds to Hg, there is no change from the free ligand C=S (181.6 ppm) peak. This suggests that the ligand may be dissociating at room temperature. Similar results have been obtained for a related rhodium system[15]. The C=O peak has shifted from 166.6 ppm to 170.4 ppm in the complex, and this is not suggestive of the carbonyl oxygen binding to mercury but X-ray structural analysis shows it is H-bonded to the aniline N-H. In the ^1H NMR of

[15] D. Cauzzi, M. Lanfranchi, G. Marzolini, G. Predieri, A. Tiripicchio, M. Costa, R. Zanoni, *J. Organomet. Chem.*, 1995, **488**, 115.

$C_6H_5CON=C(OX)NHR$ (X = C_2H_5, R = 2,4,6-tri-*tert*-butylphenyl or 2,4,6-triphenylphenyl or 2,6-diisopropylphenyl), the ethoxy group displays the usual quadruplet signal for the CH_2 and triplet for the CH_3 protons with the expected 2:3 integral. The aromatic proton chemical shifts of BzE^tBPA and BzE^iPPA remain similar to the free ligands. The resonances for the methyl groups on the t-butyl and isopropyl moieties are similar to the free ligand values.

The ^{13}C NMR spectra of BzE^tBPA and BzE^iPPA are similar to that of the free ligands, except for the presence of some new resonances. The two new peaks at 14.9 ppm and 63.7 ppm in BzE^tBPA and 14.6 ppm and 63.8 ppm in BzE^iPPA, are consistent with the CH_3 and CH_2 of the ethoxy group (**Fig. 3.5**). The peak at 178.4 ppm in BzE^tBPA and 177.9 ppm in BzE^iPPA suggests that this resonance is the imino carbon of C=N.

The ^1H NMR spectrum of ABz^iPPu exhibits a peak at 9.94 ppm assigned to an N-H moiety with the expected intensity. The chemical shifts for the acetyl protons were observed at 2.29 ppm with the expected intensity.

The ^{13}C NMR spectrum of ABz^iPPu display 3 peaks at 172.4 ppm, 171.7 ppm and 152.5 ppm which are consistent with the three C=O moieties. A new peak at 25.3 ppm may belong to the CH_3 of the acetyl moiety.

In the ^1H NMR spectrum of ^tBPtu, intensities of the Ar-CH and ^tB-CH_3 are in accordance with the ratio of the expected proton type. In the ^{13}C spectrum the absence of a peak for the carbonyl carbon of Bz^tBPtuH in the product gives support for its hydrolysis to ^tBPtu. ^tBPtu displays a C=S resonance at 183.0 ppm.

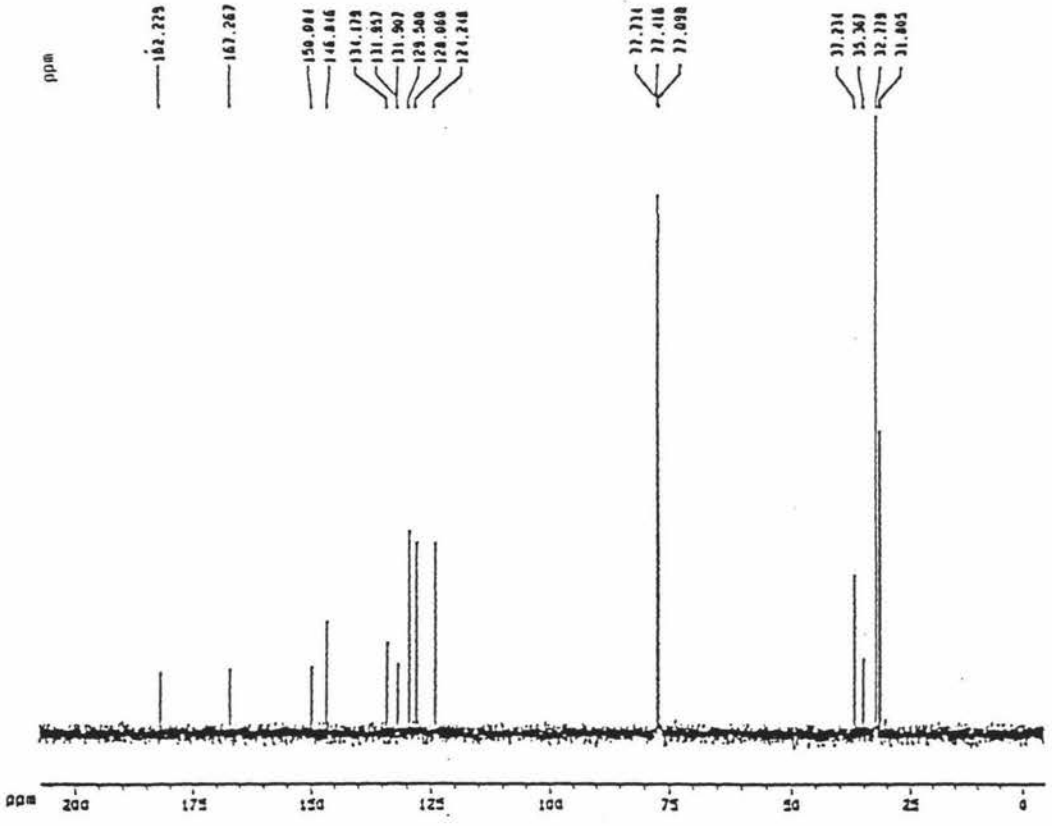

(a) ^{13}C NMR Spectrum of the Free Ligand (Bz^{t}BPtuH).

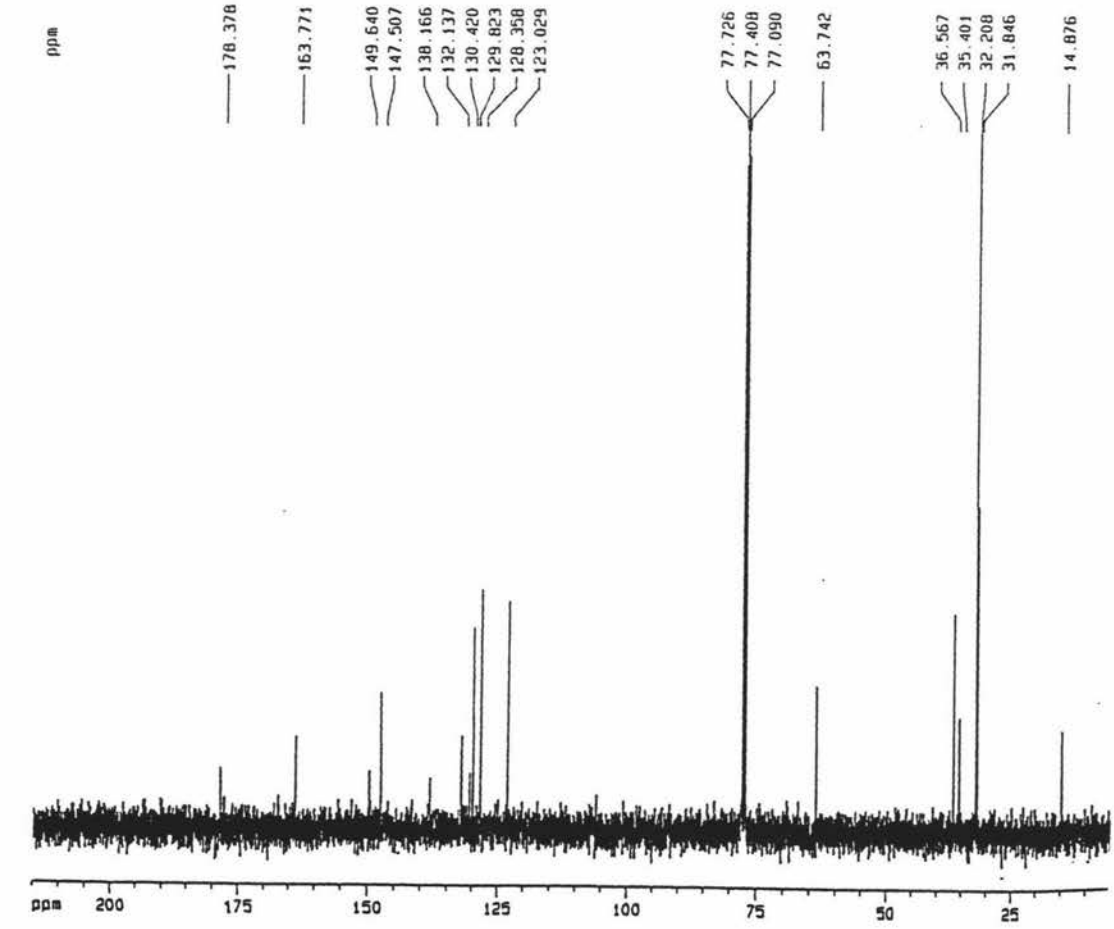

(b) ^{13}C NMR Spectrum of BzE^{t}BPA.

Figure 3.5 ^{13}C NMR Spectra of **(a)** Bz^{t}BPtuH **(b)** BzE^{t}BPA.

Table 3.3 ^{1}H chemical shift data for the products[a]

Compounds	^{1}H NMR ($CDCl_3$, TMS, ppm) δ_{N-H}	δ_{Ar-CH}	$\delta_{O-CnH2n+1}$	$\delta^{t}_{B-CH3\ or}\ ^{i}_{P-CH3\ and\ CH}$
$[Hg(Bz^{t}BPtuH)_2Cl_2]$	8.47s (1H) 8.44s (1H)	7.38-7.78m (7H)		1.46s (18H), 1.50s (9H)
$[Hg(Bz^{i}PPtuH)_2Cl_2]$	11.44s (1H)	7.21-8.31m (8H)		1.16d (6H), 1.26d (6H) 2.96sept. (2H)
$BzE^{t}BPA$ 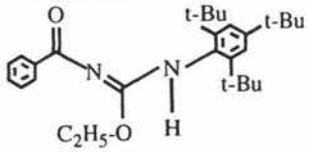	11.73s (1H)	7.25-7.51m (7H)	4.41-4.46q (2H) (-O-$\underline{CH_2}$-CH_3) 1.22-1.26t (3H) (-O-CH_2-$\underline{CH_3}$)	1.34s (18H), 1.37s (9H)
$BzE^{i}PPA$[9] 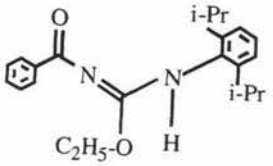	11.48s (1H)	8.37-7.21m (8H)	4.55q (2H) (-O-$\underline{CH_2}$-CH_3) 1.32t (3H) (-O-CH_2-$\underline{CH_3}$)	1.23dd (12H), 3.14sept. (2H)
$BzM^{t}BPA$ 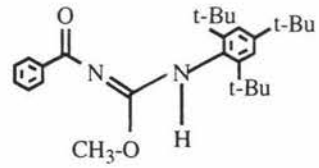	8.34s (1H)	7.25-7.52m (7H)	4.08s (3H) (-O-$\underline{CH_3}$)	1.18s (18H), 1.57s (9H)
BzEPPA 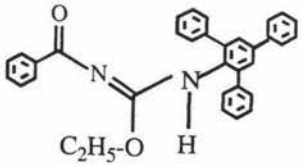	11.46s (1H) 8.10s (1H)	7.21-7.67m (22H)	3.96-4.01q (2H) (-O-$\underline{CH_2}$-CH_3) 0.96-0.99t (3H) (-O-CH_2-$\underline{CH_3}$)	
$ABz^{i}PPu$ [b] 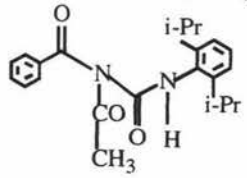	2.29 (3H) ($\delta_{acetyl-CH3}$)	9.36s (1H)	7.15-8.03m (8)	1.20d (6H), 1.33d (6H) 3.15sept.(2H)
$^{t}BPtu$ 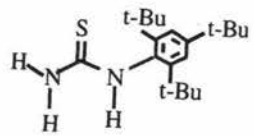	[c]	7.23-7.40s (2H)		1.20s (18H), 1.62s (9H)

[a] Recorded at 400MHz, chemical shifts are relative to $Si(CH_3)_4$ [TMS], solvent $CDCl_3$ unless stated otherwise.
[b] Contains $Bz^{i}PPtuH$ as a minor impurity. [c] No peaks; s = singlet, d = doublet, m = multiplet, sept = septuplet.

Table 3.4 ^{13}C chemical shift data for the products[a]

Compounds	^{13}C NMR ($CDCl_3$, ppm)				
	$\delta_{C=S}$ or $\delta_{C=N}$	$\delta_{C=O}$	$\delta_{O\text{-}CnH2n+1}$	$\delta_{Ar\text{-}CH}$ $\delta_{Ar\text{-}C\ (quat.)}$	$\delta^{t}_{B\text{-}CH3\ and\ C(quat.)}$ or $\delta^{i}_{P\text{-}CH3\ and\ CH}$
$[Hg(Bz^{t}BPtuH)_2Cl_2]$	181.1 (C=S)	170.4		123.9-150.8 [7Ar-CH, 5Ar- $C_{(quat.)}$]	31.4 (3C), 32.5 (6C) 35.1 ($1C_{(quat.)}$) 36.8 ($2C_{quat}$)
$[Hg(Bz^{i}PPtuH)_2Cl_2]$	181.2 (C=S)	171.0		124.6-145.5 [8Ar-CH, 4Ar-$C_{(quat.)}$]	23.5 (2C), 24.8 (2C) 29.3 ($2C_{(tert.)}$)
$BzE^{t}BPA$	178.4 (C=N)	163.8	63.7 (-O-$\underline{CH_2}$-CH_3) 14.9 (-O-CH_2-$\underline{CH_3}$)	123.0-149.6 [7Ar-CH, 5Ar-$C_{(quat.)}$]	31.8 (3C), 32.2 (6C) 35.4 ($1C_{(quat.)}$) 36.6 ($2C_{(quat.)}$)
$BzE^{i}PPA$[9]	177.9 (C=N)	162.6	63.8 (-O-$\underline{CH_2}$-CH_3) 14.6 (-O-CH_2-$\underline{CH_3}$)	123.3-145.6 [8Ar-CH, 4Ar-$C_{(quat.)}$]	23.3 (2C), 24.0 (2C) 28.8 ($2C_{(tert.)}$)
$ABz^{i}PPu$ 25.3 (3C) ($\delta_{acetyl\text{-}CH3}$)		172.4 171.7 152.5		124.2-145.9 [8Ar-CH, 4Ar-$C_{(quat.)}$] 25.3 (acetyl C)	23.5 (2C), 24.8 (2C) 29.27 ($2C_{(tert.)}$)
$BzM^{t}BPA$	178.4 (C=N)	164.0	54.6 (-O-$\underline{CH_3}$)	123.1-149.9 [7Ar-CH, 5Ar-$C_{(quat.)}$]	31.9 (3C), 32.1 (6C) 35.4 ($1C_{(quat.)}$) 36.6 ($2C_{(quat.)}$)
BzPPtuH	178.0 (C=N)	161.8	64.1 (-O-$\underline{CH_2}$-CH_3) 14.5 (-O-CH_2-$\underline{CH_3}$)	127.6-140.8 [22Ar-CH, 8Ar-$C_{(quat.)}$]	
$^{t}BPtu$	183.00 (C=S)			149.5 [$1C_{(quat.)}$] 123.9 [2 *m*-CH]	31.8 (3C), 32.1 (6C) 35.0 ($1C_{(quat.)}$) 37.0 ($2C_{(quat.)}$)

[a] Recorded at 400MHz, solvent $CDCl_3$; quat = quaternary, tert = tertiary.

3.2.1.4 Description of the Crystal Structures

3.2.1.4.1 Crystal Structure of [Hg(Bz^{i}PPtuH-$\kappa^{1}S$)$_2$Cl$_2$]

The structure of the [Hg(Bz^{i}PPtuH-$\kappa^{1}S$)$_2$Cl$_2$] is shown in **Fig. 3.6** with crystal data and structure refinement details given in **Table 3.5**, selected bond lengths and angles in **Table 3.6** and selected torsion angles in **Table 3.7**. The complex has a distorted tetrahedral monomeric structure as detected for the [Co(Bz^{t}BPtuH-$\kappa^{1}S$)$_2$Cl$_2$] complex. The two Bz^{i}PPtuH ligands are bound to the Hg atom by two S donor atoms [Hg–S(1) = 2.5930(6) Å and Hg–S(1A) = 2.5127(6) Å] and two Cl atoms [Hg–Cl(1) = 2.3831(7) Å and Hg–Cl(2) = 2.5469(6) Å]. The two Hg–S distances are similar but the two Hg–Cl distances are significantly different The C–S distances, at 1.705(2) Å are longer than the free ligand (1.679(3) Å), due to the coordination with Hg. Three bond angles are remarkable; two are greater [Cl(1)–Hg–S(1) = 120.22(3)° and Cl(1)–Hg–S(1A) = 121.63(3)°] and one is less [S(1A)–Hg–S(1) = 94.72(2)°] than the tetrahedral angle, but the other one is close to the tetrahedral angle [Cl(1)–Hg–Cl(2) = 107.96(3)°]. The bond lengths of the imine system are similar to the free ligand. [The geometry of the ligand is very similar to that in the [Cu(Bz^{t}BPtuH-$\kappa^{1}S$)$_2$Cl] and [Co(Bz^{t}BPtuH-$\kappa^{1}S$)$_2$Cl$_2$] complexes].

The torsion angles along the central chains [C(19)–N(1)–C(20)–N(2) and C(19a)–N(1a)–C(20a)–N(2a)] of the two ligands are small (7.7(4)° to 2.0(2)°) implying the chain is close to planar. The phenyl rings are twisted out of the plane of central chain. For example, for the isopropyl-substituted ring the C(6)–C(1)–N(2)–C(20) torsion angles are close to 90° [87.9(3)° for ligand 1 and –89.5(3)° for ligand 2]. For the benzoyl ring the twist is smaller with the C(14)–C(13)–C(19)–O(1) torsion angle being 23.0(3)° for ligand 1 and -144.0(3)° for ligand 2.

The intramolecular hydrogen bond between N(2)–H and O(1) (2.019(6) Å in ligand 1 and 1.873(6) Å in ligand 2) results in an almost planar six membered ring with the N(2), C(20) and N(1) atoms in the central part of the molecule. As well in the crystal, two different molecules are linked together by two equivalent hydrogen bonds (N(2)–H…O(1) = 2.419(5) Å) in a centrosymmetric fashion.

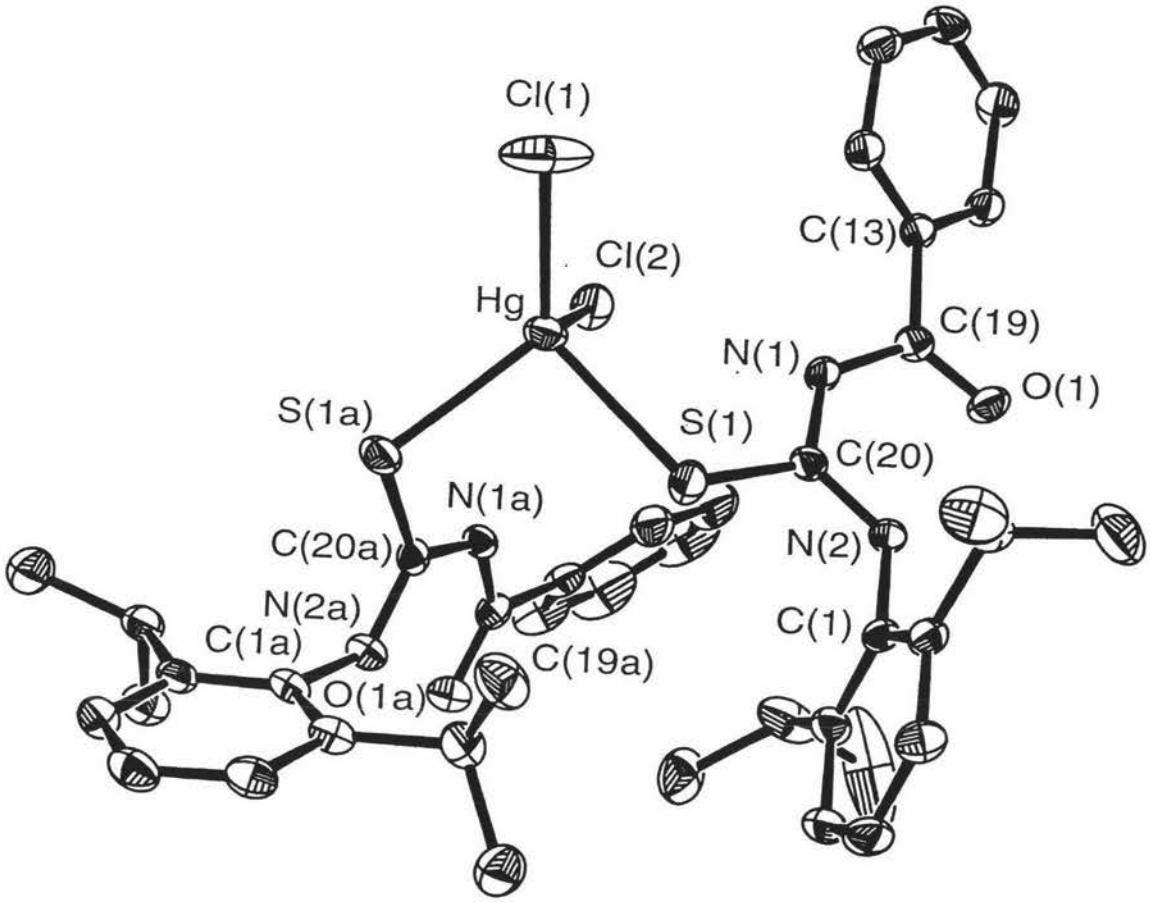

Figure 3.6 ORTEP diagram for the complex [Hg(Bz^{i}PPtuH-κ^{1}*S*)$_2$Cl$_2$] showing the numbering system used. Thermal ellipsoids are at the 50% probability level. Hydrogen atoms have been omitted for clarity

Table 3.5 Crystal data and structure refinement for $[Hg(Bz^{i}PPtuH\text{-}\kappa^{1}S)_2Cl_2]$

Identification code	ik2	
Empirical formula	$C_{40}H_{48}Cl_2HgN_4O_2S_2$	
Formula weight	952.43	
Temperature	150(2) K	
Wavelength	0.71073 Å	
Crystal system	Triclinic	
Space group	P-1	
Unit cell dimensions	a = 11.8741(1) Å	α = 93.057(1)°
	b = 13.5231(1) Å	β = 112.169(1)°
	c = 14.1961(1) Å	γ = 101.39°
Volume	2048.81(3) $Å^3$	
Z	2	
Density (calculated)	1.544 Mg/m^3	
Absorption coefficient	4.027 mm^{-1}	
F(000)	956	
Crystal size	0.22 x 0.20 x 0.12 mm^3	
Theta range for data collection	1.55 to 26.34°.	
Index ranges	$-14 \le h \le 14$, $-16 \le k \le 16$, $-17 \le l \le 17$	
Reflections collected	19035	
Independent reflections	8226 [R(int) = 0.0178]	
Absorption correction	Semi-empirical from equivalents	
Max. and min. transmission	0.6436 and 0.4711	
Refinement method	Full-matrix least-squares on F^2	
Data / restraints / parameters	8226 / 0 / 460	
Goodness-of-fit on F^2	1.017	
Final R indices [I>2sigma(I)]	R1 = 0.0203, wR2 = 0.0499	
R indices (all data)	R1 = 0.0228, wR2 = 0.0511	
Largest diff. peak and hole	0.718 and -1.064 $e.Å^{-3}$	

Table 3.6 Selected bond lengths [Å] and angles [°] for [Hg(Bz^{i}PPtuH-κ^1*S*)$_2$Cl$_2$] with estimated standard deviations in parentheses

Bond lengths:

	Ligand 1		*Ligand 2 (labelled a)*
Hg-Cl(1)	2.3831(7)	Hg-Cl(2)	2.5469(6)
Hg-S(1)	2.5930(6)	Hg-S(1A)	2.5127(6)
S(1)-C(20)	1.705(2)	S(1A)-C(20A)	1.709(2)
C(1)-N(2)	1.451(3)	C(1A)-N(2A)	1.452(3)
C(13)-C(19)	1.492(3)	C(13A)-C(19A)	1.487(3)
C(19)-O(1)	1.224(3)	C(19A)-O(1A)	1.224(3)
C(19)-N(1)	1.393(3)	C(19A)-N(1A)	1.402(3)
N(1)-C(20)	1.379(3)	N(1A)-C(20A)	1.382(3)
C(20)-N(2)	1.324(3)	C(20A)-N(2A)	1.319(3)

Bond angles:

Cl(1)-Hg-Cl(2)	107.96(3)	S(1A)-Hg-S(1)	94.72(2)
Cl(1)-Hg-S(1)	120.22(3)	Cl(1)-Hg-S(1A)	121.63(3)
Cl(2)-Hg-S(1)	102.23(2)	S(1A)-Hg-Cl(2)	107.90(2)
C(20)-S(1)-Hg	110.61(8)	C(20A)-S(1A)-Hg	106.24(8)
C(6)-C(1)-N(2)	118.8(2)	C(6A)-C(1A)-N(2A)	118.9(2)
C(2)-C(1)-N(2)	118.3(2)	C(2A)-C(1A)-N(2A)	117.3(2)
C(3)-C(2)-C(7)	121.5(2)	C(3A)-C(2A)-C(7A)	122.4(2)
C(1)-C(2)-C(7)	121.3(2)	C(1A)-C(2A)-C(7A)	120.8(2)
C(1)-C(6)-C(10)	122.1(2)	C(1A)-C(6A)-C(10A)	123.1(2)
C(5)-C(6)-C(10)	120.4(2)	C(5A)-C(6A)-C(10A)	120.0(2)
C(14)-C(13)-C(19)	117.8(2)	C(14A)-C(13A)-C(19A)	122.5(2)
C(18)-C(13)-C(19)	122.0(2)	C(18A)-C(13A)-C(19A)	116.6(2)
O(1)-C(19)-N(1)	121.5(2)	O(1A)-C(19A)-N(1A)	122.3(2)
O(1)-C(19)-C(13)	123.1(2)	O(1A)-C(19A)-C(13A)	121.4(2)
N(1)-C(19)-C(13)	115.4(2)	N(1A)-C(19A)-C(13A)	116.3(2)
C(20)-N(1)-C(19)	127.0(2)	C(20A)-N(1A)-C(19A)	125.0(2)
N(2)-C(20)-N(1)	119.0(2)	N(2A)-C(20A)-N(1A)	117.3(2)
N(2)-C(20)-S(1)	120.3(2)	N(2A)-C(20A)-S(1A)	120.3(2)
N(1)-C(20)-S(1)	120.8(2)	N(1A)-C(20A)-S(1A)	122.3(2)
C(20)-N(2)-C(1)	121.8(2)	C(20A)-N(2A)-C(1A)	124.9(2)

Table 3.7 Selected torsion angles [°] for [Hg(Bz^{i}PPtuH-κ^1*S*)$_2$Cl$_2$]

	Ligand 1		*Ligand 2 (labelled a)*
C(14)-C(13)-C(19)-N(1)	-157.9(2)	C(14A)-C(13A)-C(19A)-N(1A)	35.3(3)
C(18)-C(13)-C(19)-N(1)	28.2(3)	C(18A)-C(13A)-C(19A)-N(1A)	-147.6(2)
C(14)-C(13)-C(19)-O(1).	23.0(3)	C(14A)-C(13A)-C1(9A)-O(1A)	-144.0(3)
C(18)-C(13)-C(19)-O(1)	-150.9(2)	C(18A)-C(13A)-C(19A)-O(1A)	33.1(3)
C(6)-C(1)-N(2)-C(20)	87.9(3)	C(6A)-C(1A)-N(2A)-C(20A)	-89.5(3)
C(2)-C(1)-N(2)-C(20)	-91.9(3)	C(2A)-C(1A)-N(2A)-C(20A)	94.0(3)

3.2.1.4.2 Crystal Structure of BzE^{t}BPA

The structure of 1-benzoyl-[2-ethoxyl-3-(2,4,6-tri-*tert*-butylphenyl)-amino]aldimine (BzE^{t}BPA) is shown in **Fig. 3.7**, with crystal data and structure refinement details given in **Table 3.8**. Selected bond lengths and angles are listed in **Table 3.9** and selected torsion angles given in **Table 3.10**. In the structure the bonds C(25)–O(1) of the benzoyl moiety and C(26)–O(2) of the ethoxy group adopt a *trans* orientation with respect to one another, so as to minimise non-bonded steric interactions. The C(25)–O(1) bond distance of 1.238(3) Å is similar to the free ligand C(25)–O(1) (1.226(3) Å) distance and consistent with a double bond. There is no S in this compound as it is replaced by the OC_2H_5 moiety. The bond length N(1)–C(26) at 1.323(3) Å is shorter than the equivalent bond length in the free ligand (N(1)–C(26) = 1.395(4) Å), but it is within the range of C=N bond distances[11] [calculated N=C = 1.29 Å]. As well, the approximate coplanarity of the atoms N(2), C(26), N(1), C(25) and O(1) suggests the existence of a conjugated system of N(2)–C(26)–N(1)–C(25)–O(1), as has been observed in a similar system by Shen *et al.*[11]. As in the free ligand the benzoyl phenyl ring is almost co-planar with the central chain with the C(20)–C(26)–C(19)–C(25)–N(1) torsion angle being 5.4(3)°. In contrast, the *tert*-butyl substituted phenyl ring is twisted by approximately 90° to the plane of the central chain. For example, the torsion angle, C(6)–C(1)–N(2)–C(26) is 85.4(3)°. Also the *ortho-tert*-butyl groups are pushed back with the C(1)–C(2)–C(7) and the C(1)–C(6)–C(11) angles both being 124.0(2)°.

The intramolecular hydrogen bond between N(2)–H and O(1) [1.964(6) Å] results in an almost planar six-membered ring with the C(25), N(1) and C(26) atoms in the central part of the molecule. There are no intermolecular hydrogen bonds.

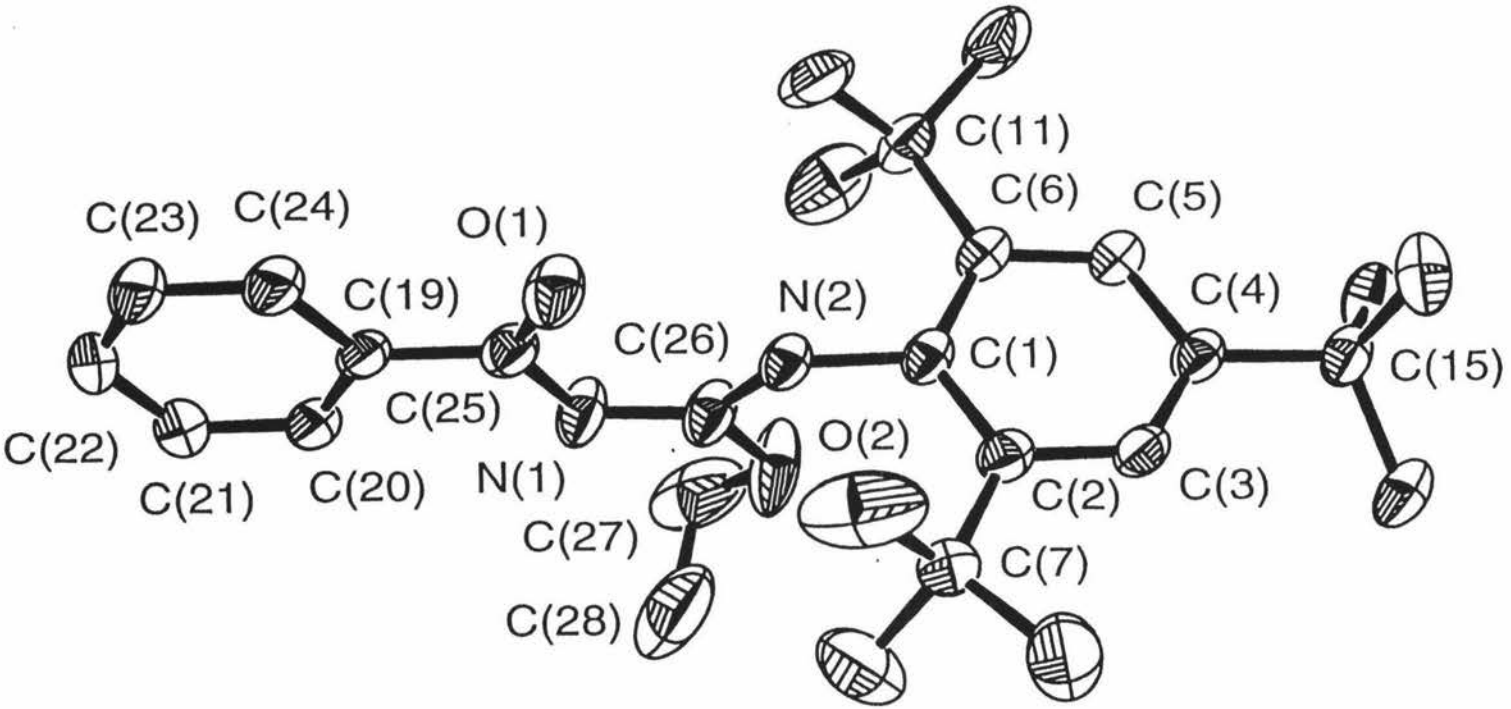

Figure 3.7 ORTEP diagram for the compound BzE^{t}BPA showing the numbering system used. Thermal ellipsoids are at the 50% probability level. Hydrogen atoms have been omitted for clarity

Table 3.8 Crystal data and structure refinement for BzE^tBPA

Identification code	ic9
Empirical formula	$C_{28}H_{40}N_2O_2$
Formula weight	436.62
Temperature	150(2) K
Wavelength	0.71073 Å
Crystal system	Monoclinic
Space group	P2(1)/n
Unit cell dimensions	a = 13.3527(3) Å $\alpha = 90°$
	b = 10.3922(2) Å $\beta = 108.316(1)°$
	c = 19.5155(4) Å $\gamma = 90°$
Volume	2570.85(9) $Å^3$
Z	4
Density (calculated)	1.128 Mg/m^3
Absorption coefficient	0.070 mm^{-1}
F(000)	952
Crystal size	0.42 x 0.35 x 0.20 mm^3
Theta range for data collection	1.64 to 26.39°.
Index ranges	$-16 \le h \le 16$, $-13 \le k \le 8$, $-23 \le l \le 24$
Reflections collected	14348
Independent reflections	5209 [R(int) = 0.0247]
Absorption correction	Semi-empirical from equivalents
Max. and min. transmission	0.9861 and 0.9711
Refinement method	Full-matrix least-squares on F^2
Data / restraints / parameters	5209 / 0 / 289
Goodness-of-fit on F^2	1.051
Final R indices [I>2sigma(I)]	R1 = 0.0758, wR2 = 0.1851
R indices (all data)	R1 = 0.0974, wR2 = 0.2031
Largest diff. peak and hole	0.724 and -0.695 $e.Å^{-3}$

Table 3.9 Selected bond lengths [Å] and angles [°] for BzE^{t}BPA with estimated standard deviations in parentheses

Bond lengths:

C(1)-N(2)	1.445(3)
C(19)-C(25)	1.500(3)
C(25)-O(1)	1.238(3)
C(25)-N(1)	1.371(3)
N(1)-C(26)	1.323(3)
C(26)-N(2)	1.318(3)
C(26)-O(2)	1.333(3)
O(2)-C(27)	1.629(6)

Bond angles:

C(6)-C(1)-N(2)	118.9(2)
C(2)-C(1)-N(2)	119.0(2)
C(3)-C(2)-C(7)	119.4(2)
C(1)-C(2)-C(7)	124.0(2)
C(3)-C(4)-C(15)	121.5(2)
C(5)-C(4)-C(15)	121.3(2)
C(5)-C(6)-C(11)	118.7(2)
C(1)-C(6)-C(11)	124.0(2)
C(20)-C(19)-C(25)	122.0(2)
C(24)-C(19)-C(25)	118.9(2)
O(1)-C(25)-N(1)	126.3(2)
O(1)-C(25)-C(19)	120.0(2)
N(1)-C(25)-C(19)	113.6(2)
C(26)-N(1)-C(25)	119.2(2)
N(2)-C(26)-N(1)	127.2(2)
N(2)-C(26)-O(2)	113.4(2)
N(1)-C(26)-O(2)	119.5(2)
C(26)-N(2)-C(1)	125.3(2)
C(26)-O(2)-C(27)	116.9(2)

Table 3.10 Selected torsion angles [°] for BzE^{t}BPA

C(20)-C(19)-C(25)-N(1)	5.4(3)
C(24)-C(19)-C(25)-N(1)	-176.4(2)
C(20)-C(19)-C(25)-O(1)	-174.6(2)
C(24)-C(19)-C(25)-O(1)	3.7(4)
C(6)-C(1)-N(2)-C(26)	85.4(3)
C(2)-C(1)-N(2)-C(26)	-95.3(3)

3.2.1.4.3 Crystal Structure of ABz^{i}PPu

The structure of 1-acetyl-1-benzoyl-3-(2,6-diisopropylphenyl)urea (ABz^{i}PPu) is shown in **Fig. 3.8**, with crystal data and structure refinement details given in **Table 3.11**, selected bond lengths and angles are in **Table 3.12** and selected torsion angles in **Table 3.13**. The S atom in the free ligand has been replaced by an O atom with the C(20)–O(3) bond length (1.212(2) Å) while the benzoyl C(19)–O(1) is 1.191(3) Å, in comparison to the 1.226(3) Å in the free ligand. Both bond lengths are consistent with C=O groups. The two C=O groups are *trans* to each other as the free ligand. Particular interest in this compound is the acetyl moiety attached to the N(1) nitrogen atom. The bond lengths of C(19)–N(1) and N(1)–C(20) (1.461(3) Å and 1.420(3) Å respectively) are longer than the free ligand (C(25)–N(1) = 1.379(4) Å and N(1)–C(26) = 1.395(4) Å respectively), but the N(2)–C(20) (1.329(3) Å) bond distance is not significantly different to the free ligand (N(2)–C(26) =1.326(4) Å). This is part of a peptide bond system. The orientations of the two phenyl rings with respect to the central chain is similar to the previous structures.

In this molecule the intramolecular hydrogen bond is between N(2)–H and O(2) of the acetyl moiety is 1.947(6) Å, resulting in an almost planar six-membered ring with the C, N(1) and C(20) atoms in the central part of the molecule. In the other molecules studied in this thesis the hydrogen bond is between the N(2)–H and O(1) of the benzoyl moiety. As well, in the crystal, two different molecules are linked together by intermolecular hydrogen bonds between C(17)–H and O(3) with C(17)–H...O(3) = 2.426(6) Å thus forming chains.

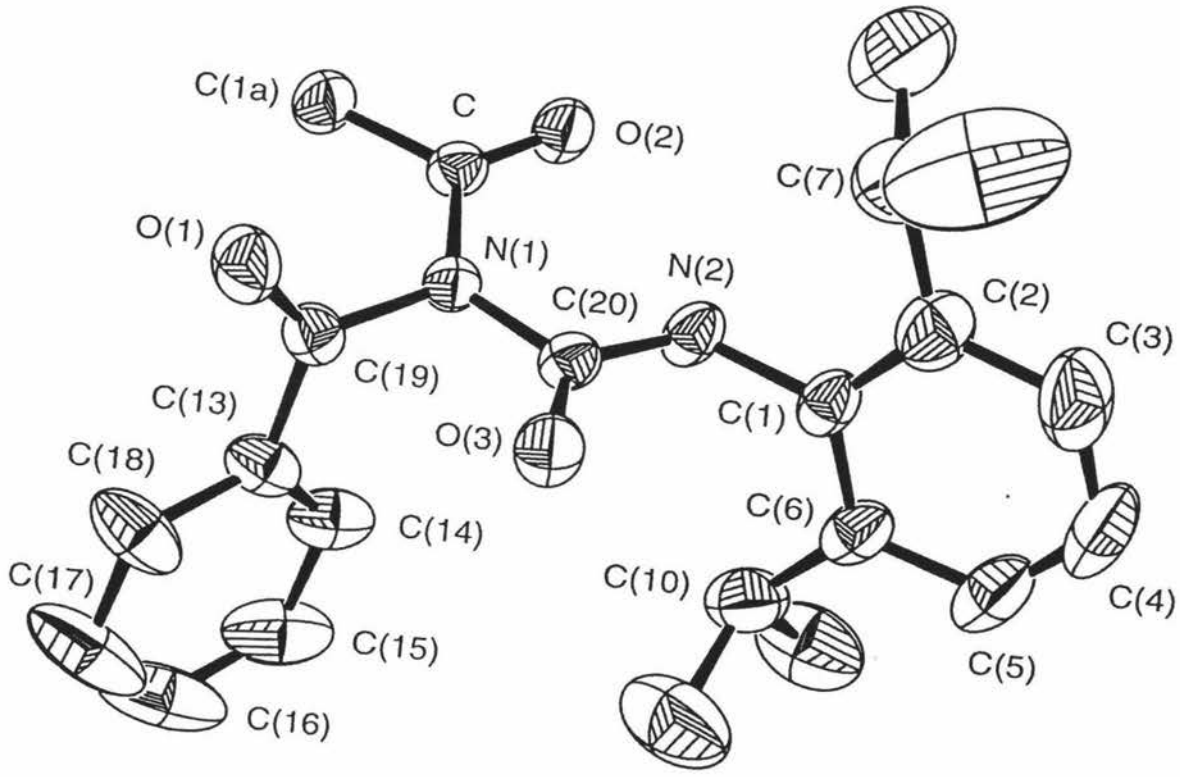

Figure 3.8 ORTEP diagram for the compound ABz^{i}PPu showing the numbering system used. Thermal ellipsoids are at the 50% probability level. Hydrogen atoms have been omitted for clarity

Table 3.11 Crystal data and structure refinement for ABz^{i}PPu

Identification code	ika	
Empirical formula	$C_{22}H_{26}N_2O_3$	
Formula weight	366.45	
Temperature	150(2) K	
Wavelength	0.71073 Å	
Crystal system	Monoclinic	
Space group	P2(1)/n	
Unit cell dimensions	a = 8.9983(1) Å	$\alpha = 90°$.
	b = 13.4870(1) Å	$\beta = 100.81°$.
	c = 16.6451(1) Å	$\gamma = 90°$.
Volume	1984.22(3) Å^3	
Z	4	
Density (calculated)	1.227 Mg/m^3	
Absorption coefficient	0.082 mm^{-1}	
F(000)	784	
Crystal size	0.52 x 0.28 x 0.24 mm^3	
Theta range for data collection	1.96 to 26.60°.	
Index ranges	$-11 \le h \le 11$, $-16 \le k \le 16$, $-20 \le l \le 20$	
Reflections collected	17841	
Independent reflections	4121 [R(int) = 0.0320]	
Completeness to theta = 0.50°	100.0 %	
Absorption correction	Semi-empirical from equivalents	
Max. and min. transmission	0.9806 and 0.9587	
Refinement method	Full-matrix least-squares on F^2	
Data / restraints / parameters	4121 / 4 / 262	
Goodness-of-fit on F^2	1.040	
Final R indices [I>2sigma(I)]	R1 = 0.0617, wR2 = 0.1591	
R indices (all data)	R1 = 0.0825, wR2 = 0.1757	
Largest diff. peak and hole	0.500 and -0.331 e.Å^{-3}	

Table 3.12 Selected bond lengths [Å] and angles [°] for ABz^{i}PPu with estimated standard deviations in parentheses

Bond lengths:

N(1)-C	1.388(2)
N(1)-C(20)	1.420(3)
N(1)-C(19)	1.461(3)
N(2)-C(20)	1.329(3)
N(2)-C(1)	1.432(3)
O(1)-C(19)	1.191(3)
O(2)-C	1.216(3)
O(3)-C(20)	1.212(2)
C-C(1A)	1.490(3)
C(13)-C(19)	1.467(3)

Bond angles:

C-N(1)-C(20)	127.0(2)
C-N(1)-C(19)	120.4(2)
C(20)-N(1)-C(19)	112.4(2)
C(20)-N(2)-C(1)	123.3(2)
O(2)-C-N(1)	121.8(2)
O(2)-C-C(1A)	121.7(2)
N(1)-C-C(1A)	116.4(2)
C(2)-C(1)-N(2)	118.4(2)
C(6)-C(1)-N(2)	119.1(2)
C(1)-C(2)-C(7)	121.5(2)
C(3)-C(2)-C(7)	121.7(3)
C(5)-C(6)-C(10)	121.0(2)
C(1)-C(6)-C(10)	121.5(2)
C(14)-C(13)-C(19)	121.9(2)
C(18)-C(13)-C(19)	118.1(2)
O(1)-C(19)-N(1)	120.0(2)
O(1)-C(19)-C(13)	124.6(2)
N(1)-C(19)-C(13)	115.4(2)
O(3)-C(20)-N(2)	126.7(2)
O(3)-C(20)-N(1)	117.6(2)
N(2)-C(20)-N(1)	115.7(2)

Table 3.13 Selected torsion angles [°] for ABz^{i}PPu

C(20)-N(2)-C(1)-C(2)	-99.1(3)
C(20)-N(2)-C(1)-C(6)	84.1(3)
C(14)-C(13)-C(19)-O(1)	169.2(2)
C(18)-C(13)-C(19)-O(1)	-9.4(3)
C(14)-C(13)-C(19)-N(1)	-8.6(3)
C(18)–C(13)-C(19)-N(1)	172.8(2)

3.3 Conclusions

With $HgCl_2$, compounds of the type $[Hg(LH)_2Cl_2]$ (LH = Bz^{t}BPtuH, Bz^{i}PPtuH or BzFPtuH) were isolated as well as $[Hg(BzPtuH)Cl_2]$. With $Hg(Ac)_2$, the ligands (in alcoholic solvents) are converted to $[C_6H_5CON{=}C(OX)NHR]$ (R = 2,4,6-tri-*tert*-butylphenyl, 2,4,6-tri-phenylphenyl, 2,6-diisopropylphenyl, *p*-fluorophenyl or phenyl, X = C_2H_5; and R = 2,4,6-tri-*tert*-butylphenyl, X = CH_3, or $CH_2C_6H_5$) while in CH_2Cl_2 $[C_6H_5CON(COCH_3)C(O)NHR]$ (R = 2,6-diisopropylphenyl) or NHCN-tri-(*t*-butyl)phenyl are obtained. With sodium ethoxide in alcohol and water NH_2-C(S)NH-tri-(*t*-butyl)phenyl was isolated.

For $[Hg(LH)_2Cl_2]$ (LH = Bz^{t}BPtuH, Bz^{i}PPtuH or BzFPtuH) the ligand remains neutral and binds through the S atom to form a monomeric distorted tetrahedral complex, but the ligands dissociate at room temperature in solution. The stoichiometry of the $HgCl_2$ reaction product is independent of the reactant ratio.

The reactions with $Hg(Ac)_2$ in alcohol result in a loss of a proton from the benzoyl N-H, then the removal of sulfur and the subsequent reaction of the anion of the solvent to form the product $[C_6H_5CON{=}C(OX)NHR]$. CH_3COO^- is a stronger base than the Cl^-, therefore desulfurisation occurs with $Hg(Ac)_2$ and complexation with $HgCl_2$. The possible mechanism for this reaction with ethanol is given in **Scheme 3.1**. The intermediate mercury complex was unstable, its lifetime was short and it decomposed to form HgS as a black solid and a new colourless compound containing no sulfur. The microanalytical and spectroscopic data confirm the loss of sulfur and the involvement of the ethanol in the final product to give $[C_6H_5CON{=}C(OEt)NHR]$. Here the EtO^- group attacks the C=S carbon. The S is bound to Hg^{2+} and this directs the EtO^- to the C=S carbon.

With CH_2Cl_2 as the solvent, the reactions are slow and low yielding. The reaction of Bz^{i}PPtuH with $Hg(Ac)_2$ or AgAc results in the formation of the new compound ABz^{i}PPu, however with Bz^{t}BPtuH the new compound ^{t}BPc was formed. In the formation of ABz^{i}PPu, HgS or Ag_2S is formed and the CH_3COO^- anion is converted into an acetyl group, with a urea being formed. The X-ray crystal structure and

spectroscopic data confirm the final product. A possible mechanism (based on Castro[16]) for this reaction is given in **Scheme 3.2**.

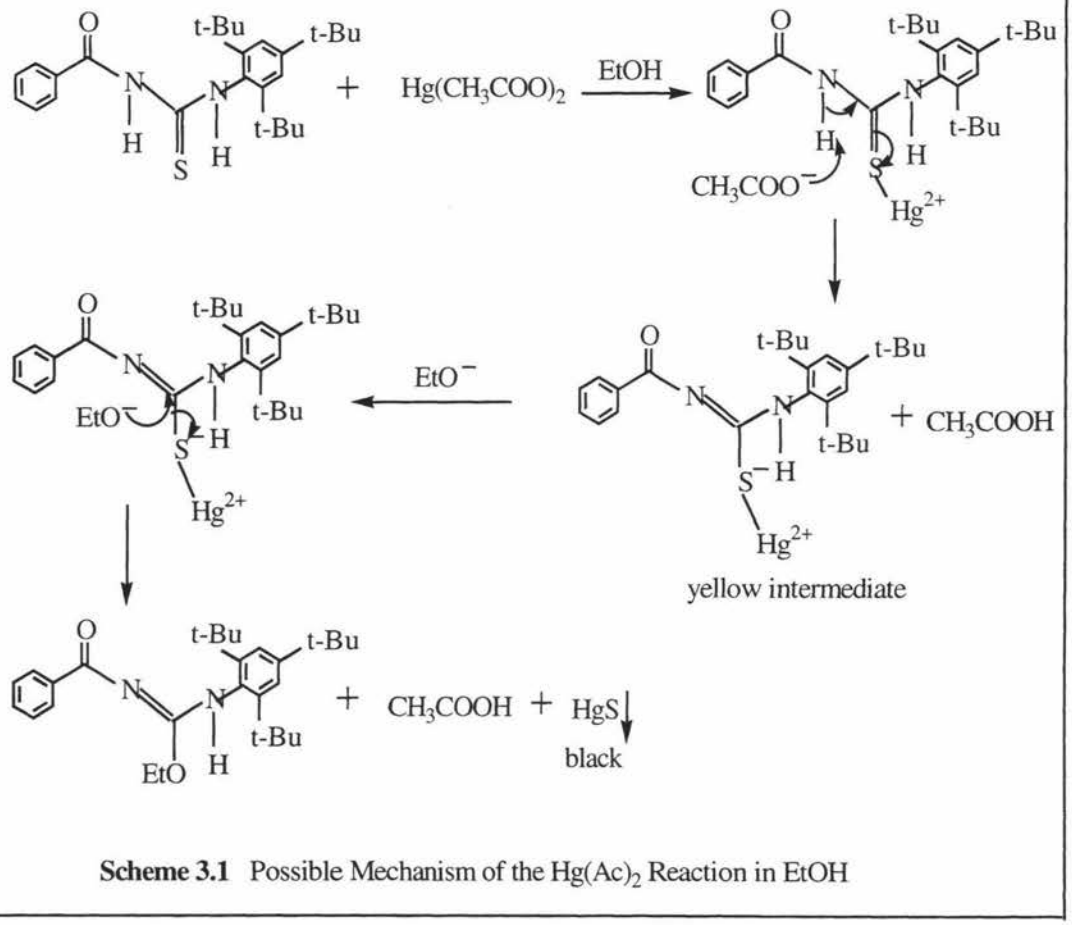

Scheme 3.1 Possible Mechanism of the $Hg(Ac)_2$ Reaction in EtOH

[16] E.A. Castro, *Chem. Rev.*, 1999, **99**, 12, 3505.

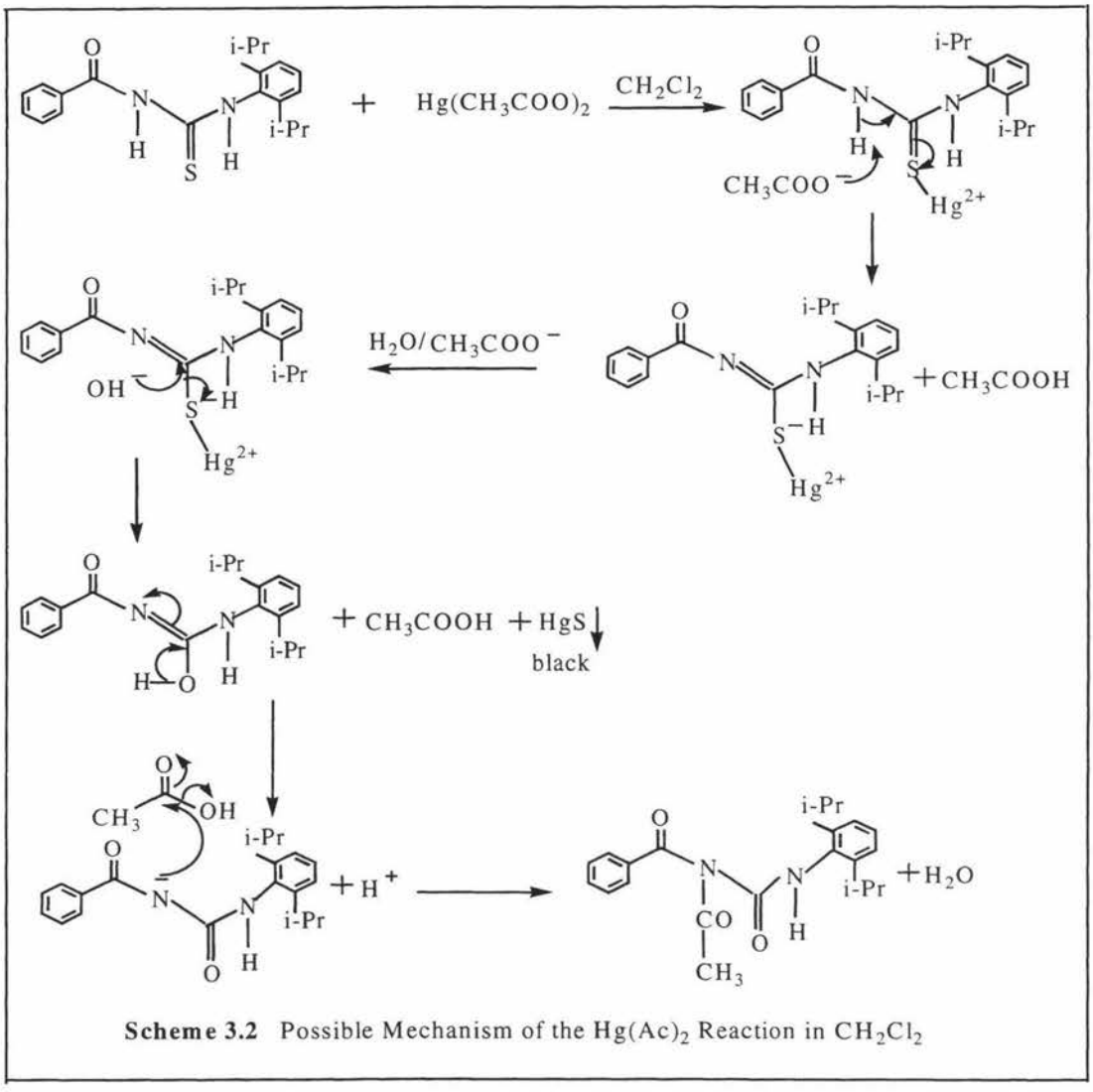

Scheme 3.2 Possible Mechanism of the $Hg(Ac)_2$ Reaction in CH_2Cl_2

Selected thiocarbonyls, such as thiourea, thioacetamide, thiobenzamide, phenylthiourea and 4,4'-bis(dimethylamino)thiobenzophenone, reacted with $Hg(Ac)_2$ and are desulfurised, whereas thiocamphor, dithizone and bis(diphenyl-thiophosphoryl)amide are not (**Scheme 3.3**).

According to the mechanism of the $Hg(Ac)_2$/thiocarbonyl reaction in ethanol (**Scheme 3.1**), the reaction is enhanced if there is an ionizable proton in the substance. Therefore with thiourea, thioacetamide, thiobenzamide and phenylthiourea desulfurisation occurred and produced cyanamide, acetonitrile, benzonitrile and phenylcyanamide respectively even at room temperature. However, the reaction of 4,4'-bis(dimethylamino)thiobenzophenone with $Hg(Ac)_2$ is very sluggish (refluxed for 2 days) and HgS was produced in 60% yield. Possibly aerial oxidation resulted in the formation of 4,4'-bis(dimethylamino)benzophenone.

Even though dithizone, and bis(diphenylthiophosphoryl)amide contain ionizable protons the bidentate anions form the appropriate mercury complexes. These chelated complexes are very stable and cannot be easily disrupted and eliminate HgS. Thiocamphor does not have an ionizable proton, but also forms a complex that does not eliminate HgS.

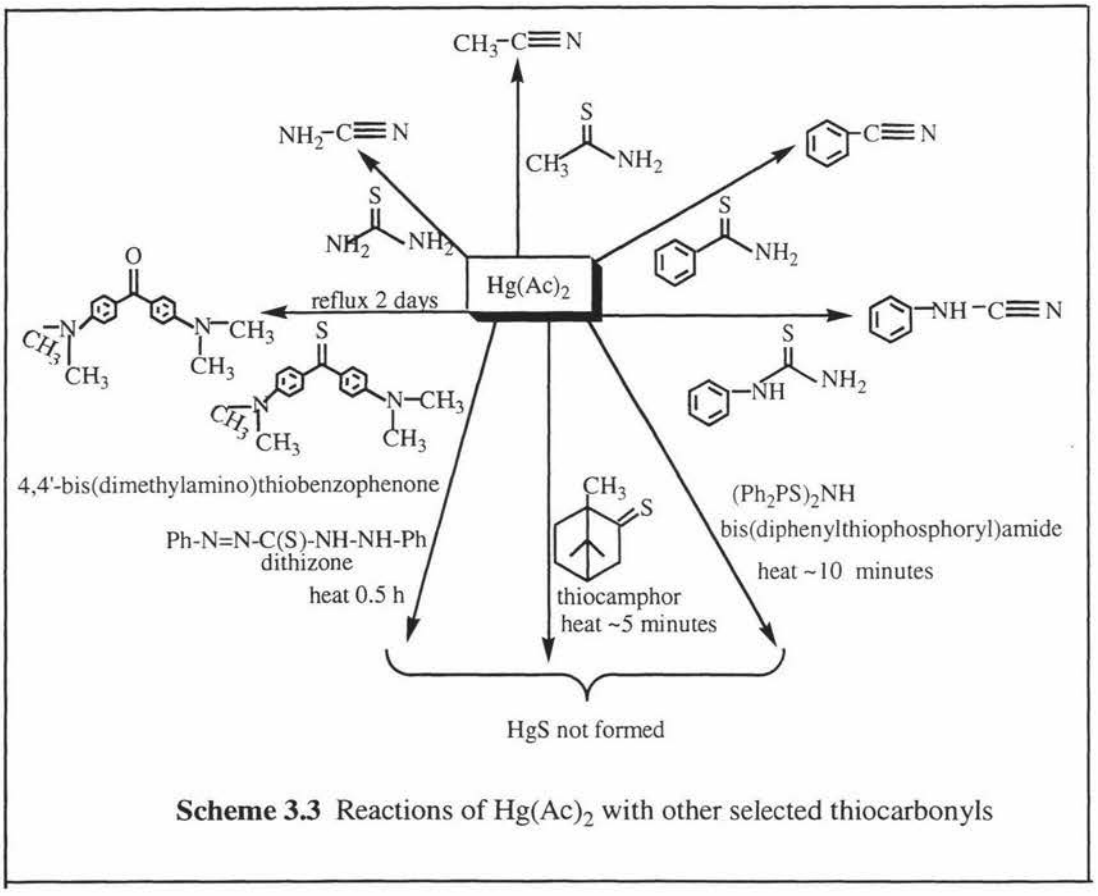

Scheme 3.3 Reactions of $Hg(Ac)_2$ with other selected thiocarbonyls

Replacing $Hg(Ac)_2$ with $Cd(Ac)_2$ and refluxing with Bz^{t}BPtuH in ethanol resulted in the formation of some CdS, unreacted starting material and a little BzE^{t}BPA. No reaction was observed with Zn^{2+} or UO_2^{2+} acetate.

Therefore the ability to perform this reaction is influenced by the softness of the group 12 metals and decreases in the order:

$$Hg(Ac)_2 >> Cd(Ac)_2 >> Zn(Ac)_2 \text{ (no reaction)} .$$

Castro[16] has studied the kinetics of methanolysis of benzoyl aryl thioureas (ArNHC(S)NHC(O)Ph) and found that these thioureas are one order of magnitude more acidic than their oxygen derivatives, and that they react faster with methoxide anion by two orders of magnitude. The hard oxynucleophile EtO^- is more reactive towards hard electrophilic centers (C=O) than soft centers (C=S), hence in the absence of Hg^{2+} ions the EtO^- ion is directed towards the C=O carbon atom.

The mechanism for ethanolysis of Bz^{t}BPtuH with C_2H_5ONa is given in **Scheme 3.4**.

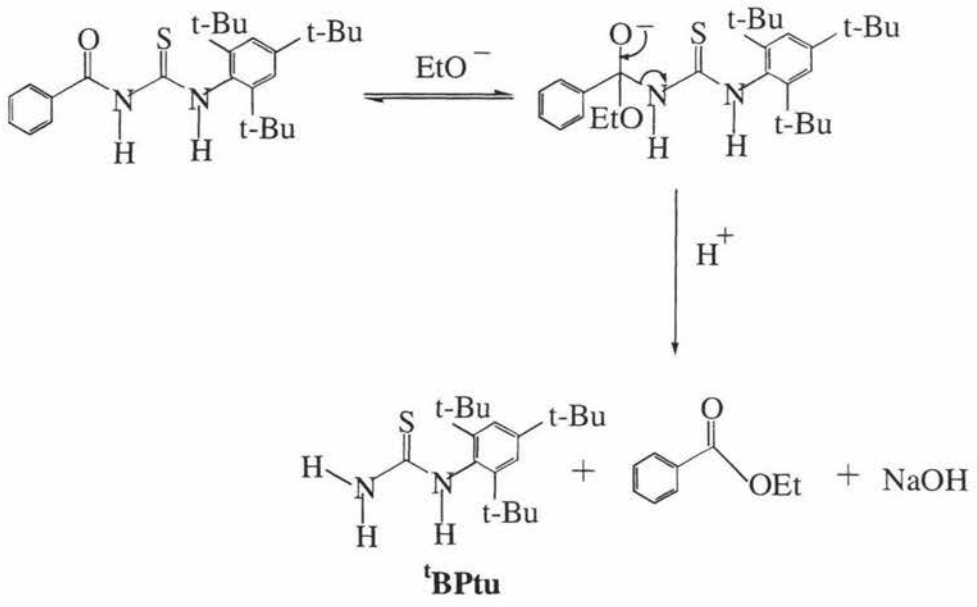

Scheme 3.4 Possible Mechanism of the EtONa Reaction

A summary of the reactions of Bz^{t}BPtuH and Bz^{i}PPtuH is given in **Scheme 3.5**.

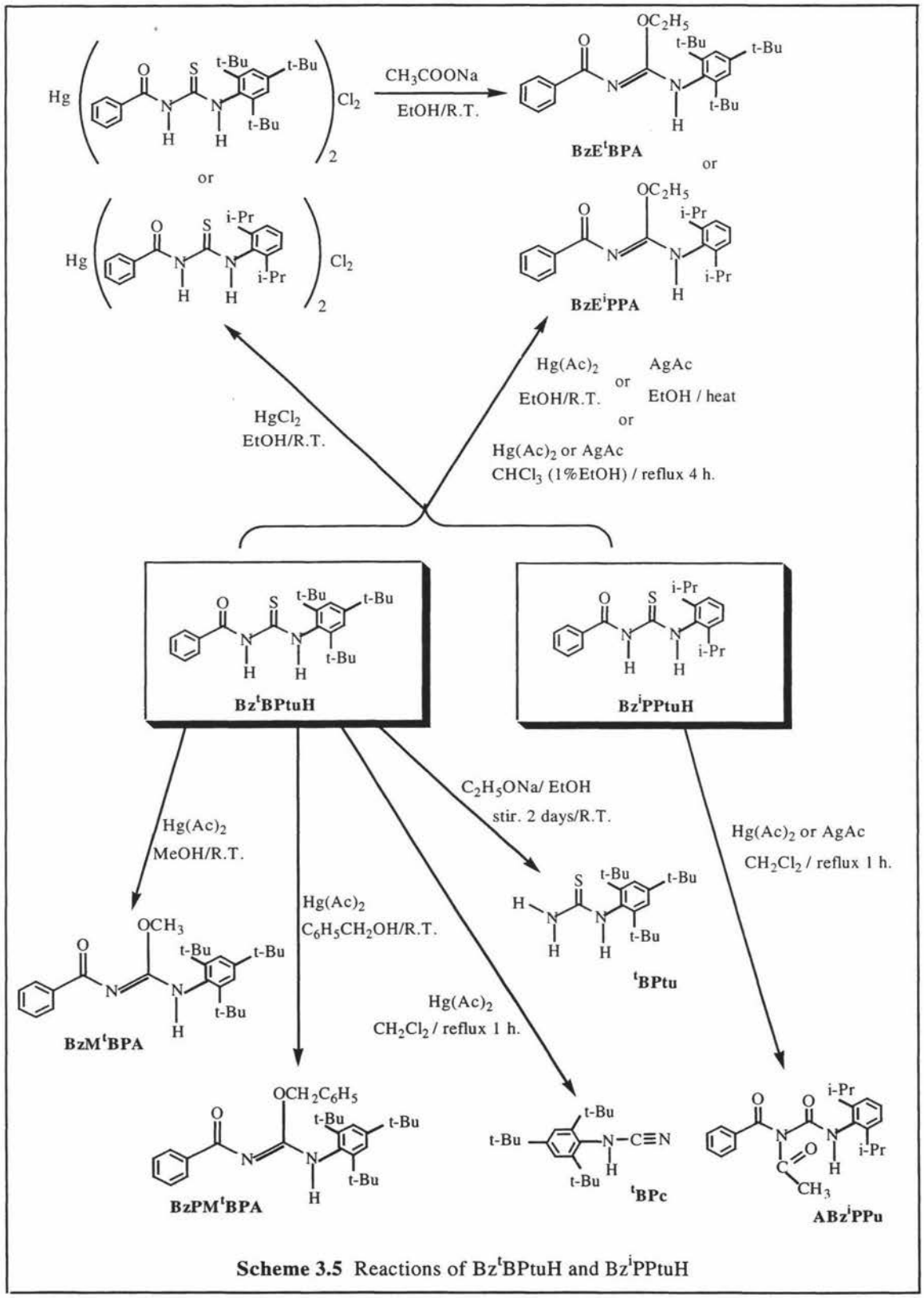

Scheme 3.5 Reactions of Bz^{t}BPtuH and Bz^{i}PPtuH

CHAPTER FOUR

Interactions of 1-Benzoyl-3-(2,4,6-tri-*tert*-butylphenyl)thiourea and Related Ligands with I_2 and Br_2

4.0 INTRODUCTION

As alluded to Chapter 2, the interaction of NiI_2 with the Bz^tBPtuH ligand resulted in the formation of $Ni(Bz^tBPtuH)_2I_2$. An attempt to grow crystals from the filtrate unexpectedly produced crystals of the I_2 adduct of Bz^tBPtuH. The crystal structure of this compound will be discussed later in this chapter. This thermal reaction however is not the most convenient way to make this complex, but this has led us to prepare and study iodine adducts of the title ligands. A study of these interactions will be one focal point of this chapter.

Lin *et al.*[1] and other earlier workers have shown that the interaction of thiourea with iodine can result in variety of different compounds, depending on the conditions under which the reaction takes place.

Spectrophotometric studies of solutions of iodine and thiourea in CH_2Cl_2 have indicated the presence of a 1:1 molar complex (Lang 1962)[2]. As well Lin *et al.*[1] have succeeded in growing deep red-brown crystals of a complex of the same composition, but unfortunately, due to instability of the crystals, they were not able to determine the crystal structure. A colorless compound with a thiourea-iodine molar ratio of 2:1 in $EtOH/H_2O$ obtained by McGowan (1886)[3], was later found to be formamidine disulfide diiodide monohydrate, $[(NH_2)_2C\text{-}S\text{-}S\text{-}C(NH_2)_2]^{2+}\ 2I^-.H_2O$ [4].

---

[1] G.Hung-Yin Lin and H. Hope, *Acta Cryst., Sect. B,* 1972, **28**, 643.
[2] R.P. Lang, *J. Am. Chem. Soc.*, 1962, **84**, 1185.
[3] G. McGowan, *J. Chem. Soc.*, 1886, **49**, 195.
[4] O. Foss, J. Johnsen and O. Tvedten, *Acta Chem. Scand.*, 1958, **12**, 1782.

However, in 1912, Werner[5] obtained a yellow solid by evaporation of a light-yellow solution in the reaction of thiourea with iodine in 2:1 molar ratio in benzene or CH_2Cl_2 at room temperature. The structure of this compound was unknown.

Lin *et al.*[1] prepared yellow crystals of composition $[(NH_2)_2CS]_2.I_2$ by reacting thiourea with iodine in 2:1 molar ratio in CH_2Cl_2 and the X-ray crystal structure showed the compound to contain the bis(thiourea)iodine(I) ion, $[I(SC(NH)_2)_2]^+I^-$.

Cristiani *et al.*[6] were able to isolate crystals of the diiodine adducts of penta atomic ring substrates containing thio- or seleno-amido groups as donors.

Esseffar *et al.*[7] have carried out an experimental and theoretical study on some thicarbonyl-I_2 molecular complexes and detected two different kinds of complexes. One with the CT band in the 300 nm region and the other one in the 350 nm region. The former one corresponds to the molecule of iodine which lies in the same plane of the C=S group, while in the latter one the I_2 moiety is almost perpendicular to that plane. This may be due to bulky substituents around the thiocarbonyl group and to the different nature of the HOMO[7].

Boyle *et al.*[8] have studied the reactions of the thioamides, thiourea (tu), 1-ethyl-2-thiourea (etu), 1,3-dimethyl-2-thiourea (dmtu), 1,3-diethyl-2-thiourea (detu), 3-methylbenzothiazole-2-thione (mbtt), and 3-methylrhodanine (mrh), with one equivalent of diiodine. It has been shown that these materials lie on a CT-ionic borderline. The crystal structure of dmtu-I_2 has been determined and is shown to be ionic and of the form $[I(dmtu)_2]^+I_3^-$.

In this work, the interaction of the title ligands with iodine was studied to determine the nature of the products formed. To the best of our knowledge no studies have been done on the interaction of I_2 with these ligands. However some chemical reactions have been done with Br_2 and *N*-acylthiourea derivatives.

Corsaro *et al.*[9] have postulated that in no case were bromine-thioamide

---

[5] E.A. Werner, *J. Chem. Soc.*, 1912, **101**, 2166.

[6] F. Cristiani, F. Demartin, F.A Devillanova, F. Isaia, G. Saba and G. Verani, *J.Chem. Soc. Dalton Trans.*, 1992, 3553.

[7] M. Esseffar, W. Bouab, A. Lamsabhi, J.-L.M. Abboud, R. Notario and M. Yáñez, *J. Am. Chem. Soc.*, 2000, **122**, 2300.

[8] P.D. Boyle, J. Christie, T. Dyer, S.M. Godfrey, I.R. Howson, C. McArthur, B. Omar, R.G. Pritchard and G.Rh. Williams, *J. Chem. Soc. Dalton Trans.*, 2000, 3106.

[9] A. Corsaro, A. Compagnini, G. Perrini and G. Purrello, *J. Chem. Soc. Perkin Trans.,I*, 1984, 897.

adducts isolated because of their rapid decomposition both upon exposure to moisture and storage at room temperature. Therefore they were generated in ice-cooled conditions.

Simoyi *et al.*[10] have performed a kinetic study of the oxidation of thiourea by aqueous bromine in different pH ranges.

Chan *et al.*[11] have prepared *N*-acylthiourea derivatives and H_2O_2/Br_2 were used as oxidants for the oxidative cyclization under various conditions.

Allegra *et al.*[12] have investigated the structure of the 1:1 adduct of thiophane (a thioether) with bromine by X-ray and nmr methods. In this adduct they claim the structure is more ionic [like **Fig. 4.1** (a)] than the donor structure [**Fig. 4.1** (b)].

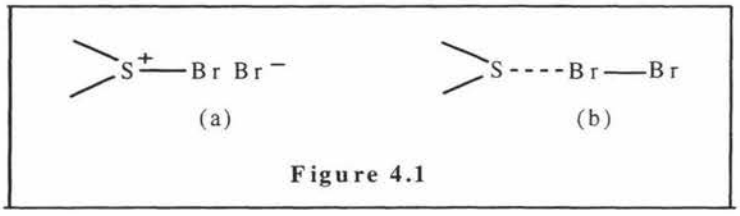

Figure 4.1

Vaughan *et al.*[13] have studied the crystal and molecular structures of $(CH_3)_2SBr_2$, $(CH_3)_2SBr_{2.5}$ and $(CH_3)_2SBr_4$ by high resolution powder synchrotron X-ray diffraction. The first, synthesised by the addition of Br_2 to dimethyl sulfide at room temperature, was isolated as the charge-transfer adduct, $(CH_3)_2S{\rightarrow}Br_2$. The other two, contain the $(CH_3)_2SBr^+$ bromodimethylsulfonium cation, which was synthesised by addition in the reverse order at –30 °C.

To the best of our knowledge no X-ray studies have been done on molecules containing thiocarbonyl-bromine adducts. This, along with a study of the nature of the oxidised products in two thiocarbonyl cases will be the second focal point for this chapter.

---

[10] R.H. Simoyi and I.R. Epstein, *J.Phys. Chem.*, 1987, **91**, 5124.

[11] C.W. Chan, C.M. Dominic Ng, J. Ho and K.C. Tin, *Indian J. Chem.*, 1997, **36B**, 216.

[12] G. Allegra, G.E. Wilson, Jr., E. Benedetti, C. Pedone and R. Albert, *J. Am. Chem. Soc.*, 1970, **92**, (13), 4002.

[13] G.B.M. Vaughan, A.J. Mora, A.N. Fitch, P.N. Gates and A.S. Muir, *J. Chem. Soc., Dalton Trans.*, 1999, 79.

4.1 Experimental

4.1.1 Instrumentation

Elemental analyses, ^{1}H and ^{13}C NMR spectra, Electronic spectra, mass spectra, IR spectra and melting points were performed as described previously. Fourier-transform Raman Spectra obtained from solid-state samples were carried out with a FRA 106 FT-Raman accessory mounted on a Bruker IFS66 FT-IR vacuum instrument, operating with an exciting frequency of 1064 nm (Nd YAG laser) by courtesy of Graham A. Bowmaker, University of Auckland, New Zealand.

4.1.2 Materials

All the reagents and solvents were of analytical grade and used without further purification. Aldrich Chemical Co Ltd. supplied iodine and bromine.

4.1.3 Preparation of Complexes

[(Bz^{t}BPtuH-κ^{1}S)I_2]

This complex may be prepared from either Method (a) or Method (b).

Method (a): To Bz^{t}BPtuH 0.2120g, (0.5000 mmol) dissolved in ~10 ml of $CHCl_3$, was added 0.1270g (0.5000 mmol) of I_2 in ~20 ml of the same solvent. The red brown solution, which formed at once, was reduced in volume using a rotary evaporator and the orange solid, was filtered off and washed with hexane. Yield, 0.2680g (79%). m.p. 154.4-155.9 °C. Anal. Found: C, 45.87; H, 5.21; N, 4.19; S, 4.59%. Calculated for $C_{26}H_{36}I_2N_2OS$: C, 46.02; H, 5.31; N, 4.13; S, 4.72%. Crystals suitable for X-ray analysis were grown by recrystallisation from $CHCl_3$.

Method (a): To Bz^{t}BPtuH 0.2120g, (0.5000 mmol) dissolved in ~10 ml of $CHCl_3$, was added 0.1905g (0.7500 mmol) of I_2 in ~20 ml of the same solvent. The dark red solution, which formed at once, was reduced in volume using a rotary evaporator and

the purple black crystals were filtered and washed with hexane, and dried in *vacuo.* Yield, 0.3014g (89%). m.p. 149-151 °C. Anal. Found: C, 45.73; H, 5.43; N, 4.17; S, 4.66%. Calculated for $C_{26}H_{36}I_2N_2OS$: C, 45.87; H, 5.31; N, 4.13; S, 4.72%.

The analytical results of method (a) and (b) are the same, hence the reaction has occurred in 1:1 molar ratio, indicating that only one product was formed under these conditions.

[(BzPPtuH-κ^{1}S)I$_2$]

To BzPPtuH 0.2420g, (0.5000 mmol) dissolved in ~10 ml of $CHCl_3$, was added 0.1270g (0.5000 mmol) of I_2 in ~20 ml of the same solvent. The dark red solution, which formed at once, was reduced to dryness using a rotary evaporator. A red brown oil formed and this was triturated in petroleum ether (5-8 drops) in an icebath. The red brown product, which formed, was filtered off and washed with petroleum ether and dried in *vacuo.* Yield, 0.2698g (73%), m.p. 191.4-191.8 °C. Anal. Found: C, 52.05; H, 3.25; N, 3.79; S, 4.34%. Calculated for $C_{32}H_{24}I_2N_2OS$: C, 52.97; H, 3.35; N, 3.92; S, 4.32%.

[(Bz^{i}PPtuH-κ^{1}S)I$_2$]

To Bz^{i}PPtuH 0.1700g, (0.5000 mmol) dissolved in ~10 ml of $CHCl_3$, was added 0.1270g (0.5000 mmol) of I_2 in ~20 ml of the same solvent. The red brown solution, which formed at once was reduced in volume using a rotary evaporator. The red brown product that formed after the addition of cold hexane (0.5 ml), was filtered, washed with hexane and air-dried to give 0.0410g of crude product, which was recrystallised, from $CHCl_3$. The dark brown micro crystals were isolated by vacuum filtration, washed with hexane, and dried in *vacuo.* Yield, 0.1120g (37.7%), m.p. 183-184 °C. Anal. Found: C, 40.60; H, 3.96; N, 4.96; S, 5.39%. Calculated for $C_{20}H_{24}I_2N_2OS$: C, 40.40; H, 4.04; N, 4.71; S, 5.38%.

[(BzFPtuH-κ^{1}S)I$_2$]

To BzFPtuH 0.2740g, (1.000 mmol) dissolved in ~10 ml of $CHCl_3$, was added 0.2540g (1.000 mmol) of I_2 in ~20 ml of the same solvent. The dark red brown solution, which formed at once was reduced in volume using a rotary evaporator. A red brown product was formed after the addition of cold hexane (3-4 drops) to the $CHCl_3$

solution, and this was filtered and washed with hexane and dried in *vacuo*. Yield, 0.3847g (72.8%), m.p. 112.6-115.2 °C. Anal. Found: C, 31.84; H, 1.91; N, 5.29; S, 6.01%. Calculated for $C_{14}H_{11}FI_2N_2OS$: C, 31.82; H, 2.08; N, 5.30; S, 6.06%.

[(BzPtuH-κ^1S)I_2]

To BzPtuH 0.2560g, (1.000 mmol) dissolved in ~10 ml of $CHCl_3$, was added 0.2540g (1.000 mmol) of I_2 in ~20 ml of the same solvent. The dark red brown solution, which formed at once, was reduce in volume using a rotary evaporator. A red brown product, which formed after the addition of cold hexane (3-4 drops) to the $CHCl_3$ solution, was filtered off and washed with hexane and dried in *vacuo*. Yield, 0.2298g (45%), m.p. 112.6-115 °C. Anal. Found: C, 33.21; H, 2.16; N, 5.70; S, 6.39%. Calculated for $C_{14}H_{12}I_2N_2OS$: C, 32.94; H, 2.35; N, 5.49; S, 6.27%.

[(Bz^{i}PPtuH-κ^1S)Br_2]

A solution of Br_2 (0.0532g, 0.3329 mmol) in $CHCl_3$ (~10 ml) was slowly added dropwise at 0^0C to Bz^{i}PPtuH (0.1133g, 0.3332 mmol) in $CHCl_3$ (~10 ml) with continuous stirring. The light yellow solution, which formed, was reduced in volume using a rotary evaporator. The yellow solid was filtered off under argon gas and washed with petroleum ether and dried in *vacuo*. Yield, 0.0500g (30%). m.p. 92-94 °C. Anal.Found: C, 46.98; H, 4.89; N, 5.62; S, 6.07; Br, 23.45%. Calculated for $C_{20}H_{24}Br_2N_2OS \cdot \frac{1}{8}CHCl_3$: C, 46.91; H, 4.68; N, 5.43; S, 6.22; Br, 31.97%. The reason for the discrepancy in the bromine chemical analysis probably derives from the instability of $CHCl_3$/pentane.

Upon aging the reaction mixture a colourless precipitate formed and the nature of this product has yet to be determined.

2-benzamido-5,7-di-tert-butylbenzothiazole hydrobromide (B^{t}BBTH)

A solution of Br_2 (0.0399g, 0.2496 mmol) in $CHCl_3$ (~10 ml) was slowly added dropwise at 0 °C to Bz^{t}BPtuH (0.1060g, 0.2500 mmol) in $CHCl_3$ (~10 ml) with continuous stirring. The light yellow solution was reduced to dryness using a rotary evaporator. Petroleum ether (0.5 ml) was added to the cold brown oil and the yellow white compound was filtered and washed with petroleum ether to give a pink white product, which was dried in *vacuo*. Yield, 0.0440g (39%). m.p. 158.7-159 °C.

Anal.Found: C, 58.87; H, 6.20; N, 6.26; S, 6.71; Br, 19.17%. Calculated for $[C_{22}H_{27}N_2SO]^+Br^-$: C, 59.07; H, 6.04; N, 6.26; S, 7.16; Br, 17.87%. Crystals suitable for X-ray analysis were grown by recrystallisation from $CHCl_3$/pentane.

The Interaction of BzPPtuH with Br_2

A solution of Br_2 (0.1598g, 1.000 mmol) in $CHCl_3$ (~10 ml) was slowly added dropwise at 0 °C to BzPPtuH (0.4840g, 1.000 mmol) in $CHCl_3$ (~10 ml) with continuous stirring. The light yellow solution, which formed, was reduced to dryness using a rotary evaporator. The yellow fluffy oil/solid formed was triturated in petroleum ether (5-8 drops) at 0 °C and the yellow product, which formed, was filtered off and washed with petroleum ether and dried in *vacuo*. Yield, 0.5602g. m.p. did not melt below 200 °C. Anal.Found: C, 64.25; H, 3.98; N, 4.81; S, 5.24; Br, 21.22%. Crystals (m.p. > 200 °C) suitable for X-ray analysis were grown by recrystallisation from $CHCl_3$/pentane. Further investigations into this reaction will be necessary to determine the nature of the product(s).

4.2 Results and Discussion

4.2.1 Physicochemical Studies and Characterization of the Complexes

4.2.1.1 Synthesis and Reactivity of the Complexes

The complexes $(LH)I_2$ (LH = Bz^{t}BPtuH, BzPPtuH, Bz^{i}PPtuH, BzFPtuH or BzPtuH) were prepared by reacting I_2 with the appropriate ligand LH in a 1:1 molar ratio as described in the experimental. The red brown complexes $(LH)I_2$ were isolated according to the following equation:

$$I_2 + LH \rightarrow (LH)I_2$$

Yields ranged from 37-79%. $(Bz^tBPtuH)I_2$ was also prepared when the molar ratio was 3:2.

As well, reaction of Bz^{i}PPtuH with Br_2 produced a rare example of a bromine adduct (see the X-ray crystal structure **Fig. 4.3**) according to the following equation:

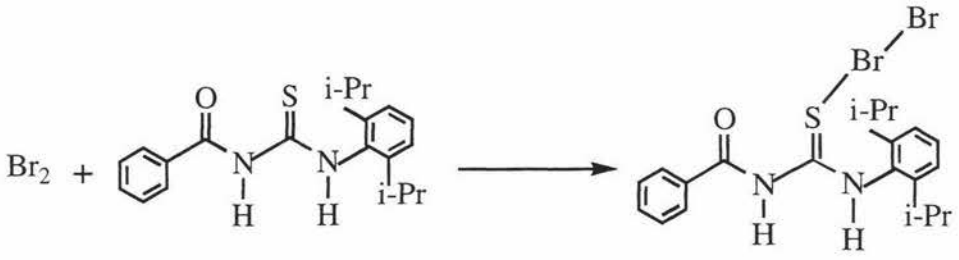

For the other LH compounds, pure bromine adducts were not isolated.

In contrast, addition of $Br_{2(l)}$ in $CHCl_3$ to Bz^{t}BPtuH in a 1:1 molar ratio in ice-cooled conditions does not produce a stable adduct but converts to the pinkish white oxidised product, 2-benzamido-5,7-tri-tert-butylbenzothiazole hydrobromide (B^{t}BBTH) (see the X-ray crystal structure **Fig. 4.4**) and interestingly, eliminates *t*-butyl bromide according to the following equation:

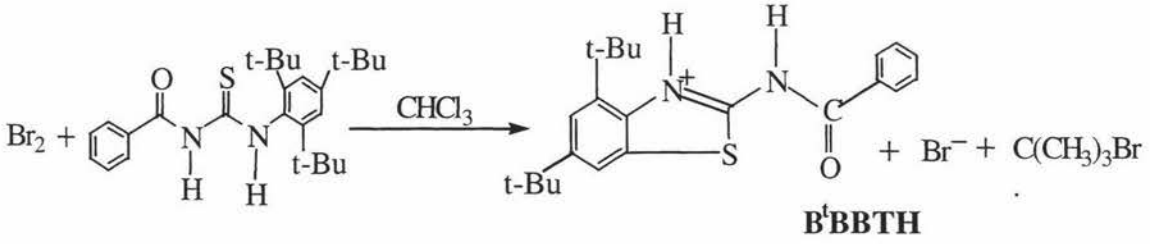

B^{t}BBTH

The reaction of Br_2 with BzPPtuH, is complex and the products have yet to be fully characterised. The bromine adduct Bz^{i}PPtuH $\rightarrow$ Br_2 (above) is unstable and converts to a white solid on standing.

4.2.1.2 IR and Raman Spectroscopic Studies of the Compounds

Infrared spectra were recorded in the range 400–4000 cm^{-1}, the far-i.r. spectra in the range 50–400 cm^{-1} and the FT-Raman spectra in the range 300–100 cm^{-1}. The ν(C=O) stretching frequencies of $(LH)I_2$ (LH = Bz^{t}BPtuH, BzPPtuH, Bz^{i}PPtuH, BzFPtuH or BzPtuH), as well as $[(Bz^{i}PPtuH)Br_2]$ are higher (7-15 cm^{-1}) than the free ligand values and this is direct evidence that C=O is not coordinated to I_2 or Br_2. The binding of the C=S group to I_2 is confirmed by the X-ray structure of $[(Bz^{t}BPtuH)I_2]$

which is shown in Section **4.2.1.5**. One of the most striking characteristics of the infrared spectra of thiocarbonyl compounds[14] is the fact that the C-S stretching mode appears very often coupled with other vibrational modes, which makes the band assignment difficult[7]. The experimental C=S stretching frequencies are only known[14] for a very limited set of thiocarbonyl compounds[7].

One of the ν(N-H) stretching frequencies of $(LH)I_2$ (Bz^tBPtuH, Bz^iPPtuH, and BzPtuH) is greater (~95, ~81 and ~66 cm^{-1}), while the other one is less (~12, ~49 and ~134 cm^{-1}) respectively than the ligand, whereas in $(BzFPtuH)I_2$ both frequencies are higher (~169 and ~67 cm^{-1}) than the free ligand.

The variation of the ν(N-H) stretching frequency of $[(Bz^iPPtuH)Br_2]$ is almost the same as for $[(Bz^iPPtuH)I_2]$ (~ +101 and ~ −44 cm^{-1}).

A adduct bond formation between a donor and diiodine stabilizes the lone pair of electrons of the donor by mixing the donor orbital with the σ^* antibonding orbital of I_2. One of the consequences of this is the lowering of the I-I bond order[15]. The more effective the interaction with the donor, the lower is the I-I bond order. Consequently, Raman spectroscopy provides a powerful tool to elucidate the interaction by means of the shifts of the ν(I-I) vibration in a complex with respect to that of free diiodine[16,17,18].

The FTRaman spectral data for the $(LH)I_2$ (LH = Bz^tBPtuH, Bz^iPPtuH, BzFPtuH or BzPtuH) compounds are collected in **Table 4.1** together with the assignments of the ν(I-I) (~138–155 cm^{-1}) and ν(I–S) (~165–177 cm^{-1}) vibrations. FTIR spectra show similar band positions to the FTRaman spectra. 'Free' diiodine in the solid state exhibits a single Raman band at 180 cm^{-1}, which moves to a lower wavenumber upon co-ordination to a donor atom, reflecting a reduction in I–I bond order[8]. 5,5-dimethyl-2-thioxoimidazolidin-4-one-diiodine[6] and 5,5-Dimethylimidazolidine-2,4-dithione- diiodine (1/1)[6] show strong bands at 158 cm^{-1} and 152 respectively, and 5,5-dimethylimidazolidine-2,4-dithionediiodine (1/2)[6] shows two peaks at 143ms and 165s

---

[14] M.T. Molina, M. Yáñez, O. Mó, R. Notario and J.-L.M. Abboud, in *The Chemistry of Functional Groups.Suppl.* A3: *The chemistry of double-bonded functional groups*; S. Patai, Z. Rappoport, Eds.; John Wiley and Sons: New York 1997.

[15] K.F. Purcell and J.C. Kotz, *Inorganic Chemistry,* Sanders, Philadelphia, PA, 1977.

[16] T.J. Marks, *Ann. N.Y. Acad. Sci.*, 1978, **313**, 594.

[17] M.A. Cowie, A. Gleizes, G.W. Grynkewich, D.W. Kalina, M.S. McClure, R.P. Scaringe, R.C. Teitebaum, S.L. Ruby, J.A. Ibers, C.R. Kannewurf and T.J. Marks, J. *Am. Chem. Soc.*, 1979, **101**, 2921.

[18] R.C. Teitebaum, S.L. Ruby and T.J. Marks, *J. Am. Chem. Soc.*, 1979, **101**, 7568; 1980, **102**, 3322.

cm^{-1}, whereas for the $[N(PPh_3)_2]^+[I_2(SCN)]^-$ [19] salt the ν(I–I) stretch was at 132–136 cm^{-1} and ν(I-S) at 192 cm^{-1}. The ν(I-I) band of $[(Bz^tBPtuH)I_2]$ is a doublet, at 138, 150 cm^{-1}, presumably due to factor group splitting, since the structural data implies only one molecule in the asymmetric unit.

The FTRaman spectrum of $Bz^iPPtuHBr_2$ displays a ν(Br–Br) stretch at 201 cm^{-1} (**Table 4.2**), whereas that for solid bromine is ≈300 cm^{-1} [20]. For $(CH_3)_2S{\rightarrow}Br_2$ the ν(Br–Br) stretch has been observed at 215 cm^{-1} [13] and this is similar to 201 cm^{-1} of $Bz^iPPtuHBr_2$.

Because $Bz^iPPtuHBr_2$ is metastable and is converted to an unknown oxidised product, or is easily converted to a Br_3^- salt in a small excess of Br_2, it was difficult to reproduce the purity of the sample in several attempts, hence the FTRaman spectrum was variable too.

---

[19] G.A. Bowmaker and D.A. Rogers, *J. Chem. Soc. Dalton Trans.*, 1981, 1146.

[20] J.J. Blaha, W. Brittain, C.E. Meloan and W.G. Fateley, *Applied Spectroscopy,* 1980, **34**, 636.

Table 4.1 Selected FTIR and FTRaman bands for iodine adducts

	IR[a] (cm^{-1})					R[b] (cm^{-1})		
Compound	ν(C=O)	ν(N-H)	ν(I-I)	ν(I-S)	Other bands	ν(I-I)	Other bands	ν(I-S)
[(Bz^{t}BPtuH)I_2]	1684vs	3316vw 3209vwbr	149s 139s	177w	345w 293w 248vw 64vw	138s 150m	292vw 258vw 115w	177w
[(BzPPtuH)I_2	1682vs	3309w 3190w						
[(Bz^{i}PPtuH)I_2]	1681vs	3318m 3188mbr	148s	171w	366w 292w 257w	145s	—	—
[(BzFPtuH)I_2][c]	1680vs	~3300w ~3198w	146s	~160sh	352vw 290w 219m 200w	139s	363vw 292vw 220w 115w	165w
[(BzPtuH)I_2][c]	1680vs	~3350w ~3150w	156m	170m	372w 275w 169w	155s	279vw 109w	175w

[a] Recorded in KBr. [b] Crystalline compounds in the 350-50 cm^{-1} range. [c] As nujol mull on NaCl. vs = very strong, s = strong, d = doublet, m = medium, w = weak, vw = very weak, br = broad.

Table 4.2 Selected FTIR and FTRaman bands for bromine compounds

	IR[a] (cm^{-1})				R[b] (cm^{-1})	
Compounds	ν(C=O)	ν(N-H)	ν(Br-Br)	Other bands	ν(Br-Br)	Other bands
[(Bz^{i}PPtuH)Br_2][c]	1682vs	3338m 3193mbr	[d]	—	201m	—
B^{t}BBTH	1695vs	3217vw 3110vw	—	—	—	—

[a] As nujol mull on NaCl. [b] Crystalline compounds in the 350-50 cm^{-1} range. [c] In other attempts the Br_3^- ion (band at 140 cm^{-1}) was also detected showing the variability in the purity of the samples. [d] Not recorded. vs = very strong, s = strong, d = doublet, m = medium, w = weak, vw = very weak, br = broad.

4.2.1.3 ^{1}H and ^{13}C NMR Spectroscopic Studies of Selected Compounds

The ^{1}H NMR data for selected compounds are shown in **Table 4.3** and ^{13}C NMR data in **Table 4.4**. In all the $(LH)I_2$ complexes (LH = Bz^{t}BPtuH, BzPPtuH, Bz^{i}PPtuH, BzFPtuH or BzPtuH) only one N-H proton was recorded and it is slightly higher than the free ligand, suggesting non-coordination of the N–H groups. Very little change has occurred in the chemical shifts of the aliphatic protons in Bz^{t}BPtuH and Bz^{i}PPtuH. B^{t}BBTH displays two N–H absorptions at 10.29 and 9.92 ppm, one is slightly lower and the other one is similar to the free ligand (N–H = 12.25 and 9.23 ppm). In the spectrum for $[(Bz^{i}PPtuH)Br_2]$, the usual doublet of doublets bands at 1.31 and 1.24 ppm is observed for the isopropyl methyls, however a new triplet band also appears at 1.19 ppm. This is probably due to the presence of *o*-isopropyl methyl groups of a possible oxidised product.

Two sets of isopropyl CH protons are observed at 2.93 and 3.07 ppm, the latter is consistent with $[(Bz^{i}PPtuH)Br_2]$, while the former may also be assigned to the oxidised product.

The ^{13}C chemical shifts for the C=S and C=O carbons of $(LH)I_2$ (LH = Bz^{t}BPtuH, BzPPtuH, Bz^{i}PPtuH, BzFPtuH or BzPtuH) are relatively constant with little change from the free ligand. This indicates that at room temperature the I_2 is dissociating from the adduct. For 5,5-dimethyl-2-thioxoimidazolidin-4-one-diiodine[6] the C=S carbon moves to lower chemical shift (–2.1 ppm) indicating that it is less dissociable. In the spectrum of $[(Bz^{i}PPtuH)Br_2]$ all the peaks are doubled which may be due to an oxidised product.

Table 4.3 ^{1}H chemical shift data for the adducts and oxidised product [a]

Complexes	^{1}H NMR ($CDCl_3$, TMS, ppm) δ_{N-H}	δ_{Ar-CH}	$\delta^{t}_{B-CH3\ or}\ ^{i}_{P-CH3\ and\ CH}$
[(Bz^{t}BPtuH)I_2]	10.08s (1H)	6.99-8.34m (7H)	1.36s (18H), 1.40s (9H)
[(BzPPtuH)I_2]	9.50s (1H)	7.23-7.85m (22H)	
[(Bz^{i}PPtuH)I_2]	10.15s (1H)	7.26-7.76m (8H)	1.22d (6H), 1.36d (6H) 2.97sept. (2H)
[(BzFPtuH)I_2]	9.82s (1H)	7.12-8.03m (9H)	
[(BzPtuH)I_2]	9.77s (1H)	7.25-8.04m (10H)	
[(Bz^{i}PPtuH)Br_2]	10.97 (1H) 10.06 (1H)	7.26-8.21m (8H)	1.24d (6H), 1.31d (6H) 1.19t (12H) 2.93sept. (2H) 3.06sept. (2H)
B^{t}BBTH	10.29 (1H) 9.92 (1H)	7.28-8.52m (7H)	1.42s (9H), 1.68s (9H)

[a] Recorded at 400MHz, chemical shifts are relative to $Si(CH_3)_4$ [TMS], solvent $CDCl_3$. S = singlet, d = doublet, t = triplet, m = multiplet, sept = septuplet.

Table 4.4 ^{13}C chemical shift data for the adducts and oxidised product [a]

complexes[b]	^{13}C NMR ($CDCl_3$, ppm) $\delta_{C=S}$	$\delta_{C=O}$	$\delta_{Ar\text{-}CH}\delta_{Ar\text{-}C\ (quat.)}$	$\delta^{t}_{B\text{-}CH3\ and\ C(quat.)}$ or $\delta^{i}_{P\text{-}CH3\ and\ CH}$
$[(Bz^{t}BPtuH)I_2]$	179.6	168.4	124.6-151.5 [7Ar-CH, 5Ar-$C_{(quat.)}$]	31.7 (3C), 32.8 (6C) 35.5 (1$C_{(quat.)}$) 37.2 (2$C_{(quat.)}$)
$[(BzPPtuH)I_2]$	178.4	167.7	127.7-142.9 [22Ar-CH, 8Ar-$C_{(quat.)}$]	
$[(Bz^{i}PPtuH)I_2]$	179.6	168.3	124.7-145.6 [8Ar-CH, 4Ar- $C_{(quat.)}$]	23.5 (2C), 24.8 (2C) 29.4 (2$C_{(tert.)}$)
$[(BzFPtuH)I_2]$	178.2	168.2	116.7-163.5 [9Ar-CH, 3Ar- $C_{(quat.)}$]	
$[(BzPtuH)I_2]$	177.6	168.2	125.3-136.4 [10Ar-CH, 2Ar- $C_{(quat.)}$]	
$[(Bz^{i}PPtuH)Br_2]$	181.6 178.87	168.1	123.9-145.3 [8Ar-CH, 4Ar- $C_{(quat.)}$]	23.1 (2C),23.3 (2C) 24.2 (2C), 24.5 (2C) 29.1 (2$C_{(tert.)}$) 29.1 (2$C_{(tert.)}$)
$B^{t}BBTH$	165.6 (C=N)	163.5	116.5-150.8 [7Ar-CH, 5Ar-$C_{(quat.)}$]	30.2 (3C), 31.4 (3C) 35.1 (1$C_{(quat.)}$) 35.5 (1$C_{(quat.)}$)

[a] Recorded at 400MHz, solvent $CDCl_3$. Quat = quaternary, tert = tertiary.

4.2.1.4 Electronic Absorption and Mass Spectroscopic Data for the Complexes

The electronic absorption spectra for $(LH)I_2$ (LH = $Bz^{t}BPtuH$, $Bz^{i}PPtuH$, BzFPtuH or BzPtuH) in $CHCl_3$ (**Table 4.5**) display a CT band at 498, 499, 507 and 505 nm (ε = 650, 674, 750 and 733) respectively due to coordinated I_2. As well, absorptions appearing at 359, 359, 327 and 360 nm (ε = 2490, 2322, 2500 and 2270) may be assigned as S $\rightarrow$ I–I charge transfer bands and these indicate that S is coordinated to

iodine. Pure I_2 has a electronic absorption at 509 nm (ε = 900) in $CHCl_3$[21]. Other I_2 adducts show similar spectroscopic characteristics to our compounds[7].

There is no parent ion M^+ present in the mass spectrum of [($Bz^tBPtuH)I_2$] in **Table 4.5**, but only LH^+.

Table 4.5 Electronic absorption[a] and Mass spectroscopic data[b] for the complexes

	UV-vis λ/nm (ε_{max}/dm^3 mol^{-1}cm^{-1})		
	Assignment		(+)FAB Mass spectra
Compounds	CT (C=S→I_2)	CT (I_2)	m/z (rel. int., %)
[($Bz^tBPtuH)I_2$]	420 (sh) 359 (2490)	498(sh)(650)[c]	no M^+ but LH^+ 425(17) [LH = $C_{26}H_{37}N_2OS$]$^+$ 367(100) [L–($C(CH_3)_3$)]$^+$ 105(25) [C_6H_5CO]$^+$
[($Bz^iPPtuH)I_2$]	420 (sh) 359 (2322)	499(sh)(674)	—
[(BzFPtuH)I_2]	327 (2500)	507 (750)	—
[(BzPtuH)I_2]	420 (sh) 360 (2270)	505 (733)	—
B^tBBTH			[(M-Br)(^{81}Br)]$^+$ 366 (53) 105(37) [C_6H_5CO]$^+$

[a] In $CHCl_3$. [b] 3-nitrobenzylalcohol matrix. [c] pure I_2 has a band at 509 nm (ε = 900).

[21] F. Freeman, J.W. Ziller, H.N. Po and M.C. Keindl, *J. Am. Chem. Soc.*, 1988, **110**, 2586.

4.2.1.5 Description of the Crystal Structures

4.2.1.5.1 Crystal Structure of [(Bz^{t}BPtuH-κ^1*S*)I_2]

The structure of the complex [(Bz^{t}BPtuH-κ^1*S*)I_2] is shown in **Fig. 4.2** with crystal data and structure refinement details given in **Table 4.6** and selected bond lengths and angles given in **Table 4.7**. Two independent molecules are contained in the asymmetric unit showing no significant differences from one another. One of the independent molecules (molecule 1) has been arbitrarily selected for the purpose of this discussion. As in the free ligand, the O and S atoms adopt a *trans* orientation with respect to one another, so as to minimise non-bonded steric interactions. In the structure the C(25)–O(1) distance (1.217(5) Å) is a little shorter than the free ligand C(25)–O(1) distance (1.226(3) Å) or to the calculated C=O (1.22 Å) double bond distance, but it is similar to the C(4)-O(7) distance of (1.211(4) Å) 5,5-dimethyl-2-thioxoimidazolidin-4-one-diiodine[6]. The C(26)–S(1) distance (1.701(4) Å) is longer than the C(26)–S distance of the free ligand (1.679(3) Å) suggesting lengthening upon coordination to I_2, but it retains some double bond character. The conformation of the molecule with respect to the phenyl rings is similar to the free ligand. The S...I–I fragment is practically linear (S(1)–I(1)–I(2) = 178.3(3)°).

The bond distances S(1)–I(1) (2.731(1) Å) , I(1)–I(2) (2.8537(4) Å) and bond angles of S(1)–I(1)–I(2) (178.3(3)°) and C(26)–S–I(1) (105.2(2)°) are similar to equivalent bond lengths and angles in 5,5-dimethyl-2-thioxoimidazolidin-4-one-diiodine[6] (S(6)–I(1) = 2.773(1) Å, I(1)–I(2) = 2.802(1) and S(6)–I(1)–I(2) = 176.14(2)°, C=S–I(1) = 104.5(1)°). As well, Ph_3PSI_2 and $(Me_2N)_3PSI_2$ adopt a charge-transfer structure with an approximately linear S–I–I bond (177.98(6)°) and *d*(I–I), 2.856(1) Å[22]. Therefore in all these structures the *d*(I–I) distance is significantly increased compared to that of solid diiodine (2.694 Å)[7]. The greater the S donor power the shorter is the S...I and longer the I–I bond distance[6].

The intramolecular hydrogen bond, N(2)–H...O(1) equals 2.015(6) Å which results in an almost planar six membered ring with C(25), N(1) and C(26) atoms in the

---

[22] W.I. Cross, S.M. Godfrey, S.L. Jackson, C.A. McAuliffe and R.G. Pritchard, *J. Chem. Soc., Dalton Trans.*, 1999, 2225.

central part of the molecule. As well in the crystal, the molecules are linked together by intermolecular N–H...O interactions (N(2)–H...O(1) = 2.604(6) Å) and three unequal C–H(*tert*-butyl)...I(2) (3.197(6), 3.216(6) and 3.242(6)) interactions (second and third H-bonds are from the same complex, whereas the third one is from another complex).

In contrast thiourea forms an anionic compound with I_2 (in 2:1 molar ratio). The compound consists of bis(thiourea)iodine(I) cations, $I[SC(NH)_2]_2^+$, and iodide anions[1]. For thiourea–I_2 complexes, such as $(tu)_x(I_2)_y$ (tu = thiourea, x = 2, y = 1 or 3, when x = 3, y = 5), S–I distances in the range 2.43 – 2.62 Å were observed[8]. These are shorter and stronger than that for Bz^{t}BPtuH (S(1)–I(1) = 2.731(1) Å).

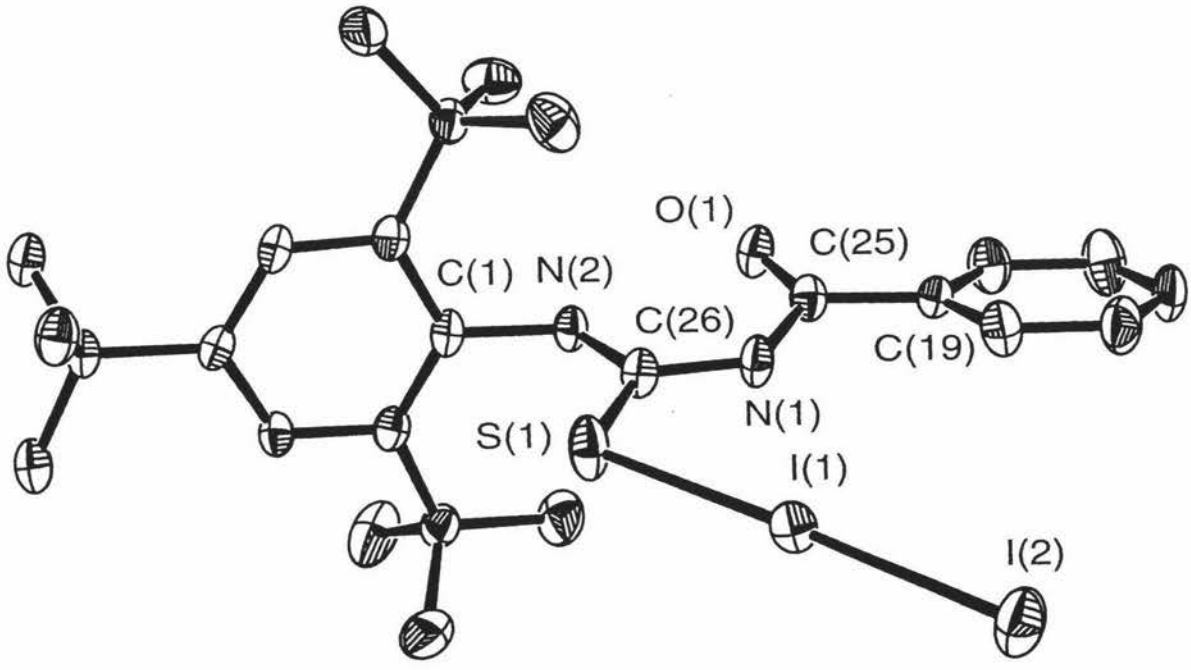

Figure 4.2 ORTEP diagram for the complex [(Bz^{t}BPtuH-κ^1*S*)I_2] showing the numbering system used. Thermal ellipsoids are at the 50% probability level. Hydrogen atoms have been omitted for clarity

Table 4.6 Crystal data and structure refinement for [(Bz^{t}BPtuH-κ^1*S*)I$_2$]

Identification code	ic6	
Empirical formula	$C_{52}H_{72}I_4N_4O_2S_2$	
Formula weight	1356.86	
Temperature	150(2) K	
Wavelength	0.71073 Å	
Crystal system	Triclinic	
Space group	P-1	
Unit cell dimensions	a = 9.6564(1) Å	α = 104.284(1)°
	b = 14.0151(2) Å	β = 94.165(1)°
	c = 22.3483(1) Å	γ = 100.706(1)°
Volume	2857.62(5) Å^3	
Z	2	
Density (calculated)	1.577 Mg/m^3	
Absorption coefficient	2.294 mm^{-1}	
F(000)	1344	
Crystal size	0.38 x 0.36 x 0.03 mm^3	
Theta range for data collection	0.95 to 26.45°.	
Index ranges	$-12 \leq h \leq 12$, $-17 \leq k \leq 17$, $-27 \leq l \leq 27$	
Reflections collected	26796	
Independent reflections	11520 [R(int) = 0.0344]	
Absorption correction	Semi-empirical from equivalents	
Max. and min. transmission	0.9344 and 0.4761	
Refinement method	Full-matrix least-squares on F^2	
Data / restraints / parameters	11520 / 0 / 577	
Goodness-of-fit on F^2	1.024	
Final R indices [I>2sigma(I)]	R1 = 0.0438, wR2 = 0.1100	
R indices (all data)	R1 = 0.0574, wR2 = 0.1184	
Largest diff. peak and hole	1.605 and -1.382 e.Å^{-3}	

Table 4.7 Selected bond lengths [Å] and angles [°] for [(Bz^{t}BPtuH-κ^1*S*)I_2] with estimated standard deviations in parentheses

Bond lengthes:

	Molecule 1	*Molecule 2*
I(1)-I(2)	2.8537(4)	2.8286(5)
S(1)-I(1)	2.731(1)	2.723(1)
C(26)-S(1)	1.701(4)	1.707(5)
C(1)-N(2)	1.449(5)	1.451(5)
C(26)-N(2)	1.306(5)	1.310(6)
N(1)-C(26)	1.384(5)	1.375(6)
C(25)-N(1)	1.382(6)	1.402(6)
C(25)-O(1)	1.217(5)	1.214(6)

Bond angles:

S(1)-I(1)-I(2)	178.3(3)	178.6(4)
C(26)-S(1)-I(1)	105.2(2)	105.1(2)
C(6)-C(1)-N(2)	119.6(4)	118.4(4)
C(2)-C(1)-N(2)	117.3(4)	118.2(4)
O(1)-C(25)-N(1)	121.7(4)	121.4(4)
O(1)-C(25)-C(19)	123.7(4)	124.0(5)
N(1)-C(25)-C(19)	114.6(4)	114.6(4)
C(25)-N(1)-C(26)	128.2(4)	127.3(4)
N(2)-C(26)-N(1)	118.6(4)	119.3(4)
N(2)-C(26)-S(1)	121.7(3)	121.3(3)
N(1)-C(26)-S(1)	119.7(3)	119.3(4)
C(26)-N(2)-C(1)	122.0(4)	121.5(4)

4.2.1.5.2 Crystal Structure of [(Bz^{i}PPtuH-κ^1*S*)Br_2]

The structure of the complex [(Bz^{i}PPtuH-κ^1*S*)Br_2] is shown in **Fig. 4.3** with crystal data and structure refinement details given in **Table 4.8** and selected bond lengths and angles given in **Table 4.9**. The crystal structure of the adduct [(Bz^{i}PPtuH-κ^1*S*)Br_2] contains one molecule and a $CHCl_3$ molecule in the asymmetric unit. The complex [(Bz^{i}PPtuH-κ^1*S*)Br_2] is similar to the previously discussed [(Bz^{t}BPtuH-κ^1*S*)I_2]. The C(19)–O(1) distance is 1.224(3) Å, which is similar to the free ligand 1.224(3) Å, while the C(20)–S(1) distance 1.724(2) Å, is longer than the Bz^{t}BPtuH 1.679(3) Å suggesting lengthening upon coordination to Br_2, but it still retains some double bond character. The S(1)–Br(1) distance is 2.4036(6) Å, and the Br(1)–Br(2) distance is 2.6118(4) Å. The S(1)–Br(1)–Br(2) bond angle is 175.99(2)° is close to linear. This compares well with the linear arrangement of S–Br–Br of 1-bromothiophanium bromide[12] and $(CH_3)_2SBr_2$[13] with S–Br and Br–Br bond lengths 2.321(4) and 2.724(2) Å for the former, and 2.329(6) Å and 2.705(3) Å in the latter respectively. The S–Br(2)–Br(1) bond angle of 1-bromothiophanium bromide is 178(3)°, whereas the S–Br(1)–Br(2) bond angle of $(CH_3)_2SBr_2$ is 176.1(2)°. In all these structures the interaction between the sulfur (donor) atom and the bromine molecule (acceptor), and the consequent lengthening of the Br–Br distance from the value in molecular Br_2 [2.287(10) Å][13], provide evidence for the charge-transfer nature of these complexes.

As in the other molecules, the [(Bz^{i}PPtuH-κ^1S)Br_2] adduct also contains an intramolecular hydrogen bond , with N(2)—H…O(1) equal to 2.030(6) Å, in the central part of the molecule. As well in the crystal, the molecules are linked together by intermolecular N–H…O interactions (N(2)–H…O(1) = 2.421(4) Å) and Br(1)…Br(1) interactions (3.791(2) Å).

Also there are intermolecular hydrogen bonds with chloroform molecules in the lattice with Br(2)…H—CCl_3 = 2.727(5) Å, C—H(iso-propyl)…Cl–$CHCl_2$ = 2.890(6) Å and C—H(aromatic ring)…Cl–$CHCl_2$ = 2.828(6) Å.

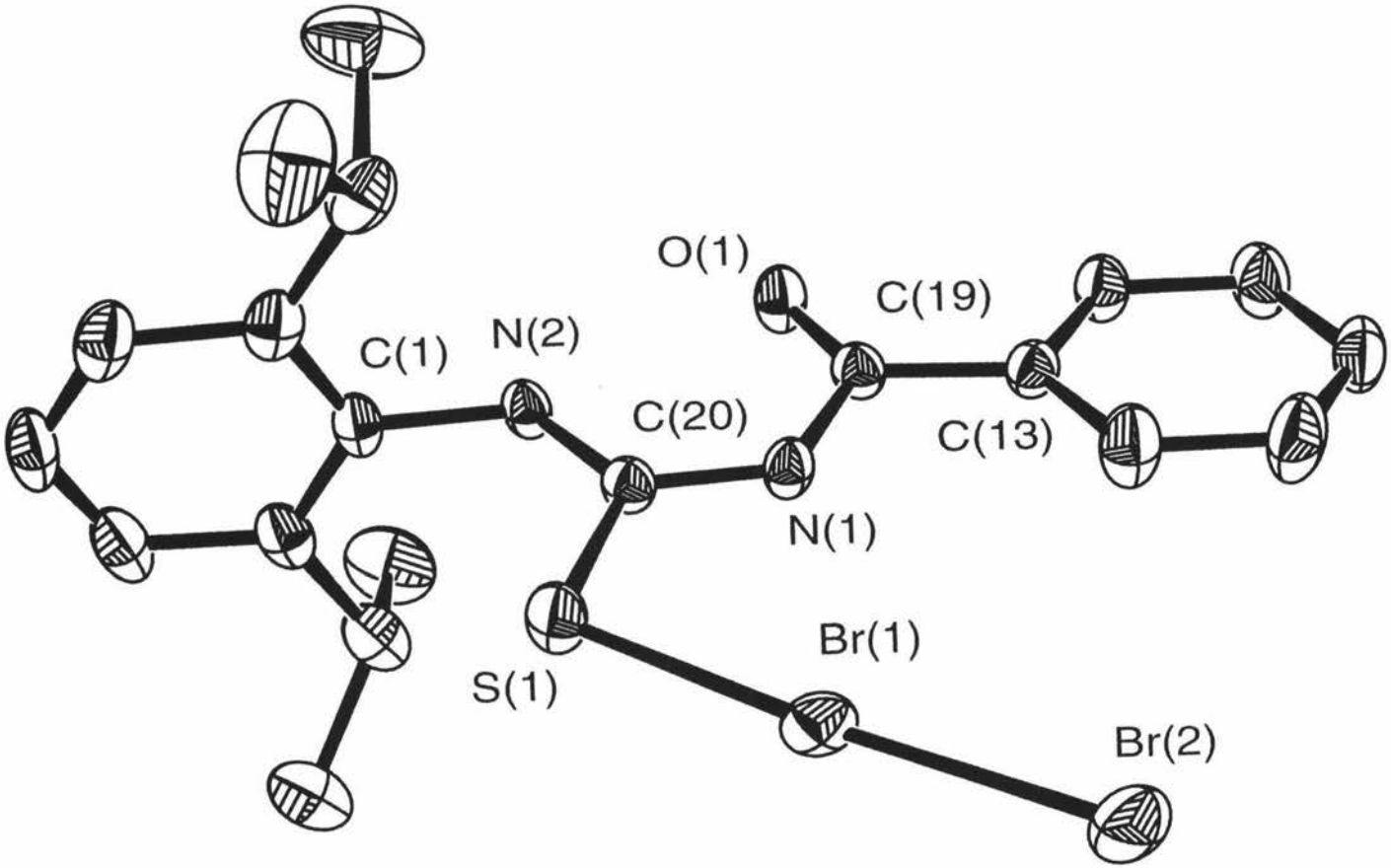

Figure 4.3 ORTEP diagram for the complex [($Bz^{i}PPtuH$-$\kappa^{1}S$)Br_2] showing the numbering system used. Thermal ellipsoids are at the 50% probability level. Hydrogen atoms have been omitted for clarity

Table 4.8 Crystal data and structure refinement for [($Bz^{i}PPtuH$-$\kappa^{1}S$)Br_2]

Identification code	ik4bra
Empirical formula	$C_{21}H_{25}Br_2Cl_3N_2OS$
Formula weight	619.66
Temperature	150(2) K
Wavelength	0.71073 Å
Crystal system	Monoclinic
Space group	C 2 / c
Unit cell dimensions	a = 15.7969(7) Å $\alpha = 90°$
	b = 20.0906(7) Å $\beta = 93.953(1)°$
	c = 16.3648(7) Å $\gamma = 90°$
Volume	5181.3(4) $Å^3$
Z	8
Density (calculated)	1.589 Mg/m^3
Absorption coefficient	3.535 mm^{-1}
F(000)	2480
Crystal size	0.19 x 0.17 x 0.14 mm^3
Theta range for data collection	1.64 to 26.40°.
Index ranges	$-19 \leq h \leq 19$, $-25 \leq k \leq 25$, $-20 \leq l \leq 20$
Reflections collected	22873
Independent reflections	5286 [R(int) = 0.0268]
Absorption correction	Semi-empirical from equivalents
Max. and min. transmission	0.6374 and 0.5532
Refinement method	Full-matrix least-squares on F^2
Data / restraints / parameters	5286 / 0 / 271
Goodness-of-fit on F^2	1.024
Final R indices [I>2sigma(I)]	R1 = 0.0271, wR2 = 0.0678
R indices (all data)	R1 = 0.0359, wR2 = 0.0730
Largest diff. peak and hole	0.765 and -0.583 $e.Å^{-3}$

Table 4.9 Selected bond lengths [Å] and angles [°] for [(Bz^iPPtuH-κ^1S)Br_2] with estimated standard deviations in parentheses

Bond lengths:

Br(1)-Br(2)	2.6118(4)
Br(1)-S(1)	2.4036(6)
S(1)-C(20)	1.724(2)
N(1)-C(20)	1.360(3)
N(1)-C(19)	1.392(3)
N(2)-C(20)	1.314(3)
N(2)-C(1)	1.450(2)
C(19)-O(1)	1.224(3)

Bond angles:

S(1)-Br(1)-Br(2)	175.99(2)
C(20)-S(1)-Br(1)	100.97(7)
C(20)-N(1)-C(19)	127.5(2)
C(20)-N(2)-C(1)	121.8(2)
C(2)-C(1)-N(2)	118.1(2)
C(6)-C(1)-N(2)	117.9(2)
O(1)-C(19)-N(1)	121.0(2)
O(1)-C(19)-C(13)	123.9(2)
N(1)-C(19)-C(13)	115.1(2)
N(2)-C(20)-N(1)	120.8(2)
N(2)-C(20)-S(1)	119.1(2)
N(1)-C(20)-S(1)	120.1(2)

4.2.1.5.3 Crystal Structure of B^{t}BBTH

The structure of the 2-benzamido-5,7-di-*tert*-butylbenzothiazole hydrobromide (B^{t}BBTH) is shown in **Fig. 4.4**, with crystal data and structure refinement details given in **Table 4.10**. Selected bond lengths and angles are listed in **Table 4.11,** and selected torsion angles given in **Table 4.12**. Two independent molecules are contained in the asymmetric unit showing no significant differences from one another. One of the independent molecules (molecule 1) has been arbitrarily selected for the purpose of this discussion. The molecule B^{t}BBTH has a heterocyclic ring structure with separate Br^- anions. The cation, contains a protonated benzothiazole ring, which is formed by the loss of a t-butyl group. The S and carbonyl group are *cis* with respect the C(15)–N(2) bond, which is similar to that in 2-(2-chloropropionamido)benzothiazole[23]. Particular interest in this molecule is the angle at S in the thiazoline ring is close to a right angle (C(15)–S(1)–C(6) = 89.4(2)°) which is similar to the C(1)–S(1)–C(16) angle of 2-(2-chloropropionamido)benzothiazole (87.2(3)°)[23].

In the thiazole ring, the endocyclic C=N bond length of N(1)–C(15) at 1.327(5) Å is similar to the equivalent bond length in the free ligand, (N(2)–C(26) 1.326(4) Å), but longer than its equivalent found in the neutral 2-(2-chloropropionamido)benzothiazole molecule at 1.290(8) Å[23]. These distances are consistent with some double bond character. The N(1)–C(1) bond length of 1.402(5) Å is longer than that for N(1)–C(15) and approaches that of a single bond with some double bond character. Similarly the S(1)–C(6) and S(1)–C(15) bond lengths are 1.757(4) Å and 1.715(4) Å respectively and lie between a double and a single carbon-sulfur bond. These bonds are similar in length to those found in 2-(2-chloropropionamido)benzothiazole[23]. The exocyclic N-C bonds N(2)–C(15) (1.358(5) Å) and N(2)–C(16) (1.389(5) Å) also display partial double bond character.

The C(18)–C(17)–C(16)–O(1) torsion angle, at about 7°, shows the benzoyl phenyl ring is slightly twisted out of the plane of the central part of the molecule.

The benzothiazole moiety can be considered rigorously planar (torsion angle C(15)–N(1)–C(1)–C(6) is –0.1(5)°). The *tert*-butyl groups are not pushed back as in

---

[23] M. Annese, A.B. Corradi, L. Forlani, C. Rizzoli and P. Sgarabotto, *J. Chem. Soc. Perkin Trans.* 2, 1994, 615.

other structures and the torsion angles show the groups to be approximately in the plane of aromatic ring (C(6)–C(1)–C(2)–C(7) = 177.2(3)°).

There are no intramolecular H-bonds, instead there are short intramolecular contacts with the carbonyl oxygen and S atom (S(1)...O(1) = 2.724(4) Å in Molecule 1 and 2.709(4) Å in Molecule 2) forming an almost planar pseudo S(1)–C(15)–N(2)–C(16)–O(1) cycle. This is considerably less than the sum of the van der Waals radii, 3.3 Å, but comparable with that found in the related compound 2-(2-chloropropionamido)benzothiazole (S...O = 2.741(4) Å)[23].

The packing in the structure is determined by several hydrogen bonds of type Br^-...H. In Molecule 1 and Molecule 2 (or Molecule A) (**Fig. 4.5**) the contacts are as follows: Br(2)...H–N(1) = 2.448(6) Å, Br(2)...H–N(2) = 2.416(6) Å, Br(2)...H–C(22) = 2.842(6) for Molecule 1, and Br(2)...H–C(5A) = 2.799(6) Å, Br(2)...S(1A) = 3.610(5) Å and O(1A)....H–C–C(7)(t-butyl) = 2.536(6) Å in Molecule 2. For Molecule 2, similar hydrogen bonds of the type Br(1)...H–N(1A) and Br(1)...H–N(2A) are also observed as well as bonds of the type Br(1)...H–C–C(7A)(t-butyl) = 3.059(7) Å and Br(1)...H–C(5) = 2.838(6) Å (**Fig. 4.5**).

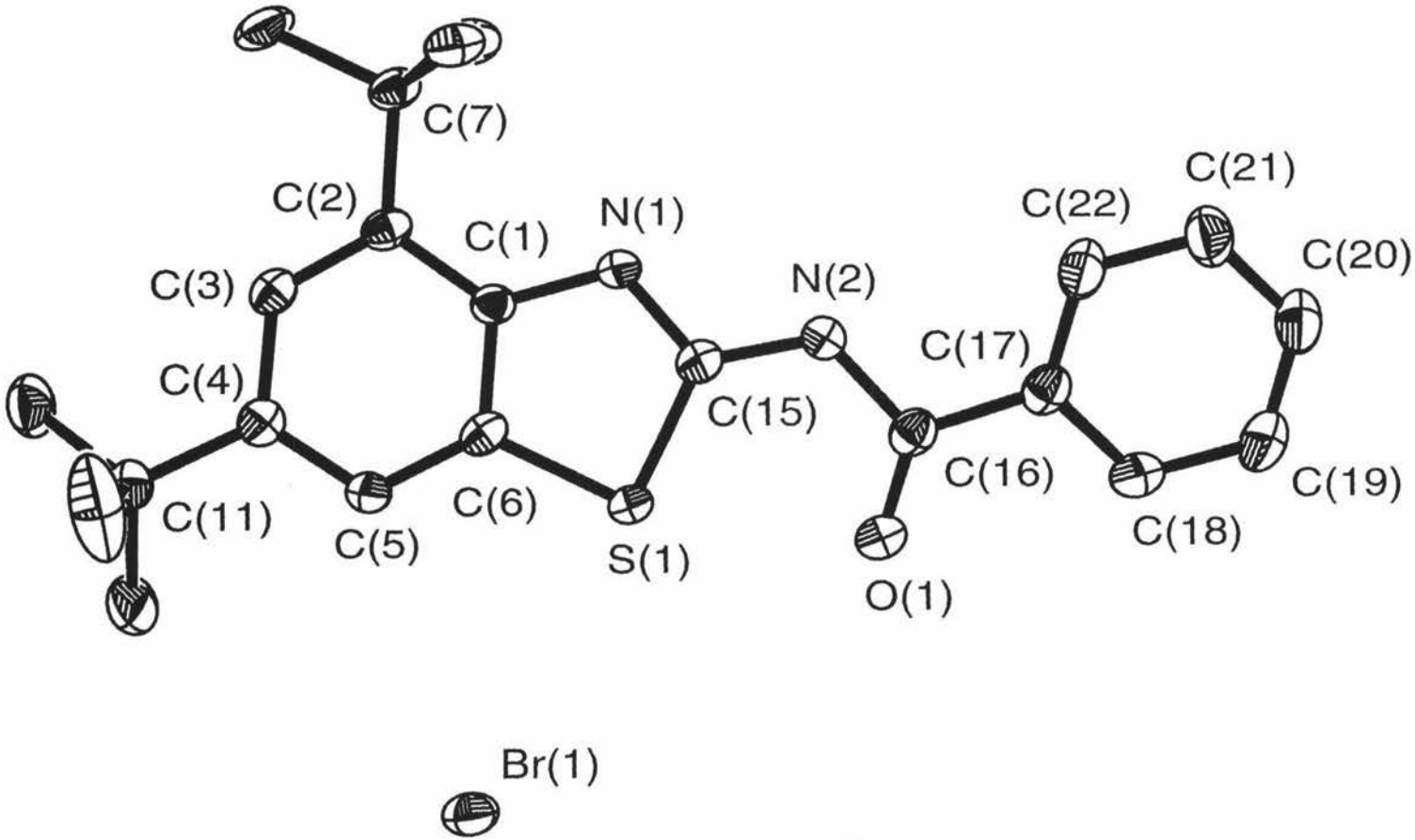

Figure 4.4 ORTEP diagram for the compound B^{t}BBTH showing the numbering system used. Thermal ellipsoids are at the 50% probability level. Hydrogen atoms have been omitted for clarity

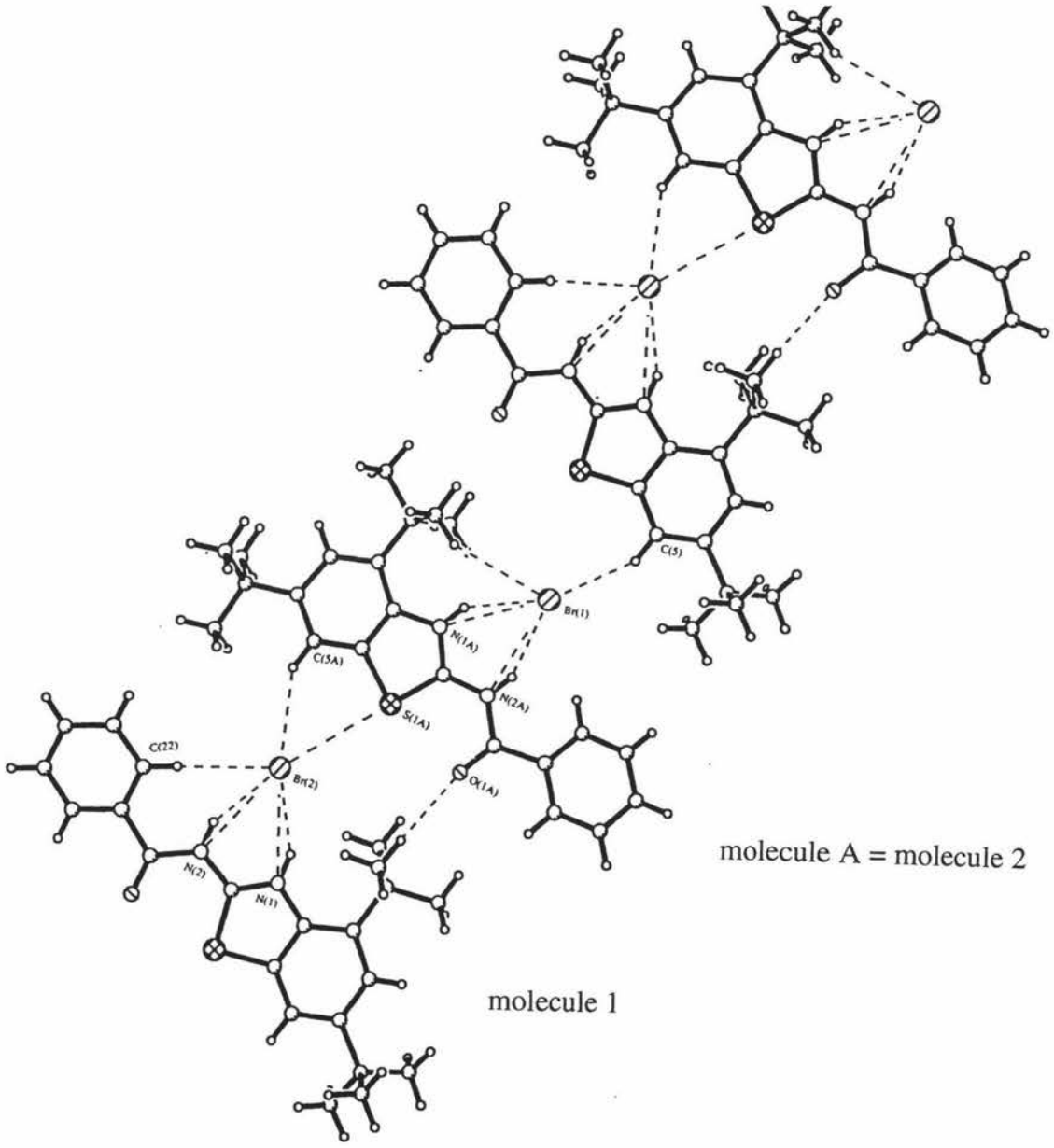

Figure 4.5 Intermolecular hydrogen bonding between B^{t}BBTH molecules

Table 4.10 Crystal data and structure refinement for B^{t}BBTH

Identification code	ic1bra	
Empirical formula	$C_{22}H_{27}BrN_2O_S$	
Formula weight	447.43	
Temperature	150(2) K	
Wavelength	0.71073 Å	
Crystal system	Monoclinic	
Space group	P2(1)/c	
Unit cell dimensions	a = 16.9031(2) Å	$\alpha = 90°$
	b = 22.8703(3) Å	$\beta = 101.54°$
	c = 11.8392(1) Å	$\gamma = 90°$
Volume	4484.31(9) Å^3	
Z	8	
Density (calculated)	1.325 Mg/m^3	
Absorption coefficient	1.940 mm^{-1}	
F(000)	1856	
Crystal size	0.16 x 0.12 x 0.12 mm^3	
Theta range for data collection	1.23 to 26.39°.	
Index ranges	$-21 \le h \le 20$, $-28 \le k \le 24$, $-13 \le l \le 14$	
Reflections collected	25884	
Independent reflections	9115 [R(int) = 0.0435]	
Absorption correction	Semi-empirical from equivalents	
Max. and min. transmission	0.8006 and 0.7466	
Refinement method	Full-matrix least-squares on F^2	
Data / restraints / parameters	9115 / 0 / 487	
Goodness-of-fit on F^2	1.019	
Final R indices [I>2sigma(I)]	R1 = 0.0536, wR2 = 0.1096	
R indices (all data)	R1 = 0.0890, wR2 = 0.1267	
Largest diff. peak and hole	2.206 and -2.048 e.Å^{-3}	

Table 4.11 Selected bond lengths [Å] and angles [°] for B^{t}BBTH with estimated standard deviations in parentheses

Bond lengths:

	Molecule 1	*Molecule 2*
S(1)-C(15)	1.715(4)	1.717(4)
S(1)-C(6)	1.757(4)	1.755(4)
N(1)-C(15)	1.327(5)	1.329(5)
N(1)-C(1)	1.402(5)	1.409(5)
N(2)-C(15)	1.358(5)	1.358(5)
N(2)-C(16)	1.389(5)	1.388(5)
O(1)-C(16)	1.214(4)	1.216(5)
C(1)-C(6)	1.398(5)	1.397(5)
C(16)-C(17)	1.493(5)	1.490(6)

Bond angles:

C(15)-S(1)-C(6)	89.4(2)	89.3(2)
C(15)-N(1)-C(1)	114.3(3)	114.2(3)
C(6)-C(1)-N(1)	110.6(3)	110.3(3)
N(1)-C(15)-S(1)	114.1(3)	114.0(3)
C(1)-C(6)-S(1)	111.7(3)	112.1(3)
C(15)-N(2)-C(16)	122.6(3)	122.5(3)
N(1)-C(15)-N(2)	119.5(3)	119.7(3)
N(2)-C(15)-S(1)	126.4(3)	126.2(3)
O(1)-C(16)-N(2)	120.4(4)	120.4(4)
O(1)-C(16)-C(17)	124.2(3)	123.4(4)
N(2)-C(16)-C(17)	115.3(3)	116.2(3)
C(3)-C(2)-C(7)	123.0(3)	122.1(3)
C(1)-C(2)-C(7)	122.4(3)	123.1(3)
C(5)-C(4)-C(11)	120.2(3)	122.5(3)
C(3)-C(4)-C(11)	120.8(3)	119.4(4)

Table 4.12 Selected torsion angles [°] for B^{t}BBTH

	Molecule 1	*Molecule 2*
C(15)-N(1)-C(1)-C(6)	-0.1(5)	-1.8(5)
N(1)-C(1)-C(6)-S(1)	-0.4(4)	1.0(4)
C(15)-S(1)-C(6)-C(1)	0.6(3)	0.0(3)
C(1)-N(1)-C(15)-S(1)	0.6(4)	1.8(4)
C(6)-S(1)-C(15)-N(1)	-0.7(3)	-1.0(3)
C(6)-C(1)-C(2)-C(7)	177.2(3)	-179.3(3)
N(1)-C(1)-C(2)-C(7)	-0.2(6)	-0.2(6)
C(7)-C(2)-C(3)-C(4)	-176.3(4)	178.0(3)
O(1)-C(16)-C(17)-C(18)	7.2(6)	19.9(6)
N(2)-C(16)-C(17)-C(18)	-169.7(4)	-161.2(4)
O(1)-C(16)-C(17)-C(22)	-172.2(4)	-155.6(4)
N(2)-C(16)-C(17)-C(22)	10.8(6)	23.4(6)

4.3 Conclusions

The I_2 adducts of the LH ligands were obtained in 1:1 molar ratio as well as the metastable Br_2 adduct [(Bz^{i}PPtuH)Br_2] which was surprisingly prepared. The X-ray crystal structure of [Bz^{t}BPtuH)I_2] shows a long I–I bond distance 2.8537(4) Å, longer than the solid diiodine bond distance 2.694 Å[7]. The S–I bond distance is 2.731(1) Å. As well, the Br_2 adduct also shows a long Br–Br bond distance of 2.6118(4) Å, which is greater than the free molecular Br_2 bond distance (2.287(10) Å) and an S–Br bond distance of 2.4036(6) Å.

Spectroscopic studies on these adducts show the ν(I–I) stretching frequencies are found in the range 138–155 cm^{-1} which is lower than the free ν(I–I) stretch of 180 cm^{-1}. As well the ν(Br–Br) stretching frequency of 201 cm^{-1} in the Br_2 adduct has dropped from the solid bromine molecule (~300 cm^{-1}). The electronic spectrum of the I_2 adducts display CT bands due to S→I–I and I_2. According to Esseffar *et al.*[7], iodine adducts that absorb at around 350 nm should show structures where the I_2 moiety is perpendicular to the C=S bond. [Bz^{t}BPtuH-κ^1*S*)I_2] absorbs at 359 nm and the

I_2 lies in the same plane as the C=S group, which would appear not to follow the above prediction.

In the reaction of Bz^{t}BPtuH with Br_2 it was found that an oxidation product could also be produced. Thus the Br_2 adduct that initially formed in ice-cooled conditions with Bz^{t}BPtuH was converted to a novel heterocyclic ring compound, 2-benzamido-5,7-di-*tert*-butylbenzothiazole hydrobromide (B^{t}BBTH) at room temperature. This compound is ionic with Br^- anions and cations, which contain a protonated benzothiazole ring. A special feature of this reaction is the loss of a *t*-butyl group during the benzothiazole formation. The nature of the products formed from similar reactions with BzPPtuH and Bz^{i}PPtuH, has yet to be resolved.

A proposed mechanism for the formation of benzothiazole product is given in **Scheme 4.1.**

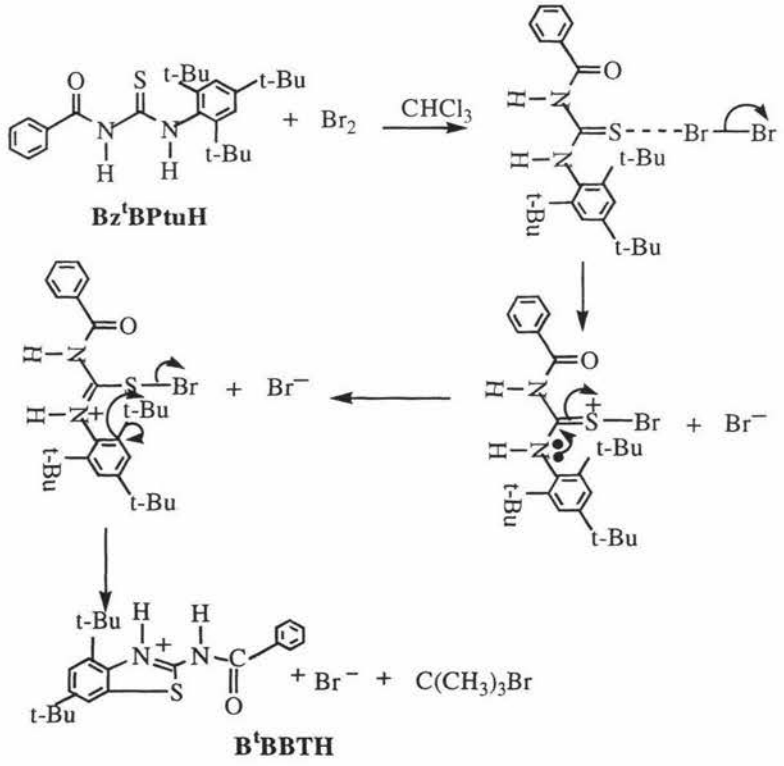

Scheme 4.1 Possible Mechanism of the Oxidation of Bz^{t}BPtuH with Br_2

The formation of *t*-butylbromide during the reaction was detected using ^1H and ^{13}C NMR. *Tert*-butyl protons were located at 1.50 ppm while the methyl carbons were found at 36.8 ppm and the C-Br carbon at 62.6 ppm, consistent with the presence of *t*-butyl bromide.

CHAPTER FIVE

Rh(I) Cycloocta-1,5-diene Complexes Containing 1-Benzoyl-3-(2,4,6-tri-*tert*-butylphenyl)thiourea and Related Ligands and the Coordination Chemistry with Pt(II)

5.0 INTRODUCTION

This chapter describes a selected aspect of rhodium(I) chemistry, with emphasis on the synthesis of [Rh(COD)(LH)Cl] (LH = Bz^{t}BPtuH, BzPPtuH, Bz^{i}PPtuH, BzFPtuH or BzPtuH) and a NMR study of the fast olefin (alkene) interchange of cycloocta-1,5-diene (COD), as well as the coordination chemistry of Bz^{t}BPtuH and Bz^{i}PPtuH ligands with platinum(II).

Rotondo *et al.*[1] has studied the fast olefin site interchange of COD in a Rh(I) square planar derivative [Rh(COD)(Ph_2PPy)Cl] and shown that the asymmetric cyclic diolefin complexes of rhodium(I) and iridium(I) have temperature-dependent ^{1}H NMR spectra indicating exchange of olefinic protons between non-equivalent sites.

Cauzzi *et al.*[2] have synthesised [Rh(COD)(Hbztu)Cl] (Hbztu = PhC(O)NHC(S)NH$(CH_2)_2CH_3$) by reacting Hbztu with [{Rh(COD)Cl}$_2$] in CH_2Cl_2 at room temperature and anchored rhodium with XGbztu (thiourea-functionalized xerogel) (**Fig. 5.1**) to give rhodium(I) species tethered by an Rh–S coordinate linkage. These new benzoylthiourea-functionalized hybrid materials, were prepared by the sol-gel process. The anchored rhodium(I) (Rh/XGbztu) species are very active, insoluble and recoverable catalysts for the hydroformylation of styrene, which exhibit remarkably

---

[1] E. Rotondo, G. Battaglia, C.G. Arena and F. Faraone, *J. Organomet. Chem.,* 1991, **419**, 399.

[2] D. Cauzzi, M. Lanfranchi, G. Marzolini, G. Predieri, A. Tiripicchio, M. Costa and R. Zanoni, *J. Organomet. Chem.,*1995, **488**, 115.

different behaviors depending on the density of the benzoylthiourea function on these xerogels.

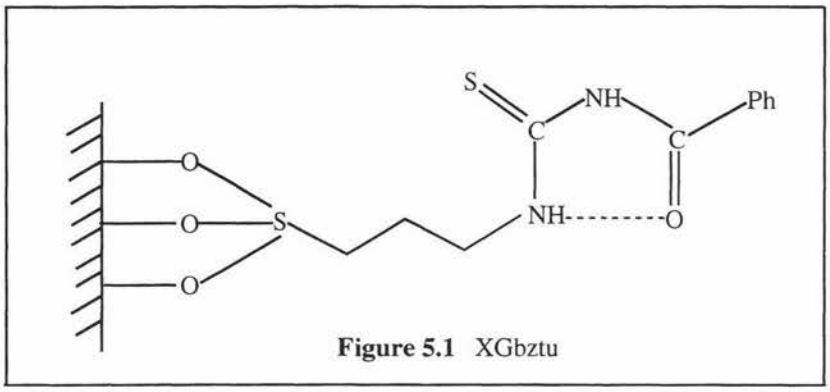

Figure 5.1 XGbztu

Kemp *et al.*[3] have shown an unusual mode of coordination of 1-benzoyl-3-phenylthiourea (H_2L^2) to Rh(I). The doubly deprotonated anion of the ligand molecule forms a bridging ligand to two metal centres, where the amidic nitrogen atom ($\kappa N'$) coordinates to one Rh(I) atom, while the 1-acylthiourea moiety binds to a second Rh(I) atom in the more usual bidentate ($\kappa^2 S,O$) fashion yielding a dinuclear rhodium(I) complex $[(PPh_3)_2(CO)Rh(\mu\text{-}L^2\text{-}\kappa N' :\kappa^2 O,S)Rh(PPh_3)(CO)].(CH_3)_2CO$, by reacting the ligand with $[Rh(CO)_2Cl]_2$ and PPh_3. The structure was determined by X-ray crystallography.

Koch *et al.*[4] and others, have shown that the co-ordination of the 1-aroyl-3,3-dialkylthioureas usually leads to very stable anionic bidentate-S,O co-ordination to Pd(II) [5], Pt(II) [6], and Rh(III) [7]. On the other hand the coordination chemistry of 1-aroyl-3-alkylthioureas is strongly influenced by an intramolecular hydrogen bond between the carbonyl atom of the aroyl moiety and the thiourea NH group, resulting in coordination through the S atom of the neutral ligand[8].

---

[3] G. Kemp, A. Roodt, W. Purcell and K.R. Koch, *J. Chem. Soc., Dalton Trans.,* 1997. 4481.

[4] K.R. Koch, Y. Wang and A Coetzee, *J. Chem. Soc., Dalton Trans.,* 1999, 1013.

[5] G. Fitzl, L. Beyer, R. Sieler, R. Richter, J. Kaiser and E. Hoyer, *Z. Anorg. Allg. Chem.,* 1977, **433**, 237.

[6] A. Irving, K.R. Koch and M. Matoetoe, *Inorg. Chim. Acta,*1993, **206**, 193.

[7] W. Bensch and M. Schuster, *Z. Anorg. Allg. Chem.,* 1992, **615**, 93.

[8] S. Bourne and K.R. Koch, *J. Chem. Soc., Dalton Trans,* 1993, 2071.

5.1 Experimental

5.1.1 Instrumentation

Elemental analyses, ^{1}H and ^{13}C NMR spectra, electronic spectra, mass spectra, IR spectra and melting points were performed as described previously.

5.1.2 Materials

All the reagents and solvents were of analytical grade and used without further purification. [{RhCl(COD)}$_2$] was prepared as previously reported[9]. Aldrich Chemical Co Ltd. supplied $K_2[PtCl_4]$.

5.1.3 Preparation of Complexes

The Rh complexes were prepared according to the method described in Cauzzi *et al.*[2] and the Pt complexes according to the Bourne *et al.*[8] with slight modifications.

[Rh(COD)(Bz^{t}BPtuH-κ^1S)Cl]

A mixture of Bz^{t}BPtuH (0.2920g, 0.6886 mmol) and [{RhCl(COD)}$_2$] (0.1700g, 0.3449 mmol) in 5 ml of CH_2Cl_2 was stirred at room temperature for 1 h under a brisk flow of argon gas. Hexane was added to the orange solution and the solvent was reduced to near dryness by rotary evaporation. The orange product formed was triturated in hexane and the yellow product was filtered and washed with hexane. Yield, 0.3470g (75%), m.p. 158-161.4 °C. Anal. Found: C, 61.13; H, 7.50; N, 4.12; S, 4.39%. Calculated for $C_{34}H_{48}ClN_2ORhS$: C, 60.86; H, 7.16; N, 4.17; S, 4.77%. Crystals suitable for X-ray analysis were grown by recrystallisation from $CHCl_3$/pentane.

---

[9] G. Giordano and R.H. Crabtree, *Inorg. Synth.*, 1979, **19**, 218.

[Rh(COD)(BzPPtuH-κ^1S)Cl]

A mixture of BzPPtuH (0.3339g, 0.6898 mmol) and [{RhCl(COD)}$_2$] (0.1700g, 0.3449 mmol) in 5 ml of CH_2Cl_2 was stirred at room temperature for 1 h under a brisk flow of argon gas and the solvent was reduced volume (5 ml) by rotary evaporation. To the orange solution was added hexane (5 ml) and the yellow product, which formed, was filtered and washed with hexane/ethanol (10:1 v/v). Yield, 0.4500g (89%), m.p. 180-182 °C. Anal. Found: C, 65.06; H, 4.90; N, 3.96; S, 4.29%. Calculated for $C_{40}H_{36}ClN_2ORh$ S: C, 65.72; H, 4.93; N, 3.83; S, 4.38%.

[Rh(COD)(Bz ^{i}PPtuH-κ^1S)Cl]

A mixture of Bz^{i}PPtuH (0.2345g, 0.6897 mmol) and [{RhCl(COD)}$_2$] (0.1700g, 0.3449 mmol) in 5 ml of CH_2Cl_2 was stirred at room temperature for 2 h under a brisk flow of argon gas and the solvent was reduced to near dryness by rotary evaporation. The dark orange product formed was triturated in hexane and the yellow product, which formed, was filtered and washed with hexane/ethanol (10:1 v/v). Yield, 0.3416g (84%), m.p. 165-166.2 °C. Anal. Found: C, 57.11; H, 6.37; N, 4.69; S, 5.42%. Calculated for $C_{28}H_{36}ClN_2ORhS$: C, 57.29; H, 6.14; N, 4.77; S, 5.46%.

[Rh(COD)(BzFPtuH-κ^1S)Cl]

A mixture of BzFPtuH (0.1890g, 0.6897 mmol) and [{RhCl(COD)}$_2$] (0.1700g, 0.3449 mmol) in 5 ml of CH_2Cl_2 was stirred at room temperature for 2 h under a brisk flow of argon gas, then the resulting dark orange solution was reduced to dryness by rotary evaporation and the dark brown oil formed was triturated in hexane/ethanol (10:1 v/v, 10 drops) and left to stand for one day in a fridge. The orange yellow product, which formed, was filtered and washed with hexane/ethanol (10:1 v/v). Yield, 0.3007g (83.7%), m.p. 132.8-134.7 °C. Anal. Found: C, 49.49; H, 4.59; N, 6.16; S, 6.76%. Calculated for $C_{22}H_{23}ClFN_2ORhS$: C, 50.73; H, 4.42; N, 5.38; S, 6.15%.

[Rh(COD)(BzPtuH-κ^1S)Cl]

A mixture of BzPtuH (0.1766g, 0.6898 mmol) and [{RhCl(COD)}$_2$] (0.1700g, 0.3449 mmol) in 5 ml of CH_2Cl_2 was stirred at room temperature for 1 h under a brisk flow of argon gas, and the solvent was reduced to dryness by rotary evaporation. The orange yellow product formed was washed with cold hexane/ethanol

(10:1 v/v,) and the yellow product, was filtered and washed with the same hexane/ethanol mixture. Yield, 0.3100g (89%), m.p. 169-170 °C. Anal. Found: C, 51.23; H, 4.76; N, 5.74; S, 6.26%. Calculated for $C_{22}H_{24}Cl\ N_2ORhS$: C, 52.54; H, 4.77; N, 5.57; S, 6.37%.

cis-[Pt(Bz^{t}BPtuH-κ^1S)$_2$Cl$_2$][a]

To a stirred, warm (60 ^{0}C) solution of Bz^{t}BPtuH 0.2120g (0.5000 mmol) dissolved in 30 ml dioxane/H_2O (2:1 v/v) with 3 drops of conc. HCl, was added dropwise a solution of $K_2[PtCl_4]$ (0.1037g, 0.2500 mmol), in the same solvent (30 ml) over 10-15 min. The solution was allowed to stir for a further 30 min at 60 ^{0}C. The mixture was subsequently poured into water (50 ml) and left in an ice-bath. The bright yellow precipitate was filtered and washed with dioxane/EtOH (2:1 v/v) to give 0.2166g of crude product 78% yield. This was recrystallised from hot $CHCl_3$/EtOH (2:1 v/v) and rotary evaporated to reduce the volume. The light yellow product was filtered and washed with $CHCl_3$/EtOH (2:1 v/v) and diethyl ether (5 ml). Yield: 0.1249g (45%), m.p. did not melt below 200 °C. Anal. Found: C, 56.02; H, 6.68; N, 5.02; S, 5.60%. Calculated for $C_{52}H_{72}Cl_2N_4O_2PtS_2$: C, 56.01; H, 6.46; N, 5.02; S, 5.74%.

Crystals suitable for X-ray analysis were grown by recrystallisation from $CHCl_3$/pentane.

[a] Preliminary crystallographic data shows this to have a *cis* structure.

cis-[Pt(Bz^{i}PPtuH-κ^1S)$_2$Cl$_2$]

To Bz^{i}PPtuH 0.1700g (0.5000 mmol) dissolved in 30ml dioxane/H_2O (2:1 v/v) with 3 drops of conc. HCl, was added dropwise a solution of $K_2[PtCl_4]$ 0.1038g (0.2500 mmol) in the same solvent. The solution was allowed to stir for 30 min at 60 ^{0}C. The dark yellow product, which separated, was filtered and washed with dioxane/EtOH (2:1 v/v) to give 0.2300g of crude product 97% yield. This was recrystallised from hot $CHCl_3$/EtOH (2:1 v/v) and rotary evaporated to reduce the volume. The light yellow product was filtered and washed with $CHCl_3$/EtOH (2:1 v/v) and diethyl ether (5 ml). Yield: 0.0492g (20.8%), m.p. did not melt below 200 °C. Anal. Found: C, 50.46; H, 5.47; N, 5.74; S, 6.61%. Calculated for $C_{40}H_{48}Cl_2N_4O_2PtS_2$: C, 50.74; H, 5.07; N, 5.92; S, 6.76%.

5.2 Results and Discussion

5.2.1 Physicochemical Studies and Characterization of the Complexes

5.2.1.1 Synthesis of the Complexes

The complexes [Rh(COD)(LH)Cl] (LH = Bz^{t}BPtuH, BzPPtuH, Bz^{i}PPtuH, BzFPtuH, BzPtuH) were prepared by reacting [{RhCl(COD)}$_2$] with the appropriate ligand LH in a 1:2 molar ratio according to the equation below. Yields of [Rh(COD)(LH)Cl] ranged from 75-89%.

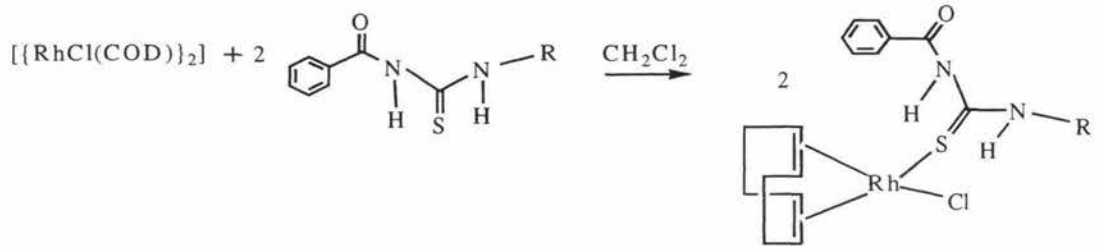

R = 2,4,6-tri-*tert*-butylphenyl (Bz^{t}BPtuH) or 2,4,6-tri-phenylphenyl (BzPPtuH) or 2,6-diisopropylphenyl (Bz^{i}PPtuH) or *p*-fluorophenyl (BzFPtuH) or phenyl (BzPtuH)

Reacting $K_2[PtCl_4]$ with LH in 1:2 molar ratio gave the yellow complexes $[Pt(LH)_2Cl_2]$ (LH = Bz^{t}BPtuH or Bz^{i}PPtuH) which were isolated according to the following equation:

$$K_2[PtCl_4] + 2LH \rightarrow \textit{cis}\text{-}[Pt(LH)_2Cl_2] + 2KCl$$

5.2.1.2 IR and Mass Spectroscopic Studies of the Compounds

Compounds of the type [Rh(COD)(LH)Cl] (LH = Bz^{t}BPtuH, BzPPtuH, or BzPtuH) or *cis*-[Pt(Bz^{i}PPtuH)$_2$Cl$_2$] display approximately the same ν(C=O) stretching frequenies as the free ligand, while LH = Bz^{i}PPtuH or BzFPtuH display a small shift to a higher wave number (6 or 12 cm^{-1} respectively), indicating that the carbonyl oxygen is not coordinated to the metal. This compares well with [Rh(COD)(Hbztu)Cl][2] (Hbztu

= $PhC(O)NHC(S)NH(CH_2)_2CH_3$), where the ν(C=O) (1669 cm^{-1}) stretching frequency is slightly lower than the free ligand (1674 cm^{-1}).

ν(N-H) stretching frequencies of [Rh(COD)(LH)Cl] (LH = Bz^tBPtuH, BzPPtuH, Bz^iPPtuH or BzPtuH) are less than those of the ligands by 86, 71, 95, and 130 cm^{-1} respectively, whereas when LH = BzFPtuH the ν(N-H) stretch is greater by 164 cm^{-1}. The ν(N-H) stretching frequency of *cis*-$[Pt(Bz^iPPtuH)_2Cl_2]$ is also less than the free ligand by 42 cm^{-1}, but this does not indicate the coordination of the N-H group in any of these compounds. Similarly the medium broad ν(N-H) stretch of $[Rh(COD)(Hbztu)Cl]^2$ is also less than the sharp broad ν(N-H) stretch of the free ligand by 48 cm^{-1}. As mentioned in Chapters 2 and 3 a decreased shift should be expected for the ν(C=S) stretching vibration, however this vibration cannot be located.

Mass spectral data give further evidence for the integrity of [Rh(COD)(Bz^tBPtuH)Cl] (see **Table 5.1**), with a $[M-Cl]^+$ peak at 635, *cis*-$[Pt(Bz^tBPtuH)_2Cl_2]$, $[(M-Cl)]^+$ at 1079 and *cis*-$[Pt(Bz^iPPtuH)_2Cl_2]$, a M^+ peak at 946.

Table 5.1 Selected IR band positions and MS data for Rh complexes

Compound	IR[a] (cm^{-1}) ν(C=O)	ν(N-H)	(+)FAB Mass spectra[b] m/z(rel. int.,%)
[Rh(COD)(Bz^{t}BPtuH)Cl]	1669vs	3135br,w	1374(18)[{$(M)_2$+Cl–H}(^{103}Rh)]$^+$ 635 (43) [M-Cl]$^+$ 562 (45) [M-(COD)]$^+$ 423 (24) [L-H]$^+$ 367 (68) [L-$(C(CH_3)_3]^+$ 105 (100) $[C_6H_5CO]^+$
[Rh(COD)(BzPPtuH)Cl]	1669vs	3137br,w	—
[Rh(COD)(Bz^{i}PPtuH)Cl]	1673vs	3142br,m	—
[Rh(COD)(BzFPtuH)Cl]	1681s	3295m	—
[Rh(COD)(BzPtuH)Cl]	1673vs	3154m,br	—
cis-[Pt(Bz^{t}BPtuH)$_2$Cl$_2$]	1675vs	3202m,br 3195m	[(M-Cl)(^{195}Pt)(^{35}Cl)]$^+$ 1079 (5) 1043 (4) [M-(2Cl+H)]$^+$ 105 (100) $[C_6H_5CO]^+$
cis-[Pt(Bz^{i}PPtuH)$_2$Cl$_2$]	1670vs	3195m,br 3150sh	[M(^{195}Pt)(^{35}Cl)]$^+$ 946 (2) 911 (20) [M-Cl]$^+$ 339 (44) [M-(L-H)]$^+$ 105(100) $[C_6H_5CO]^+$

[a] As nujol mull on NaCl. [b] 3-nitrobenzylalcohol matrix. vs = very strong, s = strong, m = medium, w = weak, br = broad, sh = shoulder.

5.2.1.3 ^{1}H and ^{13}C NMR Spectroscopic Studies of the Complexes

The ^{1}H NMR data for Rh and Pt complexes are shown in **Table 5.2** and ^{13}C NMR data in **Table 5.3**. In both thiourea/rhodium and platinum complexes the chemical shifts of the N-H protons are about the same as the free ligands except for [Rh(COD)(BzFPtuH)Cl] and [Rh(COD)(BzPtuH)Cl], where the chemical shifts are

slightly higher than the free ligand. In the ^{13}C NMR spectra, even though it is expected that the thiocarbonyl sulfur binds to Rh, there is no significant change in the chemical shift of the C=S carbon from the free ligand, suggesting that the ligand may be dissociating at room temperature. Similar results have been obtained for a related rhodium system[2] and $[Hg(Bz^tBPtuH)_2Cl_2]$ (see chapter 3 Section **3.2.2.2**). For the Pt complexes, the δ(C=S) values are lower than the free ligands (181.6 ppm for Bz^tBPtuH and 181.7 ppm for Bz^iPPtuH), suggesting S is not dissociating from Pt at room temperature and hence more strongly coordinated.

Fig. 5.2 shows how the NMR absorptions of the olefin protons vary over the temperature range 313 K – 213 K. The nearest spectrum was recorded at 313 K and then at 10 degree intervals to 213 K. The signal at 4.2 ppm is due to free COD. At low temperature (e.g. 263 K) two well separated resonances at 3.53 and 4.48 ppm, are attributable to the double bond protons *trans* to the Cl and S atoms. The structure is consistent to that observed in the crystal structure. At 313 K the system shows dynamic behavior; thus the two signals coalesce to a broad signal at about 4.25 ppm signifying a rapid interconversion of the double bonds and that the two equivalent protons H_a and the two equivalent protons H_b are rapidly interchanging (**Fig. 5.3**). Similar results were obtained with $[Rh(COD)(Ph_2PPy)Cl]$[1] complex.

The ^1H and ^{13}C chemical shifts for both the alkene CH's and CH_2's of COD compare well with those of $[Rh(COD)(Hbztu)Cl]$[2] (Hbztu = $PhC(O)NHC(S)NH(CH_2)_2CH_3$).

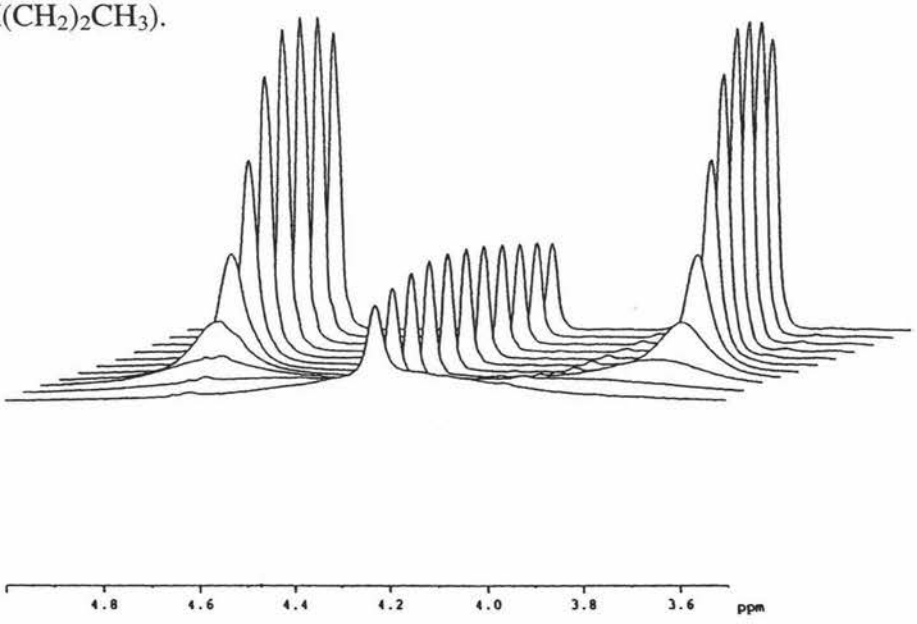

Figure 5.2 Temperature variation of the olefin proton NMR spectra for $[Rh(COD)(Bz^tBPtuH)Cl]$

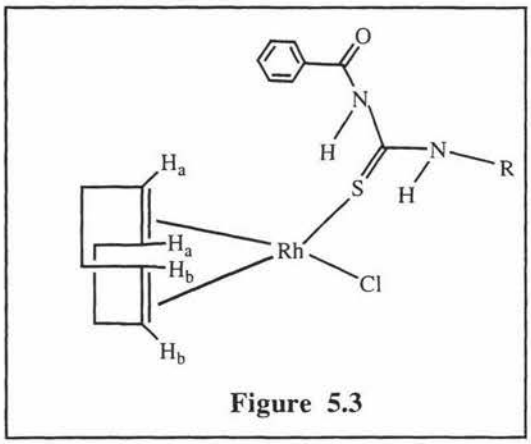

Figure 5.3

Table 5.2 ^{1}H chemical shift data for the complexes[a]

Compounds	^{1}H NMR ($CDCl_3$, TMS, ppm) δ_{N-H}	δ_{Ar-CH}	δ_{COD}	δ^t_{B-CH3} or $^i_{P-CH3}$ and CH
[Rh(COD)(Bz^{t}BPtuH)Cl]	10.24s(1H)	7.39-8.47m (7H)	4.23s,vbr (4CH) 2.50m,vbr ($4CH_2$) 1.80q ($4CH_2$)	1.34s (18H) 1.42s (9H)
[Rh(COD)(BzPPtuH)Cl]	9.88s (1H) 8.24s (1H)	7.21-8.06m (22H)	4.20s,vbr (4CH) 2.34m,vbr ($4CH_2$) 1.77q ($4CH_2$)	
[Rh(COD)(Bz^{i}PPtuH)Cl]	9.63s (1H)	7.21-8.27m (8H)	4.21s,br (4CH) 2.42m,br($4CH_2$) 1.81q ($4CH_2$)	1.18d (6H) 1.30d (6H) 3.01sept.(2H)
[Rh(COD)(BzFPtuH)Cl]	11.37s (1H) 10.36s (1H)	7.08-8.54m (9H)	4.24s (4CH) 2.44m ($4CH_2$) 1.84q ($4CH_2$)	
[Rh(COD)(BzPtuH)Cl]	11.41s (1H) 10.43s (1H)	7.27-8.22m (10H)	4.26s (4CH) 2.44m ($4CH_2$) 1.84q ($4CH_2$)	
cis-[Pt(Bz^{t}BPtuH)$_2$Cl$_2$]	8.32s (1H)	7.26-7.66m (7H)		1.33 (18H) 1.36 (9H)
cis-[Pt(Bz^{i}PPtuH)$_2$Cl$_2$]	8.30s (1H)	7.14-7.69m (8H)		1.01d (6H) 1.10d (6H) 2.84sept. (2H)

[a] Recorded at 400MHz, chemical shifts are relative to $Si(CH_3)_4$ [TMS], solvent $CDCl_3$.
s = singlet, d = doublet, q = quartet, sept = septuplet, m = multiplet, br = broad, vbr = very broad.

Table 5.3 ^{13}C chemical shift data for the complexes[a]

Compounds	^{13}C NMR ($CDCl_3$, ppm)				
	$\delta_{C=S}$	$\delta_{C=O}$	$\delta_{Ar\text{-}CH}$ $\delta_{Ar\text{-}C\ (quat.)}$	δ_{COD}	$\delta^{t}_{B\text{-}CH3\ and\ C(quat.)}$ or $\delta^{i}_{P\text{-}CH3\ and\ CH}$
[Rh(COD)(Bz^{t}BPtuH)Cl]	182.5	170.3	124.31-150.5 [7Ar-CH, 5Ar- $C_{(quat.)}$]	[b] 31.3 (CH_2)	31.8 (3C) 32.9 (6C) 35.4 ($1C_{(quat.)}$) 37.2 ($2C_{(quat.)}$)
[Rh(COD)(BzPPtuH)Cl]	180.7	169.9	127.6-142.2 [22Ar-CH, 8Ar-$C_{(quat.)}$]	79.1 (CH) 31.2 (CH_2)	
[Rh(COD)(Bz^{i}PPtuH)Cl]	182.0	170.5	124.3-145.6 [8Ar-CH, 4Ar-$C_{(quat.)}$]	82.9 (CH) 31.3 (CH_2)	23.5 (2C) 24.8 (2C) 29.2 ($2C_{(tert.)}$)
[Rh(COD)(BzFPtuH)Cl]	181.9[c] 180.8	170.1[c] 168.8	116.4-163.2 [9Ar-CH, 3Ar-$C_{(quat.)}$]	82.9 (CH) 31.3 (CH_2)	
[Rh(COD)(BzPtuH)Cl]	180.2	170.2	126.0-136.6 [10Ar-CH, $2C_{(quat.)}$]	82.9 (CH) 31.3 (CH_2)	
cis-[Pt(Bz^{t}BPtuH)$_2$Cl$_2$]	178.4	168.2	124.0-150.8 [7Ar-CH, 5Ar- $C_{(quat.)}$]		31.4 (3C) 32.4 (6C) 35.0 ($1C_{(quat.)}$) 36.7 ($2C_{(quat.)}$)
cis-[Pt(Bz^{i}PPtuH)$_2$Cl$_2$]	178.2	169.0	124.5-145.6 [8Ar-CH, 4Ar-$C_{(quat.)}$]		23.2 (2C) 24.8 (2C) 29.2 ($2C_{(tert.)}$)

[a]Recorded at 400MHz, solvent $CDCl_3$. [b]Cannot detect. [c]Split due to J(C–F).
quat = quaternary, tert = tertiary.

5.2.1.4 Description of the Crystal Structures

5.2.1.4.1 Crystal Structure of [Rh(COD)(BzPPtuH-κ^1S)Cl]

The structure of the complex [Rh(COD)(BzPPtuH-κ^1S)Cl] is shown in **Fig. 5.4** with crystal data and structure refinement details given in **Table 5.4** and selected bond lengths and angles given in **Table 5.5**. In the crystal lattice there is a CH_2Cl_2 molecule. The Rh atom is coordinated by a Cl atom, a S atom from the BzPPtuH molecule and by the COD interacting through the two C=C. If M(1) and M(2) are the midpoints of the double bonds, C(33)–C(34) and C(37)–C(38), the Rh atom displays a slightly distorted square-planar coordination. The Rh–M(1) and Rh–M(2) distances are 2.034(3) and 2.013(3) Å. The C(33)–C(34) and C(37)–C(38) distances (1.400(4) Å and 1.408(4) Å) are shorter than the other C–C distances (1.509(4) Å – 1.530(4) Å), suggesting a double bond character. As in the free ligand, the O and S atoms adopt a *trans* orientation with respect to one another, so as to minimise non-bonded steric interactions. The C(32)–S(1) distance (1.704(3) Å) is longer than the C(26)–S distance of the free ligand Bz^{t}BPtuH (1.679(3) Å), suggesting weakening of the bond upon coordination to Rh, but it retains some double bond character. This is similar to the S–C(1) distance of (1.701(4) Å) in [Rh(COD)(Hbztu)Cl] (Hbztu = PhC(O)NHC(S)NH$(CH_2)_2CH_3$)[2]. As well the C(31)–O(1) distance (1.222(3) Å) is similar to that in [Rh(COD)(Hbztu)Cl] where the O–C(5) distance is (1.214(6) Å).

As in the free molecule, an intramolecular N(2)–H...O hydrogen bond [N(2)–H...O(1) = 1.996(6) Å], results in an almost planar six membered ring with C(31), N(1) and C(32). As well another intramolecular hydrogen bond is formed by the N(1)–H with the Cl atom [N(1)–H...Cl = 2.308(6) Å]. The same interactions are observed in [Rh(COD)(Hbztu)Cl][2]. In the crystal, two different molecules are linked together by intermolecular N(2)–H...O hydrogen bond [N(2)–H...O(1) = 2.251(6) Å].

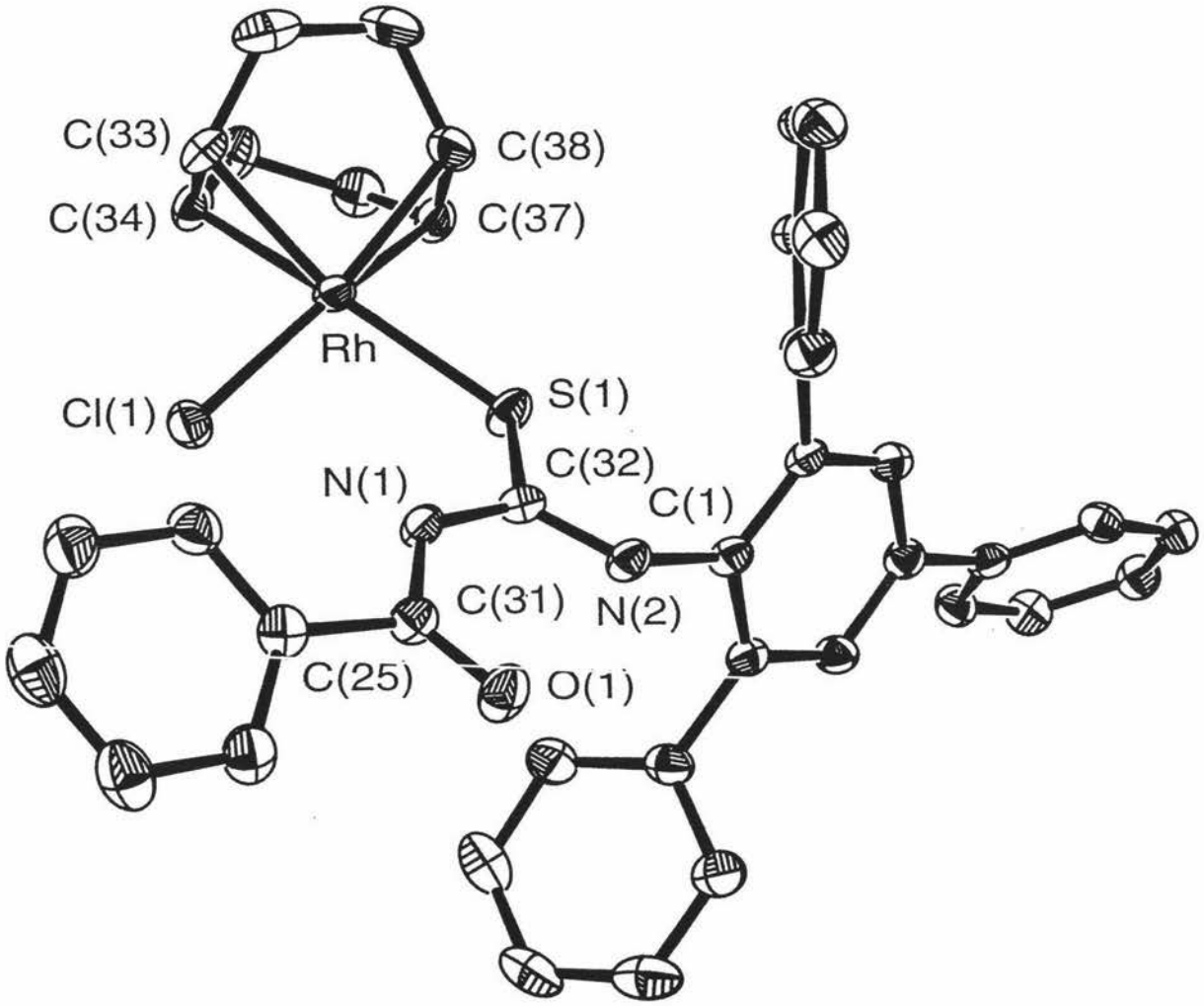

Figure 5.4 ORTEP diagram for the complex [Rh(COD)(BzPPtuH-κ^1S)Cl] showing the numbering system used. Thermal ellipsoids are at the 50% probability level. Hydrogen atoms and solvent molecules have been omitted for clarity

Table 5.4 Crystal data and structure refinement for [Rh(COD)(BzPPtuH-$\kappa^1 S$)Cl]

Identification code	iprh
Empirical formula	$C_{40}H_{36}ClN_2ORhS \cdot CH_2Cl_2$
Formula weight	816.05
Temperature	150(2) K
Wavelength	0.71073 Å
Crystal system	Triclinic
Space group	P-1
Unit cell dimensions	a = 9.5571(5) Å □ = 79.768(1)°.
	b = 12.0079(6) Å □= 86.997(1)°.
	c = 16.6720(9) Å □ = 81.623(1)°.
Volume	1862.1(2) $Å^3$
Z 2	
Density (calculated)	1.455 Mg/m^3
Absorption coefficient	0.765 mm^{-1}
F(000)	836
Crystal size	0.32 x 0.14 x 0.05 mm^3
Theta range for data collection1	24 to 26.40°.
Index ranges	-11 ≤h ≤ 11, -14 ≤ k ≤ 14, -20 ≤ l ≤ 20
Reflections collected	17852
Independent reflections	7521 [R(int) = 0.0280]
Absorption correction	Semi-empirical from equivalents
Max. and min. transmission	0.9627 and 0.7918
Refinement method	Full-matrix least-squares on F^2
Data / restraints / parameters	7521 / 0 / 442
Goodness-of-fit on F^2	1.013
Final R indices [I>2sigma(I)]	R1 = 0.0345, wR2 = 0.0744
R indices (all data)	R1 = 0.0473, wR2 = 0.0824
Largest diff. peak and hole	0.928 and -0.852 $e.Å^{-3}$

Table 5.5 Selected bond lengths [Å] and angles [°] for [Rh(COD)(BzPPtuH-κ^1*S*)Cl] with estimated standard deviations in parentheses

Bond lengths:

Rh-Cl(1)	2.3863(7)	Rh-S(1)	2.3779(7)
Rh-M(1)[a]	2.034(3)	Rh-M(2)[a]	2.013(3)
Rh-C(33)	2.143(3)	Rh-C(37)	2.120(3)
Rh-C(34)	2.153(3)	Rh-C(38)	2.140(3)
C(33)-C(34)	1.400(4)	C(37)-C(38)	1.408(4)
C(33)-C(40)	1.509(4)	C(34)-C(35)	1.519(4)
C(35)-C(36)	1.530(4)	C(36)-C(37)	1.518(4)
C(38)-C(39)	1.528(4)	C(39)-C(40)	1.528(5)
S(1)-C(32)	1.704(3)	N(1)-C(32)	1.376(3)
N(1)-C(31)	1.395(3)	N(2)-C(32)	1.328(3)
N(2)-C(1)	1.437(3)	O(1)-C(31)	1.222(3)
C(25)-C(31)	1.493(4)		

Bond angle:

S(1)-Rh-Cl(1)	96.76(3)	C(32)-S(1)-Rh	119.1(1)
C(2)-C(1)-N(2)	121.9(2)	C(6)-C(1)-N(2)	117.1(2)
C(3)-C(2)-C(7)	118.0(2)	C(1)-C(2)-C(7)	123.7(2)
C(3)-C(4)-C(13)	122.5(2)	C(5)-C(4)-C(13)	119.4(2)
C(5)-C(6)-C(19)	119.2(2)	C(1)-C(6)-C(19)	122.3(2)
C(26)-C(25)-C(31)	116.7(3)	C(30)-C(25)-C(31)	123.6(3)
O(1)-C(31)-N(1)	122.1(3)	O(1)-C(31)-C(25)	121.8(3)
N(1)-C(31)-C(25)	116.1(2)	C(32)-N(1)-C(31)	126.3(2)
N(2)-C(32)-N(1)	118.3(2)	N(2)-C(32)-S(1)	120.0(2)
N(1)-C(32)-S(1)	121.6(2)	C(32)-N(2)-C(1)	123.4(2)

[a]M(1) and M(2) are the midpoints of the bonds C(33)–C(34) and C(37)–C(38), respectively.

5.3 Conclusions

The complexes [Rh(COD)(LH)Cl] (LH = Bz^{t}BPtuH, BzPPtuH, Bz^{i}PPtuH, BzFPtuH or BzPtuH) are prepared from the reaction of $[Rh(COD)Cl]_2$ with the appropriate LH, and the complexes $[Pt(LH)_2Cl_2]$ (LH = Bz^{t}BPtuH or Bz^{i}PPtuH) by reacting $K_2[PtCl_4]$ with the appropriate LH.

The X-ray structure of [Rh(COD)(BzPPtuH-κ^1*S*)Cl] shows a square planar arrangement of the ligands about Rh, with LH binding through the sulfur atom. One of π-bonds of the COD ligand is bound to Rh and is *trans* to the Cl group while the other π-bond is bound to Rh but is *trans* to the S atom. The two equivalent protons (H_a) associated with the olefinic bonds *trans* to the Cl group have a different chemical shift from the two H_b protons on the olefin arm *trans* to the S atom at low temperature (–20 to –40 °C), but coalesce into one broad band at higher temperature (20 to 40 °C). This is due to fast interchange of the two olefinic bonds.

As observed before the presence of a possible intramolecular hydrogen bond in the ligand LH favours the formation of the complex *cis*-$[Pt(LH)_2Cl_2]$, where LH remains neutral. A preliminary X-ray structure on [Pt(Bz^{t}BPtuH-κ^1*S*)$_2$Cl$_2$] shows the complex has a *cis* structure.

Appendix

Future Work

Towards the end of Chapter 4 and 5 new lines of research appeared that are deserving of further investigations. These are now outlined.

Chapter 4

♦ Upon aging the reaction mixture containing of $Bz^{i}PPtuH$ and Br_2 (1:1 molar ratio) colourless crystals of a new product was formed and its nature needs to be studied. Reactions also need to be undertaken where the ratio is 1:1.5 and 1:2.

♦ The nature of the colourless crystals (grown in $CHCl_3$/pentane) from the reaction of BzPPtuH with Br_2 needs to be established, so that further insight into these reactions can be obtained.

♦ The reaction of the bulky ligands with interhalogen compounds e.g. IBr needs to undertaken as a follow-up to the Br_2 and I_2 reactions.

Chapter 5

♦ Pt complexes of the type $[Pt(COD)(LH)Cl]BF_4$ should be attempted to be synthesised and the COD interchange studied by ^{1}H NMR spectroscopy. The results may be compared with those for the analogous rhodium(I) system to gauge the effect of having Pt(II) in the complex.

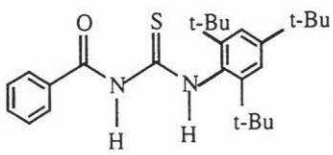

Bz^{t}BPtuH

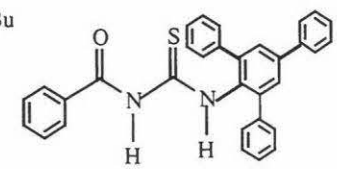

BzPPtuH

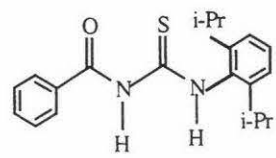

Bz^{i}PPtuH

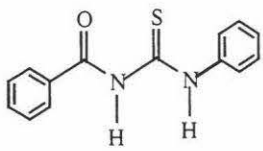

BzPtuH

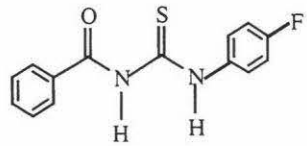

BzFPtuH

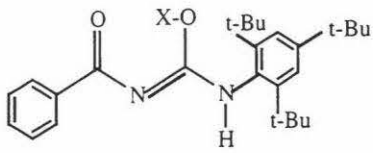

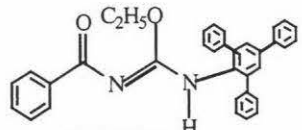

BzEPPA

BzE^{i}PPA

X = C_2H_5, 1-benzoyl-2-[ethoxyl-3-(2,4,6-tri-*tert*-butylphenyl)amino]aldimine (**BzE^{t}BPA**)

= CH_3, 1-benzoyl-2-[methoxyl-3-(2,4,6-tri-*tert*-butylphenyl)amino]aldimine (**BzM^{t}BPA**)

= $CH_2C_6H_5$1-benzoyl-2-[phenylmethoxyl-3-(2,4,6-tri-*tert*-butylphenyl)amino]aldimine (**BzPM^{t}BPA**)

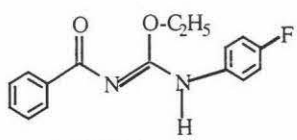

BzEFPA

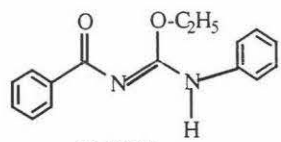

BzEPA

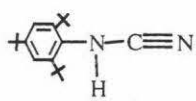

^{t}BPc

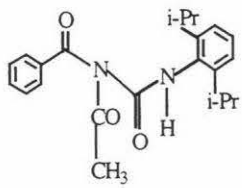

ABz^{i}PPu

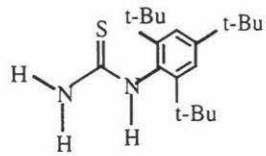

^{t}BPtu

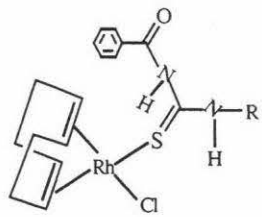

Rh(COD)(LH)Cl

LH = ^{t}BPtuH, BzPPtuH, Bz^{i}PPtuH, BzFPtuH or BzPtuH

R = 2,4,6-tri-*tert*-butylphenyl, 2,4,6-tri-phenylphenyl,
2,6-diisopropylphenyl, *p*-fluorophenyl or phenyl

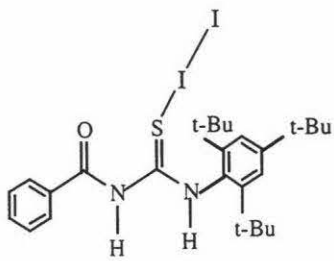

(Bz^{t}BPtuH)I_2

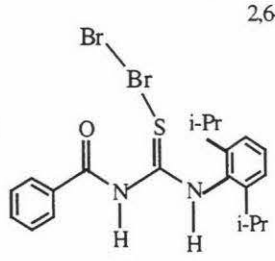

(Bz^{i}PPtuH)Br_2

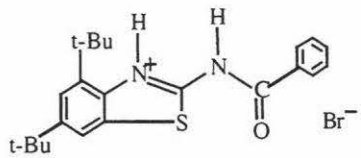

B^{t}BBTH

The structures and abbreviations of the molecules used in this thesis

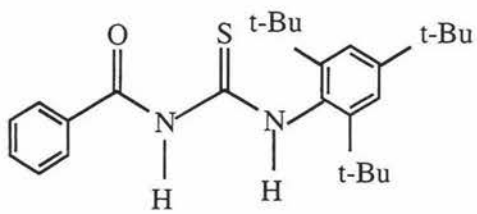

Bz^{t}BPtuH

1-benzoyl-3-(2,4,6-tri-*tert*-butylphenyl)thiourea

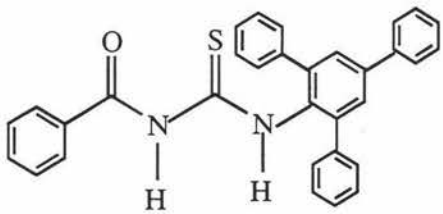

BzPPtuH

1-benzoyl-3-(2,4,6-tri-phenylphenyl)thiourea

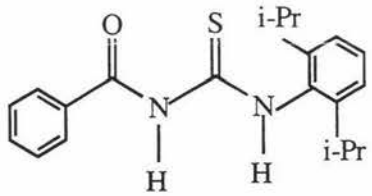

Bz^{i}PPtuH

1-benzoyl-3-(2,6-diisopropylphenyl)thiourea

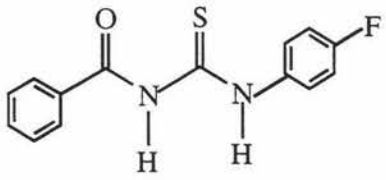

BzFPtuH

1-benzoyl-3-(4-fluorophenyl)thiourea

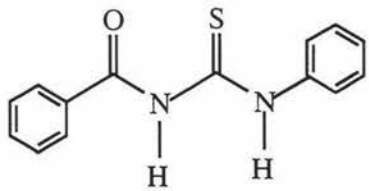

BzPtuH

1-benzoyl-3-phenylthiourea

Structures, Names and Abbreviations for the Ligands in Chapter Two

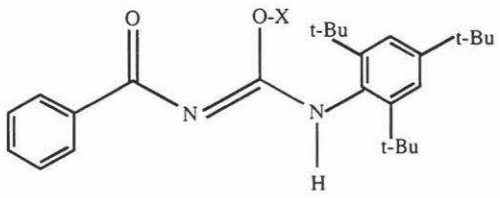

X = C_2H_5, 1-benzoyl-2-[ethoxyl-3-(2,4,6-tri-*tert*-butylphenyl)amino]aldimine (**BzE^{t}BPA**)

= CH_3, 1-benzoyl-2-[methoxyl-3-(2,4,6-tri-*tert*-butylphenyl)amino]aldimine (**BzM^{t}BPA**)

= $CH_2C_6H_5$, 1-benzoyl-2-[phenylmethoxyl-3-(2,4,6-tri-*tert*-butylphenyl)amino]aldimine

(**BzPM^{t}BPA**)

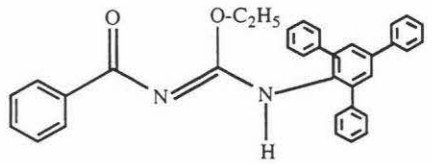

1-benzoyl-2-[ethoxyl-3-(2,4,6-tri-phenylphenyl)amino]aldimine

BzEPPA

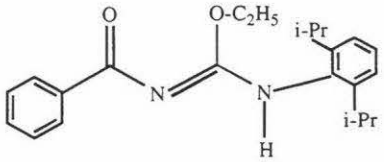

1-benzoyl-2-[ethoxyl-3-(2,6-diisopropylphenyl)amino]aldimine

BzE^{i}PPA

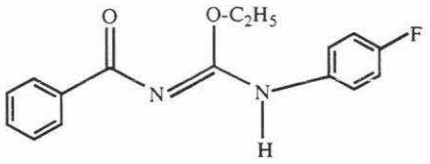

1-benzoyl-2-[ethoxyl-3-(4-fluorophenyl)amino]aldimine

BzEFPA

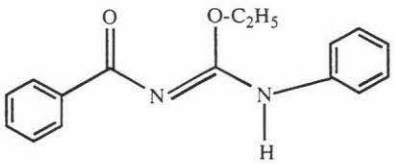

1-benzoyl-2-[ethoxyl-3-(phenyl)amino]aldimine

BzEPA

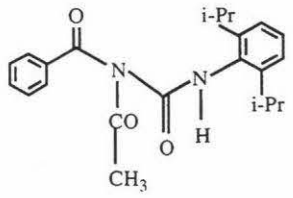

1-acetyl-1-benzoyl-*3*-(2,6-diisopropylphenyl)urea

ABz^{i}PPu

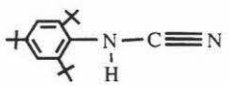

2,4,6-tri-*tert*-butylphenylcyanamide

^{t}BPc

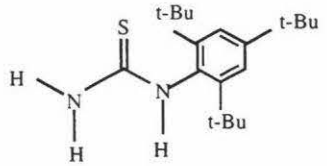

2,4,6-tri-*tert*-butylphenylthiourea

^{t}BPtu

Figure 3.1 Abbreviations, names and the structures of the compounds synthesised in this chapter.